


For Reference

NOT TO BE TAKEN FROM THIS ROOM

Ex LIBRIS
UNIVERSITATIS
ALBERTAENSIS





Digitized by the Internet Archive
in 2019 with funding from
University of Alberta Libraries

<https://archive.org/details/Cameron-Schimann1978>

THE UNIVERSITY OF ALBERTA

RELEASE FORM

NAME OF AUTHOR Monique CAMERON-SCHIMANN

TITLE OF THESIS ELECTRON MICROPROBE STUDY OF URANIUM MINERALS AND
ITS APPLICATION TO SOME CANADIAN DEPOSITS

.....

DEGREE FOR WHICH THESIS WAS PRESENTED Ph.D.

YEAR THIS DEGREE GRANTED 1978

Permission is hereby granted to THE UNIVERSITY OF
ALBERTA LIBRARY to reproduce single copies of this
thesis and to lend or sell such copies for private,
scholarly or scientific research purposes only.

The author reserves other publication rights,
and
neither the thesis nor extensive extracts from it may
be printed or otherwise reproduced without the author's
written permission.

THE UNIVERSITY OF ALBERTA

ELECTRON MICROPROBE STUDY OF URANIUM MINERALS AND ITS
APPLICATION TO SOME CANADIAN DEPOSITS

by



Monique CAMERON-SCHIMANN

A THESIS

SUBMITTED TO THE FACULTY OF GRADUATE STUDIES AND RESEARCH
IN PARTIAL FULFILMENT OF THE REQUIREMENTS FOR THE DEGREE
OF DOCTOR OF PHILOSOPHY

IN

Geology

DEPARTMENT OF GEOLOGY

EDMONTON, ALBERTA

FALL, 1978

THE UNIVERSITY OF ALBERTA
FACULTY OF GRADUATE STUDIES AND RESEARCH

The undersigned certify that they have read, and
recommend to the Faculty of Graduate Studies and Research,
for acceptance, a thesis entitled "Electron microprobe
study of uranium minerals and its application to some
Canadian deposits"
submitted by Monique CAMERON-SCHIMANN
in partial fulfilment of the requirements for the degree of
Doctor of Philosophy (Geology).

ABSTRACT

Uraniferous phases of uranium deposits commonly occur as small grains difficult to isolate by commonly used mineral separation techniques. They can be advantageously studied by electron microprobe. A review of uranium mineralogy is presented. The various aspects of electron microprobe analysis of uranium- and thorium-bearing minerals are discussed and solutions to the problems encountered are proposed. These aspects include: location of grains for analysis, instrumentation, stability of the minerals beneath the electron beam, determination of suitable X-ray emission lines, choice of standards, synthesis of glasses and selection of operating conditions.

An analytical approach is defined and tested on uranium- and thorium-bearing materials (*i.e.*, glasses and minerals). All microprobe data are corrected through the computer programme COR-2 (Hénoch *et al.*, 1973); some were also corrected using FEPAC (Springer, 1976). Compositions obtained for eight glasses and two minerals (euxenite and davidite) are compared with those previously determined through independent methods. Compositions obtained for the other minerals, namely: meta-uranocircite, sabugalite, carnotite, beta-uranophane, soddyite, thorogummite, and uranothorianite are compared with their stoichiometric compositions and analyses taken from the literature.

Three uranium deposits are studied: Baie Johan Beetz (Quebec), Charlebois Lake (Saskatchewan), and Duddridge Lake (Saskatchewan). In the first two, uranium mineralization occurs in granitic to pegmatitic rocks; in the last, it is located in meta-arkoses. Their mineralogy is described. Analyses of uranium- and thorium-bearing phases are used to define the type of deposit, and the locus of uranium and thorium mineralization in the rocks. An age is calculated from the uraninite analyses, relating the mineralization to the regional geology. The process of oxidation of uranium- and thorium-minerals is studied. Two new minerals are partly defined: a Ti-V phase, and a U-Pb-Si phase.

This study has shown that it is not only possible to identify uranium minerals from microprobe results, but also to obtain quantitative analyses, while avoiding separation and contamination. The accuracy of the analyses is best exemplified by the age determination of mineralizing events (≥ 1317 Ma at Baie Johan Beetz, with readjustment around 1150 Ma; -1750 Ma at Charlebois Lake; -2050 Ma at Duddridge Lake).

ACKNOWLEDGEMENTS

For this work, samples were provided by Dr R.A. Munday for the Duddridge Lake area; F. Morra and Fosago Exploration for the Charlebois Lake area. J.A. Smellie provided glasses and minerals of known composition, and Atomic Energy of Canada Ltd supplied some uranium standard materials. Texasgulf Inc. made it possible for the author to obtain samples from the Baie Johan Beetz region. I thank them for their contribution.

In Montreal, the Ecole Polytechnique and the Centennial College have made computer terminals available to the author for the completion of this thesis. I would like to express my gratitude to them.

I would also like to express my gratitude for all those who have helped in the realisation of this work:

Dr D.G.W. Smith for suggesting this topic and for his judicious advice and guidance;

Dr R.D. Morton for his helpful suggestions and his accessibility;

Dr H. Baadsgaard and Dr R. Cavell for discussions and for the interest they have manifested in the course of this work.

And more generally, I would like to thank the academic and technical staff of the Department of Geology, University of Alberta, particularly the technical staff of the microprobe laboratory (D.A. Tomlinson and S.L. Launspach) for their help and advice during my stay at the Department.

The microanalytical laboratory at the University of Alberta is partly supported financially by a grant (#A4254) from the National Research Council of Canada to Dr D.G.W. Smith.

TABLE OF CONTENTS

CHAPTER		PAGE
I	INTRODUCTION	1
A.	GENERAL CONSIDERATIONS	1
	1- MINERALOGY	2
	2- PETROCHEMISTRY	2
	3- METALLOGENY	4
	4- GEOCHRONOLOGY	4
B.	METHODS OF ANALYSIS	5
II	MINERALOGY OF URANIUM	10
A.	OXIDES	11
	1- ANHYDROUS OXIDES	11
	2- HYDROUS OXIDES	15
	Fourmarierite Group	16
	Other Hydrated Uranium Oxides	18
	Gummite	18
B.	MULTIPLE OXIDES	19
	Columbite Group	19
	Pyrochlore Group	20
	Others	20
C.	ARSENATES AND PHOSPHATES	21
	Uranium Micas	22
	Rhaphdophane Group	24
	Phosphuranylite Group	25
	Others	25
D.	SILICATES	25
	Thorite Group	26
	Uranophane Group	27
	Others	27
E.	CARBONATES	28
	Tricarbonate Series	28
	Others	29
F.	SULPHATES	29
G.	VANADATES	31
	Carnotite Group	31
H.	TELLURITES	32
I.	URANIUM-MOLYBDENUM MINERALS	33
J.	SELENITES	34
K.	CARBONACEOUS MATERIALS	35
III	PREVIOUS WORK	46
IV	ANALYTICAL APPROACH	49
A.	LOCATION OF GRAINS FOR ANALYSIS	50
B.	INSTRUMENTATION	51
C.	STABILITY OF MINERALS BENEATH THE ELECTRON BEAM	51
D.	SUITABLE X-RAY EMISSION LINES	54
E.	CORRECTIONS FOR MATRIX EFFECTS	56
	1- ALPHA FACTORS	57
	2- COMPREHENSIVE 'ZAF' CORRECTIONS	57

	F. PRESENCE OF WATER AND HYDROXYL IONS	66
	G. STANDARDS	70
	H. OPERATING CONDITIONS	70
V	STANDARDS	72
	A- STANDARD MATERIALS	72
	1. GENERALITIES	72
	Pure Metals	73
	Simple Compounds	74
	Alloys	74
	Glasses	75
	Minerals	76
	2. STANDARD MATERIALS	78
	B- GLASSES	78
	1. PREVIOUS WORK	79
	2. CONSTRAINTS	81
	Glass-formers	82
	Compositional Gradients	82
	Heating Equipment	83
	3. COMPOSITION	84
	4. SOURCE MATERIALS AND PREPARATION	85
	Source Materials	85
	Preparation	86
	5. RESULTS	87
	1450°C Maximum	87
	1700°C Maximum	89
VI	ANALYSIS OF STANDARD MATERIALS	91
	A- GLASSES	91
	1. GLASSES 11, 12, 13, AND 15	91
	2. GLASSES A, B, D, AND E	92
	B- MINERALS	94
	1. EUXENITE	94
	2. DAVIDITE	97
	3. META-AUTUNITE	98
	4. META-URANOCIRCITE	99
	5. SABUGALITE	99
	6. CARNOTITE	101
	7. β -URANOPHANE	102
	8. SODDYITE	103
	9. THOROGUMMITE	103
	10. URANOTHORIANITE	104
	C- CONCLUSIONS	104
VII	BAIE JOHAN BEETZ	125
	A- DESCRIPTION	125
	1. LOCALIZATION	125
	2. PREVIOUS WORK	126
	3. GEOLOGY	128
	Basement Gneisses	129
	Wakeham Basin	129
	Wakeham Group	129
	Metagabbros	131
	Younger Intrusive Rocks	132
	1- Large Bodies	133
	2- Smaller Masses, Sills, And Dykes	133

	Paleozoic Sediments	134
	4. CHRONOLOGICAL RELATIONSHIPS	134
	5. METAMORPHISM	135
	6. MINERALIZATION	136
	7. CONSIDERATIONS ON THE ORIGIN OF THE GRANITES	138
	Hypothesis For The Formation Of The Granites	141
B-	ANALYSIS	142
	1. URANINITE	143
	Age	145
	2. MONAZITE	148
	3. XENOTIME AND CHURCHITE	151
	4. SAMARSKITE	154
	5. ALLANITE	155
	6. TITANOBETAFITE	161
	7. THOROGUMMITE	162
	8. ZIRCON	164
C-	CONCLUSIONS	166
VIII	DUDDRIDGE LAKE	170
A-	DESCRIPTION	170
	1. LOCALIZATION	170
	2. PREVIOUS WORK	171
	3. GEOLOGY	173
	Granitic Gneisses	173
	Supracrustal Rocks	175
	Basic Intrusive Rocks	176
	Pegmatites And Quartz Veins	176
	Glacial Deposits	176
	4. CHRONOLOGICAL RELATIONSHIPS	177
	5. TECTONICS AND METAMORPHISM	177
	6. MINERALIZATION: Summarized From Sibbald <u>et al</u> , 1976	178
	7. SOURCE OF THE URANIUM	179
B-	ANALYSIS	179
	1. URANINITE	180
	Age	181
	2. 'BRANNERITE'	182
	3. U-Pb-Si PHASE	187
	4. Ti-V PHASE	190
	5. RUTILE	192
	6. ZIRCON	193
	7. MONAZITE	194
	8. APATITE	195
C-	CONCLUSIONS	195
IX	CHARLEBOIS LAKE	198
A-	DESCRIPTION	198
	1. LOCALIZATION	198
	2. GENERAL GEOLOGY	200
	3. DESCRIPTION OF LITHOLOGICAL UNITS	201
	A- Granitic And Tonalitic Gneisses	202
	B- Granodioritic Granofels	202
	C- Migmatites	202
	D- Calc-silicate Rocks	203
	E- Hornblende Gneiss, Amphibolite; F- Biotite	

Gneiss	203
G- Quartzite	203
H- Pink Pegmatite Dykes And Irregular Bodies Of Granitic Rocks	203
4. STRATIGRAPHY	204
5. STRUCTURE	206
6. METAMORPHISM	207
7. MINERALIZATION	208
B- ANALYSIS	209
1. APPEARANCE OF URANINITE AND MONAZITE	210
2. URANINITE	215
Age	216
3. MONAZITE	217
4. ZIRCON	218
C- CONCLUSIONS	219
X CONCLUSION	222
BIBLIOGRAPHY	228
APPENDIX I PERMANENT DATA FILE FOR COR-2	273
APPENDIX II SUGGESTIONS FOR THE ANALYSIS OF U AND TH-MINERALS	293
A- PREPARATION FOR MICROPROBE ANALYSIS OF U AND Th- MINERALS	293
B- TESTS FOR HOMOGENEITY	294
1. ENERGY DISPERSIVE ANALYSIS	295
2. WAVELENGTH DISPERSIVE ANALYSIS	295
C- OPERATING CONDITIONS	296
D- DATA PROCESSING	300
E- ELEMENTS NOT ANALYSED	301
APPENDIX III SAMPLE TEMPERATURE BENEATH THE ELECTRON BEAM	303
APPENDIX IV IDENTIFICATION AND PETROGRAPHIC DESCRIPTIONS OF SAMPLES	305

LIST OF TABLES

Table	Description	Page
1	Average abundances of thorium and uranium in the Earth's Crust and in three common rocks.	3
2	Average of unit cell dimension of uraninite in relation with the type of occurrence.	13
3	Varieties of pyrochlore.	21
4	List of uranium minerals.	36
5	Numbers and corresponding reference for table 2. ..	45
6	Microprobe composition of U_3Si for various hypothetical $U-M_4$ and $U-M_5$ absorption jump ratios.	64
7	Average atomic number for simple compounds: experimental and calculated values.	69
8	Theoretical composition of glasses A, B, D and E. .	76
9	Theoretical composition of glasses 11, 12, 13 and 15.	76
10	List of elements analysed and corresponding standards.	78
11	Systems yielding homogeneous uranium-silica glasses and reference work.	81
12	Composition of glasses 1, 2 and 3.	87
13	Composition of glasses 11, 12, 13, 15 and detailed correction factors for microprobe data computed through FEPAC.	107
14	Composition of glasses 11, 12, 13, 15 and detailed correction factors for microprobe data computed through COR-2.	108
15	Composition of glasses 11, 12, 13 and 15 as obtained from initial powders, wet chemical analysis and microprobe data corrected through FEPAC and COR-2.	109
16	Theoretical and microprobe composition of glasses A, B, D and E with detailed correction factors for data computed through COR-2.	110
17	Theoretical and analytical (COR-2) atomic proportions of Al, Si and Ca in glasses A, B, D and E.	111
18	Composition of glasses A, B, D, E and total correction factors for microprobe data computed through FEPAC.	111
19	Composition of euxenite.	112
20	Composition of euxenite and detailed microprobe correction factors.	113
21	Composition of davidite.	114
22	Composition of davidite and detailed microprobe correction factors.	115
23	Composition of autunite and meta-autunite.	116

24	Composition of metatorbernite and meta- uranocircite.	117
25	'd' spacings for sabugalite.	118
26	Composition of sabugalite.	119
27	Composition of carnotite.	120
28	Composition of β -uranophane.	121
29	Composition of soddyite.	122
30	Composition of throgummite.	123
31	Composition of uranothorianite.	124
32	Average mineralogical composition of the Lac Turgeon and Lac Ferland granites.	139
33	Composition of uraninites from the Baie Johan Beetz region.	144
34	Approximative age of uraninites from the Baie Johan Beetz region.	148
35	Composition of monazites from the Baie Johan Beetz region.	151
36	Composition of xenotimes from the Baie Johan Beetz region.	153
37	Composition of samarskites from the Baie Johan Beetz region.	155
38	Composition of allanite from the Baie Johan Beetz region.	160
39	Composition of titanobetafite from the Baie Johan Beetz region.	162
40	Composition of throgummite from the Baie Johan Beetz region.	163
41	Composition of zircons from the Baie Johan Beetz region.	165
42	Minerals from the Baie Johan Beetz region which contain uranium, thorium and rare-earth elements. .	167
43	Stratigraphy of the Duddridge Lake region.	174
44	Composition of uraninites from the Duddridge Lake region.	181
45	Age of uraninites from the Duddridge Lake region. .	182
46	Composition of 'brannerite' from the Duddridge Lake region.	186
47	Composition of U-Pb-Si phase from the Duddridge Lake region.	188
48	Composition of Ti-V phase from the Duddridge Lake region.	190
49	Composition of rutile from the Duddridge Lake region.	192
50	Composition of zircons from the Duddridge Lake region.	193
51	Thorium and uranium contents of monazites from the Duddridge Lake region.	194
52	Stratigraphy of the Charlebois Lake region.	205
53	Metamorphic mineral assemblages from the Charlebois Lake region.	207
54	Composition of uraninites from the Charlebois Lake region.	216
55	Approximative age of uraninites from the	

	Charlebois Lake region.	216
56	Uranium and thorium contents of monazites from the Charlebois Lake region.	218
57	Composition of zircon from the Charlebois Lake region.	219
58	Format for the computer file listed in table 59. ..	274
59	Listing of the permanent data file referred to in COR-2.	275
60	Basic data and suggestions for the analysis of uranium, thorium and commonly associated elements.	298
61	Elements and lines recorded with some common crystals used in WDA.	300
62	Identification of the samples from the Baie Johan Beetz region.	306
63	Petrographic description of the samples from the Baie Johan Beetz region.	307
64	Identification of the boulder samples from the Duddridge Lake region.	325
65	Petrographic description of the samples from the Duddridge Lake region.	326
66	Identification of the samples from the Charlebois Lake region.	336
67	Petrographic description of the samples from the Charlebois Lake region.	337

LIST OF FIGURES

Figure		Page
1	Variation with time of uranium count rate of a β -uranophane specimen beneath a focussed electron beam.	53
2	Partial spectra for uranium, thorium and potassium at 15 kV.	55
3	Variation of the apparent silicon concentration in U_3Si with absorption jump ratio.	63
4	Relationship between the atomic number of pure elements and their sample current/probe current ratio.	67
5	Relationship between the average atomic number of compounds and their sample current/probe current ratio.	67
6	Distribution of rare-earth elements in euxenite. ..	96
7	Geological map of the Baie Johan Beetz region.	126
8	Histogram of the age of uraninites from the Baie Johan Beetz region.	148
9	Spectra for the composition of allanite from the Baie Johan Beetz region.	156
10	Geological map of the Duddridge Lake region.	171
11	Geological map of the Charlebois Lake region.	199

LIST OF PHOTOGRAPHIC PLATES

Plate	Description	Page
1	Backscattered electron and elemental photographs of 'meta-uranocircite'.	100
2	Backscattered electron and elemental photographs of monazite in sample JB-10.	149
3	Transmitted light and elemental photographs of allanite in sample JB-15.	157
4	Reflected light, backscattered electron, and elemental photographs of 'brannerite' in sample DL-5.	184
5	Backscattered electron and elemental photographs of 'U-Pb-Si' phase in sample DL-3.	189
6	Backscattered electron and elemental photographs of uraninite in sample CL-1.	211
7	Backscattered electron and elemental photographs of monazite in sample CL-1.	212
8	Backscattered electron and elemental photographs of uraninite in sample CL-5.	214

CHAPTER I

INTRODUCTION

A. GENERAL CONSIDERATIONS

Developments in nuclear technology and the increasing demand for energy have focussed attention on uranium-bearing minerals of igneous, metamorphic and sedimentary rocks. Apart from being a major constituent in certain minerals, uranium occurs as a minor element substituting in the lattice of a substantial number of other minerals. Frequently the uraniferous phases occur as grains less than 50 microns in diameter and, because of their small size, they are difficult to study.

Investigations of uranium minerals have applications in several domains, particularly the fields of mineralogy, petrology, metallogeny, geochemistry and geochronology.

1- MINERALOGY

Although uranium is a trace element in the Earth's Crust, its minerals are numerous although not abundant. At least 120 uranium minerals have already been recognized. Because most of them are hexavalent uranium compounds, they have no structural analogues amongst other mineral groups and are therefore, of particular interest in mineralogy and crystal chemistry. Most of these hexavalent uranium minerals occur within the weathering zone but the bulk of uranium contained in the Earth's Crust occurs in the tetravalent state, often associated with thorium.

Uranium not only forms a number of distinct mineral species but also occurs as a vicarious constituent in more common rock-forming minerals such as zircon, apatite and monazite.

2- PETROCHEMISTRY

Uranium and thorium are present in the Crust in small amounts only. Average contents of some crustal materials, listed in table 1, give a rough idea of concentrations that may be expected in 'normal' rocks. The table does not include metamorphic rocks. These have compositions corresponding to those of the original precursor sedimentary or igneous rocks, but their uranium

and thorium contents appear to decrease with increasing metamorphism. Indeed, uranium and thorium tend to follow the larger ions, potassium and rubidium, and migrate away from regions of high metamorphism.

Table 1. Average abundances of thorium and uranium in the Earth's Crust and in three common rocks, in parts per million (Krauskopf, 1967).

Element	Crust	Granite	Basalt	Shale
Th	9.6	17	2.2	11
U	2.7	4.8	0.6	3.2

As shown in table 1, uranium and thorium contents of rocks are normally low, consequently their minerals can be difficult to recognize and, when metamict, to identify. Recognition of these minerals, and particularly the study of their compositions, can be of help in determining the origin of a rock (or deposit), and also in the characterization of a suite of rocks.

The first case is best exemplified by uraninite. Low temperature uraninite is normally thorium-free while high temperature uraninite is usually not. This difference in composition arises from the different geochemical properties of uranium and thorium. The second case can be seen, for example, in the identification of sedimentary beds. Suites of rocks can be typified by their heavy minerals. This facilitates the recognition and correlation

of a specific bed at different locations.

3- METALLOGENY

As the demand for uranium increases, some extremely low-grade deposits may become economical if the uranium can be extracted easily. This, for example, is the case for the Rössing deposits and Upper-Cambrian black shale deposit of Sweden. When a deposit lies on the margin of economic viability, the types of uranium minerals present, as well as their compositions, may have a bearing not only on metallogenic interpretations but also on beneficiation processes. Thus, it is important to recognize and analyse the host minerals of uranium.

4- GEOCHRONOLOGY

For the last 30 years uranium, thorium and their radiogenic products have been used to date geological events. Such determinations are most often performed by isotopic analyses on minerals containing minor amounts of uranium (and thorium), rather than on uranium minerals. This method employs mass spectrometers and involves long and tedious mineral separation, and chemical preparation. In this case microprobe analysis may be beneficial in two ways,

or rather, at two different scales. Firstly, it permits the study of the inter- and intra-grain variations of uranium-, thorium- and lead-bearing phases and thus, characterization of the various generations of a mineral species. Secondly, it may provide a very rapid method of approximate age determination using uranium- and thorium-rich minerals, such as uraninite, coffinite and thorianite. These determinations will obviously not be as precise as those made by mass-spectrometry but they may be sufficient to place an event inside a specific geological period. This latter usage is exemplified in our study of some Canadian uranium deposits discussed later in this thesis.

B. METHODS OF ANALYSIS

A number of techniques and instruments are available to study uranium bearing minerals. They can be divided into two groups.

The first requires mineral separation prior to analysis. Examples are: analysis by wet chemical techniques, X-ray fluorescence analysis, absorption and gamma-ray spectrometry, fluorimetry, neutron activation analysis; structure determination by X-ray diffraction; mineral characterization by differential thermal analysis (D.T.A.) and thermo-gravimetric analysis; isotope determination by

mass-spectrometry.

The second includes methods of in situ analysis such as optical microscopy in both reflected and transmitted light, autoradiography, radioluxography, fission track analysis, spectrometry in the optical to near infra-red wavelength region, and electron, ion and laser microprobe analysis. The latter two have not been used to date, but nevertheless remain as possibilities.

The main drawback common to the first group of techniques is the necessity for mineral separation. Indeed, uranium minerals are particularly difficult to isolate because they are often heterogeneous, fine-grained and in some cases soluble in commonly used separation liquids. Thus, many of the hexavalent uranium minerals, for example, are soluble in acetone which is commonly used to adjust the density of heavy liquids and to wash the separated aliquots. Mass-spectrometry (isotope determination) and X-ray diffraction, however, require only very small amounts of material which can often be hand selected from a crushed sample or plucked out of a rock specimen with a needle. Mass-spectrometry will usually deal only with uranium, thorium and one of their decay products and is not commonly used for complete chemical analysis. X-ray diffraction yields structural information leading to mineral identification and, in the case of simple compounds, to the determination of the ratio of the two major constituents. Uranium and/or thorium-rich minerals are often metamict as

the result of radioactivity damaging the lattice. Such minerals must be recrystallized by heating the grains to about 1000°C. When heated in this way, the final product may be chemically different from the original due to selective evaporation. Moreover, due to different conditions of crystallization, it will not necessarily be restored to its initial crystal structure.

Methods of the second group yield information of various types.

Autoradiography, radioluxography and fission track analysis are useful in locating radioactive phases, but they do not differentiate between uranium and thorium and lead only to a rough estimate of the 'richness' of a rock or mineral in radioactive constituents.

By using microscopy in reflected or transmitted light, well crystallized grains can be identified and their relationship with other constituents can be established. This method also yields a limited amount of information relative to composition. Indeed reflectance combined with micro-indentation hardness has been related to the amount of lead present in the structure of uraninite (Morton and Sassano, 1972) but this has not yet found much practical use, nor have similar experiments been carried out on other uranium and thorium minerals.

Since its introduction to the Earth Sciences around 1960, the electron microprobe has become an increasingly important tool in the study of minerals. The

capabilities of this instrument seem ideal for uranium-bearing minerals since they permit the study of small-scale chemical variations and of fine grained materials where separation is often impossible. However, a review of applications of the electron microprobe in mineralogy (Keil, 1973) shows that only very few attempts have been made to use this instrument to analyse uranium minerals. This reflects the fact that the accurate determination of uranium and thorium with the microprobe is fraught with difficulties. We have, nevertheless, chosen to explore the potential of this instrument and thus a detailed review of the difficulties encountered will be given and possible solutions discussed. The ion and laser microprobes are still rare instruments and were not available at the University of Alberta. The laser probe (Keil and Snetsinger, 1973) permits three dimensional analysis, *i.e.*, the beam can scan an area and traverse it in depth, to study for example, zoning. This can be done only at the surface with the electron microprobe. At present corrections for laser probe data are very approximate and therefore this instrument does not present any advantages over the electron microprobe. The ion probe (Andersen, 1973) gives the possibility of in situ isotopic determinations and may be very useful to study mineral growth and to date geological events. However, as in the case of the laser probe, corrections are still only approximately known, and in any case, the instrument is less applicable to simple chemical analysis and mineral

identification.

CHAPTER II

MINERALOGY OF URANIUM

To understand the problems linked with the analysis of uranium minerals, it is necessary to consider the mineralogy of uranium. Comprehensive books on this subject are those of Frondel (1958) and Heinrich (1958); a more recent summary has been tabulated by Hounsflow (1976). Because many new uranium phases have been identified since 1958, a brief updated review of the mineralogy of uranium is presented here.

Uranium minerals can be divided into ten classes (table 4, at end of chapter):

oxides

multiple oxides

arsenates and phosphates

silicates

carbonates

sulfates

vanadates

tellurites

uranium-molybdenum minerals

selenites.

Naturally occurring uranium rich carbonaceous matter has also been described.

Because the chemistry of thorium resembles that of tetravalent uranium, the tetravalent uranium minerals have thorium equivalents. The latter have been included in table 4, and in the following description.

A. OXIDES

The uranium oxides are of two types:

- 1- anhydrous i.e., uraninite (and its analogue, thorianite)
- 2- hydrous i.e., the hydrated uranyl oxides

1- ANHYDROUS OXIDES

Uraninite is essentially a tetravalent uranium oxide, having the formula UO_2 . It crystallizes in the cubic system and has a fluorite type structure; the fundamental cell is face centered with respect to the uranium ions, with the oxygen ions at $1/4$, $1/4$, $1/4$ equivalent sites.

Ramdohr (1969) has reported that many specimens of uraninite (Indus Valley, Blind River, Witwatersrand, synthetic) exhibit characteristic cleavage (111), seldom (100); but in general cleavage is not observed in natural crystals, having been destroyed by radiation effects.

Pitchblende is a descriptive name commonly used for colloform, microcrystalline uraninite.

The composition of uraninites is somewhat variable due to:

- 1- non-stoichiometry
- 2- presence of radiogenic lead
- 3- presence of elements in substitution for uranium

1- Non-stoichiometry

The variability of U/O ratio observed can be imputed to:

- 1- conditions prevailing at the time of crystallization: uraninite can crystallize in a more or less oxidized state, the degree of oxidation increasing with temperature (Berman, 1957);
- 2- self-oxidation: this is a continuous process resulting from the liberation of oxygen as uranium decays to lead, i.e.,



In $\text{UO}_{(2+x)}$, the excess oxygen is accommodated in the cubic lattice, either at position $1/2, 1/2, 1/2$ of the

cell (Alberman and Anderson, 1949), or at position $1/2, 0, 0$. In the latter case, 'normal' oxygen would be slightly displaced. The cell parameters decrease as 'x' increases. The range of 'x' for natural uraninites has not been determined but, the occurrence of $\alpha\text{-U}_3\text{O}_7$, the tetragonal equivalent of $\text{UO}_{2.33}$, has been reported (Dahlkamp and Tan, 1977). Cell dimensions and oxidation state can be correlated with the origin of the uraninite as shown in table 2.

Table 2. Averages of unit-cell dimension a_0 of untreated natural uraninites in relation to the type of occurrence. 'n' is the number of measurements used for calculation of the average. The a_0 values used to compute the average are listed in Frondel (1958) p. 24-28.

occurrence	$a_0(\text{\AA})$	n
pegmatite	5.465	59
vein	5.439	92
sediment	5.410	68

2- Radiogenic lead

This subject has been studied by Berman (1957). He showed that radiogenic lead does not replace uranium in the cubic lattice but exsolves to form orthorhombic lead monoxide. Indeed, the systematic absences of certain reflections in the X-ray pattern of some uraninites can be explained by the presence of monocellular overgrowths of PbO

on the lattice of uraninite (Berman, 1957).

3- Presence of elements in substitution for uranium.

Experimental work shows that UO_2 forms a complete solid solution with ThO_2 (Lambertson et al., 1953), CeO_2 (Fronzel, 1958), PrO_2 (Fronzel, 1958) and partial solid solution with CaO (Alberman et al., 1951), ZrO_2 (Lambertson and Mueller, 1953), Y_2O_3 (Olds, 1961) and Nd_2O_3 (Lang et al., 1956). Th, Ca, Ce, Y, Zr and Nd are thus expected to substitute for uranium in uraninites; Other rare-earths will probably enter the uraninite lattice also. These elements are abundant in high temperature uraninites (pegmatites) but absent, or nearly so, in low temperature uraninites (veins and sediments).

Elements such as Na, Bi, Zn, Cu, Mn, K, Al and Si have been reported in chemical analyses; but they might be present only as inclusions or veinlets, particularly in pitchblende which often shows fine syneresis cracks filled by 'impurities' such as quartz, calcite, hematite and galena (Geffroy and Sarcia, 1960; Fronzel, 1958).

Thorianite is the Th equivalent of uraninite with the formula ThO_2 . It generally contains U, REE and radiogenic Pb.

Compositions ranging from UO_2 to ThO_2 have been found for minerals from pegmatites; the name uranothorianite has been proposed for compositions intermediate between

uraninite and thorianite (Wells et al., 1933).

2- HYDROUS OXIDES

Hydrated uranium oxides are hexavalent uranium compounds, and have no naturally occurring thorium equivalents.

Their investigation has been made difficult by their degree of hydration and the difficulties of obtaining crystals of reasonable size. As a result, the compositions and structures of some of these oxides are poorly known.

Cations other than uranium are present as major constituents in many of the species.

Some of the hydrated oxides may be grouped together on the basis of structural similarities. They are designated here as the fourmarierite group which comprises: agrinierite, becquerelite, billielite, compregnacite, epi-ianthinite, fourmarierite, masuyite, schoepite, vandendriesscheite, metavandendriesscheite, wölsendorffite and, probably, bauranoite, calciouranoite, and metacalciouranoite.

Rameauite, roubaultite curite and vandenbrandeite do not appear to be mutually related nor related to any of the other hydrates.

Clarkeite, hydronasturan, richetite, uranosphaerite, and urgite are ill-defined. Gummite is a

generic name which applies to the alteration products of uraninite.

Fourmarierite group

Common properties of the minerals gathered in this group are (Sobry, 1971; Brasseur and Potdevin, 1960):

- crystallization in the orthorhombic system
- existence of a pseudo-hexagonal sublattice with approximate dimensions:

$$a' = 7.06 \text{ \AA}$$

$$b' = 4.08 \text{ \AA}$$

$$c' = 7.32 \text{ \AA}$$

- small $2V_x$ angle
- perfect (001) cleavage

The existence of a pseudo-hexagonal sublattice for bauranoite calciouranoite and metacalciouranoite is not certain. These were nevertheless included in the fourmarierite group on the basis of similarities with wölsendorffite (Rogova et al., 1973) and general agreement with the chemical formulae and properties of the minerals of this group, including similarity of the X-ray patterns (the ten strongest powder lines are given in Rogova et al. (1973) for bauranoite and metacalciouranoite and in Rogova et al. (1974) for calciouranoite.)

Detailed investigation of minerals of this group and some synthetic analogues have been carried out by Brasseur and Potdevin (1960), Christ and Clark (1960) and,

by Sobry (1971, 1973 a,b). It was shown that divalent and monovalent cations replace water continuously in the lattice. The following formulae were deduced:

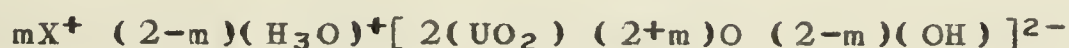


where X is a divalent cation and m ranges from 0 to 2, and:

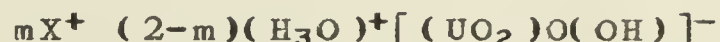


where X is a monovalent cation and m ranges from 0 to 2.

Brasseur (1962) has interpreted this replacement of water by postulating the presence of oxonium; the above general formulae thus became (Sobry, 1971):



for uranates of divalent cations, where n ranges from 0 to 2, and:



for uranates of monovalent cations, where m ranges from 0 to 2 (Sobry, 1971).

The presence of water in the form of oxonium and hydroxyl ions was further substantiated by Sobry and Rinne (1973) by means of NMR powder spectra.

Of this group, only the structure of becquerelite has been well determined. In becquerelite, uranyl ions are pentacoordinated to oxygen atoms to form sheets parallel to (001). The water of hydration is located between the (001) layers. Biellietite is isostructural with the above. (Courtois, 1968). Similarly, in other minerals of the

fourmarierite group, with the exception of masuyite ($\text{UO}_3 \cdot 2\text{H}_2\text{O}$) the uranyl ion is probably in five-fold coordination with oxygen. In masuyite, it appears to be in six-fold coordination (Sobry, 1971, 1973b; Christ and Clark, 1960)

Other hydrated uranium oxides

Curite and roubaultite are orthorhombic, rameauite is monoclinic and vandenbrandite is triclinic.

Courtois (1968) has shown that the lattice of curite is dominated by sheets parallel to (100). These sheets are made of uranyl ions in four and in five-fold coordination with oxygen. The presence of oxonium was not demonstrated.

Gummite

The term gummite is often used for any fine-grained, yellow to orange, 'uranium coloured' mineralization. It is not a mineral but a suite of alteration products which follows, more or less, this sequence:

- 1- a uraninite ore
- 2- an inner zone chiefly formed of lead uranyl oxides, resulting from the oxidation of uranium and its selective leaching relative to lead. This constitutes the traditional gummite.
- 3- an outer uranium silicate zone formed by the

reaction of the hydrated oxides with meteoric or possibly hydrothermal waters carrying silica and calcium. The carbonate rutherfordine is sometimes admixed with the silicates. Thorium and rare-earths, if contained in the original uraninite, are usually wholly removed during the formation of the silicates (Fronzel, 1956).

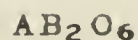
- 4- a fourth zone made of uranium phosphates may also occur (Protas, 1959).

B. MULTIPLE OXIDES

The better defined uranium and thorium multiple oxides are the members of the columbite group and those of the pyrochlore group. Others cannot be related to any group of minerals of essentially non-radioactive elements, they are: brannerite, thorutite, kobeite, zirkelite and davidite.

Columbite group

Minerals of the columbite group have the general formula:



where A is mainly occupied by Fe and Mn in variable proportions, but Y, U, Th and REE may be present.

B is Nb and Ta in variable proportions.

All are orthorhombic. Yttrotantalite and yttrocolumbite are commonly uranium rich.

Pyrochlore group

Minerals of the pyrochlore group have the general formula:



where A can be one or more of the following: Na, Ca, U, Ba, Pb;

and B is Nb, Ta and Ti in variable proportions.

Names given to the different varieties of the pyrochlore group are listed below (table 3). Betafite, tantalobetafite and titanobetafite are uranium rich varieties; all three are commonly designated as betafite. Obruchevite, tantalobruchevite and titano-obruchevite are also commonly uranium-rich.

The minerals of the pyrochlore group crystallize in the cubic system.

Others

Brannerite, thorutite, kobeite, zirkelite and davidite are generally metamict. For identification by X-ray diffraction they have to be recrystallized at temperatures between 900 and 1200°C. Recrystallized natural brannerite and thorutite as well as synthetic polymorphs have been studied by Pasbt (1954), Ostunali (1959), Patchett and

Table 3. Varieties of pyrochlore, from Tröger (1967),

A:B	Nb	Ta	Ti
Na+Ca	pyrochlore	microlite	titanopyrochlore
>15%U	betafite	tantalo- betafite	titano- betafite
Y	obruchevite	tantalo- obruchevite	titano- obruchevite
Ba(+Sr)	pandaite	rykeboerite	
Pb		Pb-microlite	

Nuffield (1960), Perez y Jorba et al. (1961), Adler and Puig (1961), and Ruh and Wadsley (1966); kobeite has been studied by Hutton (1957). It is not certain whether any of the various structures presented, all obtained on high temperature phases, correspond to the naturally occurring minerals of similar composition which are found mostly in low temperature environments (at any rate, lower than 1000°C). All but davidite have well-defined chemical formulae.

C. ARSENATES AND PHOSPHATES

Because many uranium arsenates and uranium phosphates are isostructural, the phosphates and arsenates will be reviewed as a single class. According to their composition and structure, they can be divided into three groups:

- the so-called uranium micas or torbernite group

1- phosphuranylite group

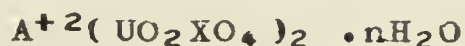
2- rhabdophane group.

Other, isolated species are: coconinoite, dumontite and walpurgite.

Uranium micas

The uranium micas are by far the best known uranyl minerals. Comprehensive studies have been made by Ross et al . (1964), Ross and Evans (1964, 1965), and Walenta (1965a).

The micas are characterized by the general formula:



where X is P or As or a mixture of both,

and A can be any one (or more) of the following:

Na₂, K₂, (NH₄)₂, (H₃O₂), Mg, Co, Fe, Cu, Ba, UO₂ and (HAl_{0.5})

All are tetragonal with perfect (001) cleavage, hence the name 'mica'. They also have significant cation exchange capacities. Their lattices are dominated by infinite sheets of (UO₂PO₄)₂⁻² or (UO₂AsO₄)₂⁻² parallel to (001). These sheets consist of uranyl ions coordinated by four oxygen atoms to four different PO₄⁻³ (or AsO₄⁻³) tetrahedra. The sheets are puckered with uranyl ions displaced upward and downward from the plane of the P or As atoms. In the fully hydrated species, adjacent sheets are related to each other

by a mirror plane lying halfway between the uranyl ions and perpendicular to the c-axes, thus leaving large cavities between the sheets. Translation of the sheets with respect to one another by a vector $(1/2, -1/2, 0)$ reduces the minimum distance between them and accounts for the loss of water.

The dimensions of the c-axes typify the different species. The unit-cell sizes of the phosphates are smaller than their arsenate equivalents. Moreover, the c-axes vary stepwise with the amount of interlayered water and, to a lesser extent, with the interlayered cations.

The exact amount of water for every species is not known accurately but as a whole it can be related to the valencies and ionic radii of the cations. According to Walenta (1965a), the water contents of the holohydrated phases are:

- 1- 10 to 12 for divalent cations i.e., 12 for the cations of small ionic radius such as Cu, Mg, Fe and Co; 10 for cations of larger radius such as Ca and Ba.
- 2- 6 for monovalent cations of large ionic radius like K and NH_3 .

These generalisations are valid for both arsenates and phosphates with the exception of barium uranyl phosphate which hosts 12 water molecules per unit cell.

The nomenclature of uranium micas takes account of

the different degrees of hydration in the following manner
(Ross and Evans, 1965):

- 1- "If only one hydrate is known, no prefix or Roman numeral will be used in the mineral name".
- 2- "If two hydrates are known, the lower hydrate will have the prefix "meta" attached to the mineral name".
- 3- "If three or more hydrates are known, the highest hydrate will have the prefix "meta" attached to the name, and the Roman numerals will in increasing order designate progressively lower hydration states".

This use of the prefix meta extends to all uranyl minerals.

Rhaphdophane group

Among uranium minerals, the rhaphdophane group includes: brockite, grayite, ningyoite and possibly the ill-defined lermontovite. These have the general formula:

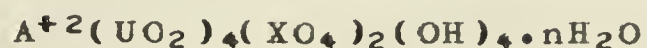


where A is two or more of the following: Ca, Th, U, and REE.

Ningyoite and grayite are orthorhombic (pseudo-hexagonal) and brockite is hexagonal (like rhaphdophane)

Phosphuranylite group

This group comprises four structural analogues, namely: phosphuranylite, arsenuranylite, renardite and bergenite. They are orthorhombic and have the general formula:



where X is either P or As;

and A is Ca, Ba or Pb.

Others

Walpurgite is a bismuth uranyl arsenate; it crystallizes in the triclinic system. Its phosphorus analogue has been described but not named (Soboleva and Pudovkina, 1957).

Dumontite is an orthorhombic lead uranyl phosphate and coconinoite is an iron-aluminium uranyl sulfo-phosphate, and is possibly monoclinic.

D. SILICATES

The silicate minerals comprise two important groups, namely:

- 1- thorite group: thorite, coffinite, and thorogummite

2- uranophane group: uranophane, barium-uranophane, boltwoodite, sodium-boltwoodite, sklodowskite, cuprosklodowskite and kasolite.

in addition to huttonite and β -uranophane, which are polymorphs of thorite and uranophane respectively, and six other species: haiweeite, metahaiweeite, ranquillite, soddyite, ursilite and weeksite.

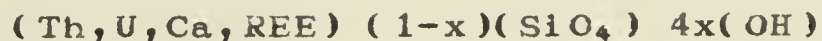
Thorite group

Minerals of the thorite group are tetragonal and isostructural with zircon (Fuchs and Hoestra, 1959). They are orthosilicates with the general formula:



where M can be one or more of: Th, U, Ca, and REE.

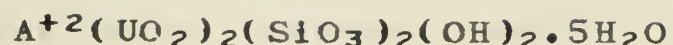
The M cation is mainly U in coffinite, and Th in thorogummite; Ca and REE are usually also present. Both minerals are hydrous due to the replacement of part of the silica by hydroxyl, thus leading to the formula:



Thorite and its polymorph huttonite are 'pure' thorium orthosilicates; huttonite is monoclinic and isostructural with monazite.

Uranophane group

Minerals of this group have the general formula:



where A can be: Ca, Ba, Cu, Pb, K₂ or Na₂.

They are monoclinic or perhaps orthorhombic in the case of boltwoodite and metaboltwoodite; they exhibit perfect (100) cleavage.

Their structure consists of chains of edge-shared (UO₄)O₅ dipyramids and SiO₄ tetrahedra. The chains are cross-linked by corner sharing to form (UO₂SiO₄)⁻² layers parallel to (100). Ca, other cations and water are located between the layers. The chain structure accounts for the common acicular habit of uranophane and its analogues.

β-uranophane is also made of chain-nuilt layers (UO₂SiO₄)⁻² but the uranium-oxygen and silica-oxygen polyhedra are oriented differently (Smith and Stohl, 1972). It is not known what natural conditions favour the formation of β-uranophane rather than uranophane.

Others

Haiweeite and metahaiweeite have essentially the same chemical formula, exept that metahaiweeite is less hydrated; both are monoclinic.

Ranquillite, soddyite, ursilite and weeksite are all orthorhombic, but each has a chemical formula which cannot be related to any other known uranium silicate.

E. CARBONATES

All uranium carbonates, except wyartite, contain uranium as the uranyl ion and all but sharpite and rutherfordine have other cations than uranium and carbon as major constituents. On the basis of chemical formulae, one series can be distinguished: the tricarbonates,

Tricarbonate series

This series is characterized by the general formula:



where A^{+2} is one or two of the following: Na_2 , Ca , K_2 or Mg .

Its members are: andersonite, bayleyite, grimselite, liebigite, rabbittite, and swartzite. Structural relations between the above are not known. Only liebigite, has been the subject of a detailed structural analyses.

Study of synthetic liebigite has shown it to crystallize in the orthorhombic system. Its "structure consists of discrete $(UO_2(CO_3)_3)^{4-}$ complexes in which three CO_3^{2-} groups lie in a plane perpendicular to the linear UO_2^{+2} ion; these planes are all nearly parallel to (100) and tilted about 45° with respect to (001). Calcium ions bond the complexes together into slablike units parallel to (010), between which water molecules are packed" (Appleman, 1956). This description leaves something to be desired since

"planes nearly parallel to (100) and tilted about 45° with respect to (001)" cannot occur in the orthorhombic system.

Others

Rutherfordine is orthorhombic and consists of layers of uranyl ions bonded in six-fold coordination with three CO₃ triangles. It is anhydrous. Wyartite is orthorhombic; it contains both tetra- and hexavalent uranium. The $U^{6+}:(UO_2)^{4+}$ ratio appears to alter rapidly in normal P,T conditions (Clark, 1960). Zellerite and metazellerite are orthorhombic calcium dicarbonates. Voglite, sharpite and studtite are ill-defined. Schroeckingerite is triclinic and commonly exhibits perfect 'micaceous' (001) cleavage. Its water content is variable (Smith, 1959).

F. SULPHATES

In the past many names have been proposed to designate uranium sulfates but only three of these substances have been adequately determined: johannite, zippeite, uranopilite (and possibly meta-uranopilite), (Fronzel 1952). Structural data on these minerals are scarce. Only the structure of johannite has been described.

Johannite crystallizes in the triclinic system.

Uranyl ions are pentacoordinated and sulfur ions are tetracoordinated. Each uranyl is bonded to three oxygens from different sulfate groups and each sulfate shares oxygen atoms with three uranyl ions; the endless chains parallel to (001), are apparently linked by pairs of $(OH)^-$ ions shared between two uranyl ions. The resulting structure consists of infinite sheets parallel to (001) cross-linked by copper atoms bonded to the fourth sulfate oxygen (Appleman, 1957).

For some time, the name zippeite was applied to a number of hydrated uranium sulphates. As suggested by Frondel (1958), the name zippeite proper is restricted to a particular mineral from Joachimsthal, Bohemia, which is orthorhombic and has the composition: $2UO_3 \cdot SO_3 \cdot 5H_2O$ or near thereto (Frondel, 1952).

Analysis of material from the type locality shows calcium; the content from six analyses ranges from 0 to 4.13% CaO (Frondel, 1958). This might be attributed to contamination of zippeite by gypsum.

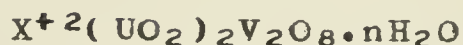
Uranopilite is monoclinic; the identity of a partly dehydrated species, meta-uranopilite, remains uncertain (Frondel, 1952).

G. VANADATES

Among the uranium vanadates, uvanite and rauvite are ill-defined. All other known minerals of uranium and vanadium fall into the carnotite group.

Carnotite group

This group is characterized by the general formula:



where X can be K₂, Ca, Ba, Cu or (AlOH).

Its members are either orthorhombic or monoclinic. Their crystal structures are known from the study of synthetic anhydrous carnotite and its cesium analogue by Appleman and Evans (1965).

Each vanadium atom is surrounded by five oxygen atoms in the form of a tetragonal pyramid. Pairs of such coordination polyhedra, with their apices pointing in opposite directions, share an edge to form $V_2O_8^{6-}$ 'divanadate' groups. The linear uranyl ion is also surrounded by five oxygen atoms in the form of a plane pentagon which shares edges with adjacent divanadate groups and uranyl coordination groups, to form infinite sheets of $[(UO_2)_2V_2O_8]^{-2}$ parallel to (001). The sheets are linked together by potassium or other cations such as Cs in the synthetic Cs-carnotite or Ca, Ba, Cu, and (AlOH) in known

minerals. Water molecules are located between the [001] layers.

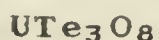
Like the uranium micas, carnotite and its analogues exhibit perfect [001] cleavage and their unit cell dimension in the z-direction is related to the number of interlayered water molecules. They also have significant cation exchange capacities.

H. TELLURITES

Three uranium tellurites have been described. All are from the Se-Au deposits of Moctezuma, Mexico. In contrast with uranyl minerals of other classes, the known uranyl tellurites are neither hydrous nor hydrated.

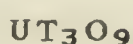
Moctezumite is a monoclinic lead uranyl tellurite.

Schmitterite and cliffordite contain only uranium and tellurium as major cations. The former crystallizes in the orthorhombic system and the latter, in the cubic system. The chemical formula proposed initially for cliffordite is (Gaines, 1969):



where both uranium and tellurium are tetravalent.

A refinement of the structure (Galy and Meunier, 1971) shows that:



where uranium is hexavalent and tellurium tetravalent, is more appropriate.

The structure of cliffordite consists of dipyramids of hexacoordinated uranyl ions linked to TeO_4^{2-} tetrahedra; cationic planes of $(\text{Te}+\text{U})$ and of Te alternate parallel to $[100]$, (Galy and Meunier, 1971).

In schmitterite, the uranyl ions are coordinated to five oxygen ions, and tellurium is bonded to four oxygen ions. The pentagonal dipyramids (UO_7) are linked side by side to form $[\text{n}(\text{UO}_5)^{4-}]$ chains elongated in the (100) direction. Tellurium bonds the chains in the (100) plane. (Structural data are from Meunier and Galy (1973) but the crystallographic axes are those chosen by Gaines (1971) in reference to the conventional orthorhombic cell). Schmitterite exhibits a good (100) cleavage.

I. URANIUM-MOLYBDENUM MINERALS

Six uranium-molybdenum minerals have been reported. Five of them, sedovite, mourite, iriginite, umohoite and moluranite contain no cations other than uranium and molybdenum; calcurmolite combines calcium with molybdenum and uranium.

The chemical formulae of these minerals are difficult to ascertain and, except for umohoite, they are

ill-defined. The difficulty arises from the coexistence of multivalent elements namely uranium (+4,+6) and molybdenum (+5,+6); their oxidation state cannot be derived from quantitative chemical analyses because it is not known, in most cases, how essential oxygen present as O^{-2} and possibly also as $(OH)^{-1}$ is shared between the the uranium and molybdenum cations.

Deliens (1975) reported a calcium-magnesium-uranium-molybdenum mineral which might be a new species.

J. SELENITES

Four uranium selenites have been described. All were found in the oxidation zone of the Musonoi Cu-Co deposit in Shaba, Zaire.

In these minerals, water and cations such as Ba, Cu, and Pb occur with hexavalent uranium and selenium. The minerals appear structurally unrelated to each other though three of them, derricksite, guilleminite and marthosite crystallize in the orthorhombic system; demesmaeckerite is triclinic.

K. CARBONACEOUS MATERIALS

The materials carburan, sogrenite and thucholite are not minerals but uranium-rich carbonaceous matter of indefinite composition.

These substances are more or less oxidized and more or less polymerized hydrocarbon. Aside from the major constituents, carbon and uranium, they may host thorium, REE and vanadium (Geffroy and Sarcia, 1960). In particular cases where the uranium content is high, microscopic examination of polished section permits the distinction of fine particles of uraninite in the carbonaceous matter (Davidson and Bowie, 1951; Schidlowski, 1966c). Heavy liquid separation allowed Nekrasova, (1958) to recover a heavy fraction which yielded an X-ray pattern similar to that of uraninite. It thus appears that, in most cases, uranium in carbonaceous matter occurs as uraninite rather than as a uranium-carbon complex.

The name thucholite is mainly used for material found in pegmatitic dykes; it contains Th, U, C, O and H.

Table 4. List of uranium minerals (reference number and corresponding author(s) are listed in table 5).

Name	Formula*	References
ARSENATES		
abernathyite	$K_2(UO_2)_2(AsO_4)_2 \cdot 8H_2O$	32, 33, 69
arsenuranylite	$Ca(UO_2)_4(AsO_4)_2 \cdot 6H_2O$	4
hallimondite	$Pb_2(UO_2)(AsO_4)_2$	84, 85
heinrichite	$Ba(UO_2)_2(AsO_4)_2 \cdot 10-12H_2O$	46
hügelite	$Pb_2(UO_2)_3(AsO_4)_2(OH) \cdot 3H_2O$	86
kahlerite	$Fe(UO_2)_2(AsO_4)_2 \cdot nH_2O$	32
metaheinrichite	$Ba(UO_2)_2(AsO_4)_2 \cdot 8H_2O$	46
metakahlerite	$Fe(UO_2)_2(AsO_4)_2 \cdot 8H_2O$	82
metakircheimerite	$Co(UO_2)_2(AsO_4)_2 \cdot 8H_2O$	32, 83
metalodevite	$Zn(UO_2)_2(AsO_4)_2 \cdot 10H_2O$	2
metanovacekite	$Mg(UO_2)_2(AsO_4)_2 \cdot 4-8H_2O$	82
meta-uranospinite	$Ca(UO_2)_2(AsO_4)_2 \cdot 8H_2O$	82
metazeunerite	$Cu(UO_2)_2(AsO_4)_2 \cdot 8H_2O$	32, 33
novacekite	$Mg(UO_2)_2(AsO_4)_2 \cdot 12H_2O$	32, 33
sodium-uranospinite	$(Na_2, Ca)(UO_2)_2(AsO_4)_2 \cdot 5H_2O$	52
troegerite	$(UO_2)_3(AsO_4)_2 \cdot 12H_2O$	32, 33, 84
uranospinite	$Ca(UO_2)_2(AsO_4)_2 \cdot 10H_2O$	32, 33, 52
walpurgite	$(BiO)_4(UO_2)(AsO_4)_2 \cdot 3H_2O$	32, 33
zeunerite	$Cu(UO_2)_2(AsO_4)_2 \cdot 10-16H_2O$	32, 38

* When available, the formulae came from Fleischer (1975)

Table 4 cont'd.....

CARBONATES

andersonite	$\text{Na}_2\text{Ca}(\text{UO}_2)(\text{CO}_3)_3 \cdot 6\text{H}_2\text{O}$	32, 33
bayleyite	$\text{Mg}_2(\text{UO}_2)(\text{CO}_3)_3 \cdot 18\text{H}_2\text{O}$	32, 33
dakeite	synonym of schoeckingerite	32
diderichite	synonym of rutherfordine	32
grimselite	$\text{K}_3\text{Na}(\text{UO}_2)_{23} \cdot \text{H}_2\text{O}$	86
liebigite	$\text{Ca}_2\text{U}(\text{CO}_3)_4 \cdot 10\text{H}_2\text{O}$	32, 33
mckelveyite	$(\text{Na}, \text{Ca})(\text{Ba}, \text{Y}, \text{U})_2(\text{CO}_3)_3 \cdot \text{H}_2\text{O}$	24, 55
metazellerite	$\text{Ca}(\text{UO}_2)(\text{CO}_3)_2 \cdot 3\text{H}_2\text{O}$	22
neogastunite	synonym of schroeckingerite	32
rabbittite	$\text{Ca}_3\text{Mg}_3(\text{UO}_2)_2(\text{CO}_3)_6(\text{OH})_4 \cdot 18\text{H}_2\text{O}$	32, 33
rutherfordine	$\text{UO}_2(\text{CO}_3)$	32, 33
schroeckingerite	$\text{NaCa}_3(\text{UO}_2)(\text{CO}_3)_3(\text{SO}_4)\text{F} \cdot 10\text{H}_2\text{O}$	75
sharpite	$(\text{UO}_2)(\text{CO}_3) \cdot \text{H}_2\text{O} (?)$	33
swartzite	$\text{CaMg}(\text{UO}_2)(\text{CO}_3)_3 \cdot 12\text{H}_2\text{O}$	32, 33
voglite	$\text{Ca}_2\text{Cu}(\text{UO}_2)(\text{CO}_3)_4 \cdot 6\text{H}_2\text{O} (?)$	32
wyartite	$\text{Ca}_3\text{U}^{+4}(\text{UO}_2)_6(\text{CO}_3)_2(\text{OH})_{16}$ $\cdot 3-5\text{H}_2\text{O}$	21, 47
zellerite	$\text{Ca}(\text{UO}_2)(\text{CO}_3)_2 \cdot 5\text{H}_2\text{O}$	22, 45

HYDRATED OXIDES

agrinierite	$(\text{K}_2, \text{Ca}, \text{Sr})\text{U}_3\text{O}_{10} \cdot 4\text{H}_2\text{O}$	16
bauranoite	$\text{BaU}_2\text{O}_7 \cdot 4-5\text{H}_2\text{O}$	66

Table 4 cont'd.....

becquerelite	$\text{CaU}_6\text{O}_{19} \cdot 11\text{H}_2\text{O}$	20, 32, 33
billietite	$\text{BaU}_6\text{O}_{19} \cdot 11\text{H}_2\text{O}$	20, 32, 33
calciouranite	$(\text{Ca}, \text{Ba}, \text{Pb})\text{U}_2\text{O}_7 \cdot 5\text{H}_2\text{O}$	67
clarkeite	$(\text{Na}, \text{Ca}, \text{Pb})_2\text{U}_2(\text{O}, \text{OH})_7$	32, 33
compreignacite	$\text{K}_2\text{U}_6\text{O}_{19} \cdot 11\text{H}_2\text{O}$	64
curite	$\text{Pb}_2\text{O}_5\text{O}_{17} \cdot 4\text{H}_2\text{O}$	32, 33
epi-ianthinite	variety of schoepite	
fourmarieite	$\text{PbU}_4\text{O}_{13} \cdot 4\text{H}_2\text{O}$	20, 32, 33
hydronasturan	$\text{UO}_2 \cdot 2.3-5\text{UO}_3 \cdot 7\text{H}_2\text{O}$	41
ianthinite	$\text{UO}_2 \cdot 5\text{UO}_3 \cdot 10\text{H}_2\text{O}$	32, 33
masuyite	$\text{UO}_3 \cdot 2\text{H}_2\text{O} (?)$	20, 32, 33
metacalciouranite	$(\text{Ca}, \text{Na}, \text{Ba}, \text{Pb}, \text{K})\text{U}_2\text{O}_7 \cdot 1.7\text{H}_2\text{O}$	66
meta-		
vandendriesscheite	$\text{PbU}_7\text{O}_{22} \cdot n\text{H}_2\text{O}$	20
paraschoepite	variety of schoepite	
rameauite	$\text{K}_2\text{CaU}_6\text{O}_{20} \cdot 9\text{H}_2\text{O}$	16
richetite	hydrated Pb, U oxide	32
roubaultite	$\text{Cu}_2(\text{UO}_2)_3(\text{OH})_{10} \cdot 5\text{H}_2\text{O}$	14
schoepite	$\text{UO}_3 \cdot 2\text{H}_2\text{O}$	20
unnamed	$\text{PbU}_2\text{O}_7 \cdot n\text{H}_2\text{O}$	25
uranosphaerite	$\text{Bi}_2\text{U}_2\text{O}_9 \cdot 3\text{H}_2\text{O}$	20
urgite	$\text{UO}_3 \cdot n\text{H}_2\text{O}$	46
vandendriesscheite	$\text{PbU}_7\text{O}_{22} \cdot 12\text{H}_2\text{O}$	20
vandenbrandeite	$\text{Cu}(\text{UO}_2)_2 \cdot 2\text{H}_2\text{O}$	32, 33
wölsendorffite	$(\text{Pb}, \text{Ca})\text{U}_2\text{O}_7 \cdot 2\text{H}_2\text{O}$	63

Table 4 cont'd.....

MOLYBDATES		
calcurmolite	$\text{Ca}(\text{UO}_2)_3(\text{MoO}_4)_3(\text{OH})_2 \cdot 11\text{H}_2\text{O}$	71
iriginite	$\text{U}(\text{MoO}_4)_2(\text{OH})_2 \cdot 2\text{H}_2\text{O}$	26, 79
moluranite	$\text{UO}_2 \cdot 3\text{UO}_3 \cdot 7\text{MoO}_3 \cdot 20\text{H}_2\text{O}$	26, 42, 78
mourite	$4(\text{U}^{6+}\text{O}_2) \cdot 2\text{Mo}^{5+}\text{O}_2(\text{OH})_2$ $\quad \quad \quad \cdot \text{Mo}^{6+}\text{O}_2(\text{OH})_2$ or $4(\text{U}^{4+}\text{O}_2 \cdot 5\text{Mo}^{6+}\text{O}_2(\text{OH})_2$	
sedovite	$\text{U}(\text{MoO}_4)_2$	74
umohoite	$\text{UO}_2 \cdot \text{MoO}_4 \cdot 2-4\text{H}_2\text{O}$	48, 50
OXIDES		
absite	synonym of brannerite	
betafite	$(\text{Ca}, \text{Na}, \text{U})_2(\text{Nb}, \text{Ta})_2\text{O}_6(\text{OH})$	32, 33, 80
brannerite	UTi_2O_6	32, 33, 62
broggerite	synonym of uraninite	
cleveite	synonym of uraninite	
davidite	$(\text{U}, \text{Fe}^{2+}, \text{Ca}, \text{La})_6(\text{Ti}, \text{Fe}^{3+})_{15}$ $\quad \quad \quad (\text{O}, \text{OH})_{36}$	32, 33
ferutite	synonym of davidite	42, 52
gummite	generic term	30, 32
kobeite	$(\text{Y}, \text{U})(\text{Ti}, \text{Nb})_2(\text{O}, \text{OH})_6$	58
lodochnikite	synonym of brannerite	42, 62, 78
obruchevite	$(\text{Y}, \text{Na}, \text{Ca}, \text{U})(\text{Nb}, \text{Ta}, \text{Ti}, \text{Fe})_2$ $\quad \quad \quad (\text{O}, \text{OH})_7$	42, 80
parapitchblende	synonym of uraninite	
pitchblende	synonym of uraninite	

Table 4 cont'd.....

samarskite	$(Y, Ce, U, Ca, Pb)(Nb, Ta, Sn)_2O_6$	44, 62
samieresite	synonym of betafite (?)	43
thorianite	ThO_2	32, 33
thorutite	$(Th, U, Ca)_2Ti_2(O, OH)_6$	44, 62
uferite	synonym of davidite	42, 78
ulrichite	synonym of uraninite	
uraninite	UO_2	32, 33
uranothorianite	variety of thorianite	32
yttrocolumbite	$(Y, U, Fe)(Nb, Ta)O_6$	53
yttrotantalite	$(Y, U, Fe)(Ta, Nb)O_6$	53
zirconolite	synonym of zirkelite	65
zirkelite	$(Ca, Th, REE)Zr(Ti, Nb)_2O_7$	65

PHOSPHATES

autunite	$Ca(UO_2)_2(PO_4)_2 \cdot 10-12H_2O$	32, 33
bassetite	$Fe(UO_2)_2(PO_4)_2 \cdot 8H_2O$	32, 33
bergenite	$Ba(UO_2)_4(PO_4)_2(OH)_4 \cdot 8H_2O$	8
brockite	$(Ca, Th, Ce)PO_4 \cdot 2H_2O$	29
coconinoite	$Fe_2Al_2(UO_2)(PO_4)_4(SO_4)(OH)_2 \cdot 20H_2O$	87
dewindtite	synonym of renardite (?)	32
dumontite	$Pb_2(UO_2)_3(PO_4)_2(OH)_4 \cdot 3H_2O$	32, 33
eyletterite	$(Th_{0.5}Al_{3.5})[(PO_4)(SiO_4)]_2(OH)_6 (?)$	81

Table 4 cont'd.....

grayite	$(\text{Th}, \text{Pb}, \text{Ca})\text{PO}_4 \cdot \text{H}_2\text{O}$	32, 33
lermontovite	$(\text{U}, \text{Ca}, \text{REE})_3\text{PO}_4 \cdot 6\text{H}_2\text{O}$	42, 78
meta-ankoleite	$\text{K}_2(\text{UO}_2)_2(\text{PO}_4)_2 \cdot 6\text{H}_2\text{O}$	38
meta-autunite	$\text{Ca}(\text{UO}_2)_2(\text{PO}_4)_2 \cdot 2-6\text{H}_2\text{O}$	32, 33, 68
metatorbernite	$\text{Cu}(\text{UO}_2)_2(\text{PO}_4)_2 \cdot 8\text{H}_2\text{O}$	32, 33, 70
meta-uranocircite	$\text{Ba}(\text{UO}_2)_2(\text{PO}_4)_2 \cdot 8\text{H}_2\text{O}$	32, 33
ningyoite	$(\text{U}, \text{Ca}, \text{Ce})(\text{PO}_4)_2 \cdot 1-2\text{H}_2\text{O}$	56
parsonite	$\text{Pb}_2(\text{UO}_2)_2(\text{PO}_4)_2 \cdot \text{H}_2\text{O}$	32, 33
phosphuranylite	$\text{Ca}(\text{UO}_2)_2(\text{PO}_4)_2 \cdot 7\text{H}_2\text{O}$	32, 333
przhevalskite	$\text{Pb}(\text{UO}_2)_2(\text{PO}_4)_2 \cdot 4\text{H}_2\text{O}$	42, 78
pseudoautunite	$(\text{H}_3\text{O})_4\text{Ca}_2(\text{UO}_2)_2(\text{PO}_4)_4 \cdot 5\text{H}_2\text{O} ?$	73
renardite	$\text{Pb}(\text{UO}_2)_4(\text{PO}_4)_2(\text{OH})_4 \cdot 7\text{H}_2\text{O}$	32, 33
sabugalite	$\text{HAl}(\text{UO}_2)_4(\text{PO}_4)_4 \cdot 16\text{H}_2\text{O}$	32, 33
salleeite	$\text{Mg}(\text{UO}_2)_2(\text{PO}_4)_2 \cdot 8\text{H}_2\text{O}$	32
sodium-autunite	$\text{Na}_2(\text{UO}_2)_2(\text{PO}_4)_2 \cdot 8\text{H}_2\text{O}$	18
torbernite	$\text{Cu}(\text{UO}_2)_2(\text{PO}_4)_2 \cdot 8-12\text{H}_2\text{O}$	32, 33
unnamed	$\text{Bi}_4(\text{UO}_2)_2(\text{PO}_4)_2 \cdot 3\text{H}_2\text{O}$	78
unnamed	$(\text{UO}_2)_3(\text{PO}_4)_2 \cdot 12\text{H}_2\text{O}$	6
uramphite	$(\text{NH}_4)(\text{UO}_2)(\text{PPG}_4) \cdot \text{H}_2\text{O}$	57
uranosphatite	$\text{Ca}(\text{UO}_2)_2(\text{AsO}_4)_2 \cdot 10\text{H}_2\text{O}$	32, 33
SULFATES		
johannite	$\text{Cu}(\text{UO}_2)_2(\text{SO}_4)_2(\text{OH})_2 \cdot 6\text{H}_2\text{O}$	32, 33
peligotite	synonym of johannite (?)	32

Table 4 cont'd.....

uranopilite	$(\text{UO}_2)_6(\text{SO}_4)(\text{OH})_{10} \cdot 12\text{H}_2\text{O}$	32, 33
zippeite	$(\text{UO}_2)_2(\text{SO}_4)(\text{OH})_2 \cdot 4\text{H}_2\text{O} (?)$	31, 32, 33
SELENITES		
demesmaekerite	$\text{Pb}_2\text{Cu}_5(\text{UO}_2)_2(\text{SeO}_3)_6(\text{OH})_6 \cdot 2\text{H}_2\text{O}$	12
derriksite	$\text{Cu}_4(\text{UO}_2)(\text{SeO}_3)_2(\text{OH})_3 \cdot \text{H}_2\text{O}$	15
guilleminite	$\text{Ba}(\text{UO}_2)_3(\text{SeO}_3)_2(\text{OH})_4 \cdot 3\text{H}_2\text{O}$	60
marthozite	$\text{Cu}(\text{UO}_2)_3(\text{SeO}_3)_3(\text{OH})_2 \cdot 7\text{H}_2\text{O}$	13
SILICATES		
barium-uranophane	$\text{Ba}(\text{UO}_2)_2(\text{SiO}_3)_2(\text{OH})_2 \cdot 5\text{H}_2\text{O}$	5
beta-uranophane	$\text{Ca}(\text{UO}_2)_2(\text{Si}_2\text{O}_7) \cdot 6\text{H}_2\text{O}$	32, 33, 79
boltwoodite	$\text{K}_2(\text{UO}_2)_2(\text{SiO}_3)_2(\text{OH})_2 \cdot 5\text{H}_2\text{O}$	49
cheralite	synonym of uraninite	
coffinite	$\text{U}(\text{SiO}_4)_{1-x}(\text{OH})_{4x}$	32, 33, 34
cuprosklodowskite	$\text{Cu}(\text{UO}_2)_2\text{Si}_2\text{O}_7 \cdot 6\text{H}_2\text{O}$	32, 33
gastunite	Ca, Pb uranyl silicate (?)	32
haiweeite	$\text{Ca}(\text{UO}_2)_2\text{Si}_6\text{O}_{15} \cdot 12\text{H}_2\text{O}$	50
huttonite	ThSiO_4	31, 32
kasolite	$\text{Pb}(\text{UO}_2)\text{SiO}_4 \cdot \text{H}_2\text{O}$	32, 33
laplandite	$\text{Na}_4\text{CeTiPSi}_7\text{O}_{22} \cdot 5\text{H}_2\text{O}$	27
metahaiweeite	$\text{Ca}(\text{UO}_2)_2\text{Si}_6\text{O}_{15} \cdot 5\text{H}_2\text{O}$	54
nenadkevite	synonym of coffinite (?)	61
orlite	synonym of kasolite (?)	42, 78

Table 4 cont'd.....

ranquillite	synonym of haiweeite	1
sklodowskite	$\text{Mg}(\text{UO}_2)_2\text{Si}_2\text{O}_7 \cdot 6\text{H}_2\text{O}$	32, 33
soddyite	$(\text{UO}_2)_5\text{Si}_2\text{O}_9 \cdot 6\text{H}_2\text{O}$	32, 33
sodium-boltwoodite	$\text{Na}_2(\text{UO}_2)_2(\text{SiO}_3)_2(\text{OH})_2 \cdot 5\text{H}_2\text{O}$	19
thorite	ThSiO_4	32, 33, 34
thorogummite	$\text{Th}(\text{SiO}_4)_{1-x}(\text{OH})_{4x}$	32
umbozerite	$\text{Na}_3\text{Sr}_4\text{ThSi}_8(\text{O}, \text{OH})_{24}$	28
uranophane	$\text{Ca}(\text{UO}_2)_2\text{Si}_2\text{O}_7 \cdot 6\text{H}_2\text{O}$	31, 32, (77)
uranothorinite	variety of thorianite	34
uranotile	synonym of uranophane	32
ursilite	$(\text{Ca}, \text{Mg})_2(\text{UO}_2)_2\text{Si}_5\text{O}_{14} \cdot 9-10\text{H}_2\text{O} (?)$	17
weeksite	$\text{K}_2(\text{UO}_2)_2\text{Si}_5\text{O}_{15} \cdot 4\text{H}_2\text{O}$	59
TELLURITES		
cliffordite	UTe_3O_9	36-39
moctezumite	$\text{Pb}(\text{UO}_2)(\text{TeO}_3)_2$	36, 39
schmitterite	UO_2TeO_3	35
VANADATES		
carnotite	$\text{K}_2(\text{UO}_2)_2(\text{VO}_4)_2 \cdot 3\text{H}_2\text{O}$	32, 33
curienite	$\text{Pb}(\text{UO}_2)_2(\text{VO}_4)_2 \cdot 5\text{H}_2\text{O}$	11
francevillite	$(\text{Ba}, \text{Pb})(\text{UO}_2)_2(\text{VO}_4)_2 \cdot 5\text{H}_2\text{O}$	32, 33
fritzscheite	$\text{Mn}(\text{UO}_2)_2(\text{VO}_4)_2 \cdot 10\text{H}_2\text{O}$	32

Table 4 cont'd.....

metatyuyaminite	$\text{Ca}(\text{UO}_2)_2(\text{VO}_4)_2 \cdot 3-5\text{H}_2\text{O}$	32,33
metavanuralite	$\text{Al}(\text{UO}_2)_2(\text{VO}_4)_2(\text{OH}) \cdot 8\text{H}_2\text{O}$	10
rauvite	$\text{Ca}(\text{UO}_2)_2\text{V}_{10}\text{O}_{28} \cdot 16\text{H}_2\text{O}$	32,33'
sengierite	$\text{Cu}(\text{UO}_2)_2(\text{VO}_4)_2 \cdot 8-10\text{H}_2\text{O}$	32,33
strelkinit	$\text{Na}_2(\text{UO}_2)_2(\text{VO}_4)_2 \cdot 6\text{H}_2\text{O}$	3
tyuyamunit	$\text{Ca}(\text{UO}_2)_2(\text{VO}_4)_2 \cdot 5-8\text{H}_2\text{O}$	32,33
uvanite	$\text{U}_2\text{V}_6\text{O}_{21} \cdot 15\text{H}_2\text{O}$	32,33
vanuralite	$\text{Al}(\text{UO}_2)_2(\text{VO}_4)_2(\text{OH}) \cdot 11\text{H}_2\text{O}$	7,10
vanuranylite	$[(\text{H}_3\text{O}), \text{Ba}, \text{Ca}, \text{K}]_{1.6}$ $(\text{UO}_2)_2(\text{VO}_4)_2 \cdot 4\text{H}_2\text{O} (?)$	9

CARBONACEOUS COMPOUNDS

carburan**	40
sogrenite**	38,78
thucholite**	23,72

** Not a mineral name

Table 5. Numbers and corresponding reference for table 4

1	Abledo <u>et al.</u> (1960)	47	Guillemin and Protas (1959)
2	Agrinier <u>et al.</u> (1972)	48	Hamilton and Kerr (1959)
3	Alekseeva <u>et al.</u> (1974)	49	Honea (1961)
4	Belova (1958a)	50	Kamhi (1959)
5	Belova (1959b)	51	Kopchenova <u>et al.</u> (1962)
6	Belova <u>et al.</u> (1963)	52	Kopchenova and Skvortsova (1957)
7	Branche <u>et al.</u> (1963)	53	Lima de Faria (1958)
8	Bulteman and Moh (1959)	54	McBurney and Murdoch (1969)
9	Burynova <u>et al.</u> (1965)	55	Milton <u>et al.</u> (1965)
10	Cesbron (1970)	56	Muto <u>et al.</u> (1959)
11	Cesbron and Morin (1968)	57	Nekrasova (1957)
12	Cesbron <u>et al.</u> (1965)	58	Hutton (1957)
13	Cesbron <u>et al.</u> (1969)	59	Outerbridge <u>et al.</u> (1960)
14	Cesbron <u>et al.</u> (1970)	60	Pierrot <u>et al.</u> (1965)
15	Cesbron <u>et al.</u> (1971)	61	Polikarpova (1957)
16	Cesbron <u>et al.</u> (1972)	62	Pcvitailis (1963)
17	Chernikov (1957)	63	Protas (1959)
18	Chernikov <u>et al.</u> (1957)	64	Protas (1964)
19	Chernikov <u>et al.</u> (1975)	65	Pudovkina <u>et al.</u> (1974)
20	Christ and Clark (1960)	66	Rogova <u>et al.</u> (1973)
21	Clark (1960)	67	Rogova <u>et al.</u> (1974)
22	Coleman <u>et al.</u> (1966)	68	Ross (1963)
23	Davidson and Bowie (1951)	69	Ross and Evans (1964)
24	Desautels (1967)	70	Ross <u>et al.</u> (1964)
25	Emerson and Wright (1957)	71	Rupnitskaya (1958)
26	Epshtein (1959)	72	Schidłowski (1966c)
27	Eskova <u>et al.</u> (1974)	73	Sergeev (1964)
28	Eskova <u>et al.</u> (1974)	74	Skvortsova and Sidorenko (1965)
29	Fisher and Meyrowitz (1962)	75	Smith (1959)
30	Fron del (1952)	76	Smith and Marienko (1971)
31	Fron del (1956)	77	Smith and Stohl (1972)
32	Fron del (1958)	78	Soboleva and Pudovkina (1957)
33	Fron del <u>et al.</u> (1956)	79	Stephenson (1964)
34	Fuchs and Gebert (1958)	80	Tröger (1967)
35	Gaines (1965)	81	Van Wambecke (1972)
36	Gaines (1969)	82	Walenta (1958a)
37	Gaines (1971)	83	Walenta (1958b)
38	Gallather and Atkin (1966)	84	Walenta (1965b)
39	Galy and Meunier (1971)	85	Walenta (1972)
40	Geffroy and Sarcia (1960)	86	Walenta and Wimmennauer (1961)
41	Getseva (1956)	87	Young <u>et al.</u> (1966)
42	Getseva and Savel'va (1956)		
43	Gorzhevskaya <u>et al.</u> (1965)		
44	Gotman and Khapaev (1958)		
45	Granger (1963)		
46	Gross and Corey (1958)		

CHAPTER III

PREVIOUS WORK

In the analysis of uranium and thorium minerals, the electron microprobe has been used mostly in qualitative studies such as identification, distribution of the various constituents of a phase and for the determination of approximate ratios of elements present. Examples of such applications are given by Agrinier et al. (1972); Barthel and Mehnert (1970); Cesbron et al. (1972); Frenzel et al. (1975); Kleykamp (1973); Ramdohr et al. (1965); Schidlowski (1966 a,b,c); Van Wambecke (1972); and Walenta (1972). Quantitative analyses have been reported by Ferris and Ruud (1971) and by Steacy et al. (1974) for brannerite and by Grandstaff (1974) and Morton and Sassano (1972) for uraninite. Ferris and Ruud (1971) corrected their analytical data for matrix effects using semi-empirical factors developed by Ziebold and Ogilvie (1966), but they did not state what emission line they have used for uranium. Steacy et al. (1974) gave no information about emission lines or corrections. Grandstaff (1974) used M-emission lines for

uranium and thorium, but made no mention of corrections for matrix effects. Morton and Sassano (1972) used uranium M-lines, but also gave little information regarding corrections.

Other applications of the electron microprobe in the study of uranium compounds are found in the field of metallurgy where it is mainly used to study migration phenomena (for example; Adda et al., 1960; Adda et al., 1961; Alcock and Grieveson, 1961). Binary systems, however, have been analysed quantitatively with success by Büchner (1973), Colby (1964) and Kirianenko et al. (1963). Büchner (1973) and Colby (1964) established calibration curves relating average atomic number and beam current to probe current ratios. The determination of this ratio for an unknown allowed them to deduce its average atomic number and hence the proportions of its constituents. This approach is only viable with binary compounds of very different atomic number. Kirianenko et al. (1963) applied the conventional 'ZAF' corrections as suggested by Castaing (1951, 1960) and Castaing and Deschamps (1955) for L_3 and M_4 emission lines. Good results were thus obtained for binary alloys but no attempts have been made to test and to apply this method with uranium minerals.

A survey of the geological literature indicates that investigations of uranium and thorium minerals are generally performed on separate fractions by X-ray diffraction, differential thermal analysis, wet chemistry

and, for uranium and thorium exclusively, by γ -ray-spectrometry, neutron activation and track-etch procedures.

CHAPTER IV

ANALYTICAL APPROACH

Before undertaking the analysis of uranium minerals with the electron microprobe, certain problems need to be considered:

- A. location of grains for analysis
- B. instrumentation
- C. stability of the minerals beneath the electron beam
- D. selection of suitable X-ray emission lines
- E. corrections for matrix effects
- F. presence of water and hydroxyl ions
- G. choice of standards
- H. operating conditions

A. LOCATION OF GRAINS FOR ANALYSIS

Uranium and thorium minerals usually make up only a small proportion of a rock, occurring as sparsely disseminated grains in a matrix of other minerals. To obtain polished thin sections containing these trace minerals, areas of high radioactivity were selected by means of autoradiography. Autoradiographs were acquired by pressing slices of rock for 12 to 24 hours against a strip of Ilford Industrial G X-ray diffraction film. Autoradiographs of the polished thin sections were also acquired first by the technique outlined above and when it became available, by radioluxography (Dooley, 1976). The latter requires shorter exposure (about 15 minutes for uraninite). The polished thin sections were then studied under reflected and transmitted light, and physically suitable radioactive grains were selected for analysis. It should be noted that transmitted light observations usually exaggerate the size of radioactive grains, the reason being that they are commonly surrounded by a zone of radiation damage which may be opaque like the radioactive grains themselves. Photographs of selected grains were taken in reflected light (x40) and used as maps during the analyses to avoid time consuming searches in relocating grains.

B. INSTRUMENTATION

The instrument used is an Applied Research Laboratories (ARL-EMX) electron microprobe with three wavelength dispersive spectrometers (WDS), and an Ortec (6200) energy dispersive spectrometer (EDS). One WDS with a RbAP crystal was used for light elements. The other two were used for heavier elements with EDDT, LIF and ADP crystals.

Results were at various times acquired on punched cards, cassette tapes or via typewriter print-outs.

Even though both wavelength dispersive and energy dispersive spectrometers were available, the latter was not used for quantitative analysis because it has poor resolution relative to the first (about two orders of magnitude difference). Problems of overlap and interference would be more important when using EDS; for example, L-lines of the various rare-earth elements would overlap one another.

C. STABILITY OF MINERALS BENEATH THE ELECTRON BEAM

Many of the uranium minerals are hydrous. DTA data (Ambartsumian, 1957) on some hexavalent uranium minerals indicate a first endothermic peak in the range of 100° to 200°C. Thus, it can be anticipated that such minerals will

be easily degraded in the vacuum chamber by the electron beam. Degradation of the specimen is manifested by a slight increase in X-ray intensity for major elements as the water is driven off. This change of intensity is usually of the order of 5% and follows the pattern illustrated by a uranophane specimen in figure 1. Darkening of the analysed areas is also visible for most of the hexavalent uranium minerals analysed. Degradation effects are minimized by keeping the power in the beam as low as possible while retaining sufficient intensity for analysis; by sweeping the beam over a small area of the sample during analysis; by defocussing the beam to about a diameter of 20 microns; and whenever possible, by moving the sample continuously during analysis.

Lead is commonly present in older uranium and thorium minerals as a result of radioactive decay process. This lead is 'out of place' in the minerals, is weakly bonded, and can be readily mobilized under the electron beam. For example, lead in a uraninite sample was driven away from the area of beam impact when attempting to analyse for uranium using an operating voltage of 20 kV and 25 kV; probe current of 10^{-6} A; beam diameter of 10-20 microns. The effect was not observed when proceeding as outlined above for the hydrous minerals.

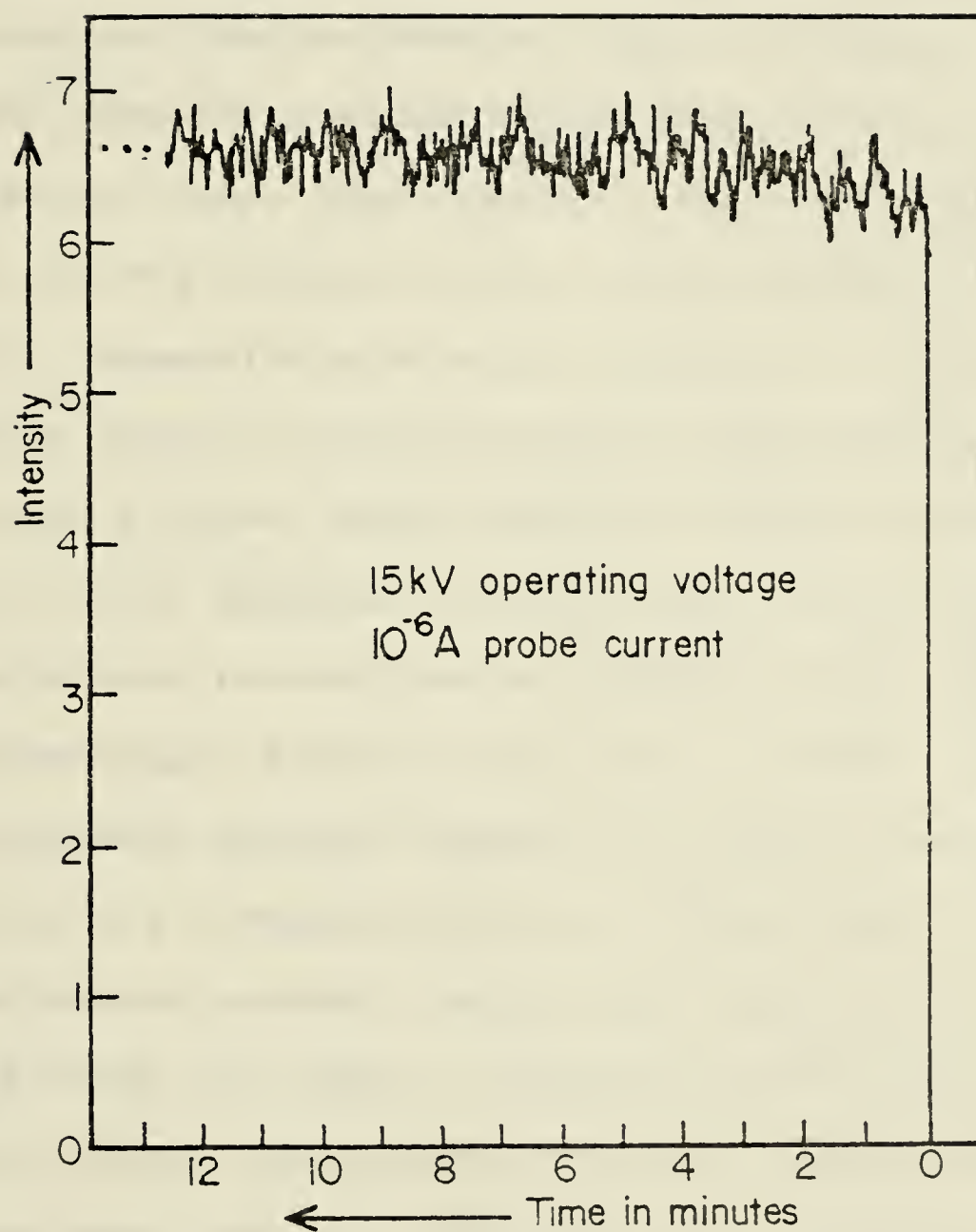


Figure 1. Variation with time of uranium count rate of a β -uranophane specimen under a focussed electron beam.

D. SUITABLE X-RAY EMISSION LINES

With elements of high atomic number two sets of lines may be used namely: L- and M-lines. As a general rule, the line of highest intensity is chosen. The L-lines of uranium and thorium have too high an energy to be diffracted by the commonly available analysing crystals as first order radiation. Also, they require a high operating voltage (at least 25 kV) combined with a probe current of at least 10^{-7} A, incompatible with the analysis of minerals which degrade easily beneath the beam. These problems are avoided by using M-lines, which require a lower voltage to excite them, can be measured as first order radiations, and give satisfactory intensities at suitable probe current. Disadvantages from M-lines arise, however, from interference between uranium and thorium lines and between uranium and potassium lines as illustrated in figure 2. Interference between uranium and thorium is minimized by using Th- $M\alpha$ and U- $M\beta$; a correction factor to subtract the minor thorium contribution from the uranium $M\beta$ peak has been established. For the instrument and crystals used, i.e., EDDT for uranium and ADP for thorium, the contribution of thorium to uranium $M\beta$ is equal to 1.62% of the intensity of the thorium $M\alpha$ measured at the peak centre. When potassium is present (as in carnotite) U- $M\alpha$

When using wavelength dispersive spectrometers, another reason for preferring U- $M\beta$ is the greater efficiency

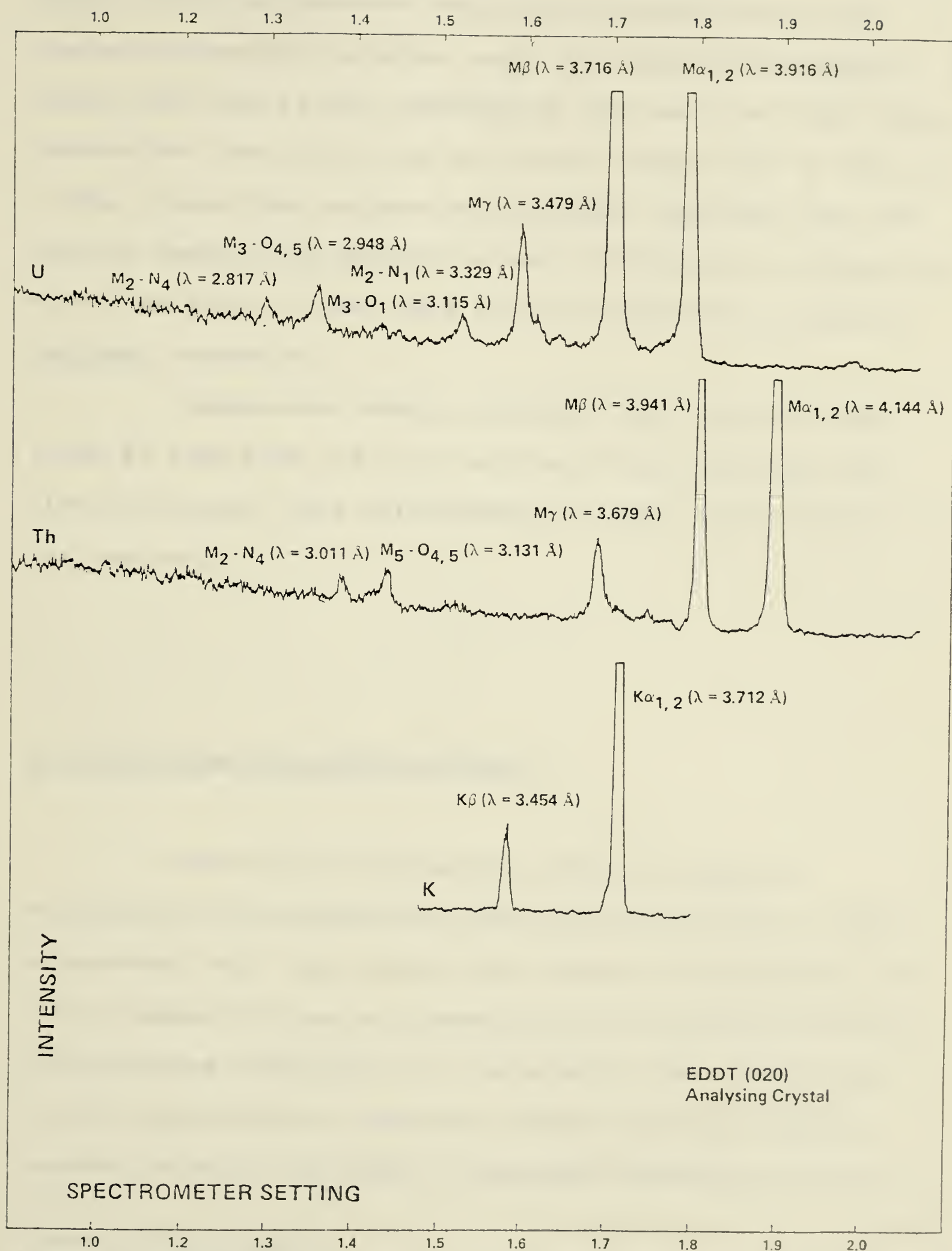


Figure 2. Partial spectra for uranium, thorium, and potassium at 15 kV. Recorded by wavelength spectrometry.

of the Ar-filled detector for the U-M β radiation. In the sealed proportional counter used, the critical excitation energy for Ar-K is just exceeded by the energy of U-M β line, whereas the U-M α line lies on the low energy side of the Ar-K edge. Hence U-M β is much more strongly absorbed than the U-M α by argon. This feature is well illustrated in figure 2, where the width of U-M β peak clearly indicates its greater recorded intensity.

Background reading positions were usually taken 0.005 Å¹ away from the peak position. These settings were altered whenever they corresponded to other lines present in the spectra.

E. CORRECTIONS FOR MATRIX EFFECTS

Quantitative microprobe analysis requires correction of the analytical data for matrix effect. These corrections take into account the effects of absorption (A) atomic number (Z) and of fluorescence (F) by characteristic and continuum radiations. At the present time, application of the corrections to commonly analysed minerals usually results in about one order of magnitude reduction of the

¹ This is measured on a LiF geared spectrometer calibrated in wavelength of the radiation which is diffracted.

error which would otherwise remain. Particularly in the determination of compounds of high average atomic number, the corrections may be substantial. They are commonly applied as:

- 1- alpha factors, or as
- 2- comprehensive 'ZAF' corrections.

1- ALPHA FACTORS

These are determined either theoretically through comprehensive 'ZAF' calculations for hypothetical compounds or experimentally by comparing the intensities of simple compounds, ideally comparing a metal with its oxide (Bence and Albee, 1968; Albee and Ray, 1970).

2- COMPREHENSIVE 'ZAF' CORRECTIONS

These are carried out through iterative applications of a set of equations, some theoretical, some empirical. Considerable uncertainties surround the M-line parameters used in these corrections, in particular the mass absorption coefficients and the fluorescence yields.

The comprehensive 'ZAF' corrections were preferred to the alpha-factors because the latter could not be

obtained experimentally since suitable standards were lacking. Neither could they be determined theoretically, as the accuracy of the 'ZAF' corrections first needed to be verified.

Very few computer programmes are capable of applying the full matrix corrections when M-emission lines are involved. COR-2 (Hénoc et al., 1973) and FEPAC (Springer, 1976a) will perform such calculations. COR-2 was used when this work was initiated, because it was the only one available, but later, results obtained through both programmes were compared for some of the analyses.

Corrections applied by both programmes have been summarized by Springer (1976a) for FEPAC, and by Heinrich (1973) for COR-2. In brief, the following are used:

Atomic number corrections:

1- backscatter factor

FEPAC: polynomial expression after Duncumb (1973; private communication, in Heinrich (1973))

COR-2: polynomial expression from Duncumb (1973; private communication, in Heinrich (1973))

2- mean ionization potential

FEPAC: after Berger and Seltzer (1964)

COR-2: after Berger and Seltzer (1964)

3- stopping power

FEPAC: abbreviated (Poole and Thomas, 1962) form of the penetration function with a mean value for the electron energy.

COR-2: after Bethe et al. (1938)

Absorption corrections:

1- method

FEPAC: after Heinrich and Yakowitz (1975)

COR-2: after Philibert (1963)

2- absorption coefficients

FEPAC: after Heinrich (1966), computed from polynomials according to Springer and Nolan (1976)

COR-2: after Heinrich (1966)

3- emission and critical absorption energies

FEPAC: computed from polynomials after Springer and Nolan (1976)

COR-2: after Bearden (1967)

Characteristic fluorescence:

1- method

FEPAC: after Reed (1965)

COR-2: modified version of Reed (1965)

2- fluorescence yields

FEPAC: after Colby as described by Springer (1976b)

COR-2: measured values (probably after Fink et al. (1966))

3- absorption efficiency factors

FEPAC: after Colby as described by Springer (1976b)

COR-2: after Philibert (1963)

Continuum fluorescence:

FEPAC: as described by Springer (1976b)

COR-2: after Hénoc (1968)

Application of the corrections:

FEPAC: re-iteration according to the Wegstein method described by Springer (1976c)

COR-2: modified version of Criss and Birks (1966).

Discrepancies in the results calculated by these two programmes will arise not only from the difference in the basic equations used for the ZAF corrections, but also, from the procedures of application of these corrections and from the use of different sets of parameters.

Modifications were made to adapt COR-2, which was written for a UNIVAC system, first to the IBM 360/67, and then to the AMDAHL computer now in use at the University of Alberta.

More significant modifications, discussed below, dealt with the permanent data file. The data file used is listed in appendix I.

Fluorescence yields and Coster-Krönig coefficients

Fluorescence yields and Coster-Krönig coefficients were updated, using the 'best values' suggested by Bambynek et al. (1972). Where these parameters were not available, a

value was determined by interpolation from neighbouring elements. Both fluorescence yields and Coster-Krönig coefficients are used to determine primary intensities and to correct for fluorescence by characteristic and continuum radiations (Coster-Krönig coefficients are limited to L-lines).

Mass absorption coefficients

Mass absorption coefficients are used in the corrections for both absorption and fluorescence effects. COR-2 utilized the mass absorption coefficients defined by Heinrich (1966). The mass absorption coefficient for a particular element increases smoothly with increasing wavelength except at absorption edges where it drops sharply. On the low energy side of absorption edges the mass absorption coefficient is calculated as a function of the mass absorption coefficient on the high energy side by using the 'absorption jump ratio'. Mass absorption coefficients and jump ratios are known for wavelengths shorter than M_1 edges. For wavelengths longer than M_1 edges, data are scarce, and experimental and calculated values do not agree with each other at all well. Hence, mass absorption coefficients (and jump ratios) in this region are only rough approximations. No data between M_4 and M_5 edges are available nor are there any data covering the region between and beyond N edges. These uncertainties and omissions affect the corrections for:

- absorption of sodium K-emission lines by uranium and thorium in the N region,
- fluorescence of sodium, magnesium, aluminium, silicon, phosphorus, sulfur and chlorine K-radiations by uranium and thorium M-lines.

For our purpose we have determined empirical jump ratios at the M_4 and M_5 edges of uranium and thorium. A first approximation of the jump ratios was obtained through the analysis of a uranium-silicon alloy (U_3Si). Analyses were performed at operating voltages of 15 kV and 20 kV. Uranium and silicon were analysed simultaneously against uranium oxide and silicon metal respectively. The 'ZAF' corrections were applied to the data using a range of values for M_4 and M_5 jump ratios. The best value was assumed to be the one which yielded similar results for both voltages. Results are listed in table 6. Figure 3 illustrates the variation of the computed compositions with hypothetical absorption jump ratios. The stoichiometric composition of the alloy is, in weight percentages: U:96.22; Si:3.78. Our results for operating voltages of 15 and 20 kV are in agreement as U:95.01; Si:3.50 (weight percentages) using absorption jump ratios of 1550.

Possible causes for the discrepancy between experimental and stoichiometric compositions are:

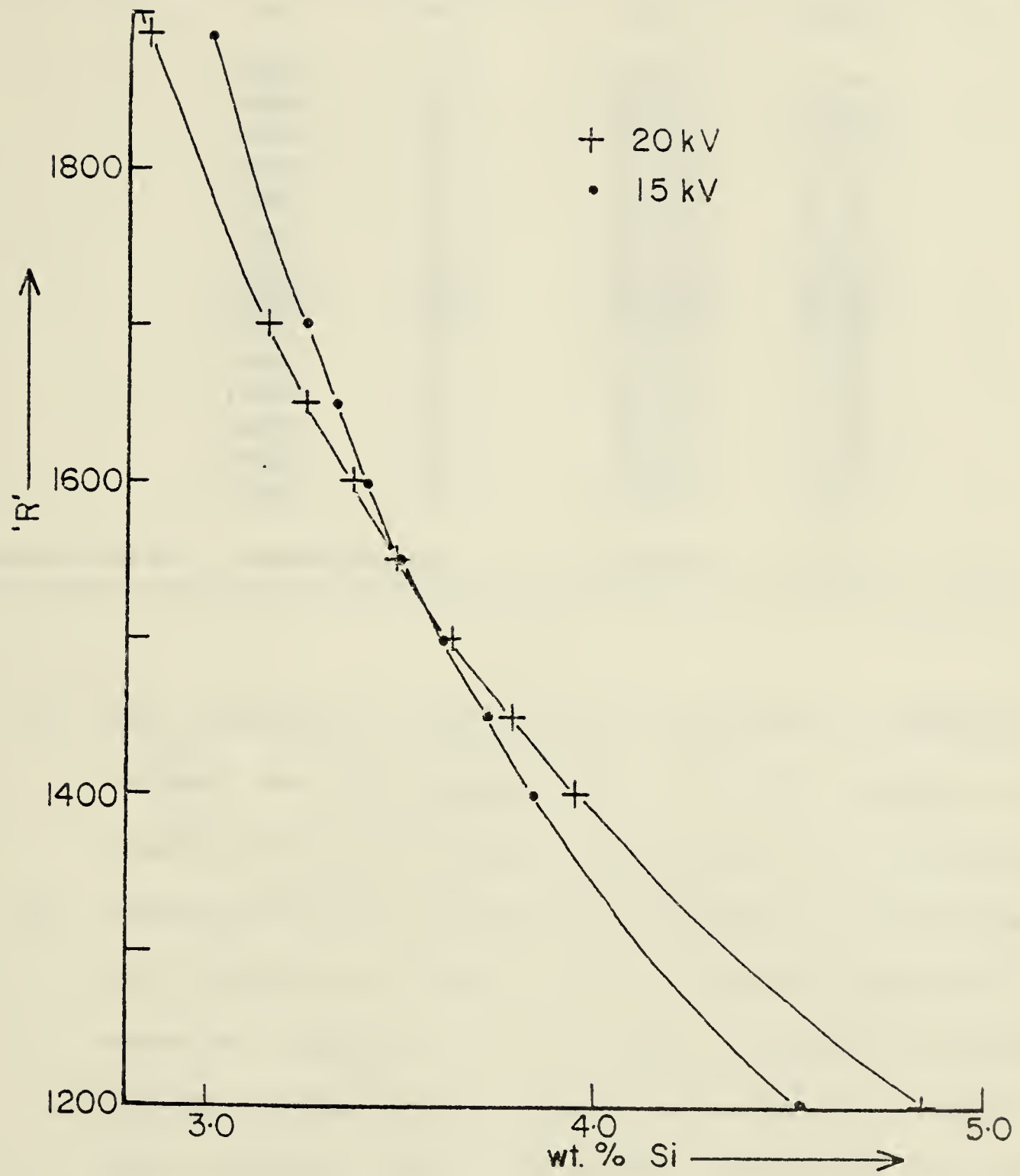


Figure 3. Variation of the apparent silicon concentration in U_3Si with jump ratio ('R').

Table 6. Composition of U_3Si in weight percentages. Results from electron microprobe analysis at 15 kV and 20 kV are given for various hypothetical $U-M_4$ and $U-M_5$ absorption jump ratios.

R	kV	% U	% Si
1400	15	95.23	3.86
1400	20	95.31	3.95
1450	15	94.81	3.73
1450	20	95.29	3.78
1500	15	94.80	3.61
1500	20	95.26	3.63
<u>1550</u>	<u>15</u>	<u>94.78</u>	<u>3.51</u>
<u>1550</u>	<u>20</u>	<u>95.24</u>	<u>3.49</u>
1600	15	94.77	3.42
1600	20	95.22	3.37
1650	15	94.76	3.33
1650	20	95.20	3.26
1700	15	94.76	3.25
1700	20	95.19	3.16
stoichiometric composition		96.22	3.78

- 1- The presence of U_3Si_2 in the analysed or excited volume; the two phases U_3Si and U_3Si_2 coexist in our sample, with an average grain size of 10 microns.
- 2- Oxidation of the alloy: no information concerning the oxidation of U_3Si in air at room temperature could be found, but this alloy is known to develop a uranium oxide coating (U_3O_8) when heated at $350^\circ C$ in air (Feraday, 1971). Oxidation could have occurred during polishing or subsequent handling.
- 3- Inaccurate corrections: it is not, at this stage, possible to judge the validity of the corrections applied.

Our standards, uranium oxide and silicon metal are stable

under the analytical conditions employed and do not alter between or during manipulations. Their compositions have been well determined. Hence they are unlikely sources of error.

The validity of our empirical factors was further checked through analysis of uranium glasses of known composition (tables 8, and 9). Similar factors were used for thorium; they were tested through analysis of thorium glasses (tables 8, and 9). Results for these glasses are discussed in a following chapter. Suffices it to say at this juncture that agreement between theoretical and experimental compositions is satisfactory. It should be kept in mind though that M_4 and M_5 absorption jump ratios of 1550 for uranium and thorium may not be of any absolute significance; they are simply empirical factors valid for microprobe analysis with an operating voltage of 15 kV to 20 kV.

We had no means of defining an empirical absorption jump ratio for uranium at the N_1 edge, although this would be required for the analysis of sodium. Such factors, however, would be determinable through the analysis of uranium and sodium-bearing compounds of known composition.

F. PRESENCE OF WATER AND HYDROXYL IONS

Water and OH cannot be determined directly by the electron microprobe, but their presence affects the 'ZAF' corrections. Their presence is reflected in the average atomic number (\bar{Z}) of minerals and consequently in the fraction of electrons backscattered during analysis. Estimation of the average atomic number as a function of backscattered electrons was envisaged. Two types of function are possible:

- 1- the first relates the amount of backscattered electrons of a finite energy and constant angle to \bar{Z} ;
- 2- the second, relates the total amount of backscattered electrons to \bar{Z} .

We were not equipped to effect the measurements required by the first type of calibration, but values for the second type can be acquired by measuring the sample current to probe current ratio (SC:PC; i.e., 1 - backscattered electrons). A calibration curve was thus established by plotting atomic number for pure elements against the sample current to probe current ratios (fig. 4). This relationship was tested for simple compounds.

The average atomic number of compounds can be calculated in a number of ways (Büchner, 1973):

$$\bar{Z} = \text{sum of: } C_w \cdot Z \quad (1)$$

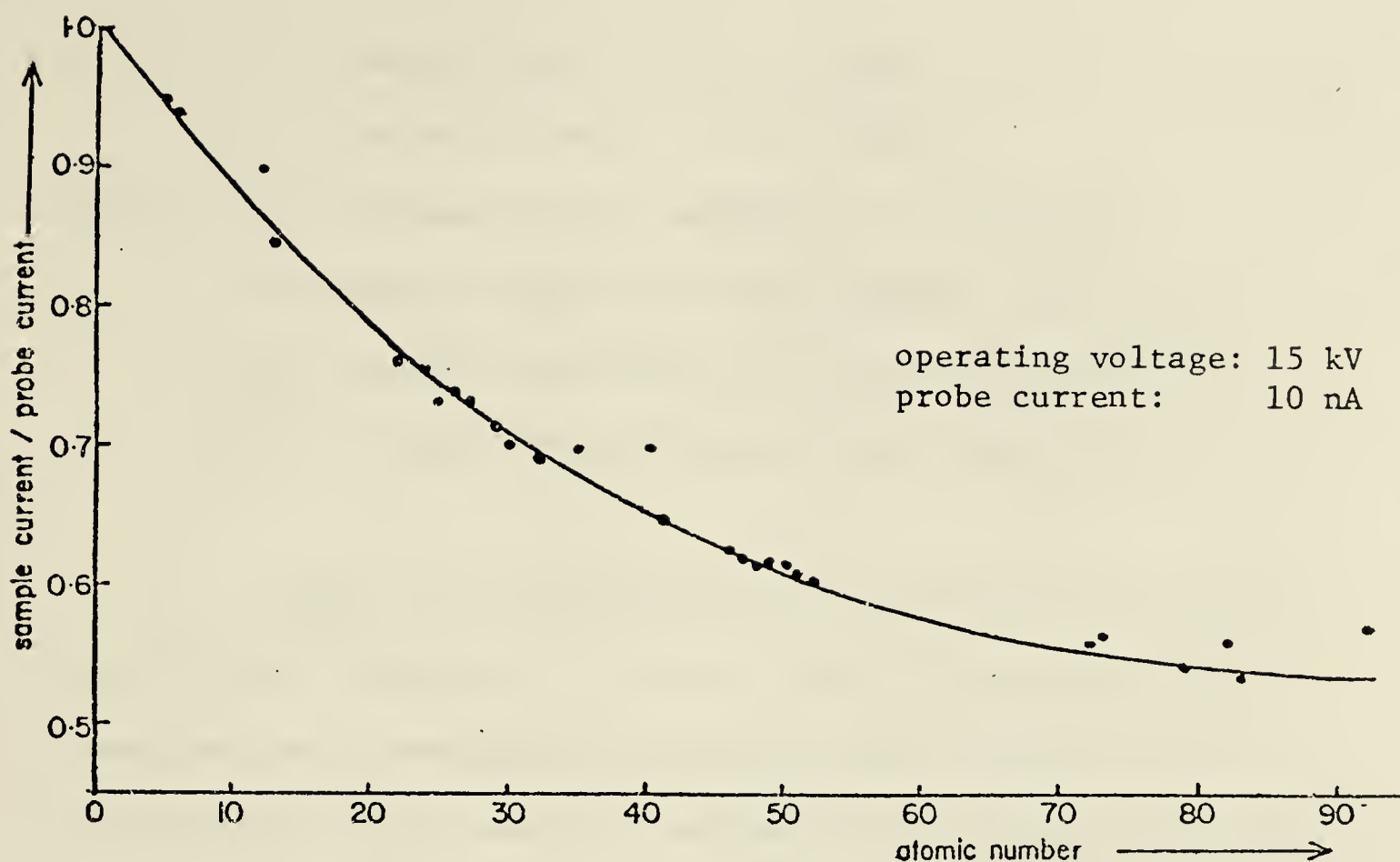


Figure 4. Relationship between the atomic number of pure elements and their sample current/probe current ratio.

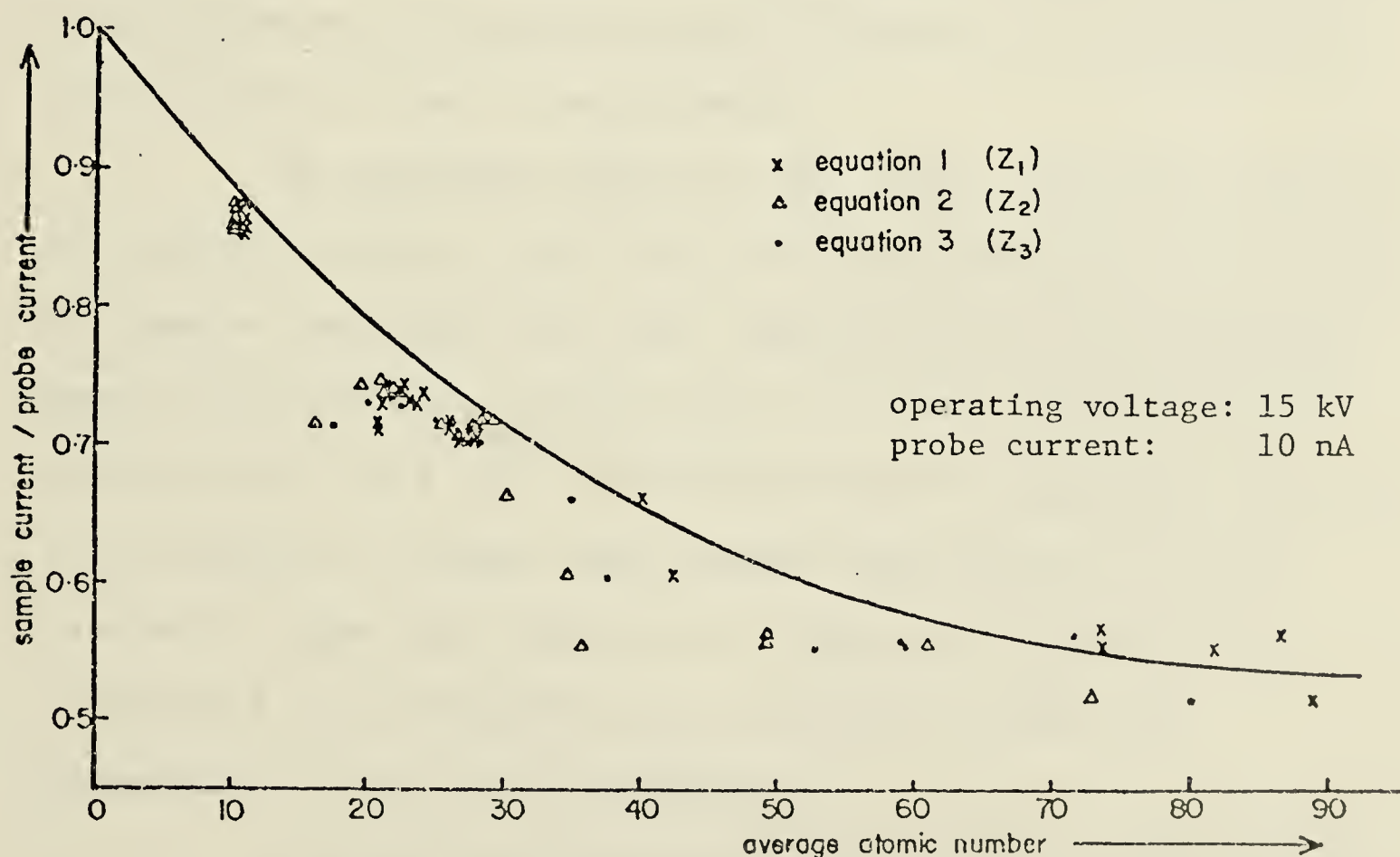


Figure 5. Relationship between the average atomic number of compounds and their sample current/probe current ratio. The average atomic numbers were calculated using equations 1, 2, and 3 (see text). The curve is that of figure 4.

$$\bar{Z} = \text{sum of: } Ca \cdot Z \quad (2)$$

$$\bar{Z} = \text{sum of: } Ca \cdot Z^2 \quad (3)$$

where : \bar{Z} = average atomic number of a compound;

Z = atomic number of each element involved;

C_w = weight proportion of the constituents;

Ca = atomic proportion of the constituents.

When \bar{Z} is calculated on the basis of atomic proportions (equation 2 and 3), the presence of light elements has a noticeable effect, while when it is calculated on the basis of weight proportions (equation 1) the effect of light elements becomes minor. Büchner (1973) was successful in using equation (3) to estimate the average atomic number of binary alloys and hence, in deducing the proportions of their constituents.

To determine which of the three equations applies to our calibration curve the SC:PC was measured for a number of simple compounds and their experimental \bar{Z} value deduced from the calibration curve (fig. 5). These experimental \bar{Z} values agree best with their theoretical homologues obtained from equation 1, i.e., when weight proportions are used (table 7). Thus the presence of water and hydroxyl ions modifies \bar{Z} only slightly and its effect on the 'Z' corrections will not be critical.

For most uranium minerals, \bar{Z} plots in the second half of the calibration curve where the slope is low i.e., variations in SC:PC ratios vary only slightly with \bar{Z} . Hence,

Table 7. Average atomic number for some simple compounds: \bar{Z}_0 was obtained experimentally from figure 5; \bar{Z}_1 , \bar{Z}_2 and \bar{Z}_3 were calculated respectively from the equations 1, 2 and 3 (see text).

compound	\bar{Z}_0	\bar{Z}_1	\bar{Z}_2	\bar{Z}_3
SiO ₂	11.5	10.8	10.0	10.4
Al ₂ O ₃	13.0	10.6	10.0	10.2
AlSiO ₅	12.0	10.7	10.0	10.3
FeS ₂	22.0	20.6	19.3	19.9
CuFeS ₂	25.0	23.8	22.0	22.8
CoS	26.0	22.8	21.1	21.8
ZnS	27.0	25.4	24.0	25.0
NiS	27.5	23.4	21.6	22.4
Ni _{56.4} -Fe _{43.7}	29.0	27.1	27.1	27.1
FeS	30.0	22.2	20.8	21.4
Fe ₂ O ₃	30.5	20.6	15.3	17.6
FeAsS	31.0	27.3	25.0	26.0
Ni _{88.3} -Fe _{10.6}	31.5	27.8	27.8	27.8
Ni _{5.1} -Fe _{94.9}	32.0	26.1	26.1	26.1
Ni _{62.8} -Fe _{37.2}	32.5	27.2	27.2	27.2
Sb ₂ S ₃	40.5	41.1	30.0	34.6
PbS (synthetic)	71.0	73.2	49.0	59.1
PbS (galena)	73.0	73.2	49.0	59.1
UO _{2.1}	75.0	81.6	35.1	52.7
U ₃ Si	91.0	89.0	72.5	80.0

this curve cannot be used to estimate the amount of water and hydroxyl ion present. This amount must be calculated by difference from the corrected data after oxygen has been added in stoichiometric proportions.

G. STANDARDS

Ideally, pure homogeneous stable uranium and thorium minerals or compounds are desirable, however, such are not available. Acquisition and synthesis of standards is discussed in the following chapter.

H. OPERATING CONDITIONS

Operating conditions used are briefly listed below. A more complete outline of suggestions for the analysis of uranium, thorium, and commonly associated elements is given in appendix II.

Samples and standards were carbon-coated to ensure conductivity. Constituents of the selected grains were identified using the energy dispersive spectrometer.

In brief, the following operating conditions were employed for quantitative analysis:

- Operating voltage : 15 kV
- Aperture current : $1 \cdot 10^{-6}$ A
- Beam diameter : 1 to 20 microns
- Dispersing crystal for uranium $M\alpha$ and $M\beta$ lines:
EDDT
- Dispersing crystal for thorium $M\alpha$ line : ADP
- Counting period (per point, or area) : 50

seconds, integrated aperture current monitored continuously.

The choice of crystals was dominated by the crystals available.

Readings were acquired in the following sequence:

- upper background on samples and then on standards: five counting periods (totalling 250 sec)
- peak on samples and then on standards: ten counting periods (totalling 500 sec)
- lower background on standards and then on samples: five counting periods (totalling 250 sec).

Corrections for fluctuation of the probe current were applied i.e., PC:AC ratios were measured every hour or so and all results were normalised to a constant probe current.

CHAPTER V

STANDARDS

A- STANDARD MATERIALS

1. GENERALITIES

Standard materials containing uranium, thorium and other commonly associated elements are required for two purposes:

- 1 - as analytical standards;
- 2 - as reference materials to test the analytical approach and to define some parameters involved in the correction factors (such as the absorption coefficients for uranium M and N lines).

Standard materials ought to meet the following criteria:

- 1- homogeneity: the electron microprobe results must be representative of the specimen's composition as

previously determined by independent techniques;

- 2- accurately known composition;
- 3- stability under the electron beam.

Ideally, standards and specimens should have similar compositions. When this is the case, correction factors for both standards and specimens are similar and hence, tend to cancel out, thus minimizing the effect of inaccurately known factors. In this respect, uranium minerals are particularly exacting as they show a wide variety of compositions and average atomic numbers. Thorium minerals are less demanding. Their range of composition is more limited and all have high average atomic numbers.

Five categories of material were considered:

- 1- pure metals
- 2- simple compounds such as oxides
- 3- alloys
- 4- glasses
- 5- minerals.

Their properties and availability are discussed next.

Pure metals

Uranium and thorium metals comply with the criteria aforementioned criteria but they oxidize rapidly in air at room temperature (Elston, 1960; Flahaut 1963). It was noted that they develop an oxide coating within a week when kept in a vacuum dessicator. Because it is tedious and undesirable to repolish standards before use, uranium and

thorium metals do not constitute good, practical standards.

Simple compounds

Uranium and thorium dioxide and lead sulfide meet the aforementioned criteria and can easily be obtained. They have high average atomic numbers similar to thorium and tetravalent uranium minerals. Sintered uranium and thorium oxides were made available respectively by the A.E.C.L. and by Dr K. Norrish (C.S.I.R.O., Adelaide, Australia). Galena, already available in the University of Alberta microprobe laboratory, was used as a lead sulfide standard.

Alloys

Many alloys would be stable under the electron beam but their composition is difficult to establish for our purpose. Alloy specimens are often made of fine-grained phases, each having the same constituents but in different proportions. These phases may be difficult to distinguish on well polished carbon coated surfaces. Most uranium and thorium alloys, like uranium and thorium oxides, have high average atomic number. Hence, they would constitute good standards for the analysis of minerals such as uraninite and thorianite, which also have high average atomic number. However, standards of lower average atomic number would be better for analysis of hexavalent uranium minerals.

Glasses

A review of the literature on uranium- and thorium-bearing glasses yielded little information relevant to our purposes, since most glasses described contained less than 1 wt% of the elements concerned. However, indications that glasses containing as much as 50 wt% uranium oxide can be produced were given by Chakrabarty (1969); Heynes and Rawson (1961); Wirkus and Wilder (1960b, 1961, 1962) and by Wilder et al. (1963). At first, glasses seemed to promise an elegant source for standards as their composition could be pre-established at will. Homogeneity and stability under the electron beam, however, appeared unpredictable.

Six glasses were kindly provided by J.A.T. Smellie (Institute of Geological Sciences, Grays Inn Road, London) but two of them proved to be inhomogeneous. Compositions for the remaining four (A,B,D,E) are given in table 8. The author synthesized four satisfactory glasses (11,12,13,15) and their compositions are given in table 9. Their preparation is discussed further in the second part of the present chapter. Glasses containing rare-earths were also available in the microprobe laboratory (Drake and Weill, 1972).

Table 8. Theoretical composition of glasses A,B,D and E in weight percentages (Smellie *et al.*, 1978).

glass	A	B	D	E
SiO ₂	41.95	40.08	42.01	39.91
Al ₂ O ₃	31.04	30.08	31.00	29.96
CaO	26.08	25.05	25.98	24.97
ThO ₂	-	-	1.01	5.17
U ₃ O ₈	0.92	4.78	-	-
Total	99.99	99.99	100.00	100.01

Table 9. Theoretical composition of glasses 11,12,13 and 15 in weight percentages.

glass	11	12	13	15
MgO	7.44	7.41	7.40	4.60
Al ₂ O ₃	29.82	29.63	29.55	28.52
SiO ₂	37.12	37.03	37.07	35.62
CaO	7.47	7.42	7.42	7.11
V ₂ O ₅	-	-	-	2.15
TiO ₂	-	-	-	4.19
ZrO ₂	-	2.46	-	-
ThO ₂	-	8.02	18.54	-
UO ₂	18.17	8.03	-	17.82
Total	100.00	100.00	99.98	100.01

Minerals

The stability of uranium and thorium minerals under the electron beam was discussed in a previous chapter. Compositions of thorium and tetravalent uranium minerals are difficult to ascertain on the micron scale because these minerals are often zoned (e.g. allanite), or crossed by syneresis cracks (e.g. uraninite). Moreover, they are often characterized by complex chemistry. Computer reduction of

microprobe data from such minerals is thus long and costly. For these reasons they should not be used as standards in the analysis of simple compounds (such as many hexavalent uranium minerals).

Although minerals do not appear to be suitable for analytical standards, some well characterized minerals would be ideal materials to test the validity of our analytical approach. Two such samples, namely euxenite and davidite were kindly provided by Smellie (tables 19 and 21).

Other specimens were available in the collections of the University of Alberta Mineral Museum, although their identification was often found to be in error when they were examined with the microprobe. Physically suitable specimens were selected and their identifications were checked by X-ray powder diffraction and by qualitative electron microprobe analysis. Finally their compositions were assumed to be stoichiometric. Identified specimens used in testing the analytical approach are: carnotite, sabugalite, soddyite, meta-autunite, uranothorianite, thorogummite and β -uranophane. For other elements, a collection of well characterized standards of common rock forming minerals was also available in the microprobe laboratory of the Department of Geology. In general, these are uranium- and thorium-free.

2. STANDARD MATERIALS

Materials finally selected as analytical standards are summarized in table 10.

Table 10. List of elements analysed and corresponding standards. Less frequently used standards are in parenthesis.

Element	Standard
U	UO ₂ , (glass-11)
Th	ThO ₂ , (glass-13)
Pb	PbS, (Pb metal)
REE	glasses
Mg, Al, Si, Ca	common minerals, (glasses 11, 13)
P, Ca	Ca ₂ P ₂ O ₇ , apatite
elements with Z = 10 to 56	common minerals

B- GLASSES

The synthesis of glasses containing uranium, thorium, and other commonly associated elements was envisaged with hopes of obtaining standards with as much as 50 wt% UO₂, such as is present in many of the uranyl minerals.

1. PREVIOUS WORK

In the literature uranium bearing glasses has stemmed mainly from three interests:

- 1- the use of uranium as a colouring agent;
- 2- the study of diffusion phenomena;
- 3- the fabrication of nuclear fuel materials.

Literature concerning the first two fields is abundant but deals only with glasses containing small amounts of uranium, rarely above 1 wt%. Literature on the fabrication of glasses as possible nuclear fuel materials is very scarce but deals with higher uranium contents (up to 60 wt% UO_2).

Wirkus and Wilder (1960a) have discussed the principles involved in forming glasses containing uranium. From their work it appears that seven oxides are likely to act as glass formers. They are: B_2O_3 , SiO_2 , GeO_2 , P_2O_5 , As_2O_3 , As_2O_5 , and Sb_2O_3 . Theoretical considerations, such as neutron poisoning capacities, permit the elimination of B_2O_3 , GeO_2 , As_2O_3 , As_2O_5 and Sb_2O_3 for nuclear-fuel applications, leaving only P_2O_5 and SiO_2 . For our purpose we have not investigated phosphorus-based glasses because phosphorus-rich compounds are likely to deteriorate under the electron beam under normal analytical conditions (operating voltage : 15 kV; probe current : $0.1 \cdot 10^{-6}$ A). Systems known to form silica based uranium-rich glasses are listed in table 12. Wirkus and Wilder (1960b) have studied

the limit of composition within which glass formation occurs in combination with uranium oxide, silica and various intermediate agents (although not glass-formers, the intermediate agents can act as and/or replace part of the glass-formers in glass frameworks). The systems known to form silica-bases glasses listed in table 11 were submitted to a maximum temperature of 1250°C . They concluded that "... uranium glasses containing up to 45 wt% UO_2 , present as an integral part of the structure can be prepared. Forty percent or more silica is required in these glasses to provide the glassy framework. The remainders of the glass formula should consist of modifiers such as Na_2O and CaO and/or intermediates such as TiO_2 . Alumina is a suitable intermediate also in the absence of TiO_2 ". The studies of Heynes and Rawson (1961) dealt with higher temperatures (1800°C maximum). Their results on the limits of composition of silica based uranium glasses are compatible with those of Wirkus and Wilders (1960b). More recent work on the SiO_2 - Na_2O - UO_2 systems as been carried out by Chakrabarty (1969) who synthesized glasses at temperatures ranging from 850°C to 1260°C ; high sodium content (10 to 45.5 wt% Na_2O) leads to low melting temperatures.

Table 11. Systems yielding homogeneous uranium-silica-glasses with their maximum uranium dioxide content in weight percentage and reference work.

System	UO ₂	reference
UO ₂ -SiO ₂ -Na ₂ O-TiO ₂	45	Wirkus and Wilder, 1960b.
UO ₂ -SiO ₂ -Al ₂ O ₃ -CaO-TiO ₂	16	"
UO ₂ -SiO ₂ -Al ₂ O ₃ -CaO-Na ₂ O-K ₂ O	6	"
UO ₂ -SiO ₂ -CaO-Na ₂ O-TiO ₂	38	"
UO ₂ -SiO ₂ -Al ₂ O ₃ -CaO-Na ₂ O	41	"
UO ₂ -SiO ₂ -Al ₂ O ₃ -Na ₂ O	36	"
UO ₂ -SiO ₂ -CaO-UO ₂ -ZrO ₂	31	"
UO ₂ -SiO ₂ -CaO-Na ₂ O-Y ₂ O ₃	35 -	"
UO ₂ -SiO ₂ -CaO-Na ₂ O-Y ₂ O ₃	38	"
UO ₂ -SiO ₂ -Na ₂ O-TiO ₂ -PbO	31	"
UO ₂ -SiO ₂ -Al ₂ O ₃ -BeO	40	Heynes and Rawson, 1961
UO ₂ -SiO ₂ -Al ₂ O ₃ -MgO	50	"
UO ₂ -SiO ₂ -Al ₂ O ₃ -ZrO ₂	40	"
UO ₂ -SiO ₂ -Al ₂ O ₃ -ThO ₂	40	"
UO ₂ -SiO ₂ -Al ₂ O ₃ -ThO ₂	60	"
UO ₂ -SiO ₂ -MgO-ThO ₂	50	"
UO ₂ -SiO ₂ -Na ₂ O	52	Chakrabarty, 1969

2. CONSTRAINTS

In attempt to synthesize glasses we had to take the following points into account:

- 1 - the preparation must include a glass-former in sufficient amount;
- 2 - enough material must be prepared to check for the presence and extent of possible compositional gradients;
- 3 - the availability of heating equipment bearing in mind the refractory properties of uranium and thorium oxides.

Glass-formers

As previously mentioned, the only data we have found dealt with silica- and phosphorus-based uranium glasses. Phosphorus was considered unsuitable of electron microprobe standards. The other possible glass-formers mentioned by Wirkus and Wilder (1960) were discarded because we preferred using already known systems. In addition, antimony and arsenic would have posed problems regarding their final oxidation state. Boron cannot be analysed with the equipment we were to use and finally, germanium is relatively expensive.

Compositional gradients

These could arise through contamination from the containers and through evaporation. A composition gradient in the sample can easily be detected with the microprobe. Slices of the samples were made into polished sections. The polished sections contained part of the crucible and adjacent glass. Line scanning was carried out (with the electron microprobe) across the section from bottom to top and side to side of the glass slice, while simultaneously recording the variations in intensity for three elements. Differences in composition between the initial and final product can only be measured by independent methods. Ten gramme loads were considered sufficient because they provided enough material for wet chemical analysis and also because in such a volume contamination by the container

might affect only the border of the glass. This, of course, supposes that the silica-based glass is highly viscous and does not mix rapidly in the molten state.

Heating equipment

Ten gramme loads can be heated in induction or muffle furnaces. An induction furnace was occasionally available at the Department of Physics. It was installed for use in vacuum with a graphite crucible. For use in air, it would have been necessary to install an iridium susceptor of adequate shape. This would have been costly and difficult to obtain. The muffle furnaces were equipped for use in a normal atmosphere only. The muffle furnaces were preferred to induction furnaces to avoid possible reduction of uranium or other constituents. At first an M-Blue 'Rad-O-Glow' muffle furnace with a maximum temperature of 1460°C was used. At a later stage, a Deltech 'DT-31' muffle furnace capable of reaching a temperature of 1700°C became available.

3. COMPOSITION

In our first attempts, we tried compositions studied by Wirkus and Wilder (1960b) but our results were unsatisfactory due to high contents of sodium, titanium, and zirconium oxides. Sodium-rich glasses (>8 wt% Na_2O) were unstable under the electron beam, and titanium- and zirconium-rich mixtures (>10 wt% TiO_2 , >10 wt% ZrO_2) reacted with both ALUNDUM® and recrystallized alumina crucibles in the molten state. When a higher temperature furnace (1700°C) became available, sodium-free and low-titanium and zirconium mixtures were prepared. Phase diagrams for systems combining the glass constituents considered were studied. In attempting to keep the melting temperatures of the mixtures to a minimum, the constituents of this mixtures were combined in proportions close to those of the eutectic compositions of relevant systems.

Because of the high temperatures involved and the narrow fields of composition-yielding glasses (Wirkus and Wilder, 1960b; Heynes and Rawson 1961), only four specimens were thus obtained.

4. SOURCE MATERIALS AND PREPARATION

Source materials

The source materials are: SiO_2 , Al_2O_3 , CaCO_3 , Na_2CO_3 , MgCO_3 , TiO_2 , ZrO_2 , V_2O_5 , ThO_2 and UO_2 . UO_3 was used in mixture #1 (table 12). All are reagent grade products; their manufacturers are:

- Fisher Scientific Co. Ltd for SiO_2 , CaCO_3 , Na_2CO_3 , and MgCO_3 ;
- Alfa Products for ZrO_2 , and UO_3 ;
- Analar Products Ltd for Al_2O_3 , and V_2O_5 ;
- Var-Lac-Oil Chem. Ltd for ThO_2 , and UO_2 .

The constituents were treated along the line suggested by Edgar (1973) and kept in a vacuum dessicator prior to mixing.

- SiO_2 , Al_2O_3 , TiO_2 , ZrO_2 were dried at 950°C for 12 hours.
- CaCO_3 and MgCO_3 were transformed (into the oxides CaO and MgO respectively) by heating them at 950°C for 12 hours in air.
- V_2O_5 and Na_2CO_3 were dried at 300°C in air.
- ThO_2 , UO_2 and UO_3 came in bottles packed under nitrogen and required no treatment.

Preparation

Ten gramme loads were prepared by weighing all the constituents on a precision balance and dry mixing by hand in an agate mortar for at least 20 min. Then the mixtures were placed in a loosely covered crucible and initially heated to 900°C in air for 12 hours to allow a preliminary degassing. Afterwards, the temperature was brought to either 1460 or 1650°C depending on the furnace and kept at this maximum temperature for one hour. The M-Blue furnace took 20 hours to reach its maximum temperature (1460°C) while the Deltech furnace reached 1650°C within 3 hrs. The furnace was then turned off and the crucible allowed to cool to about 1200°C before removing. Cooling took approximately 1 hr.

A means of obtaining homogeneous glass commonly described in the literature consists of successive grinding, mixing, and melting of the mixture. We have not done so to avoid extensive contamination by the crucible. Indeed, regrinding the whole glass would have resulted in a higher alumina content in the final product, since contamination would have occurred during each melting period. Disregarding the contaminated marginal glass would have required too large an initial load (the Deltech furnace could not take more than ten gramme loads). Homogeneity and stability of the final products were checked by electron-microprobe analysis. It was found that aluminium contamination did not extend beyond 2 mm from the contact and that the central part of the glass was in most cases, homogeneous.

Inhomogeneous products were rejected and new loads were prepared. Samples for quantitative microprobe work and independent wet chemical analysis were taken from the central, apparently contamination-free, parts of the glasses.

5. RESULTS

1450°C maximum

Glasses with melting temperatures below 1460°C were either unstable to electron beam irradiation (#2, 3 table 12) or inhomogeneous and highly contaminated by the crucible in which they were prepared. Inhomogeneity and

Table 12. Composition of glasses 1,2 and 3 in weight percentages.

glass	1	2	3
Al ₂ O ₃	7.81	-	-
SiO ₂	68.60	40.02	43.74
Na ₂ O	11.87	7.98	7.58
CaO	4.34	-	-
TiO ₂	7.38	3.99	3.38
ZrO ₂	-	-	-
ThO ₂	-	-	45.30
UO ₃	-	48.01	-
Total	100.00	100.00	100.00

contamination were due to the highly corrosive nature of the mixtures containing 10 wt% titanium or zirconium oxide,

which reacted with the ALUNDUM® crucibles. The instability to electron beam irradiation (15 kV; PC = $0.1 \cdot 10^{-6} \text{A}$) is manifested by the decreasing count rate for sodium. Decrease occurs not only under a stationary focussed beam, but also under a focussed beam sweeping an area of 300 square microns (glass #2). In no case did sodium follow the migration pattern described by Borom and Hanneman (1967) who observed a substantial increase in the sodium count rate with time. The ease of migration of sodium seems to be related to the presence of uranyl ions. Indeed, of the three glasses numbered 1, 2 and 3 (table 12), the least stable is the uranium glass even though it contains less sodium than the other two. It may be that in the presence of the large dumbbell-shaped uranyl ions, silica forms a loose glass-framework. Temperatures of the samples at the point of impact were calculated from the equation developed by Friskney and Haworth (1967), (Appendix III). For a focussed beam (15 kV; PC = $1.0 \cdot 10^{-6} \text{A}$) striking a carbon coated obsidian sample, the estimated temperature is 218°C. At such a temperature, sodium oxide will not volatilize. Some other process is needed to explain the decreasing count rate. If this temperature (218°C) is realistic or even underestimated by a factor of three, the beam could not have melted the sample and therefore the mechanism proposed by Lineweaver (1963) does not apply.

The experiments suggested the following sequence of events:

- 1 - neutralization of sodium at the surface of the specimen by the impinging electrons;
- 2 - evaporation of sodium metal and formation of a concentration gradient. The vapour pressure of sodium metal at 150-200°C is 10^{-4} to 10^{-6} torr similar to that in the sample chamber. Such temperatures are comparable with the estimated temperature (218°C).
- 3 - the concentration gradient induces diffusion from the interior of the specimen to the point of impact. At this stage, migration would be controlled by the diffusion coefficient, which is controlled by the concentration gradient (at the temperatures considered).

No other experiments were carried out with additives such as lithium and potassium. The first cannot be analysed with the electron microprobe and the second would have posed problems from overlapping peaks (K-K α and U-M β).

1700°C maximum

Glasses 11,12,13 and 15 (table 9) are stable beneath the electron beam under normal analytical conditions. Glass samples were produced as truncated cones 0.8 cm high, and 1 cm to 1.5 cm across. Contamination by the recrystallized alumina crucible was detected in all four charges but did not extend more than 2 mm from the crucible into the glass. It was not possible to make a series of

glass standards combining uranium with a number of commonly associated elements all in sufficient amounts (about 5 wt%).

This follows from the compositional restrictions arising from the presence of a glass-former in sufficient amounts (40%) and from the high temperatures required (in many instances, higher than 1700°C).

CHAPTER VI

ANALYSIS OF STANDARD MATERIALS

To test the analytical approach, known compounds were analysed. Results are compared with the known and theoretical compositions and, in the case of most mineral specimens, with analytical results taken from the literature.

A- GLASSES

1. GLASSES 11, 12, 13, AND 15

Compositions for glasses 11, 12, 13, and 15 are given in table 13. With the exception of glass 15, it appears that aluminium contamination has occurred over the entire volume of the glasses. In general, the microprobe data corrected by FEPAC agree best with the composition of

the initial powders while data corrected by COR-2 agree well with the wet chemistry results. Because of the difference in aluminium contents between the powders and the corresponding glasses, the latter do not constitute reliable standards.

As shown in table 14, corrections for fluorescence by the continuum are small. Most important are the atomic number and absorption effects. This arises from the difference in average atomic number between the glasses and the standards. (Standards used are listed in table 10, for general analyses; in table 13, and 16 for the analyses of glasses 11, 12, 13, and 15; and glasses A, B, D, and E respectively.) The overall correction factor as calculated by both COR-2 and FEPAC (tables 14 and 15) are important for all elements concerned with the exception of calcium.

2. GLASSES A, B, D, AND E

The presence of molybdenum in our results and its absence in the theoretical composition¹ (table 16) is probably the most striking difference between these sets of values. Molybdenum comes from contamination of the glasses by the molybdenum container during fusion. Glasses were prepared according to the method described by Smellie (1972). With the exception of glass B, other values do not

¹ composition obtained from weighing the constituents

agree very well. The differences are best seen when the atomic proportions of the main constituents are compared. In table 17, the atomic proportions of aluminium, silicon and calcium are recalculated to 100. It can be seen that the theoretical proportions for all four glasses are similar. Our results show variable proportions from one glass to the other with aluminium being low. The discrepancies between theoretical and microprobe compositions cannot be due to the effect of thorium and uranium since the compositions of the glasses with the highest amounts of thorium and uranium, namely E and B, are in better agreement than those with less thorium and uranium. Also, the amounts of uranium and thorium are rather low compared with the differences observed. Discrepancies are found whichever correction program is utilized i.e., COR-2 (table 16) or FEPAC (table 18). This suggests that the discrepancies in composition are real and arise from contamination by molybdenum and probably from segregation of the other constituents during fusion. Corrections for continuum fluorescence are negligible. Atomic number and absorption corrections are very important for molybdenum, thorium and, uranium. This arises from the markedly different average atomic number of the glasses compared to those of the standards (PbMoO_4 , ThO_2 , and UO_2). Silicon, aluminium and calcium were analysed against a plagioclase standard.

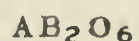
B- MINERALS

1. EUXENITE

Discrepancies between the two sets of analytical results can be seen for major and minor elements (table 19). These arise, at least in part, from the higher sensitivity of the methods used by Smellie et al. (1978); indeed, some elements determined by atomic absorption spectrophotometry, flame emission spectrophotometry and neutron activation analysis were not detected by the microprobe. Another likely reason is the presence of impurities in the aliquots analysed by Smellie, a concentration of 0.12 wt% MnO, for example, would have been detected by the microprobe had it been present in the excited volume of this sample. Our low total is due to water (reported by Smellie et al., 1978) and perhaps to other volatile elements which were not determined.

Differences can be appreciated by expressing the analysis in terms of the general formula for euxenite, and by comparing the distribution of rare-earths with that of other euxenite analyses.

The group formula of euxenite is:



where A = U, Th, Fe⁺², Ca, REE;

and B = Ti, Ta, Nb, Fe⁺³.

On this basis one finds for Smellie's analysis:

sum of A = 35.16

sum of B = 64.84 including all iron as Fe^{+3}

Microprobe results can be calculated to yield the group formula:

sum of A = 33.33 including 0.34 Fe^{+2}

sum of B = 66.67 including 1.52 Fe^{+3}

It can be seen that our result agrees with the theoretical formula for euxenite ($A/B = 1/2$) while those of Smellie will at best yield an A/B ratio of 1/1.84.

The distribution of rare-earths for both analyses are compared to those of eight samples taken from the literature (fig. 6). The trend of the microprobe results is in good agreement with the average trend of other euxenite samples (Butler, 1958) while that of Smellie et al. (1978) disagrees, mainly for gadolinium and neodymium.

Three facts support the validity of our results:

- 1- The presence of unexpected elements in the analysis of Smellie et al. (1978), such as aluminium, potassium and magnesium. These likely come from mineral impurities.
- 2- The distribution of rare-earths in our analysis is in better agreement with that of other euxenite analyses (fig. 6).
- 3- Finally, our results are in good agreement with the

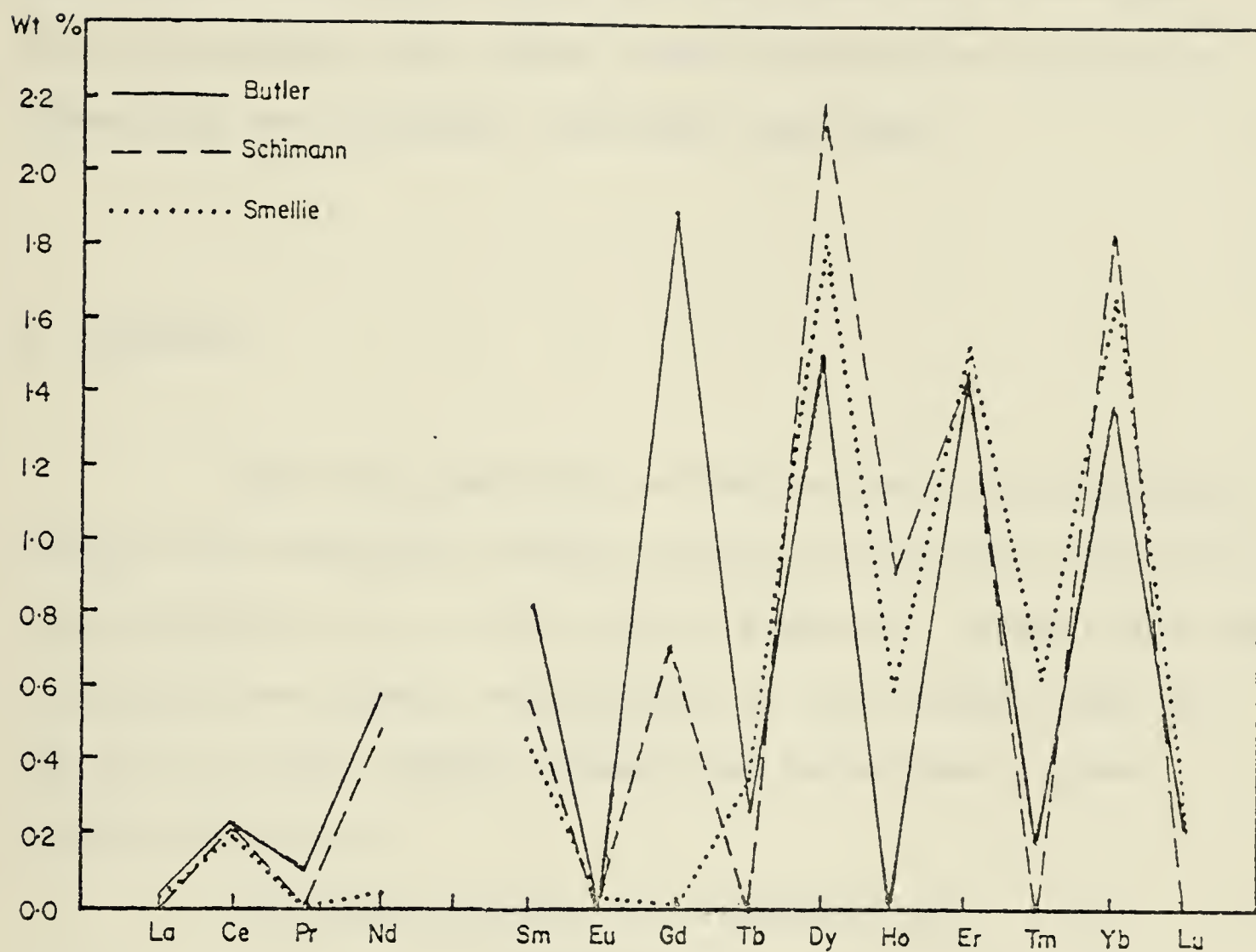


Figure 6. Distribution of rare-earth elements in the euxinite standard in weight percentages, as analysed by Smellie (1975) and by Schimann, compared to the average distribution for 8 euxinite samples analysed by Butler (1958). The samples of Butler are from South-West Africa, Nansek (Uganda), Vegusdal and Arendal (Norway), Fitamalama (Madagascar), Brazil, and Rio Lagone (Mozambique). For a better comparison, the average values for Butler's analyses were recalculated for a sum equal to the average sum of rare-earths in Smellie's and Schimann's analyses.

structural formula of euxenite.

As can be seen in table 20, the corrections for fluorescence are low except for tantalum and ytterbium, while absorption and atomic number effects are important, especially for niobium, tantalum, and lead.

2. DAVIDITE

Some discrepancies in the two sets of analytical results from davidite (table 21) can be seen for major and minor elements. As in the case of euxenite, reasons for this difference are higher sensitivity of the methods used by Smellie, and the likely presence of impurities in his mineral aliquots.

The group formula for davidite is:



where A = U, Ca, Zr, Th, Fe^{+2} , REE;

and B = Ti, Fe^{+3} , V, Cr.

On this basis the analysis of Smellie et al. (1978) gives:

sum of A = 23.67, including 16.63 Fe^{+2}

sum of B = 70.90, including 13.74 Fe^{+3} .

Our results yield:

sum of A = 24.37, including 18.63 Fe^{+2}

sum of B = 73.10, including 15.81 Fe^{+3} .

In the first case the Fe^{+2}/Fe^{+3} ratio is equal to 0.55, in

the second it is 0.54. Because the oxidation states of iron thus calculated agree very well with each other, it is concluded that the discrepancies in composition are real i.e., that the composition given by Smellie is different from that of our specimen because the original material was not homogeneous.

Corrections for microprobe analysis are listed in table 22, and standards used are given in table 10. The continuum fluorescence effect is low although not always negligible while the other three factors are important.

3. META-AUTUNITE

Our results for meta-autunite (table 23) are in very good agreement with the theoretical and synthetic meta-autunite, although phosphorus is somewhat higher than expected. The concentration of phosphorus was checked using several different standards and different operating voltages, and essentially the same results were obtained. Undoubtedly this analysis shows that we can recognise the mineral from its composition.

4. META-URANOCIRCITE

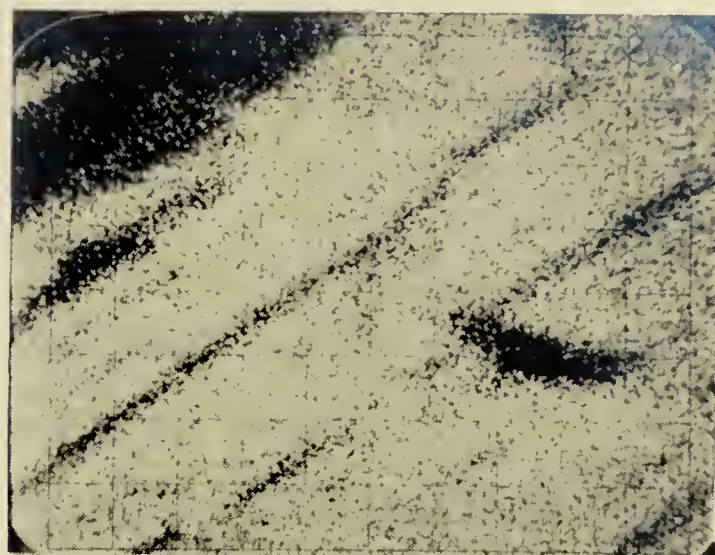
Table 24 shows the compositions of metatorbernite and meta-uranocircite. Our analysis falls between these two end-members but closer to meta-uranocircite. The relatively low sum for the cations in our results ($\text{Ca} + \text{Cu} + \text{Ba} = 0.86$) is caused by the segregation of barium into cleavage planes. It is not known whether this segregation occurs during analysis or during sample preparation, but scanning photographs show local concentrations of barium and perhaps copper (plate 1). X-ray powder diffraction and microscopic examination on separate fractions revealed the presence of only one compound, with properties close to those of meta-uranocircite. The phosphorus and uranium contents and their atomic proportions are in excellent agreement with both theoretical compositions and with previous analyses.

5. SABUGALITE

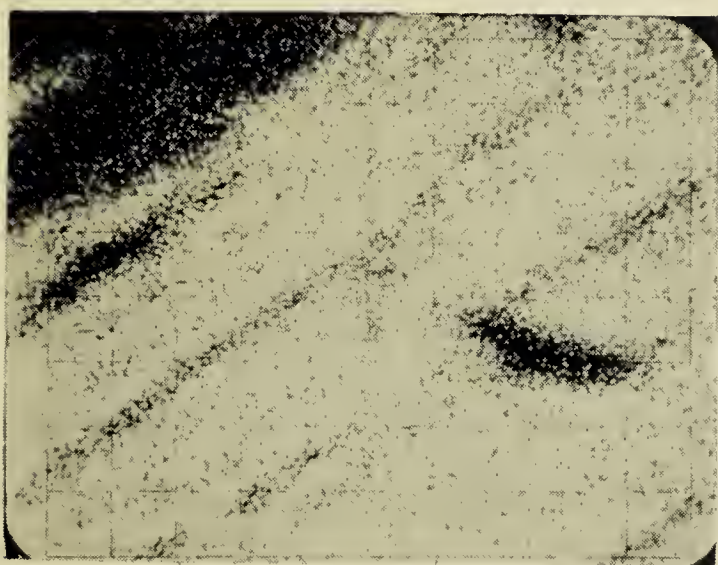
The mineral we have analysed was identified as sabugalite by X-ray diffraction (Table 25). Our results (Table 26) are in excellent agreement with the uranium and phosphorus contents and atomic proportions of theoretical and analytical compositions of sabugalite (natural and synthetic). The aluminium content of our analysis is relatively high compared with the type material (sample 3)



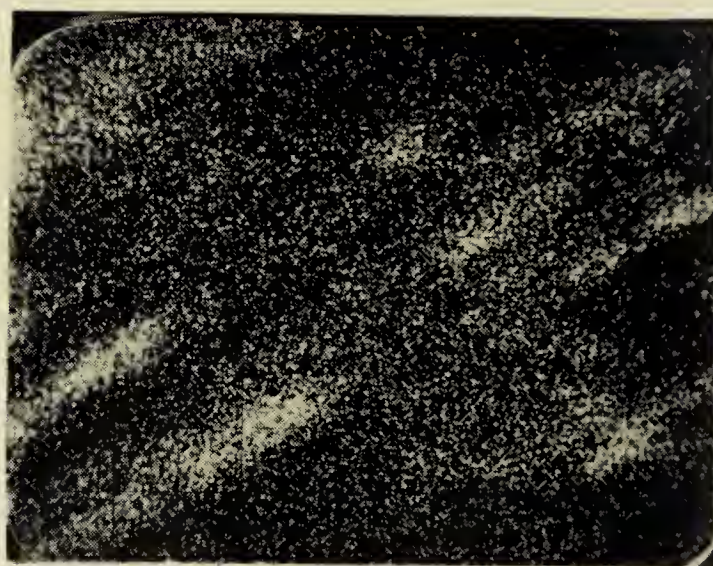
bs



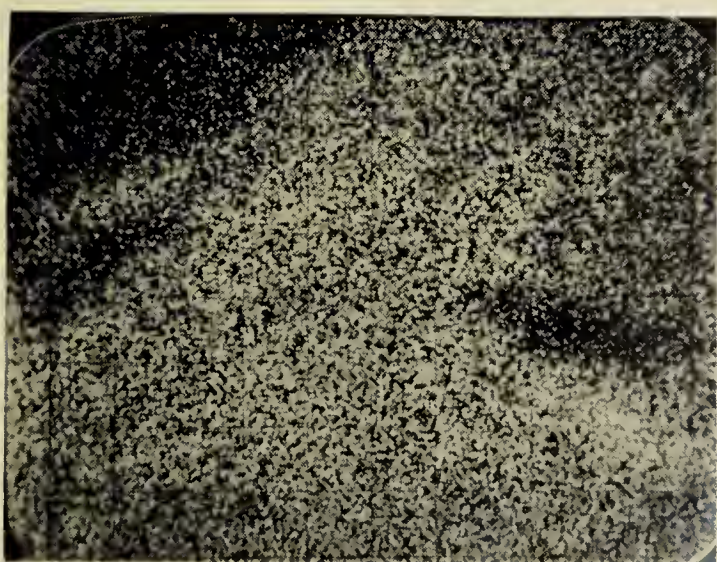
P



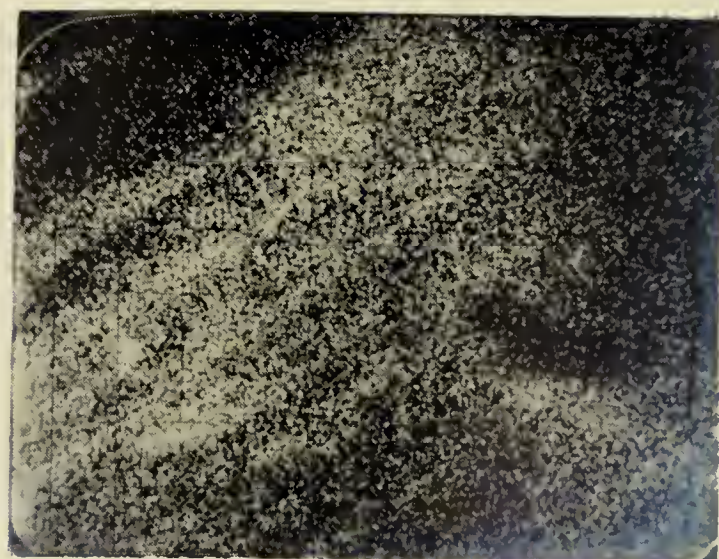
U



Ba



Cu (background)

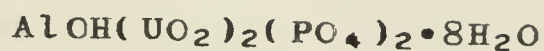


Cu

0 25 50
microns

Plate I : Backscattered electron (bs) and elemental photographs of 'meta-uranocircite'.

and the theoretical composition but not incompatible with the synthetic 'sabugalite' (sample 4). Three analyses using different standards led to similar results suggesting the following structural formula:



where OH is grouped together with Al for charge compensation. Because of the highly hydrated character of the mineral, investigation by infra-red and Raman spectroscopy did not yield any information on the nature of hydrogen and oxygen in sabugalite, *i.e.*, on their presence as OH, H or H₃O in addition to H₂O.

In light of these facts it appears that in sabugalite, the aluminium content may vary without much change in the cell dimensions.

6. CARNOTITE

Our results (table 27) agree well with other analyses of carnotite, especially when the composition is recalculated on the basis of an 'ideal' water content of 5.98%. Potassium is low and water calculated by difference is high compared with the theoretical values. This high apparent water content is probably due to the presence of impregnation and mounting materials in the excited volume during microprobe analysis. This is likely as carnotite, in our specimen, occurred only as a fine coating (about 20

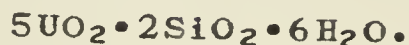
micron thick) on quartz and feldspar grains of an arkose sample. The discrepancy in the potassium content is not surprising since the analysis of potassium existing with uranium poses interference problems and K-K β line is used. Considering this difficulty our results are very satisfactory, and carnotite is easily recognized and characterized by such analyses.

7. β -URANOPHANE

Table 28 shows analyses of β -uranophane. The material we analysed formed a very thin film (20-30 micron thick) on a rock specimen. It is very fine-grained and somewhat porous so that the plastic used as an impregnating and mounting material is probably present in the excited volume during microprobe analysis. This is responsible for the apparent high water content. When our results are recalculated to 100% on the basis of the theoretical water content, the analysis is very similar both to those previously reported and to the theoretical composition.

8. SODDYITE

Our results (table 29) compare very well with the previous analysis of the type material. When iron and lead are grouped together with uranium in the calculation of the structural formula, results agree best with:



The precision of microprobe analysis, however, does not allow us to make a definite choice between the two possible structural formulae for soddyite.

9. THOROGUMMITE

Our results (table 30) yield a high total; this is probably caused by the loss of P_2O_5 , together with water when H_2O^+ was determined on a separate fraction. Phosphorus would then be included twice in the total, firstly as P_2O_5 (in the microprobe determination) and, secondly as part of ' H_2O^+ '. Our silicon and calcium contents are very high relative to other analysis.

10. URANOTHORIANITE

Our results (table 31) agree well with the theoretical composition and with other analyses taken from the literature and especially with sample 3. All three samples (2, 3 and 4) are from Ceylon.

C- CONCLUSIONS

Compositions of glasses determined by various methods are not in perfect agreement. Discrepancies in the aluminium content of glasses 11, 12, and 13 are opposite to those of glasses A, B, D, and E. In both cases these discrepancies are, at least in part, due to the procedures of glass synthesis. In practice, these glasses do not constitute good analytical standards.

The determination of magnesium in the presence of uranium, when corrections are applied through COR-2, is not satisfactory. It appears that the corrections made are not suitable for magnesium, nor probably for other elements of lower atomic number, such as, sodium. It can be expected that the sodium concentrations would also be underestimated in the presence of thorium.

From analyses of mineral specimens using the techniques outlined in a previous chapter, it appears

possible to obtain accurate determinations of the compositions of uranium and thorium minerals using the electron microprobe. It has proven feasible not only to identify these minerals in situ but also to obtain completely plausible values for minor concentrations.

Corrections to our data are important because the elements involved are of widely differing atomic numbers and also because standards and unknowns have very different average atomic numbers. A comparison between data corrected by FEPAC and COR-2 shows not only the remaining inadequacy of our knowledge concerning the precise size of the matrix effects, but also the usefulness of the applied corrections.

It appears that corrections applied by FEPAC give better results than those applied by COR-2. Owing to the fact that FEPAC does not print out detailed ZAF corrections¹, it is difficult to trace back the sources of the differences in the results. Better results, however, may in part arise from the standardization of the various parameters needed through the use of mathematical expressions. Because these parameters are linked, not only in theory, but also by their mathematical expressions, they are more compatible with the group treatment effected to correct for interactions of the various elements.

¹ The data were run through FEPAC by Dr Springer in Toronto, using the original version of the programme.

Comparisons between analytical compositions and stoichiometric compositions of minerals show that minerals can easily be identified by microprobe. Deviation from stoichiometry for both microprobe results and analyses of other workers, may be due to imprecise determinations, but also to the unusually large error that will arise when structural formulae are calculated from weight concentrations where heavy elements, such as uranium, thorium, and lead dominate. This is best exemplified by soddyite for which no definite structural formula has yet been accepted. Atomic proportions of the major constituents in minerals containing heavy and light elements, are in general better established from structural determinations rather than through chemical analyses.

Precision and accuracy expected in the analysis of uranium and thorium minerals are best illustrated by euxenite and davidite. It appears possible to study any zonal or other variations in mineral chemistry and, of course, to identify minerals; but special care must be taken when comparing minerals determined by different methods. This inconvenience is largely compensated by the ability to analyse for all constituents (with $Z > 9$) from a small area i.e. enough to avoid mineral separation and contamination.

Finally, it should be pointed out that hydrated uranium minerals lose only part of their water in the course of analysis.

Table 13. Composition in weight percentages of glasses 11, 12, 13, 15, and total correction factor for the combined effect of sample and standard (CF) for microprobe data computed through FEPAC. Oxygen is calculated by stoichiometry. Standards are listed below.

Glass-11			Glass-13		
	wt%	CF		wt%	CF
Mg	4.40	1.169	Mg	4.30	1.377
Al	15.82	1.126	Al	17.50	1.101
Si	17.03	1.169	Si	17.33	1.162
Ca	5.16	1.002	Ca	5.26	0.994
U ⁴⁺	16.89	1.385	Th	16.21	1.380
O	40.69		O	39.74	
Total	99.99		Total	100.34	

Glass-12			Glass-15		
	wt%	CF		wt%	CF
Mg	4.35	1.152	Mg	2.76	1.186
Al	16.76	1.114	Al	15.07	1.120
Si	16.58	1.169	Si	16.32	1.157
Ca	5.18	1.003	Ca	5.01	0.992
Zr	1.66	1.472	Ti ⁴⁺	1.28	1.082
Th	6.95	1.402	V ⁵⁺	2.51	1.201
U ⁴⁺	7.14	1.426	U ⁴⁺	15.99	1.378
O	41.35		O	41.07	
Total	99.97		Total	100.01	

Standards

Mg: MgO	V: V-metal
Al: corundum	Zr: zircon
Si: quartz	Th: ThO ₂
Ca: plagioclase glass	U: UO _{2.1}
Ti: rutile	

Table 14. Composition in weight percentages of glasses 11, 12, 13, and 15, correction factors for atomic number (Z), absorption (A), characteristic fluorescence (F), continuum fluorescence (Fc), and total correction factor for the combined effect of sample and standard (CF) for microprobe data computed through COR-2.

Glass-11						
	mprobe	Z	A	F	Fc	CF
Mg	3.88	0.960	1.083	0.991	0.999	1.029
Al	16.71	0.971	1.233	0.994	0.999	1.189
Si	17.91	0.955	1.289	1.000	0.999	1.229
Ca	5.10	0.963	1.032	1.000	0.999	0.992
U ⁺⁴	15.27	1.340	0.935	0.995	1.001	1.249
O	41.93					
Total	100.80					
Glass-12						
	mprobe	Z	A	F	Fc	CF
Mg	4.07	0.964	1.130	0.990	0.999	1.078
Al	17.89	0.976	1.223	0.994	0.999	1.189
Si	17.58	0.959	1.294	0.999	0.999	1.240
Ca	5.18	0.968	1.037	1.000	0.998	1.001
Zr	1.63	1.198	1.209	0.999	1.000	1.444
Th	5.82	1.341	0.878	0.995	1.001	1.173
U ⁺⁴	6.40	1.347	0.947	0.999	1.003	1.278
O	42.97					
Total	101.50					
Glass-13						
	mprobe	Z	A	F	Fc	CF
Mg	4.49	0.961	1.173	0.990	0.999	1.115
Al	18.10	0.973	1.267	0.994	0.999	1.224
Si	18.02	0.956	1.338	1.000	0.999	1.277
Ca	5.19	0.964	1.051	1.000	0.999	1.012
Th	15.07	1.336	0.885	0.995	1.001	1.178
O	43.73					
Total	104.60					
Glass-15						
	mprobe	Z	A	F	Fc	CF
Mg	2.46	0.958	1.110	0.991	0.999	1.053
Al	15.90	0.970	1.227	0.994	0.999	1.181
Si	17.15	0.953	1.277	1.000	0.999	1.216
Ca	4.97	0.961	1.028	0.997	0.998	0.984
Ti ⁺⁴	1.26	1.021	1.059	1.000	0.996	1.074
V ⁺⁵	2.30	0.992	1.128	1.039	1.000	1.162
U ⁺⁴	14.41	1.338	0.932	0.995	1.001	1.242
O	41.92					
Total	100.37					

Table 15. Composition in weight percentages of glasses 11, 12, 13, and 15. Values for the initial powders (powder) and analytical results obtained from wet chemistry (wchem) and microprobe corrected through COR-2 and FEPAC are compared.

Glass-11				
	powder	wchem	COR-2	FEPAC
Mg	4.49	4.35	3.88	4.40
Al	15.77	16.76	16.71	15.82
Si	17.35	17.09	17.91	17.03
Ca	5.34	5.12	5.10	5.16
U ⁺⁴	16.02	15.87	15.27	16.89
O	41.03	41.42	41.93	40.69
Total	100.00	100.61	100.80	99.99

Glass-12				
	powder	wchem	COR-2	FEPAC
Mg	4.47	4.39	4.07	4.35
Al	15.68	16.07	17.89	16.76
Si	17.31	16.75	17.58	16.58
Ca	5.30	5.10	5.18	5.18
Zr	1.82	2.12	1.63	1.66
Th	7.05	5.74	5.82	6.95
U ⁺⁴	7.08	6.76	6.40	7.14
O	40.13	43.53	41.42	41.35
Total	100.00	100.46	101.50	99.97

Glass-13				
	powder	wchem	COR-2	FEPAC
Mg	4.46	4.38	4.49	4.30
Al	15.64	18.02	18.10	17.50
Si	17.33	16.94	18.02	17.33
Ca	5.30	5.07	5.19	5.26
Th	16.29	14.07	15.07	16.21
O	40.98	42.16	43.73	39.74
Total	100.00	100.64	104.60	100.34

Glass-15				
	powder	wchem	COR-2	FEPAC
Mg	2.77	2.83	2.46	2.76
Al	15.09	14.51	15.90	15.07
Si	16.65	16.47	17.15	16.32
Ca	5.08	4.89	4.97	5.01
Ti ⁺⁴	1.29	1.61	1.26	1.28
V ⁺⁵	2.35	2.30	2.43	2.51
U ⁺⁴	15.71	17.16	14.41	15.99
O	41.06	40.37	41.92	41.07
Total	100.00	100.14	100.37	100.01

Table 16. Composition in weight percentages of glasses A, B, D, and E, correction factors for atomic number (Z), absorption (A), characteristic fluorescence (F), continuum fluorescence (Fc), and total correction factor for the combined effect of sample and standard (CF) for microprobe data computed through COR-2. Theoretical (theor) and analytical (mprobe) compositions are compared; oxygen is calculated by stoichiometry. Standards are listed below.

Glass A							
	theor.	mprobe	Z	A	F	Fc	CF
Al	16.43	15.32	0.997	1.021	1.000	1.000	1.018
Si	19.61	19.90	0.997	0.984	1.000	1.000	0.980
Ca	18.64	18.64	0.997	1.001	1.000	1.000	0.998
Mo ⁺⁵	-	0.96	1.252	1.042	0.992	1.002	1.296
U ⁺⁴	0.78	0.70	1.385	0.914	0.993	1.005	1.265
O	44.53	44.52					
Total	99.99	100.04					

Glass B							
	theor.	mprobe	Z	A	F	Fc	CF
Al	15.92	15.81	0.988	1.051	1.001	1.000	0.997
Si	18.74	18.74	0.988	1.007	1.000	1.000	0.997
Ca	17.90	17.87	0.988	1.006	1.000	0.999	0.994
Mo ⁺⁵	-	0.29	1.241	1.051	0.993	1.002	1.302
U ⁺⁴	4.05	3.80	1.372	1.372	0.994	1.004	1.255
O	43.38	43.36					
Total	99.99	99.87					

Glass D							
	theor.	mprobe	Z	A	F	FC	CF
Al	16.41	15.16	0.992	1.024	1.000	1.000	0.992
Si	19.64	19.94	0.992	0.985	1.000	1.000	0.965
Ca	18.57	18.68	0.992	1.002	1.000	1.000	0.996
Mo ⁺⁵	-	0.85	1.246	1.043	0.993	1.003	1.293
Th	0.89	0.78	1.371	0.849	0.976	1.002	1.138
O	44.49	44.59					
Total	100.00	100.00					

Glass E							
	theor	mprobe	Z	A	F	Fc	CF
Al	15.86	15.12	0.995	1.066	1.001	1.000	1.058
Si	18.66	19.31	0.995	1.011	1.000	1.000	1.001
Ca	17.85	18.21	0.994	1.012	1.000	1.000	1.006
Mo ⁺⁵	-	0.51	1.249	0.993	1.002	1.003	1.300
Th	5.17	3.84	1.375	0.854	0.978	1.002	1.148
O	42.47	42.70					
Total	100.01	99.69					

Standards

Al: anorthoclase glass
Si: anorthoclase glass
Ca: anorthoclase glass

Mo: PbMoO₄
Th: ThO₂
U: UO_{2.1}

Table 17. Atomic proportions of Al, Si, and Ca in glasses A, B, D, and E for a sum Al + Si + Ca equal to 100. Theoretical and analytical (COR-2) values are compared.

	Glass A		Glass B	
	theoretical	analytical	theoretical	analytical
Al	34	33	34	34
Si	39	41	39	39
Ca	26	27	26	27

	Glass D		Glass E	
	theoretical	analytical	theoretical	analytical
Al	34	32	34	33
Si	39	41	39	40
Ca	26	27	26	27

Table 18. Composition in weight percentages of glasses A, B, D, and E and, total correction factors for the combined effect of sample and standard (CF) for microprobe data computed through FEPAC. Oxygen is calculated by stoichiometry.

	Glass A		Glass B	
	wt%	CF	wt%	CF
Al	15.26	1.013	15.58	1.025
Si	19.81	0.975	18.49	0.984
Ca	18.81	0.996	17.55	0.998
Mo ⁺⁵	1.13	1.362	0.34	1.357
U ⁺⁴	0.83	1.423	4.45	1.413
O	44.17		43.49	
Total	100.01		99.90	

	Glass D		Glass E	
	wt%	CF	wt%	CF
Al	15.07	1.015	14.66	1.023
Si	19.82	0.975	18.82	0.975
Ca	18.67	0.997	18.21	2.996
Mo ⁺⁵	0.99	1.363	0.59	1.351
Th	0.98	1.424	4.73	1.408
O	44.41		42.94	
Total	99.94		99.95	

Table 19. Composition of euxenite in weight percentages and in atomic proportions as obtained by wet chemistry and neutron activation (Smellie) and by electron microprobe. Atomic proportions have been calculated on a water- and oxygen-free basis.

	wt%		at.prop.	
	Smellie	mprobe	Smellie	mprobe
Na	0.08	n.d.	0.44	-
Mg	0.05	n.d.	0.27	-
K	0.02	n.d.	0.07	-
Ca	0.83	0.26	2.58	0.85
Mn	0.12	n.d.	0.26	-
Cu	0.02	n.d.	0.04	-
Zn	0.02	n.d.	0.04	-
Y	11.81	12.27	16.54	17.62
La	0.03	n.d.	0.22	-
Ce	0.19	0.21	0.16	0.19
Nd	0.04	0.49	0.04	0.44
Sm	0.47	0.58	0.39	0.49
Eu	0.03	n.d.	0.03	-
Gd	n.d.	0.73	-	0.63
Tb	0.36	n.d.	0.27	-
Dy	1.83	2.19	1.41	1.72
Ho	0.59	0.92	0.46	0.72
Er	1.52	1.44	1.13	1.10
Tm	0.64	n.d.	0.47	-
Yb	1.65	1.82	1.19	1.34
Lu	0.24	n.d.	0.17	-
Pb	0.76	1.17	0.46	0.72
Th	4.18	4.18	2.24	2.30
U	9.61	9.59	5.03	5.14
Fe	0.78	0.81	1.73	1.85
Al	0.26	0.02	1.22	0.10
Si	0.02	n.d.	0.08	-
Ti	14.45	13.74	37.54	36.66
Nb	18.04	19.65	24.28	27.00
Ta	1.76	1.65	1.21	1.16
O	25.71	24.86		
H ₂ O ⁺	3.21	N.D.		
H ₂ O ⁻	0.07	N.D.		
Total	99.87	96.58	100.00	100.00

n.d. : not detected

N.D. : not determined

Table 20. Composition in weight percentages of euxenite and correction factors for atomic number (Z), absorption (A), characteristic fluorescence (F), continuum fluorescence (Fc), and total correction factor for the combined effect of sample and standard (CF) for microprobe data computed through COR-2. Oxygen was calculated by stoichiometry.

	wt%	Z	A	F	Fc	CF
Al	0.02	0.863	1.172	1.002	0.999	0.911
Ca	0.26	0.834	1.111	0.991	0.997	0.947
Ti	13.74	0.874	1.092	0.998	0.997	0.988
Fe	0.81	0.818	1.034	0.997	1.000	0.876
Y	12.27	0.921	1.080	0.995	0.999	1.031
Nb	19.65	1.023	1.206	0.998	0.999	1.283
Ce	0.21	0.846	1.034	0.998	0.997	0.898
Nd	0.49	0.848	1.048	0.999	1.001	0.926
Sm	0.58	0.846	1.037	0.999	1.000	0.920
Gd	0.73	0.845	1.031	1.000	1.002	0.916
Dy	2.19	0.834	1.025	1.002	1.002	0.895
Ho	0.92	0.832	1.033	1.000	1.002	0.891
Er	1.44	0.830	0.020	0.999	1.001	0.881
Yb	1.82	0.833	1.010	0.999	0.996	0.873
Ta	1.65	1.024	1.001	1.000	0.983	1.277
Pb	1.17	1.134	1.115	0.999	1.001	1.312
Th	4.18	0.862	1.102	1.000	1.000	0.990
U	9.59	0.859	1.097	0.980	1.00	0.974
O	24.86					
Total	96.58					

Table 21. Composition of davidite in weight percentages and in atomic proportions as obtained by wet chemistry and neutron activation analysis (Smellie, 1976), and by electron microprobe. Atomic proportions have been calculated on a water- and oxygen-free basis.

	wt%		at.prop.	
	Smellie	mprobe	Smellie	mprobe
Na	0.07	n.d.	0.25	-
Mg	0.16	0.22	0.56	0.76
K	0.03	n.d.	0.07	-
Ca	0.58	0.20	1.26	0.42
Mn	0.07	n.d.	0.11	-
Cu	0.02	n.d.	0.03	-
Zn	0.04	n.d.	0.05	-
La	4.31	2.89	2.71	1.76
Ce	1.68	1.90	1.04	1.14
Nd	<0.04	n.d.	<0.03	-
Sm	<0.01	n.d.	<0.01	-
Eu	<0.01	n.d.	<0.01	-
Gd	<0.01	n.d.	<0.01	-
Tb	<0.01	n.d.	<0.01	-
Dy	<0.04	n.d.	<0.03	-
Ho	0.04	n.d.	<0.03	-
Er	0.08	n.d.	0.04	-
Tm	<0.09	n.d.	<0.04	-
Yb	0.08	0.07	0.04	0.03
Lu	<0.09	n.d.	<0.04	-
Pb	0.73	0.77	0.31	0.31
Th	0.21	n.d.	0.08	-
U	8.22	7.70	3.01	2.74
Fe	19.44	22.71	30.37	34.44
Al	0.69	0.35	2.22	1.09
Si	0.06	n.d.	0.17	-
Ti	28.54	30.05	51.97	53.14
V	0.58	n.d.	0.99	-
Cr	2.57	2.55	4.30	4.15
O	31.79	29.91		
H ₂ O ⁺	0.68	N.D.		
H ₂ O ⁻	0.05	N.D.		
Total	101.02	99.32	100.00	100.00

n.d.: not detected

N.D.: not determined

Table 22. Composition in weight percentages of davidite and correction factors for atomic number (Z), absorption (A), characteristic fluorescence (F), continuum fluorescence (Fc), and total corrections factor for the combined effect of sample and standard (CF) for microprobe data computed through COR-2. Oxygen was calculated by stoichiometry.

	wt%	Z	A	F	Fc	CF
Mg	0.22	1.305	0.922	0.999	1.006	1.202
Al	0.35	1.163	0.947	1.006	1.000	1.110
Ca	0.20	1.009	0.918	0.955	0.995	0.880
Ti	30.05	1.028	0.964	0.983	0.997	0.976
Fe	22.71	1.028	0.909	1.000	1.011	0.948
Cr	2.55	1.047	1.045	0.976	0.997	1.072
La	2.89	0.982	0.936	0.983	0.998	0.906
Ce	1.90	0.984	0.936	0.981	0.998	0.908
Yb	0.07	1.017	0.933	1.000	1.014	0.985
Pb	0.77	1.007	1.245	0.995	1.000	1.252
U	7.70	0.973	0.945	0.945	0.997	0.876
O	29.91					
Total	99.32					

Table 23. Composition of autunite and meta-autunite in weight percentages and recalculated structural formulae on the basis of 12 oxygen ions.

Sample	1	2	3	4	5	6	7
CaO	5.69	5.31	6.56	5.3	7.17	5.8	6.14
MgO	-	-	0.26	-	-	n.d.	-
SrO	-	-	-	0.34	-	n.d.	-
UO ₂	-	-	-	3.07‡	-	N.D.	-
UO ₃	58.00	60.84	58.85	56.91	63.00	62.2	62.58
P ₂ O ₅	14.39	13.40	14.80	14.8	15.95	17.5	15.53
H ₂ O	21.92	20.33	19.60	18.3	13.84	14.5	15.75
Total	100.00	99.98	100.07	98.72	99.96	100.0	100.00
Ca	1	1.06	1.13	0.81	1.13	0.90	1
Mg	-	-	0.01	-	-	-	-
Sr	-	-	-	0.03	-	-	-
U ⁺⁶	2	2.11	1.99	1.70	1.95	1.90	2
P	2	1.84	2.02	1.78	2.00	2.16	2
O	12	12.00	12.00	12.00	12.00	12.00	12
H ₂ O	12	11.18	10.51	8.66	6.83	6.89	8

- 1 Theoretical composition of autunite: $\text{CaO} \cdot 2\text{UO}_3 \cdot \text{P}_2\text{O}_5 \cdot 12\text{H}_2\text{O}$.
- 2 Autunite: Autun, France; Church (1875).
- 3 Autunite: Mount Painter, South Australia; Greig analyst, in Smith (1926).
- 4 Autunite: Mt. Spokane, Washington; Leo (1960), (average composition of dark green autunite). ‡uraninite impurity
- 5 Autunite: synthetic; Fairchild (1929). Probably meta-autunite.
- 6 Meta-autunite, Hummer Mine, Paradox Valley, Colorado; microprobe analysis (Cameron-Schimann). H₂O is calculated by difference.
- 7 Theoretical composition of meta-autunite I : $\text{CaO} \cdot 2\text{UO}_3 \cdot \text{P}_2\text{O}_5 \cdot 8\text{H}_2\text{O}$.

n.d.: not detected

N.D.: not determined

Table 24. Composition of metatorbernite and meta-uranocircite in weight percentages and calculated structural formulae based on 12 oxygen ions.

Sample	1	2	3	4	5	6
SiO ₂	-	0.40	n.d.	-	-	-
CaO	-	-	0.4	3.40	-	-
CuO	8.49	8.50	2.5	-	-	-
BaO	-	-	8.9	5.80	14.57	15.16
UO ₃	61.00	59.67	64.2	58.10	56.86	56.56
P ₂ O ₅	15.14	14.00	16.1	14.65	15.06	14.04
H ₂ O	15.37	15.00	7.9	17.55	13.99	14.24
Total	100.00	97.57	100.0	99.50	100.48	100.00
Si	-	0.07	-	-	-	-
Ca	-	-	0.06	0.37	-	-
Cu	1	1.03	0.28	-	-	-
Ba	1	-	0.52	0.60	0.87	1
U ⁺⁶	2	2.63	2.01	1.99	1.90	2
P	2	1.91	2.04	2.02	2.02	2
O	12	12.00	12.00	12.00	12.00	12
H ₂ O	8	8.07	3.30	9.56	7.12	8

- 1 Theoretical composition of metatorbernite:
CuO•2UO₃•P₂O₅•8H₂O.
- 2 Metatorbernite(?): Gunnis Lake Mine, Cornwall; Pisani (1861).
- 3 Metatorbernite - meta-uranocircite: Vogtland, Saxony; microprobe analysis (Cameron-Schimann). H₂O is calculated by difference.
- 4 Meta-uranocircite - autunite: Saint-Priest-La-Prugne, France; Chervet and Courtault analyst, in Chervet (1960).
- 5 Meta-uranocircite: Falkenstein; Winkler analyst in Weisbach (1877).
- 6 Theoretical composition of meta-uranocircite:
BaO•2UO₃•P₂O₅•8H₂O.

Table 25. 'd'-spacings for sabugalite (X-ray powder diffraction). In the first two columns, the spacings and intensities from material from Sabugal, Portugal (Fron del, 1951) are listed. In the last two columns, the spacings and intensities for our specimen from Cisco, Utah are given. s:strong; m:moderate; f:weak.

'd' (Å) I		'd' (Å) I	
9.69	10	9.51	s
6.56	1		
5.59	1		
4.86	9	4.87	s
4.39	4	4.46	m
3.47	8	3.44	s
3.36	1		
3.22	1/2		
3.06	1/2		
2.82	1	2.62	f
2.45	2	2.46	m
2.39	2	2.37	f
2.19	6	2.19	m
1.70	1	1.85	f
1.73	1	1.74	f
1.64	1/2	1.63	f
1.55	1	1.55	f
1.36	1	1.35	f

Table 26. Compositions of sabugalite in weight percentages and calculated structural formulae based on 24 oxygen ions.

Sample	1	2	3	4
Al ₂ O ₃	2.87	6.21	2.65	4.85
UO ₃	64.41	67.51	65.22	63.10
P ₂ O ₅	15.99	18.40	16.08	15.40
H ₂ O	16.73	7.88	15.93	16.80
Total	100.00	100.00	99.88	100.15
Al	1	1.92	0.94	1.70
U	4	3.69	4.12	3.93
P	4	4.02	4.10	4.05
O	24	24.00	24.00	24.00
H ₂ O	16	7.70	15.98	16.62

- 1 Theoretical composition of sabugalite:
 $\text{HAL}(\text{UO}_2)_4 \cdot (\text{PO}_4)_4 \cdot 4\text{H}_2\text{O}$.
- 2 Sabugalite: Cisco, Utah; microprobe analysis (Cameron-Schimann); H₂O is calculated by difference.
- 3 Sabugalite: Mina da Quarta Feira, Sabugal, Portugal; Gonyer analyst, in Frondel (1951). Ca, Mg, Ba, Cu, Fe, Mn, and As were not detected.
- 4 Synthetic 'sabugalite'; Mogin analyst, in Frondel (1958).

Table 27. Composition of carnotite in weight percentages and recalculated structural formulae based on 12 oxygen ions.

Sample	1	2	3	4	5
Na ₂ O	-	0.35	0.16	n.d.	n.d.
K ₂ O	10.44	9.58	10.00	8.5	9.3
CaO	-	0.64	0.66	n.d.	n.d.
MgO	-	0.22	0.30	n.d.	n.d.
Fe ₂ O ₃	-	0.04	0.55	n.d.	n.d.
UO ₃	63.42	65.62	62.26	57.8	63.1
V ₂ O ₅	20.16	21.12	20.57	19.9	21.6
H ₂ O	5.98	1.35	4.90	13.8	6.0
Rem.	-	0.48	0.37	-	-
Total	100.00	99.40	99.77	100.0	100.0
K	2	1.74	1.86	1.75	1.75
U	2	2.01	1.96	1.95	1.95
V	2	2.03	2.04	2.11	2.11
O	12	12.00	12.00	12.00	12.00
H ₂ O	3	0.65	2.45	7.40	2.93

- 1 Theoretical composition of carnotite:
2K₂O·2UO₃·2V₂O₅·3H₂O.
- 2 Carnotite: Cane Springs Pass, Utah; Hess and Foshag (1927). Rem. includes: Al₂O₃=0.16; insoluble=0.23; traces of CuO, PbO and P₂O₅.
- 3 Carnotite: Temple Mountain, Utah; Hillebrand (1924). Rem. includes: CuO=0.07; SO₃=0.26; insoluble=0.04.
- 4 Carnotite: unknown locality in Germany; microprobe analysis (Cameron-Schimann). H₂O is calculated by difference.
- 5 Analysis 4 recalculated on the basis of 'ideal' 6.0% (5.98%) H₂O.

n.d.: not detected

Table 28. Composition of β -uranophane in weight percentages and calculated structural formulae based on 11 oxygen ions.

Sample	1	2	3	4	5	6
CaO	6.55	7.32	7.1	6.1	6.3	6.7
UO ₃	66.80	66.29	66.9	66.5	63.0	67.2
SiC ₂	14.03	13.11	12.9	13.1	12.6	13.5
H ₂ O	12.62	12.87	12.6	14.3	18.1	12.6
CO ₂	-	tr	-	tr	-	-
Total	100.00	99.59	99.5	100.0	100.0	100.0
Ca	1	1.15	1.11	0.95	1.04	1.04
U	2	2.01	2.05	2.03	2.03	2.03
Si	2	1.91	1.87	1.90	1.94	1.94
O	11	10.94	10.74	10.83	10.84	10.84
H ₂ O	6	6.18	5.98	6.71	9.15	6.00

- 1 Theoretical composition of β -uranophane:
CaO·2UO₃·2SiO₂·6H₂O.
- 2 Uranophane: Joachimsthal; Nováček (1935), on 7.5 mg. CO₂ present in small amount of impurities, not determined.
- 3 Uranophane: Wölsendorf, Bavaria; Nováček analyst, in Steinocher and Nováček (1939), on 2mg..
- 4 Uranophane: Bigay, Puy-de-Dome, France; Branche et al. (1951).
- 5 β -Uranophane: Charlebois Lake, Saskatchewan; microprobe analysis (Cameron-Schimann). H₂O is calculated by difference.
- 6 Analysis 5 recalculated on the basis of 'ideal' 12.6% H₂O.

Table 29. Composition of soddyite in weight percentages and recalculated structural formulae based on 19 oxygen ions.

Sample	1	2	3	4
SiO ₂	7.51	7.24	7.87	7.8
Fe ₂ O ₃	-	-	-	0.5
PbO	-	-	-	1.7
UO ₃	86.19	86.24	85.27	87.4
H ₂ O	6.30	6.50	6.26‡	2.6
Total	100.00	100.00	100.00	100.0
Si	2.14	2.00	2.15	2.13
Fe	-	-	-	0.10
Pb	-	-	-	0.12
U	4.90	5.00	4.90	4.82
O	19.00	19.00	19.00	19.00
H ₂ O	5.72	6.00	5.68	2.51

- 1 Theoretical composition of soddyite for the structural formula: $12\text{UO}_3 \cdot 5\text{SiO}_2 \cdot 14\text{H}_2\text{O}$.
- 2 Theoretical composition of soddyite for the structural formula: $5\text{UO}_2 \cdot 2\text{SiO}_2 \cdot 6\text{H}_2\text{O}$.
- 3 Kasolo, Katanga district Belgian Congo (now Zaire); Schoep (1930) average of three partial analyses.
‡ probably 6.86% H₂O.
- 4 Katanga Belgian Congo (now Zaire); microprobe analysis (Cameron-Schimann); H₂O is calculated by difference.

Table 30. Composition of thorogummite in weight percentages and recalculated atomic proportions for the structural formula: $\text{Th} \cdot (1-4x)(\text{SiO}_4) \cdot 4(\text{OH})$. The amount of $(\text{OH})_4$ (i.e., x) has been calculated in amount needed for valence compensation of the cations.

Sample	1	2	3	4
ThO_2	41.44	24.46	21.20	43.1
UO_3	22.43	37.33	18.63	4.7
$(\text{Ce}, \text{La})_2\text{O}_3$		0.12	0.08	2.1
	6.69			
$(\text{Y}, \text{Er})_2\text{O}_3$		0.32	9.47	n.d.
Nb_2O_5	-	-	7.81	n.d.
CaO	0.41	1.62	-	10.0
MgO	-	0.16	-	n.d.
PbO	2.16	7.78	0.17	1.5
Al_2O_3	0.96	-	8.84	1.9
Fe_2O_3	0.84	-	2.84	n.d.
SiO_2	13.08	15.30	14.43	24.4
P_2O_5	1.19	-	2.65	2.4
H_2O^+	7.88	8.37	7.82	N.D.
H_2O^-	1.23	4.19	5.61	11.7
Rem	-	0.40	8.28	-
Total	98.32	100.05	100.05	101.8

Sample 1: $[\text{Th}_{0.49} \text{U}_{0.24}^{+6} \text{Ce}_{0.13} \text{Al}_{0.06} \text{Fe}_{0.03}^{+3} \text{Ca}_{0.02} \text{Pb}_{0.03}]$
 $[(\text{NbO}_4)_{0.67} (\text{PO}_4)_{0.5} ((\text{OH})_4)_{0.3}] \cdot 1.57\text{H}_2\text{O}$

Sample 2: $[\text{Th}_{0.01} \text{Pb}_{0.12}]$
 $[(\text{NbO}_4)_{0.87} ((\text{OH})_4)_{0.28}] \cdot 2.38\text{H}_2\text{O}$

Sample 3: $[\text{Th}_{0.19} \text{U}_{0.15}^{+6} \text{Nb}_{0.17} \text{Al}_{0.40} \text{Fe}_{0.09}]$
 $[(\text{SiO}_4)_{0.56} \text{PO}_4)_{0.09} ((\text{OH})_4)_{0.33}] \cdot 1.72\text{H}_2\text{O}$

Sample 4: $[\text{Th}_{0.35} \text{U}_{0.04}^{+6} \text{Ce}_{0.03} \text{Ca}_{0.39} \text{Pb}_{0.01} \text{Si}_{0.14} \text{Al}_{0.04}]$
 $[(\text{SiO}_4)_{0.75} (\text{PO}_4)_{0.07}] \cdot 1.30\text{H}_2\text{O}$

1 Thorogummite: Baringer Hill, Texas; Hidden and Mackintosh (1889). Atomic weight of rare-earths given as 135.

2 Thorogummite (nicolayite): Wodgina, Western Australia; Simpson (1930). Rem: $(\text{Nb}, \text{Ta})_2 \text{O}_5 = 0.40$.

3 Thorogummite: Haicheng Prefecture, South Manchuria; Yosimura and Yamada analysts in Hemmi (1951). Rem.: $\text{BeO} = 0.16$; $\text{SnO}_2 = 0.31$; $\text{Nb}_2\text{O}_5 = 7.81$. Atomic weight of (Y, Er) given as 120.

4 Thorogummite: Belafa, Madagascar; microprobe analysis (Cameron-Schimann). H_2O^- includes: loss between $110^\circ\text{C} = 4.86$; loss between $110^\circ - 750^\circ\text{C} = 5.98$; loss between $750^\circ - 1500^\circ\text{C} = 0.88$.

n.d.: not detected

N.D.: not determined

Table 31. Composition of uranothorianite in weight percentages and structural formulae based on 8 oxygen ions.

Sample	1	2	3	4	5
CaO	-	-	0.42	0.1	0.1
PbO	1.80	2.66	3.99	4.0	4.0
(Ce,La) ₂ O ₃	-	1.41	-	n.d.	n.d.
Fe ₂ O ₃	0.29	1.54	-	n.d.	tr
UO ₂	4.73	-	-	tr	-
U ₃ O ₈	-	14.54	27.94	-	29.6
UO ₃	-	-	-	25.2	-
ThO ₂	93.02	78.00	64.61	62.4	62.4
H ₂ O	-	-	0.14	2.9	2.9
Rem.	-	2.04	2.18	N.D.	N.D.
Total	99.84	100.19	97.28	94.6	99.0
Ca	-	-	0.07	0.02	0.02
Pb	0.10	0.11	0.17	0.18	0.18
Ce, La	-	0.07	-	-	-
Fe	0.05	0.18	-	-	-
U	0.23	0.49	0.98	0.98	1.09
Th	3.70	2.81	2.40	2.43	2.44
Rem.	-	0.28	0.17	-	-
O	8.00	8.00	8.00	8.00	8.00
H ₂ O	-	-	0.08	1.65	1.66

- 1 Thorianite: Betroka, Madagascar; Pisani analyst, in Lacroix (1922).
- 2 Thorianite: Ceylon; Kobayashi (1912). Rem: Sc₂O₃=0.46; CuO=0.02; SiO₂=0.20; ZrO₂=0.09; Al₂O₃=0.15; ignition loss=1.12.
- 3 Thorianite: Ceylon; Hecht (1933) Rem.: insoluble= 0.15; SnO₂(?)=0.31; REE=0.031; (Fe,Al)₂O₃=0.80; TiO₂=0.33; ZrO₂=0.56; H₂O includes loss between 110°-300°C = 0.04; loss between 300°-1000°C = 0.10.
- 4 Uranothorianite: Galle, Ceylon; microprobe analysis (Cameron-Schimann); H₂O includes: loss between 110°-300°C = 0.31; loss between 300°-1000°C = 2.55.
- 5 Analysis 4 with all U calculated as U₃O₈.

n.d.: not detected

N.D.: not determined

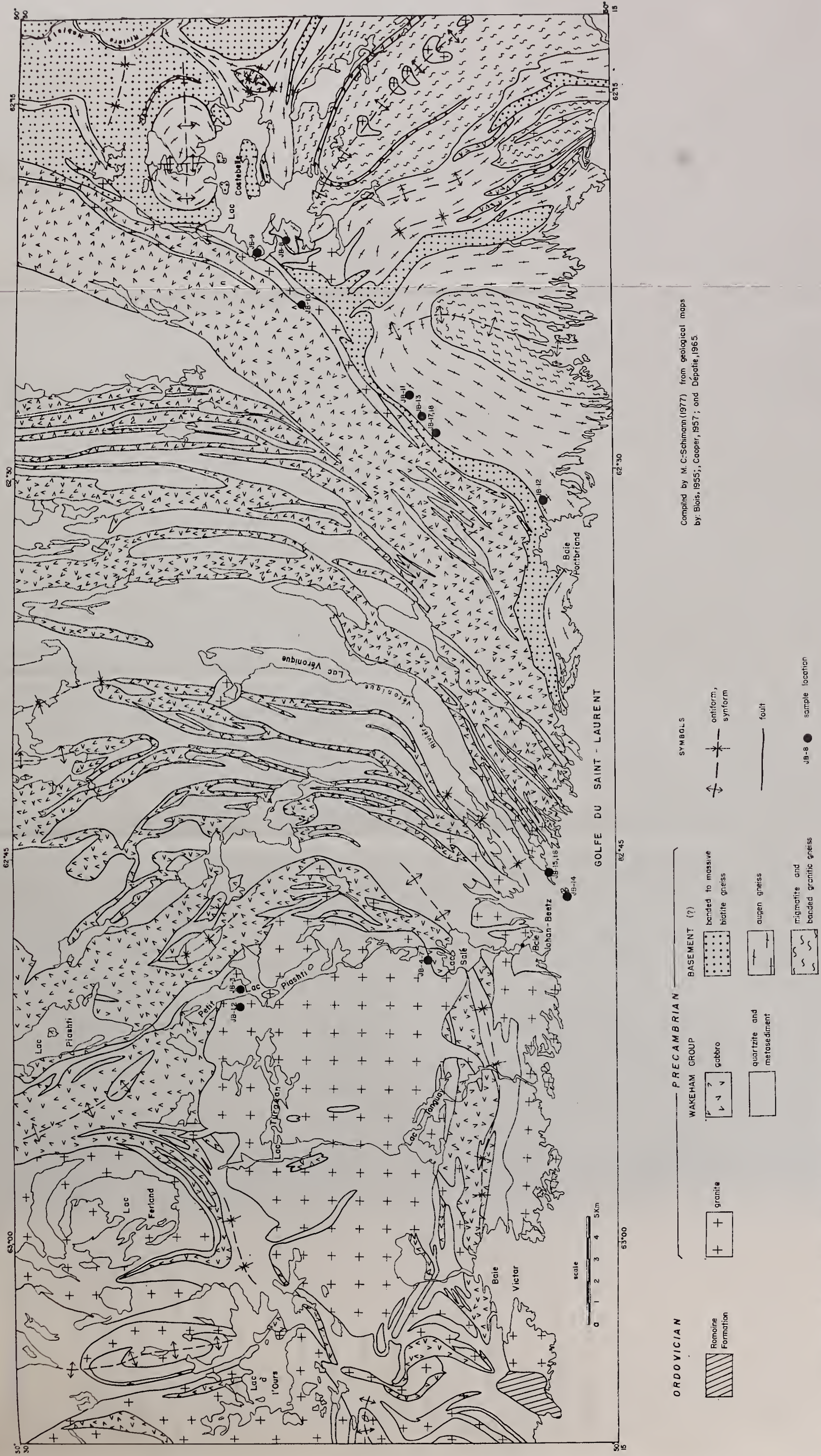
CHAPTER VII

BAIE JOHAN BEETZ

A- DESCRIPTION

1. LOCALIZATION

The Baie Johan Beetz region is part of the eastern Grenville Province. It is situated on the north shore of the Gulf of St. Lawrence in the vicinity of the village of Baie Johan Beetz, which is 55 km east of Havre St Pierre and 250 km east of Sept-Isles (fig. 7).



Compiled by M. C. Schumann (1977) from geological maps by: Blois, 1955; Cooper, 1957; and Dépatie, 1965.

Fig. 7 Geology of the Baie Johan Beetz area, Quebec, and location of samples.

2. PREVIOUS WORK

Mapping of the area (fig. 7) was done at a scale of 1 mi:1 inch by Dépatie (1964-1965), Cooper (1957) and Blais (1955). In 1975, the Geological Survey of Canada made an airborne gamma-ray spectrometer survey at a spacing of 5 km over the whole area and at a spacing of 1 km over the central part of the area.

Radioactivity in the area was first noted in the mid-fifties, but intensive exploration was not initiated until 1966 when a number of companies acquired mineral rights over the area. Search for uranium extended from the Saguenay River to Blanc Sablon. Results of the 1967 and 1968 seasons have been summarized by Baldwin (1970). Renewed activity since 1973 on many prospects has not yet defined any mineable uranium deposit. During the summer of 1976, the author had the opportunity to visit part of this area with K. Schimann while working on various prospects for Rouanda Mining Co. Ltd., a subsidiary of Texasgulf Inc..

3. GEOLOGY

The area (fig. 7) covers the southern part of a north-trending synclinal basin which extends over 3600 sq km. This basin is occupied by the Wakeham Group. The main units of this group are quartzites and calcareous quartzites cut by sills of gabbro; these rocks are metamorphosed into greenschist and amphibolite facies; they have been similarly deformed. A basement of quartzo-feldspathic gneisses, surrounds the basin. Metasediments, metagabbros and gneisses are cut by granites (Wynne-Edwards, 1972).

Quartzo-feldspathic gneisses, metasediments, metagabbros and granites all crop out in the Baie Johan Beetz area (fig. 7). The eastern part is occupied by migmatites and augen gneisses (quartzo-feldspathic gneisses). The major structural trends in this eastern part of the area are NW-SE and E-W. In the central and eastern parts of the area, the metasedimentary rocks and gabbros strike N-S to NE-SW and appear to wrap around the Lac Turgeon and the Lac Ferland granites. Smaller granitic bodies occur within the Wakeham Group where they are mostly concordant with the general structure, and within the migmatites where they also occupy the cores of major folds.

Paleozoic sediments are present in the southwestern part of the area (fig. 7).

Basement gneisses

Biotite gneiss, augen gneiss and migmatites occupy the eastern part of the map area (fig. 7). They have been briefly described by Blais (1955). Migmatites or banded granitic gneiss occupy the core of major anticlinal folds. The migmatites are flanked by augen gneiss, which in turn are bordered by quartzo-feldspathic hornblende-biotite gneiss or paragneiss (Blais, 1955).

Wakeham basin

The metasediments which occupy the Wakeham basin constitute the Wakeham Group (McPhee, 1959); they are cut by sills and dykes of metagabbro.

Wakeham Group

Metasediments are widely distributed over the central and western parts of the area (fig. 7), where they occur in bands of irregular width separated by sills of metagabbro. In the Baie Johan Beetz area, Cooper (1957) has distinguished two broad types of metasedimentary rocks. The first, by far the most common, includes fine-grained, light to dark grey, impure quartzites. Carbonate-, hematite-, and rutile-bearing quartzites are interbedded in small amounts. The second and minor type comprises micaceous quartzites, quartz-biotite schist and gneiss, and biotite schist; all are commonly interbedded with varying amounts of dark grey quartzite; rocks of this second type crop out east of Lac

Véronique. Minor amounts of coarsely crystalline limestone and a small lens of conglomerate have also been reported. The quartzites commonly exhibit primary bedding, and less frequently, ripple marks and cross-bedding. The stratigraphic relations between the two types of sediments, as reported by Cooper (1957), are not clear, but it seems reasonable to suppose that the stratigraphy proposed by Grenier (1957) for the Lake Beetz area, a region located immediately north of the Baie Johan Beetz area, is also valid for the latter; the more so in that it corresponds to the probable stratigraphy in the Victor Lake area, northwest of the Baie Johan Beetz area. In Lake Beetz area, Grenier (1957) recognized a stratigraphic sequence composed as follows: in ascending order, "first are the quartzose schists interstratified with impure quartzites, then relatively pure quartzites, succeeded finally by calcareous quartzites and phyllitic beds interstratified with pure quartzites." A geological map of Victor Lake area (Sharma, 1973) shows pelitic paragneisses with interlayered quartzitic bands in its upper parts, overlain by calcareous quartzites; the upper unit contains a marker horizon of black schist and pink crystalline limestone. These metasediments are wrapped around massifs of gneissic granite which could be interpreted as basement gneiss domes (K. Schimann, pers. comm., 1976; Bourne et al., 1977).

Thus it appears that the first type of metasediments distinguished by Cooper (1957) corresponds to

the upper part of the Wakeham Group while the second corresponds to the lower part.

Migmatites have been described by Cooper (1957). They occur east of Baie Victor and between Baie Johan Beetz and Baie Pontbriand. They are composed of rocks of the Wakeham Group and of amphibolites injected and partially assimilated by granitic material. The migmatites east of Baie Victor seem to be associated with the contact with the granite while the others, east of Baie Johan Beetz, are situated at the boundary between basement gneisses and the Wakeham Group.

Metagabbros

In the area shown in figure 7, metagabbros underlie a surface about half the size of that of the metasediments. They intrude rocks of the Wakeham Group in sill-like bodies and, locally, also occur as dykes and small discordant bodies; they are older than the granites which contain inclusions of both metagabbros and metasediments. Fresh gabbros have been reported in neighbouring areas only (Claveau, 1949; Grenier, 1957). In the Baie Johan Beetz area, the metagabbros are characterized by complete uralitization of pyroxenes, saussuritization and albitization of plagioclase and to a lesser extent, by introduction of alkalies, tourmaline and apatite. Cooper (1957) has divided them into four types, based on their degree of alteration, namely: uralite gabbro, amphibolite,

amphibolite gneiss and hybrid rocks i.e., hornblende-rich rock and quartz diorites. He reports: "The change from gabbro to amphibolite and from this to gneiss and finally to hybrid rocks is gradual. Uralite gabbro is found in the northern two-thirds of the area and amphibolite in the southern third. The remaining two types are much more local and form phases of the series (gabbroic) in the vicinity of granite, where the alteration is more intense. Amphibole gneiss occurs on the east side of the main granite mass (Lac Turgeon granite), and hybrid rocks on the south side."

Younger intrusive rocks

The younger intrusions are of granitic composition and occur throughout the whole area shown in figure 7. On the basis of their size, they may be divided into two types:

- 1- large bodies such as the Lac Turgeon and the Lac Ferland granites;
- 2- smaller masses, sills and dykes.

Both types are very heterogeneous in texture, ranging from fine-grained to pegmatitic; their composition varies from granite to quartz diorite. In general they contain abundant inclusions of basement gneisses and of quartzites, arkoses, biotite schists, and amphibolites of the Wakeham Group.

1- Large bodies

Their relation with the country rocks is controversial. Cooper (1957) has reported that the intrusive character of the Lac Ferland and the Lac Turgeon granites is evident since these exhibit cross-cutting relations with the surrounding rocks and because large tongues of granite cut indiscriminately across both the metasediments and the metagabbros. Hauseux (1976), on the other hand, has reported that the contact between the Lac Turgeon granite and the metasediments is either sharp or diffuse, and mostly conformable to bedding but can transgress it abruptly. "Sedimentary bedding can often be traced into the neighbouring granite; elsewhere, the granite is banded parallel to sedimentary bedding but is isolated from the actual sediments." It should be noted that the Lac Ferland granite is coarser grained than the Lac Turgeon granite.

2- Smaller masses, sills, and dykes

These occur in the Wakeham Group around the Lac Turgeon granite and in the basement gneisses to the west. They tend to be concordant to the general or structural trend either as sills or as small masses in the core of folds of basement gneisses. In general, they are more pegmatitic than the large bodies, in particular a phase of white muscovite pegmatite often with graphic texture is common within this group but rare in the large bodies where it is only found in the border zone.

Paleozoic sediments

Paleozoic sediments occur in the south-western part of the Baie Johan Beetz area (fig. 7). They are represented by the Lower Ordovician Romaine Formation which consists of stromatolitic dolomite with a thin basal veneer of orthoquartzitic sandstone (Poole et al., 1970).

4. CHRONOLOGICAL RELATIONSHIPS

The oldest rocks of the Baie Johan Beetz area (fig. 7) are the migmatites and augen gneisses. The Wakeham Group rests on the migmatites and gneisses; it begins with quartzose schists and impure quartzites with minor pelitic bands followed upwards by white quartzites which contain about 10 percent feldspar and minor biotite and muscovite; above these, the quartzites become fine-grained, dark grey, calcareous, and may be thinly bedded and intercalated with phyllites. The sediments are cut by sills and dykes of gabbro. Sedimentary rocks and gabbros have been metamorphosed and deformed similarly. Basement rocks, metasediments and metagabbros are cut by granites (Cooper, 1957; Grenier, 1957).

5. METAMORPHISM

The degree of metamorphism of the Wakeham Group is difficult to ascertain because of the lack of characteristic assemblages. Metamorphic minerals in the terrigenous sediments of the Wakeham Group in the Baie Johan Beetz area, are: muscovite, biotite, garnet, epidote, chlorite, amphibole and scapolite; in the crystalline limestone, the assemblage calcite + diopside + orthoclase has been described (Cooper, 1957). These place the degree of metamorphism in greenschist to amphibolite facies.

The gabbros vary from unmetamorphosed in certain parts of Lac Beetz area (Grenier, 1957), to uralite gabbros with the assemblage albite + tremolite-actinolite, or, albite + blue-green hornblende in the northern two thirds of Baie Johan Beetz area, and finally to amphibolite with the assemblage oligoclase-andesine + green hornblende + cumingtonite in the southern third of the latter. The above indicate a southward increase from greenschist to mid-amphibolite facies. This trend is corroborated by observations of Bourne *et al.* (1977) who have placed the metasediments of the northern end of the Wakeham basin (*i.e.*, approximately 50 km north of Baie Johan Beetz area) in the middle to upper greenschist facies.

A southward increase in metamorphic grade also correlates with the style of intrusion of the granites. Indeed, truly discordant intrusions occur in the northern

part of the basin, for example the two granitic bodies mapped by Sharma and Jacoby (1973) some 35 km north of the Baie Johan Beetz area; while, in the southern part, the intrusions are less distinctly discordant, like the Lac Turgeon granite, to mostly concordant, like the small masses and sills.

Superimposed on the regional metamorphic trend is a metasomatic alteration of the metagabbros related to the granites. This alteration is marked by the presence of scapolite and tourmaline increasing in amount toward the intrusions.

6. MINERALIZATION

The north shore of the Gulf of St. Lawrence is a uranium-thorium metallogenic province, the main known occurrences are near Sept-Iles, Baie Johan Beetz, Romaine and St Augustin. The host rocks of uranium and thorium are masses, dykes, and sills of granitic rocks.

In the Baie Johan Beetz area, the main showings are located in the Lac Turgeon granite, and in smaller bodies in the vicinity of the village of Baie Johan Beetz and west of Lac Costebelle. The U/Th ratio of the granites ranges from 0.1 to 10 with values clustering between 1.5 and 4.

Within the granites, radioactivity occurs either

in small pods 0.3 to 30 m in diameter or disseminated over larger surfaces (150 m in diameter). On a regional scale, Hauseux (1976) reports that "zones of uraniferous pods lie in broad bands which are approximately parallel to sedimentary bedding." This has also been observed by K. Schimann (pers. comm., 1977) but only for radiometric anomalies in granitic sills intruding either the Wakeham Group near the margin of the Lac Turgeon granite or the basement gneisses in the eastern part of the area.

Hauseux (1976) has studied the mode of occurrence of uranium in the Lac Turgeon granite. Her work has revealed "that uranium mineralization is confined to the plagioclase-rich granite characterized by brick-red feldspar, smoky quartz, magnetite, a coarse to pegmatitic grain size, and rarer uranium stain." She proposed that "the bulk of uranium is contained within metamict zircon and sparse microscopic uraninite, and also within magnetite maybe as submicroscopic uraninite from which uranium could be leached and relocated in fracture-filling matrices." Phosphuranylite and uranophane have also been reported but they represent only a minor amount of uranium.

7. CONSIDERATIONS ON THE ORIGIN OF THE GRANITES

In the Baie Johan Beetz area (fig. 7), the uranium appears confined to the granites. Therefore, knowledge of their mode of origin may shed light on the origin of the uranium mineralization in this part of the Grenville Province.

Features of the granite pertaining to their genesis are:

- 1- contact relations with the country rocks;
- 2- structural position;
- 3- composition;
- 4- type of inclusions.

1- Contact relations : Contact between the granites and their country rocks is variable. The granites are truly discordant north of the Baie Johan Beetz area (fig. 7), less discordant in the case the Lac Turgeon granite and mostly concordant in that of the smaller masses and sills. Contacts between sills and gabbros are usually sharp while those between sills and quartzites may be gradational.

2- Structural position : Emplacement of the granites appears highly dependant on the structure and competence of the country-rocks as they tend to be situated in position of less resistance. In the metasediments and metagabbros, the granites occur mostly as sills between the sediments and the gabbros, and, for the Lac Turgeon granite, as a major

antiformal structure; in the basement gneisses, they occur mostly in the noses of folds or as sills. The Lac Ferland granite seems to cut across a synclinal structure of Wakeham Group rocks and metagabbros; according to Cooper (1957) this granite predates the Lac Turgeon granite.

3- Composition : Average mineralogical compositions of the Lac Turgeon and the Lac Ferland granites are given below (table 32). These compositions are compatible with compositions obtained from the anatexis of quartzofeldspathic rocks of micaschists at temperatures of 650° to 750°C and pressures, (H₂O) of 2 to 6 kb (Winkler, 1974).

Table 32. Average mineralogical composition of the Lac Turgeon and Lac Ferland granites, from petrological study by Cooper (1957).

	Lac Turgeon	Lac Ferland
Quartz	25-35	25
biotite	5-15	15
K-feldspar	30-45	40
plagioclase	15-25	20
	(An ₁₄₋₁₇)	(An ₁₉)

4- Type of inclusions : The Lac Turgeon granite includes fragments of metagabbros and metasediments of the Wakeham Group. The frequency of inclusions of the various types of metasediments seems to be correlated with their relative amount in the Wakeham Group east of it. It should be noted that arkose inclusions are also present; arkoses are found

in the Victor Lake area (Sharma, 1973), though none have been described in the Baie Johan Beetz area. No inclusions of basement gneisses were identified. The inclusions in the Lac Turgeon granite occur in elongated zones reminiscent of the sedimentary bedding.

Information pertaining to the genesis of the granites may also be gathered from observations on the surrounding rocks and general geology:

- 1- composition of the Wakeham Group;
- 2- composition of the basement gneisses;
- 3- presence and type of migmatites;
- 4- metamorphic zonation.

1- Composition of the Wakeham Group : On the whole the Wakeham Group is highly siliceous. Certain compositions likely to yield large amounts of anatectic melts, like biotite schists and gneisses, form only a small proportion of the Wakeham Group. Arkosic formations have been reported in the Victor Lake area (Sharma, 1973) some 35 km north of the Baie Johan Beetz area, but none have been found among the sediments of the latter.

2- Composition of the basement gneisses : These are mostly quartzo-feldspathic gneisses and so ideal starting material for the generation of large amounts of anatectic melt.

3- Presence and type of migmatites : Migmatites occur in the vicinity of the Lac Turgeon granite and between Baie Johan Beetz and Baie Pontbriand. They are considered to be

injection gneisses and thus a product rather than a source of granitic melt. It should be noted also that the small granitic masses and sills are more abundant in the southern part of the Baie Johan Beetz area.

4- Metamorphic zonation : Metamorphism increases from North to South in the Wakeham basin and ranges from greenschist to amphibolite facies.

Hypothesis for the formation of the granites

A hypothesis for the formation of the granites needs to account for:

1- mechanism: anatexis in situ or intrusion from a deeper source.

2- source rock: Wakeham Group or basement rocks.

1- Mechanism : Metamorphism in the Wakeham basin corresponds to temperatures lower than that required for the formation of an anatectic melt, therefore, the granites could not be formed in situ . This is emphasized by the presence of injection migmatites only and by the absence of migmatites formed by segregation of granitic liquid.

2- Source rock : The basement rocks have a granitic composition and are a suitable source for large amount of granitic melt while rocks of the Wakeham Group likely to yield granitic melt, are present in minor quantities. In addition, the proportions of various types of sediments occurring as inclusions in the Turgeon granite are similar to those found in the Wakeham Group outside. This makes the

formation of granitic melt by partial anatexis of suitable members of the Wakeham Group, unlikely. Also, in the area (fig. 7), uranium is associated with granitic material only, and no significant radioactivity has been registered anywhere in the metasediments.

The hypothesis proposed for the formation of the granites is thus: fusion of basement rocks within deeper levels of the crust and intrusion at the various levels at which they are now observed.

B- ANALYSIS

Eighteen samples were collected in the Baie Johan Beetz region; their location is shown on figure 7. All were chosen from zones of high radioactivity independant of rock type. Identifications and petrographic descriptions for these samples are given in appendix IV.

The main constituents for all the samples are quartz, plagioclase, K-feldspar, and often biotite. Muscovite and garnet may also be present. Minor constituents include: chlorite, calcite, magnetite, ilmenite, apatite, sphene, brookite, stilpnomelane, uraninite, monazite, allanite, titanobetafite, xenotime and churchite, zircon, thorogummite, and samarskite.

Phases investigated in more detail are uraninite,

titanobetafite, samarskite, allanite, xenotime and churchite, thorogummite, and zircon. Apatite is uranium free in our samples, it was not analysed quantitatively.

1. URANINITE

Uraninite is automorphous to roundish, generally fractured, and occasionally hematized. In some samples fractures in the uraninite are filled by a slightly greenish, opaque material; some grains are made of this material only, while others are free of it. In general, uraninite tends to cluster together with other accessory minerals such as zircon, monazite, and xenotime.

The uraninite has a fairly uniform composition; no zoning could be detected. Its constituents are uranium, lead, thorium, rare-earths, yttrium, and minor amounts of calcium, iron, and silicon. Results of analyses are listed in table 33. Calcium, iron, and silicon were analysed; their content is uniform from one grain to another; they sum to 0.5-0.7 wt% when calculated as oxides ($\text{Fe}_2\text{O}_3 = 0.11$, $\text{CaO} = 0.38$, $\text{SiO}_2 = 0.16$ wt%). Rare-earth content is low and was determined for two specimens only, those with the highest rare-earth contents. One is from granitic material (JB-1B), while the other is from fracture filling material (JB-9). The rare-earth content is equal to 1.06 wt% in JB-1B ($\text{La}_2\text{O}_3 = 0.09$; $\text{Ce}_2\text{O}_3 = 0.21$; $\text{Nd}_2\text{O}_3 = 0.21$; $\text{Sm}_2\text{O}_3 = 0.15$; $\text{Er}_2\text{O}_3 =$

0.20; $\text{Gd}_2\text{O}_3 = 0.20$ wt%) and 2.02 wt% in JB-9 ($\text{Ce}_2\text{O}_3 = 0.36$; $\text{Nd}_2\text{O}_3 = 0.35$; $\text{Sm}_2\text{O}_3 = 0.40$; $\text{Er}_2\text{O}_3 = 0.45$; $\text{Gd}_2\text{O}_3 = 0.46$ wt%). In the other specimens rare-earth elements do not exceed 1 wt% (as oxides). For our analyses, oxygen is calculated

Table 33. Composition in weight percentages of uraninites from the Baie Johan Beetz region and average correction factors for microprobe data ('ZAF'). Not included in the results below are iron, silicon, and calcium oxides which make up 0.5 to 0.7 wt%.

Sample	Y_2O_3	REE_2O_3	PbO	ThO_2	UO_2-3	Total
JB-1A	1.18	N.D.	11.49	4.56	74.46	91.69
JB-1B	1.05	1.06	11.49	3.41	75.18	92.19
JB-4A	1.54	N.D.	12.72	6.02	71.43	91.71
JB-4B	1.09	N.D.	13.43	5.19	76.06	95.77
JB-4C	0.81	N.D.	13.53	5.78	75.80	95.92
JB-6A	1.37	N.D.	13.32	6.25	74.41	95.35
JB-6B	0.81	N.D.	13.36	5.78	75.80	93.75
JB-7A	1.69	N.D.	11.75	6.17	74.22	95.83
JB-7B	0.81	N.D.	13.21	9.02	72.31	95.35
JB-9	2.74	2.02	11.74	4.90	75.15	96.55
JB-13	3.06	N.D.	12.13	9.11	67.08	91.38
<hr/>						
	Y		Pb	Th	U	
'ZAF'	0.88		1.20	0.99	1.08	

N.D.: not determined

stoichiometrically for divalent lead, tetravalent uranium, and an amount of hexavalent uranium equivalent to the amount of lead present. As can be seen, all totals are low; this is unlikely to be the result of inaccuracy in the corrections since the standards for the main constituents have characteristics close to those of uraninite, i.e., corrections applied are small (table 33) with the exception

of lead which has a high absorption correction (1.17); low totals are imputed in part to silicon, iron, and calcium not being included in the totals and rare-earths not being determined for most specimens; these elements sum up to 1.7 wt% or less (as oxides). Other reasons for the low totals are the presence of carbonaceous matter and perhaps other volatiles such as helium which may be included in the grains or mineral structure, a higher oxidation state for uranium (and lead?), and hydration of the mineral. The presence of carbonaceous matter is suggested by the observation of an opaque grey, slightly greenish material which occurs together with uraninite in samples JB-4, 6 and 7. That material yielded little characteristic radiation under the electron beam. Peaks that could be detected corresponded to uranium, lead, and in some cases, to silicon. Rare-earths and thorium were not identified. One analysis of a particularly 'heavy element-rich' zone gave:

Pb: 0.26 wt%

U : 0.44 wt%

No other elements were detected.

Age

Calculation of an approximate age for the formation of uraninite was attempted. Since we have measured only elemental concentrations and not isotopic concentrations, basic decay formulae need to be somewhat simplified. We know that:

$$\text{Pb}^{206} = \text{U}^{238} (\exp(\lambda^{238}t) - 1) \quad (1)$$

$$\text{Pb}^{207} = \text{U}^{235} (\exp(\lambda^{235}t) - 1) \quad (2)$$

$$\text{Pb}^{208} = \text{Th}^{232} (\exp(\lambda^{232}t) - 1) \quad (3)$$

where λ is the decay constant. Assuming that lead in uraninite is solely of radiogenic origin, we can write:

$$\begin{aligned} \text{Pb} = & \text{U}^{238} (\exp(\lambda^{238}t) - 1) + \text{U}^{235} (\exp(\lambda^{235}t) - 1) \\ & + \text{Th}^{232} (\exp(\lambda^{232}t) - 1) \end{aligned} \quad (4)$$

The approximate power expansion of $\exp(\lambda t)$ is:

$$\exp(\lambda t) = 1 + \lambda t - (\lambda t)^2/2 \dots \quad (5)$$

When dates of about 1000 Ma are calculated, an error of about 1.5% is made when neglecting all terms but the first two in the right part of equation (5). This equation then becomes:

$$\exp(\lambda t) = 1 + \lambda t \quad (6)$$

Substituting (6) in (4):

$$\text{Pb} = \text{U}^{238}(\lambda^{238}t) + \text{U}^{235}(\lambda^{235}t) + \text{Th}^{232}(\lambda^{232}t) \quad (7)$$

The isotopic ratio of $\text{U}^{238}/\text{U}^{235}$ at present is 137.88 (Steiger and Jäger, 1977) i.e.:

$$\text{U}^{238} = 0.9927\text{U} \quad (8)$$

$$\text{U}^{235} = 0.0072\text{U} \quad (9)$$

where U is the total uranium content.

Th^{232} constitutes the whole of thorium (Th).

Replacing isotopic contents in (7) by atomic proportions yields:

$$\text{Pb} = 0.9927\text{U}(\lambda^{238}t) + 0.0072\text{U}(\lambda^{235}t) + \text{Th}(\lambda^{232}t) \quad (10)$$

When t is isolated, equation (10) becomes:

$$t = \frac{\text{Pb}}{U((0.9927\text{E}^{238}) + (0.0072\text{E}^{235})) + (\text{Th}\text{E}^{232})} \quad (11)$$

When values for E are introduced, equation (11) becomes:

$$t = \frac{\text{Pb } 10^{10} \text{ y}}{1.612\text{U} + 0.495\text{Th}} \quad (12)$$

It should be noted that when dates are calculated from analyses of elements as opposed to isotopic determinations, the following constraints arise:

- 1- The values obtained will not take account of possible diffusion of the elements concerned.
- 2- All Pb in the grains studied must be of radiogenic origin.

Because diffusion of the daughter product often takes place, the values thus calculated, will constitute minimum ages. When isotopic ratios are measured the above constraints can be alleviated by the use of concordia plots.

Ages thus calculated for eleven uraninites are listed in table 34. A histogram (fig. 8) shows two populations, one at 1152 Ma and a second at 1317 Ma.

Table 34. Approximate ages of uraninites from the Baie Johan Beetz region. Details of the calculations are given in the text; Averages and standard deviations are calculated for the two populations distinguished in figure 8.

sample	age (Ma)
JB-4A	1313
JB-4B	1306
JB-4C	1319
JB-6A	1340
JB-6B	1301
JB-7A	1166
JB-7B	1330
JB-13	1310
JB-1A	1146
JB-1B	1140
JB-9	1158
average	1317
standard deviation	14
average	1152
standard deviation	12

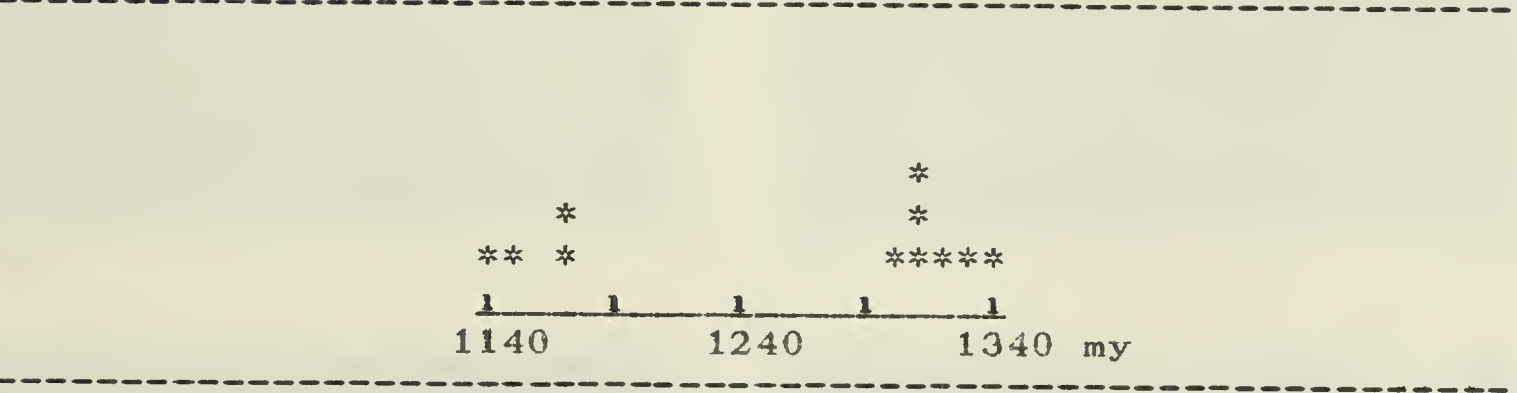
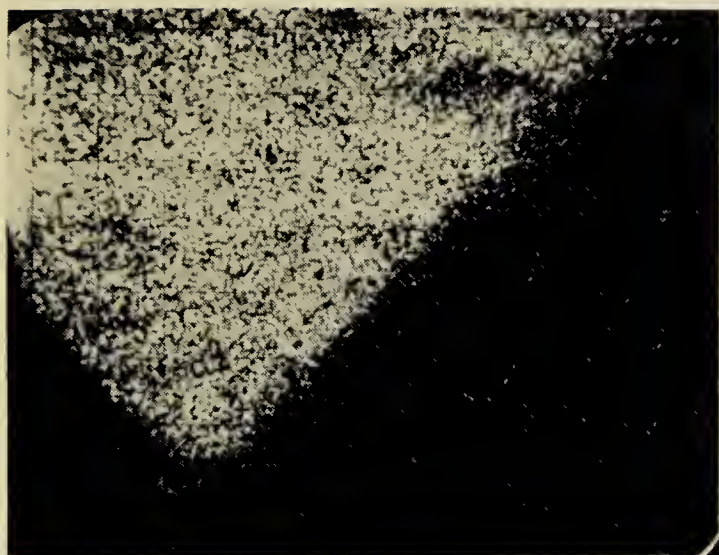
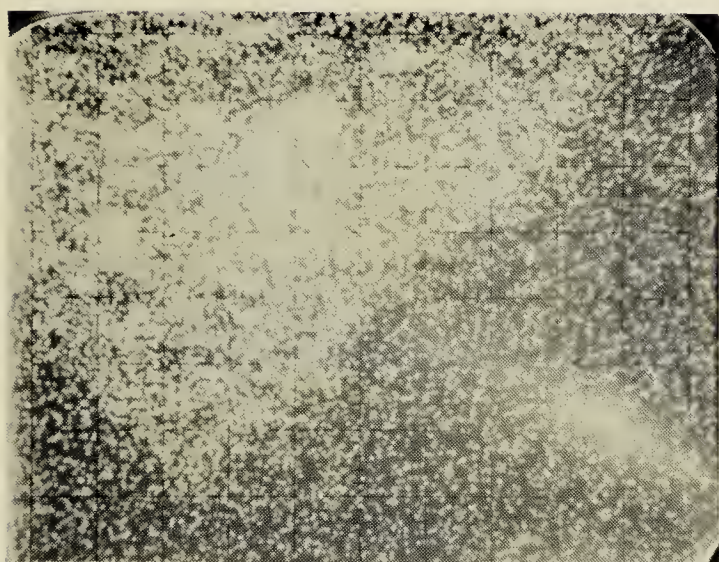
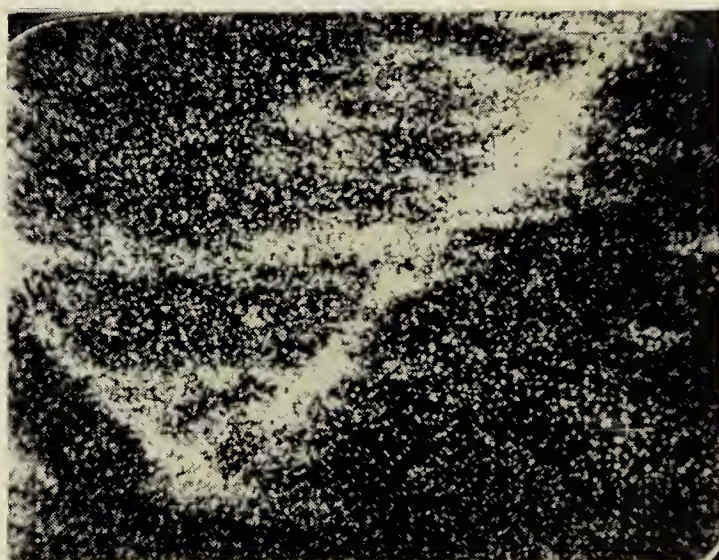
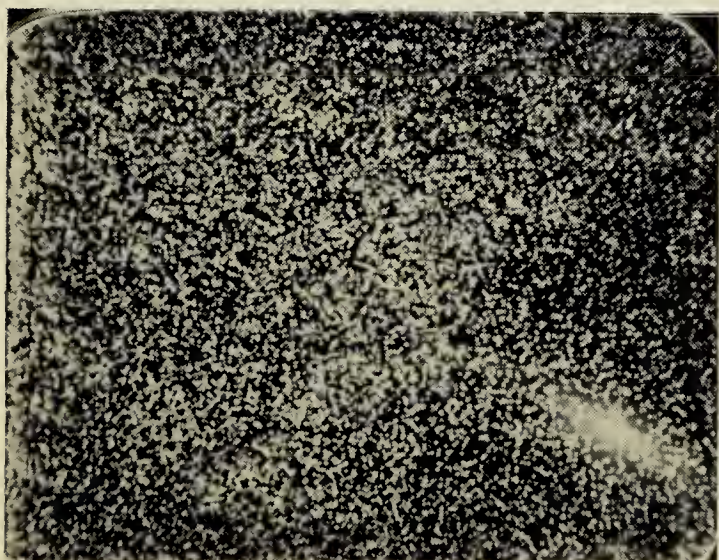


Figure 8: Histogram for the ages of uraninites

2. MONAZITE

Monazites are optically zoned and inhomogeneous. Qualitative investigations showed that the amount of uranium and thorium varied by at least a factor of two from one grain to another. Scanning photographs for phosphorus, cerium, calcium, uranium, thorium, and lead are shown in plate 2. The section of the grain studied is included in

**P****Ce****Th****U****Pb****Ca**

0 50 100
microns

Plate 2 : Backscattered electron (bs) and elemental photographs of monazite in sample JB-10.

biotite. Phosphorus and yttrium have a uniform distribution as has lead which is present only in minor amounts. Thorium and calcium are concentrated in patches; patches of calcium represent apatite which is present both inside and outside the monazite. Uranium is mainly present on the border of the grain and along lines that are prolongations of the biotite's cleavage into the monazite. There is no obvious relationship between the distribution of calcium, thorium, and uranium.

Two grains were analysed. Both analyses were done on areas covering about one sixth of the grain with one corner of the area analysed at the center of the grain; thus they are approximations to the compositions of the whole grains. From these results (table 35) it appears that monazite is an important thorium bearer while it contains little uranium (the rim of the grain was avoided for quantitative analyses). The precision of our analyses for low concentrations of lead and uranium does not enable us to estimate the age of these monazites. It should be noted however that the amount of lead increases proportionally to the amount of thorium (and uranium) indicating that the grains though different in composition, were coeval.

Table 35. Composition of monazites from the Baie Johan Beetz region in weight percentages. Oxygen is calculated by stoichiometry.

Sample	JB-1	JB-10
Al ₂ O ₃	0.08	0.19
SiO ₂	1.43	2.46
P ₂ O ₅	29.02	27.87
CaO	0.52	3.02
Fe ₂ O ₃	0.13	0.11
Y ₂ O ₃	0.54	2.38
La ₂ O ₃	16.29	10.03
Ce ₂ O ₃	31.45	24.66
Nd ₂ O ₃	10.49	11.33
Sm ₂ O ₃	2.05	3.06
Gd ₂ O ₃	1.14	0.95
Dy ₂ O ₃	tr	0.56
Ho ₂ O ₃	tr	0.65
PbO	0.26	0.52
ThO ₂	5.72	13.47
UO ₂	0.16	0.59
Total	99.28	101.85

3. XENOTIME AND CHURCHITE

In our samples, xenotime is isomorphous and optically zoned. The zoning is manifested by a difference in colour: the centre is brownish and occasionally contains small black dusty particles; the rim is colourless. Scanning photographs of part of a xenotime grain penetrated by monazite, were taken for phosphorus, yttrium, calcium, and silicon (Plate 2). They show uniform distribution of yttrium and phosphorus. Calcium and silicon have patchy distributions; they are frequently, though not always, related to each other and are often present as inclusions in xenotime rather than as a constituent of that mineral.

A more detailed investigation was conducted by traversing xenotime grains and registering elemental concentration on a chart recorder. It showed that uranium, silicon, and rare-earths are more abundant in the centres whilst phosphorus, yttrium, and iron increase in the rims.

Three analyses were done, two on one grain, centre and rim, and one over an area covering about one half of a grain, i.e., covering both centre and rim material. In the course of analysis the rim material obviously degassed to form Newton rings at the sample surface. Newton rings are caused by the accumulation of volatiles between the specimen and its carbon coating resulting in optical interference effects. The results (table 36) all have low totals but it should be noted that the totals decrease from centre to a mixture of centre plus rim, to rim. Low totals can be explained at least in part by deterioration of the mineral under the electron beam and by the presence of an undermined amount of water. Deterioration under the electron beam is likely as the area analysed became brown; but deterioration does not account for the strong reaction of the rim material relative to the centre material, nor for the gradation from centre to rim. It is thus believed that the rim material contains a higher amount of water, and is composed of churchite ($\text{YPO}_4 \cdot 2\text{H}_2\text{O}$) rather than xenotime. Three analysis of churchite listed in Vlasov (1964) show between 15 and 16 wt% water. These amounts are compatible with our results. Whether churchite has grown on xenotime or formed from

Table 36. Composition of xenotime from the Baie Johan Beetz region in weight percentages. C=centre, M=margin.

Sample	JB-10(C)	JB-10(M)	JB-15(C+M)
P ₂ O ₅	32.26	33.15	31.25
SiO ₂	5.09	0.82	4.24
Al ₂ O ₃	0.39	0.02	0.19
CaO	0.23	0.17	0.29
TiO ₂	n.d.	n.d.	tr
Fe ₂ O ₃	0.78	0.03	1.20
Y ₂ O ₃	39.94	44.01	34.61
La ₂ O ₃	0.40	0.04	0.10
Ce ₂ O ₃	0.79	n.d.	0.32
Nd ₂ O ₃	1.19	0.15	0.25
Sm ₂ O ₃	0.60	0.50	0.44
Gd ₂ O ₃	1.63	1.96	1.84
Er ₂ O ₃	3.85	4.75	4.06
WO ₃	2.02	2.58	2.68
ThO ₂	4.25	0.23	5.95
UO ₂	4.30	0.54	5.18
Total	97.72	88.95	92.60

n.d.: not detected

tr : trace

xenotime as an alteration product is unknown. Compositional differences between the centre and rim material are also evidenced by the higher content of uranium, thorium and silicon in the former. Dark particles in the centre could not be identified because they were too small. They are, however, unavoidably included in the analysis of the centre material.

4. SAMARSKITE

Samaraskite is isotropic and does not appear zoned under the microscope. Qualitative investigation with the electron microprobe, traversing one grain and registering element concentrations on a chart recorder, showed that calcium, phosphorus, and iron are more abundant in the outer part of the grain, whilst rare-earths, niobium, tungsten, and uranium concentrate in the inner part; thorium and yttrium are uniformly distributed; minor variations of titanium and iron are antipathetic. Results of two analyses done on areas covering about one sixth of the grains with one corner of the area covered at the centre of the grain, are listed in table 37. Compositions of the two grains are similar. No lead was detected in spite of the high concentration of uranium and thorium. Our totals differ from 100 by 2.4 and 0.91 wt% for JB-15 and JB-16 respectively. This probably comes from hydration of samarskite. Indeed analyses of samarskites given in Vlasov (1964) have between 0.53 and 4.62 wt% water; these values are compatible with our results.

Table 37. Composition of samarskites from the Baie Johan Beetz region in weight percentages.

Sample	JB-15	JB-16
Al ₂ O ₃	0.03	n.d.
SiO ₂	0.86	0.19
P ₂ O ₅	2.60	0.40
CaO	0.78	0.70
TiO ₂	2.42	2.62
Fe ₂ O ₃	1.01	0.80
Y ₂ O ₃	20.09	23.01
Nb ₂ O ₃	49.60	51.95
La ₂ O ₃	0.16	0.05
Ce ₂ O ₃	0.16	tr
Nd ₂ O ₃	0.69	0.82
Sm ₂ O ₃	3.00	0.89
Gd ₂ O ₃	1.69	1.55
Er ₂ O ₃	3.12	3.78
WO ₃	2.45	2.59
ThO ₂	2.85	2.47
UO ₃	6.05	6.65
Total	97.56	98.47

n.d.: not detected

5. ALLANITE

Allanite is encountered in samples JB-11, 15, 16 and 17 and it is a major constituent of sample JB-15. It is automorphous and zoned, generally fractured. In transmitted light three zones could be defined: pale green at the centre of the grains, opaque (metamict) dark green at the rim and, between the two, medium green. The latter was not always present and often was very thin. Contacts between these zones were irregular but sharp.

Compositional differences between the pale green and medium green zones are illustrated in figure 9. Spectra

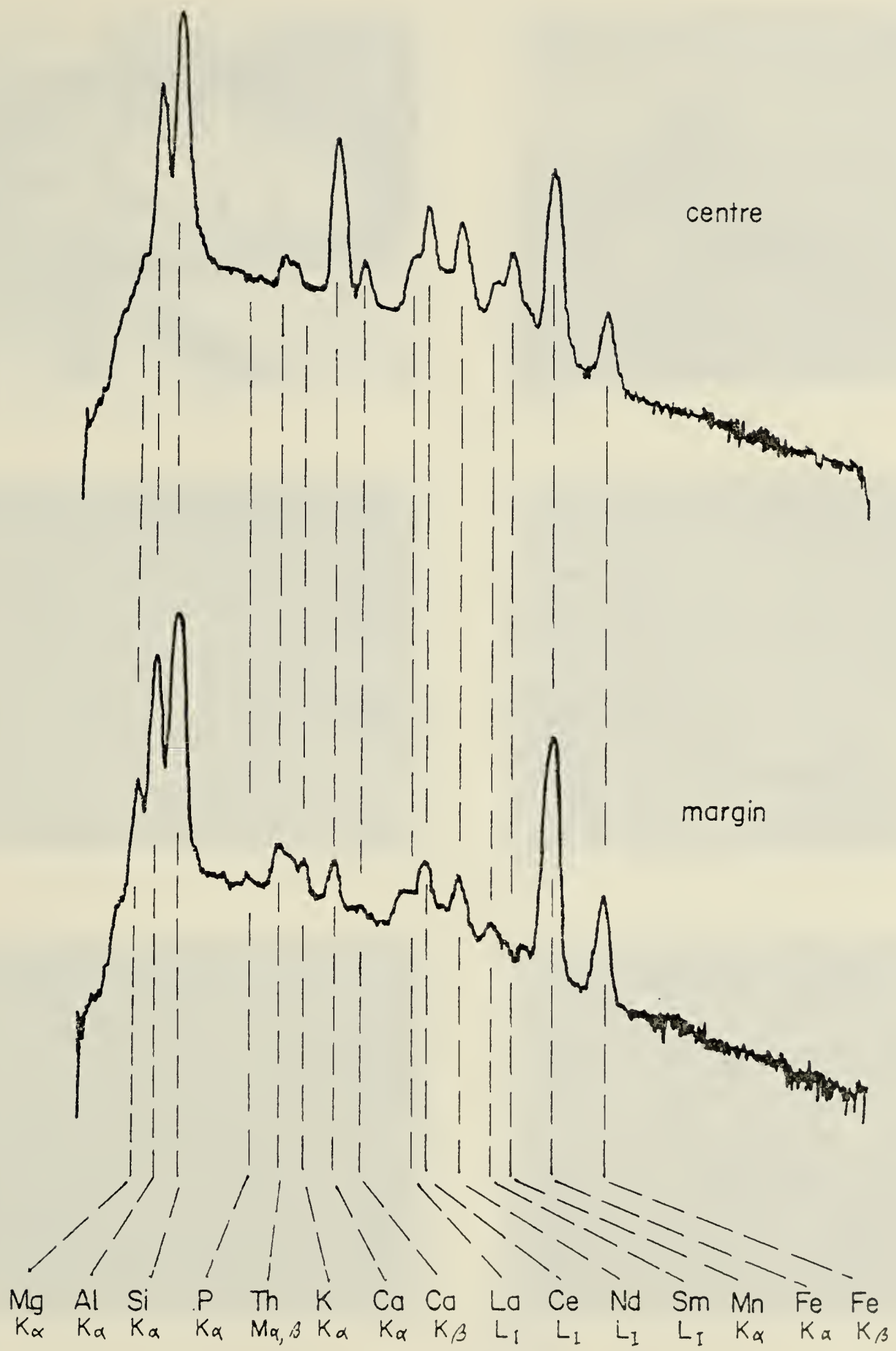
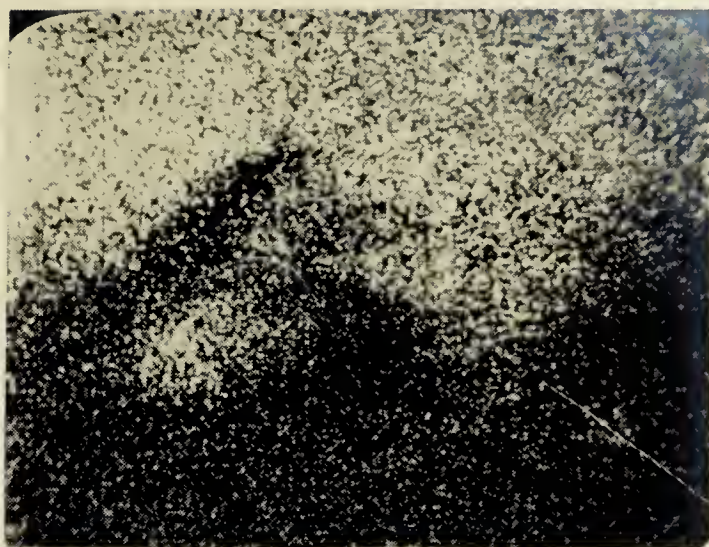


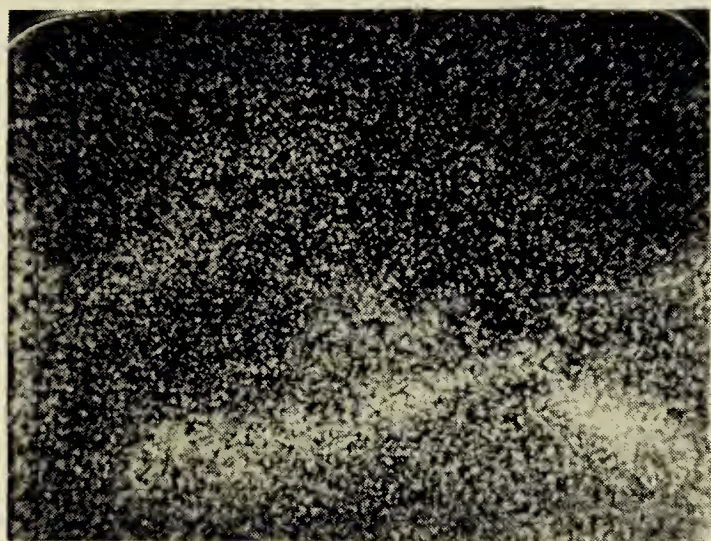
Figure 9. Spectra in logarithmic scale for the composition of allanite. Recorded by energy dispersive spectrometry.



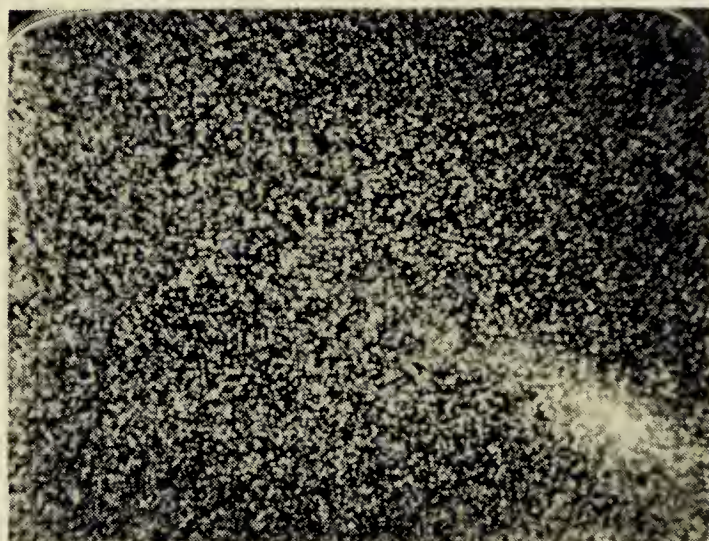
transmitted light (x10)



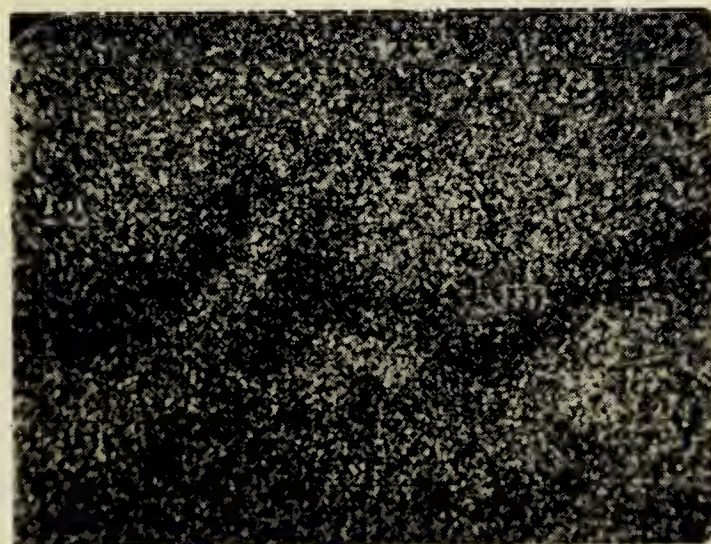
Ca



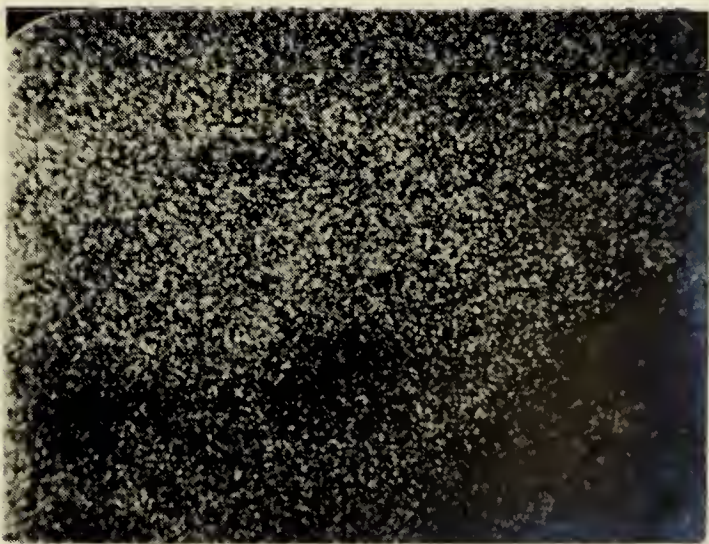
K



Th



Fe



Ce

0 50 100
microns

Plate 3: Transmitted light and elemental photographs of allanite in sample JB-15.

for the zones show that thorium, iron, and magnesium concentrate in the intermediate zone whilst calcium and rare-earths are enriched in the centre. This is corroborated by the distribution of elements shown in plate 3.

The pale green and dark green materials were analysed. Both zones were unstable under the electron beam and the areas analysed darkened rapidly. Compositions are listed in table 38; in both cases uranium was sought but not found. Low totals result from instability of the mineral under the electron beam, and from hydration.

Composition of the pale green material corresponds to that of allanite. When the atomic proportions are calculated on the basis of 13 (O,OH) for the general formula:



the cations filling the position (Ce,Ca) come to a total lower than the theoretical value. Deer et al. (1963) explain the variation of composition of allanite by the two substitutions: $\text{Ca} \leftrightarrow \text{REE}$ and $\text{Al} \leftrightarrow \text{Fe}^{+2}$. According to these authors "these substitutions are essentially sympathetic, the replacement of Ca by higher valency ions, mainly of the rare-earth groups, requiring a balancing substitution of divalent for trivalent ions in the octahedral (Fe,Al,Mg) position of the structure." Our results suggest that a fraction of the octahedral positions remain empty when trivalent and quadrivalent elements substitute for calcium. Indeed the sum of charges for elements occupying

this position equals +3.84, this compares quite well with the theoretical charge of +4.00. In this case all iron except that entering the octahedral position was assumed trivalent. Atomic proportions and charges exceed the corresponding theoretical values for the octahedral positions of allanite, i.e., 2 and 4 respectively.

The dark (metamict) material is enriched in rare-earths by a factor of 3 relative to the pale green area. Its rare-earth content (36.1 wt% REE₂O₃) exceeds the maximum rare-earth content of allanite (27 wt% REE₂O₃) (Vlasov, 1964) for the formula:



It contains less silicon, calcium and iron than the pale green allanite. Atomic proportions for the dark zone do not correspond to those of allanite nor any rare-earth silicate mineral. It remains unknown whether it is a solid solution or fine mixture of allanite and some other mineral(s), or a single phase.

Table 38. Composition of one allanite grain (pale green and dark green zones) from sample JB-15 in weight percentages and atomic proportions. The atomic proportions were calculated for an epidote formula based on 13 (O,OH).

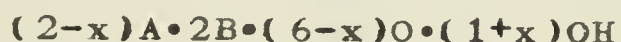
Zone	Centre	Rim
MgO	0.71	2.59
Al ₂ O ₃	17.14	15.64
SiO ₂	31.97	18.66
P ₂ O ₅	n.d.	0.15
K ₂ O	n.d.	0.44
CaO	7.18	2.57
MnO	0.95	0.24
Fe ₂ O ₃	17.20	10.44
La ₂ O ₃	1.89	8.84
Ce ₂ O ₃	7.50	22.69
Nd ₂ O ₃	4.72	7.09
Sm ₂ O ₃	1.17	1.67
Gd ₂ O ₃	1.51	3.63
Dy ₂ O ₃	1.18	0.76
Ce ₂ O ₃	n.d.	0.14
Yb ₂ O ₃	n.d.	0.12
ThO ₂	1.71	1.60
Total	94.84	97.26
Si	2.98	2.14
P	-	0.01
sum of Z =	2.98	2.15
Al	1.87	2.11
Fe ⁺³	1.02	0.90
Mg	0.11	0.44
sum of Y =	3.00	3.55
K	-	0.06
Ca	0.72	0.31
Fe	0.18	-
Mn	0.06	0.02
La	0.06	0.37
Ce	0.25	0.95
Nd	0.16	0.29
Sm	0.05	0.07
Gd	0.04	0.14
Dy	0.03	0.03
Th	0.03	0.04
sum of X =	1.58	2.28

n.d.: not detected

6. TITANOBETAFITE

Titanobetafite is rare in our samples. It was noted only in JB-1, and 10. In transmitted light it occurs as metamict reddish brown to yellowish grains. These grains could not be identified microscopically and they required chemical analysis. Qualitative microprobe investigations showed that the grains were inhomogeneous; but no systematic variations or regular zonings were established. An area covering 80 by 80 square microns was analysed; results are listed in table 39.

The total is low due to the presence of undetermined hydroxyl ions. Atomic proportions were calculated for the general formula:



The best value for x is 1.2 in agreement with the beta-fite minerals where x ranges between 0.5 and 1.5. The ratio $(Nb+Ta)/Ti$ equals 0.5, and this value is compatible with titanobetafite whose $(Nb+Ta)/Ti$ ratio ranges between 0.3 and 2.5 (Vlasov, 1964). The uranium content is high but no lead was detected suggesting that titanobetafite formed only recently in our samples or else that it underwent alteration with departure of lead and possibly some other elements. The latter hypothesis appears more realistic as the grains of titanobetafite are metamict and often stained red presumably by iron oxides.

Table 39. Composition of titanobetafite from sample JB-1 in weight percentages and atomic proportions. Atomic proportions were computed for the general formula $(2-x)A \cdot 2B \cdot (6-x)O \cdot (1+x)OH$ based on 7(O,OH). The best value for x was found to be 1.2.

CaO	1.95	Ca	0.13
FeO	1.01	Fe	0.05
Y ₂ O ₃	1.20	Y	0.04
La ₂ O ₃	2.06	La	0.05
Ce ₂ O ₃	6.31	Ce	0.15
Nd ₂ O ₃	1.94	Nd	0.04
Sm ₂ O ₃	0.46	Sm	0.01
Gd ₂ O ₃	0.83	Gd	0.01
Er ₂ O ₃	0.19	Er	-
ThO ₂	2.04	Th	0.03
UO ₂	23.77	U	0.30
		sum of A	0.81
Al ₂ O ₃	0.67	Al	0.05
SiO ₂	5.96	Si	0.36
P ₂ O ₅	0.01	P	-
TiO ₂	25.61	Ti	1.17
Nb ₂ O ₅	22.43	Nb	0.59
		sum of B	2.17
Total	96.44	O	4.8
		OH	2.2
		sum: O+OH	7.00

7. THOROGUMMITE

A bright yellow phase occurs in sample JB-10 as fillings between grains. No optical sign could be determined and it is presumed that this phase is amorphous. Under the electron beam, it deteriorates rapidly in a manner similar to that of epoxy resin though at a slower rate. Water and/or carbon oxide probably evaporate during deterioration. Phosphorus counts did not decrease during analysis. The composition of this phase was obtained by taking only two

counts for each background and peak positions and changing location at each step of the analysis. Results are listed in table 40.

Table 40. Composition of thorogummite from sample JB-10 in weight percentage and atomic proportions. The latter are based on the general formula: $\text{Th} \cdot (1-x)(\text{SiO}_4) \cdot 4x(\text{OH})$. The best value for x is 0.17.

Al_2O_3	1.97	Al	0.12
CaO	0.04	Ca	-
Fe_2O_3	1.29	Fe	0.05
Y_2O_3	7.00	Y	0.19
La_2O_3	0.26	La	0.01
Ce_2O_3	0.63	Ce	0.01
Nd_2O_3	1.06	Nd	0.02
Sm_2O_3	0.69	Sm	0.01
Gd_2O_3	0.83	Gd	0.02
Er_2O_3	1.11	Er	0.02
WO_3	0.58	W	0.01
ThO_2	42.29	Th	0.48
UO_2	11.36	U	0.13
		sum of A	1.07
SiO_2	15.05	Si	0.75
P_2O_5	1.84	P	0.08
		sum of B	0.83
Total	86.00	O	3.32
		OH	0.68
		sum: O+OH	4.00

The composition of this phase is that of thorogummite. The low total is due to deterioration of the specimen during analysis and to the presence of undetermined water. Frondel (1958), for example, reports as much as 12 wt% water (H_2O^+) for some thorogummite samples. This is compatible with our

results.

Because this thorogummite is lead-free despite its high thorium and uranium content, and since it occurs as a filling between other minerals, it must have precipitated recently.

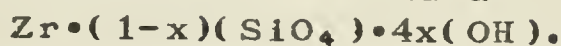
8. ZIRCON

Two types of zircons were identified through petrographic examination. The most common is clear, colourless and zoned. The other is brownish and occasionally forms a core in grains of the first type. Qualitative microprobe studies showed that the brownish zircons correspond closely to the theoretical composition (ZrSiO_4) whilst the clear zircons contain additional elements, namely: sodium, phosphorus, calcium, manganese, iron, hafnium and uranium. In the zoned zircons it was observed that iron, sodium, calcium, hafnium, and cerium vary independently from one another but in a concentric pattern; iron and manganese vary sympathetically.

Three grains were analysed, two from sample JB-8 and one from JB-18. One of the grains from JB-8 had a brownish core with a clear margin, both areas were analysed independently. In all cases the area analysed covered about 1/10 of the grain (or core and margin) and an attempt was made to return to the same area at each step of the

analysis. Results are listed in table 41. The total for the

Table 41. Composition of zircons from the Baie Johan Beetz region in weight percentages and atomic proportions. The latter are calculated for the formula:



Sample	JB-8		JB-8	JB-18
	core	margin		
Na ₂ O		2.00	2.06	4.23
CaO	-	2.09	1.83	2.48
MnO	0.05	0.27	0.10	0.17
Fe ₂ O ₃	0.21	1.33	0.50	1.45
ZrO ₂	65.90	58.52	59.46	54.43
Hf ₂ O ₃	1.48	1.94	1.81	1.88
UO ₂	0.08	0.46	0.49	1.09
SiO ₂	33.66	31.40	30.91	30.85
P ₂ O ₅	-	0.07	0.10	-
Total	101.38	98.08	97.26	96.58
Na	-	0.12	0.12	0.25
Ca	-	0.07	0.06	0.08
Mn	-	-	-	-
Fe	-	0.03	0.01	0.06
Zr	0.97	0.90	0.90	0.82
Y	0.01	0.02	0.02	0.02
U	-	-	-	0.01
sum: 'Zr'	0.98	1.02	0.90	0.99
Si	1.02	0.99	0.96	0.95
P	-	-	-	-
sum: 'Si'	1.02	0.99	0.96	0.95
O	4.00	4.00	3.84	3.80
OH	-	-	0.16	0.20
sum: O+OH	4.00	4.00	4.00	4.00

brownish core is high while totals for clear grains are low.

Hafnium, zirconium and silicon were analysed against a

zircon standards thus minimizing possible correction errors;

it is thus believed that the low total either reflects a

failure to return always to exactly the same area in the course of analysis, inaccuracy in the composition of the standard, or the presence of undetermined elements such as OH (Fron del, 1953). The first hypothesis is unlikely as the area swept became slightly darker than the rest of the grain after a few counts, making relocalization an easy task. Three of the analyses have sodium in significant amount. Sodium does not substitute for silicon in silicate minerals.

Because the sodium content of zircon varies in a concentric pattern though it is excluded from the mineral structure, it must occur either as absorbed material, such as Na(OH), or as a constituent of a mineral in solid solution with zircon; such a mineral might be epididymite: $\text{NaBeSi}_3\text{O}_7(\text{OH})$.

C- CONCLUSIONS

The samples from the Baie Johan Beetz region are enriched in uranium, thorium, and rare-earth elements. The main minerals containing these elements are listed below (table 42).

The above minerals are more abundant in samples from fracture filling (JB-9) and shear zone (JB 15, 17) materials than in those from granitic materials. It should be noted

Table 42. Minerals from the Baie Johan Beetz region which contain uranium, thorium, and rare-earth elements together with the average contents of the above elements in weight percentages.

Mineral	U(wt%)	Th(wt%)	REE(wt%)
Uraninite	75	7	1
Monazite	0.3	8	40
Xenotime	2	4	8
Samarskite	6	2.5	8
Titanobetafite	24	2	13
Allanite	1	1.5	17-35
Thorogummite	12	42	11

though that the fracture filling and shear zone materials crystallized at relatively high temperature; they are of a different type than the pitchblende-rich veins of the Massif Central (France) or Great Bear Lake (N.W.T.).

A hypothesis for the genesis of mineralization in the area studied must account for:

- 1- the association uranium, thorium and rare-earth elements suggesting a relatively high temperature of formation i.e., corresponding to pegmatite deposits rather than hydrothermal veins and sedimentary deposits;
- 2- the enrichment is restricted to remobilized granitic material and shear zones and fractures therein;
- 3- the distribution of mineralization is independant of the meta-sediments;
- 4- the minimum age of 1317 Ma for mineralization yielded by uraninites;

- 5- a period of recrystallization at about 1152 Ma, as suggested by some uraninites;
- 6- the association of carbonaceous matter with uraninites in some of the granite samples.

The age of the younger population (1152 Ma) of uraninites is compatible with the Grenville Orogeny as dated by Rb-Sr methods on rocks from the Shawinigan region, 160 km northeast of Montreal: 1094 ± 43 Ma on whole rock samples of garnet sillimanite gneiss (Barton and Doig, 1973); 1103 ± 33 Ma in whole rock samples from the St. Didace adamellites (Barton, 1971); 1105 Ma on minerals from the St. Didace granite (Goulet, 1971).

Inside the Grenville Province, the older population (1317 Ma) can be correlated with anorthosite and associated, more acidic, intrusives and also, with some metasedimentary rocks. Indeed ages ranging from 1050 Ma to 1480 Ma have been measured on anorthosites and associated acidic rocks (Wynne-Edwards, 1976), while ages of about 1300 were obtained for some metasediments: 1307 Ma for sediments from the Hastings Basin (Brown *et al.*, 1975); and a probable age of 1307 Ma for the Lake Quinn formation (Barton, 1971).

The most likely hypothesis is an enrichment in the remobilized fraction of the basement gneiss producing the granites at about 1317 Ma, with preferential concentration in fractures and shear zones during the cooling stages. It appears that lead was retained in, or not completely

expelled from, the uraninites during the subsequent Grenville Orogeny (1152 Ma). The stability of uraninites during the Grenville Orogeny might explain the apparent absence of uranium and thorium in the metasediments overlying and intruded by the granites.

CHAPTER VIII

DUDDRIDGE LAKE

A- DESCRIPTION

1. LOCALIZATION

This locality lies within northern Saskatchewan, about 80 km northwest of La Ronge, and occupies part of (fig. 10) is part of the Churchill Province, in the so-called Wollaston Lake fold belt (Money, 1968) overlying the Wollaston domain and the Rottenstone domain (Sibbald et al., 1976).

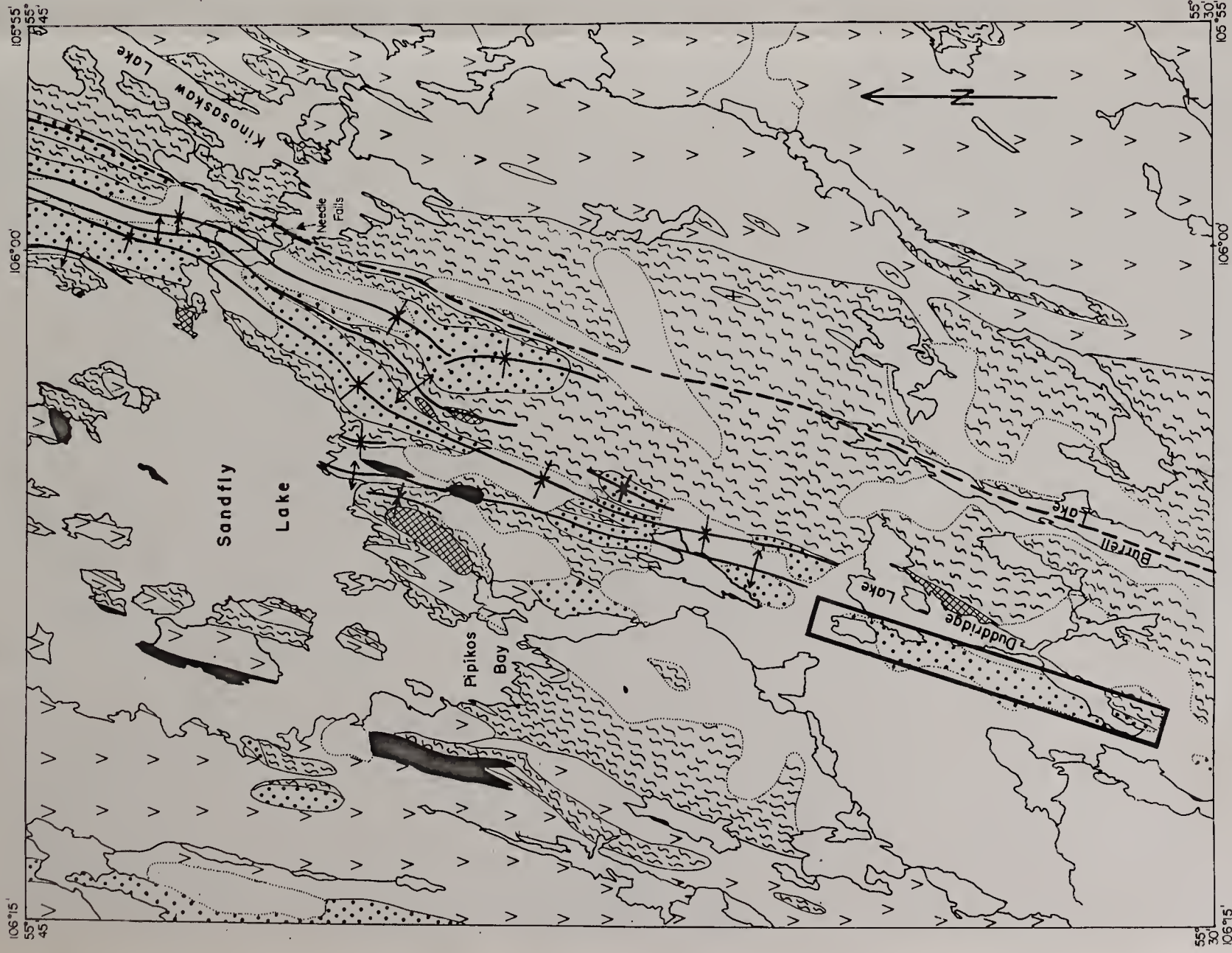


Fig. 10 Geology of the Duddridge Lake area, Saskatchewan and location of the sampled zone.

2. PREVIOUS WORK

Mapping of the area (fig. 10) was performed on a scale of 4 mi:1 inch by Frarey (1950), on a scale of 1 mi:1 inch by Money (1965, 1967), and at a scale of 2 mi:1 inch by Munday (1974a,b). The geology of the Wollaston Lake Belt has been summarized by Money (1968) and by Money et al. (1970). The geological setting of the uranium mineralization in that part of the Belt situated in northern Saskatchewan has been reviewed by Sibbald et al. (1976), and more specifically, a multiple media geochemical survey of a boulder train associated with the Duddridge Lake uranium deposit was undertaken by Haughton (1976).

Radioactivity in the Wollaston Lake Belt was first noted in 1952 by geologists of Eldorado Mining Corporation in the Foster Lake area, about 130 km northwest of Duddridge Lake. In 1968, a drill hole southwest of Wollaston Lake, about 320 km northwest of Duddridge Lake, intersected some promising uranium mineralization (Money et al., 1970). Activity was renewed in 1974 when uranium-copper mineralization was discovered in a boulder train 1500 m long and 40 m wide on the west side of Duddridge Lake. Later, in the same field season, uranium mineralization was found in part of the underlying bedrock, namely quartz-pebble conglomerate (Munday, 1974a). Following this discovery, a continuous zone of radioactivity, associated with the quartz-pebble conglomerate, was traced over a 40 km distance

from Duddridge Lake on northward to Meyers Lake (Sibbald et al., 1976). This property is now held by the Exploration Company and Noranda Exploration Company Limited. Specimens of typical rock types of the Duddridge Lake area were kindly supplied to the author by Dr R.A. Munday (Saskatchewan, Department of Mineral Resources).

3. GEOLOGY

The Duddridge Lake area (fig. 10) is part of a metamorphosed sedimentary basin. Its principal components are granitic gneiss and supracrustal rocks with variable proportions of basic intrusive rocks, all of which are cut by pegmatites and partly covered by glacial deposits. The lithological units that have been recognised in the field by Money (1965, 1968) and Munday (1974a,b) are given in table 43.

Granitic gneisses

Granitic gneisses are encountered in the northwestern and southeastern parts of the map area (fig. 10). The western granite is continuous into the subgranulite facies sequence west of the present area, i.e., in the Mudjatic domain (Munday 1972, 1973; Pearson, 1972; Sibbald, 1973). It is constituted mostly of quartzo-feldspathic gneiss of granitic to granodioritic composition,

Table 43. Stratigraphy of the Duddridge Lake area, according to Money (1965,1968), Munday (1974a, b), and Sibbald et al. (1976).

Money (1965, 1968)	Munday (1974a, b) and Sibbald et al. (1976).
Pleistocene and Recent sediments	Pleistocene and Recent sediments
----- unconformity -----	----- unconformity -----
Quartz veins (P)*	(P) Pegmatites
Pegmatites (P)	----- intrusive contact -----
----- intrusive contact -----	(remobilization of the basement gneiss)
Eastern granitic rocks (F)	----- ? ? ? -----
----- intrusive contact -----	(D) Uralitized and saussuritized gabbro
Metamorphosed intrusive rocks(epidiorite)	----- intrusive contact -----
(D)	(B) Biotite gneisses: with cordierite, sillimanite, and magnetite, but lacking garnet and graphite; with garnet, sillimanite, cordierite, and graphite, but generally lacking magnetite.
Daly Lake Group: biotite-cordierite-sillimanite rocks and associated rocks, derived from migmatite(upper arkosic and middle pelitic units).	(Q) Siliceous gneisses and granulose rocks: meta-arkose, meta-psammite, quartzite, meta-conglomerate, sericitic schist, and muscovite meta-arkose.
Meyers Lake Group: biotite-muscovite-quartz-schist, quartz-pebble meta-conglomerate(lower clastic unit).	(M) Mafic gneisses: amphibolite and hornblende-felspar gneiss, hypersthene gneiss and pyroxenite.
(S, B, Q, M, F)	(S) Mylonite derived from felsic gneiss.
----- unconformity -----	(F ₃)K-felspar augen felsic gneiss
Western granitic rocks (F)	----- unconformity -----
----- unconformity -----	(F) Felsic gneiss of granitic to granodioritic composition (Eastern and Western granites)
Archean	Archean

* Capital letters indicate corresponding units.

and, in general, is medium- to coarse-grained and equigranular with foliation that is either weak and irregular or else absent (Money, 1965). The eastern granitic rocks are located east of the Needle Falls shear zone in the so-called Rottenstone domain (Munday, 1974a,b). Its composition varies between granodiorite and quartz diorite, ranging to quartz monzonite. It is, in general, medium- to coarse-grained, equigranular with foliation that is either weak and irregular or else absent. A porphyroblastic variety is present at the contact with migmatized supracrustal rocks.

Supracrustal rocks

The supracrustal rocks occupy the main part of the map area (fig. 10). They are composed essentially of metamorphosed shales, arkosic arenites and greywacke with variable proportions of basic metavolcanic rocks. According to Sibbald et al. (1976), the main units underlying the map area are:

- 1- a clastic unit best represented by thick metamorphosed conglomerate-quartzite-argillite successions (corresponding to the Meyers Lake and Sandfly Lake Groups of Money (1965) and Money et al. (1968));
- 2- a metamorphosed pelitic to semi-pelitic unit which is often graphitic and locally displays intercalation of calc-silicates. This corresponds to

the Daly lake Group of Money (1966).

Basic intrusive rocks

Metamorphosed gabbro or epidiorite forms small bodies intrusive into the supracrustal rocks. It is a medium- to coarse-grained equigranular and massive unit (Money, 1965).

Pegmatites and quartz veins

Pegmatitic sills and lenses are common throughout the Duddridge Lake area (fig. 10). Both segregation and intrusive types have been identified (Money, 1965). Segregation pegmatites occur in biotite-cordierite-sillimanite rocks of the metapelite. Quartz veins occur mainly west of Sandfly Lake, and probably represent the youngest rocks of the area.

Glacial deposits

These cover about 25% of the map area. Uraniferous quartzite boulders have been noted west of Duddridge Lake.

4. CHRONOLOGICAL RELATIONSHIPS

Chronological relationships as established for the map area by Money (1965) and Money et al., (1968) and by Munday (1974a,b) are compared in table DL-1. In the light of a synthesis study of the southern part of the Saskatchewan Shield, (Sibbald et al., 1976), it appears that both eastern and western granitic bodies belong to the basement gneiss. The lower clastic unit lies unconformably on the basement gneiss and is overlain by the pelitic to semi-pelitic unit.

5. TECTONICS AND METAMORPHISM

The area (fig. 10) is crossed by the north-northeast trending shear zone referred to as the Needle Falls Shear Zone. Intense shearing and faulting is evident from the presence of mylonites (Munday 1974a,b).

On a large scale, the map area is located on the eastern margin of a sedimentation basin composed essentially of an Archean basement overlain by Aphebian sediments. Two major thermal events have affected the basin area. The first predates the formation of the supracrustal rocks and is characterized by metamorphism of the so-called 'basement gneiss'. The second event, of Hudsonian age, is characterized by retrograde metamorphism of the Archean basement and metamorphism of the supracrustal rocks,

accompanied by local remobilization and intense deformation in a northeastwardly direction.

In the map area, the grade of metamorphism increases westward from lower amphibolite to lower granulite facies

6. MINERALIZATION: summarized from Sibbald et al., 1976

Uranium-, cobalt-, silver-, gold-, copper- and vanadium-mineralization has been reported for the map area. Uranium mineralization was found in boulders of feldspathic quartzite and in quartz pebble conglomerate lying unconformably on the basement gneiss. It has been said to occur as pitchblende, uraninite and tyuyamunite.

Other uranium occurrences for the southeastern part of the Saskatchewan Shield have been associated with remobilized basement rocks (in pink granites and leucogranites) and with supracrustal rocks (in calc-silicates and in pegmatites within graphitic gneiss: the so-called pelite-pegmatites (Sibbald et al., 1976)).

7. SOURCE OF THE URANIUM

The source for uranium mineralization appears to lie in basement gneiss. Through the history of the region, uranium is concentrated both in remobilized parts of the gneiss and in its heavy clastic erosion products.

B- ANALYSIS

Ten samples from the Duddridge Lake region (supplied by Dr R.A. Munday) were studied. The rock types and petrographic descriptions are given in appendix IV. The main minerals are quartz, plagioclase, K-feldspar, biotite occasionally accompanied by garnet, muscovite and epidote. Minor constituents are: ilmenite, chalcopyrite, pyrite, magnetite, zoisite, sphene, rutile, calcite, apatite, arsenopyrite, cobaltite, safflorite uraninite, monazite, carnotite, 'brannerite', Ti-V compounds and a U-Pb-Si phase. The specimens are weathered and stained yellow and red by uranium and iron alteration products and in one case (DL-8), by cobalt bloom.

Our analysis centred on uraninite, brannerite, U-Ti-V compounds and the U-Pb-Si phase. Other minerals likely to contain uranium were investigated briefly, they are: apatite, rutile and monazite.

1. URANINITE

Uraninite was identified in samples DL-3, 4, 5 and 6. It is fine-grained (about 0.01 mm), occasionally automorphous and altered. Alteration is manifested by the presence of red staining, cracks and a sooty aspect. Sample DL-3 contained relatively fresh uraninite. This, however, had a sooty aspect, did not polish very well and released volatiles or oil under the electron beam, as evidenced by the formation of interference rings. Whether the volatile material was originally trapped in the mineral or was oil absorbed during polishing is unknown.

Eight grains were analysed. They contain uranium, lead and, in lesser amounts, silicon, calcium, yttrium and rare-earths plus, presumably, oxygen. Yttrium and rare-earths were determined for one grain only. Vanadium and thorium were sought but not found, sulphur did not exceed 0.02 wt %. Compositions and average correction factors are listed in table 44. All eight compositions are very close. It is, therefore, believed that the yttrium and rare-earth contents determined in one grain are a good approximation for all of the eight grains. Totals are low even when yttrium and rare-earths are accounted for. This results from the sooty, porous nature of the uraninite which contains volatile elements or compounds and the fact that it did not polish as well as desired for microprobe analysis.

Table 44. Composition of some uraninites from sample DL-3 of the Duddridge Lake region in weight percentages and average correction factors for microprobe analysis. The UO_2/UO_3 ratio was calculated to compensate for the liberation of oxygen assuming that PbO is produced from UO_2 . Correction factors do not vary by more than 1% from the average for each element.

SiO_2	CaO	TiO_2	PbO	UO_{2-3}	$(\text{REE}+\text{Y})_2\text{O}_3$	Total
0.64	0.29	0.13	16.66	75.93	N.D.	93.65
0.66	0.56	0.13	15.92	76.11	N.D.	93.38
0.96	0.50	0.07	15.47	76.13	N.D.	93.13
0.53	0.55	0.09	17.53	75.51	N.D.	94.21
0.66	0.31	0.13	15.81	76.16	N.D.	93.07
0.60	0.39	0.18	16.89	76.40	N.D.	94.46
0.58	0.31	0.12	16.36	76.71	2.78	96.86
0.51	0.32	0.23	17.16	75.85	N.D.	94.07
average ZAF correction factors						
Si	Ca	Ti	Pb	U		
1.00	0.88	0.87	1.18	1.06		

N.D.: not determined

Age

Lead to uranium ratios yield an average minimum age of 1649 Ma (maximum value of 1772 Ma). Detailed results are given in table 45 and the mode of calculation has been explained in chapter VII.

Cumming and Scott (1976) have summarized geochronological results and dated rocks from the Wollaston Lake Belt. They suggest an age of about 2650 Ma for the granites and some sedimentation as old as 2100 Ma followed by regional metamorphism around 1850 my; a later less pronounced metamorphic pulse might have taken place between 1750 and 1700 Ma and, finally a period of metamorphic activity and pegmatitic intrusion occurred around 1550 Ma

Table 45. Age calculated from the lead to uranium ratio of eight uraninites.

Pb/U (in atomic proportions)	age (Ma)
0.2697	1673
0.2568	1593
0.2493	1546
0.2857	1772
0.2547	1580
0.2719	1687
0.2644	1640
0.2785	1700
average age	1649
standard deviation	74

ago.

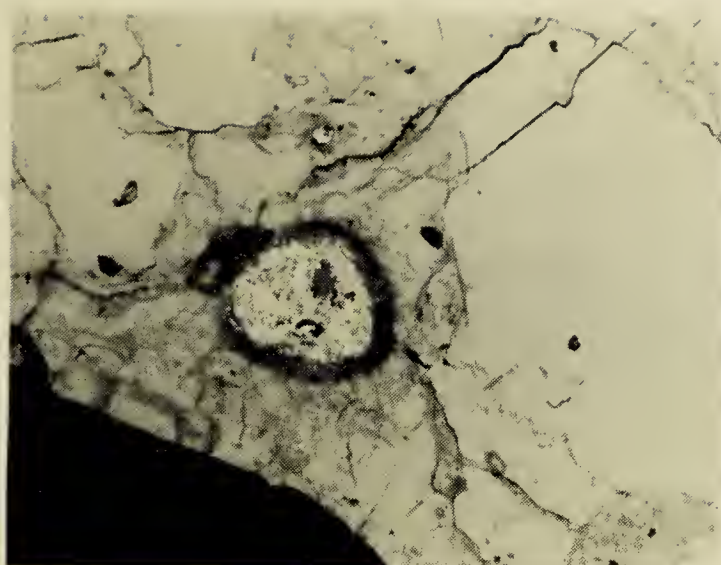
The average date of 1649 Ma (with a maximum value of 1772 Ma) obtained from our samples suggest that uranium mineralization has occurred prior to the late period of pegmatite intrusion. The uraninites have crystallized (or recrystallized) during the metamorphic period dated at 1700 to 1750 Ma.

2. 'BRANNERITE'

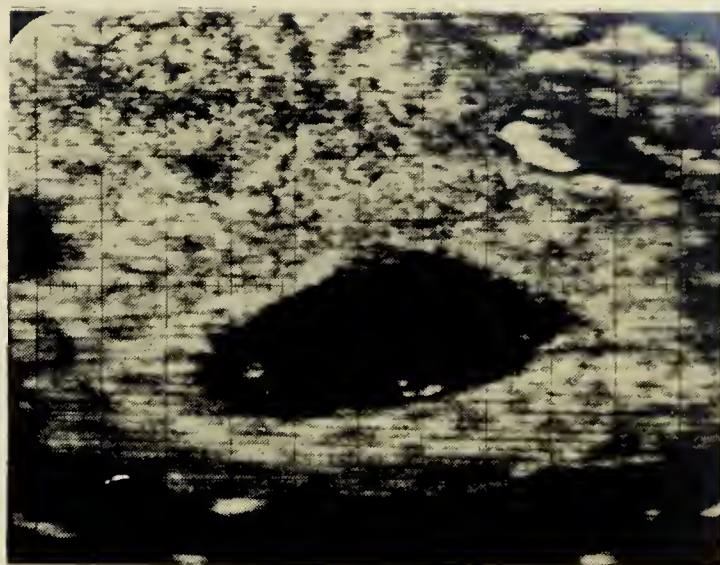
In thin section under reflected light, 'brannerite' appears as roundish grains. These are coloured in various shades of grey with a patchy aspect and sometimes have overgrowths of magnetite; they are surrounded by a red rim. Petrographic study combined with microprobe work showed that grains of 'brannerite' are inhomogeneous; they often

include major rock constituents such as quartz and feldspar, and also uraninite and one of the titanium oxide minerals. The rim is coloured by iron oxide and comprises fine particles of uraninite; it extends into the minerals surrounding 'brannerite'. A photograph in reflected light and microprobe photographs for backscattered electrons and for the main constituents, titanium, uranium, iron and lead (plate 4), illustrate the above features. The photomicrograph shows 'brannerite' in pale grey surrounded by a darker rim. The dark grey spot included in 'brannerite' is potassic feldspar. Microprobe photographs were taken for the lower left portion of the grain. The backscattered electron photograph is of three shades corresponding to three average atomic numbers. The dark band is located outside the 'brannerite' grain and the large dark spot represents potassic feldspar; both can be seen in the X-ray scanning photographs. The small dark spot is one of the titanium oxide minerals, it corresponds to the white spot in the titanium distribution photograph. The pale grey area is 'brannerite', which also appears pale grey in the titanium and uranium distribution photographs. Iron, however, is variable. Finally uraninite shows up as white areas in the backscattered electron and uranium photographs and as dark areas in the titanium photograph. Lead is associated with uranium.

It was not possible to obtain a good quantitative analysis representative of the 'brannerite'; nevertheless



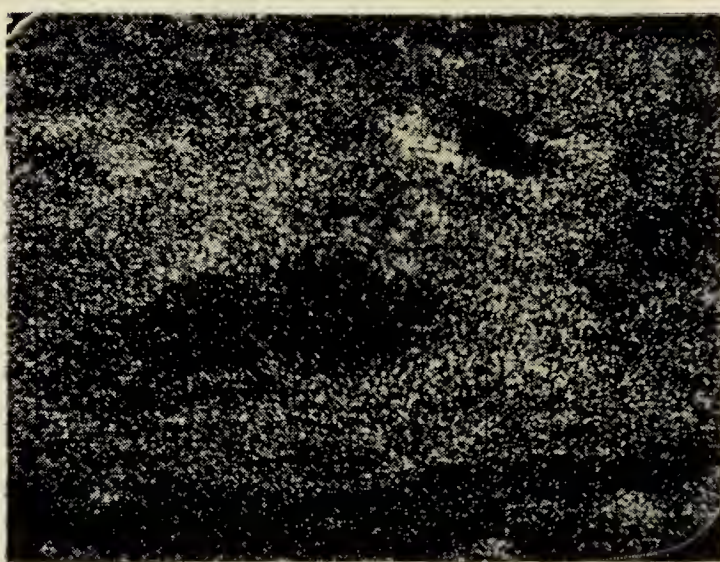
reflected light (x10)



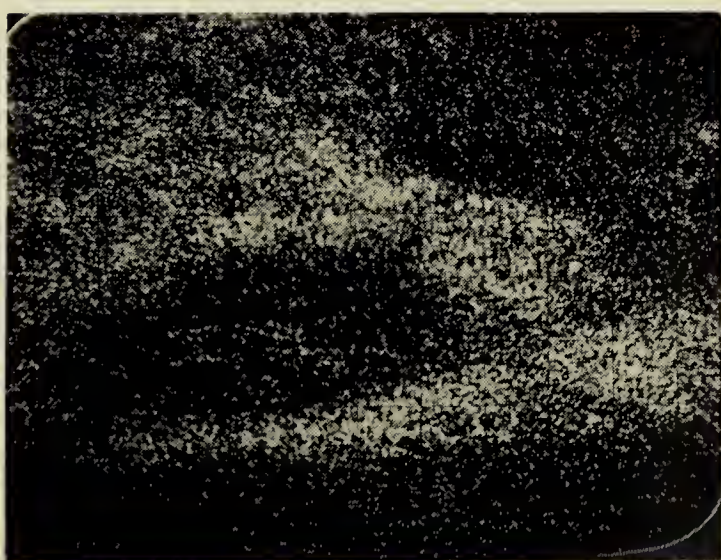
bs



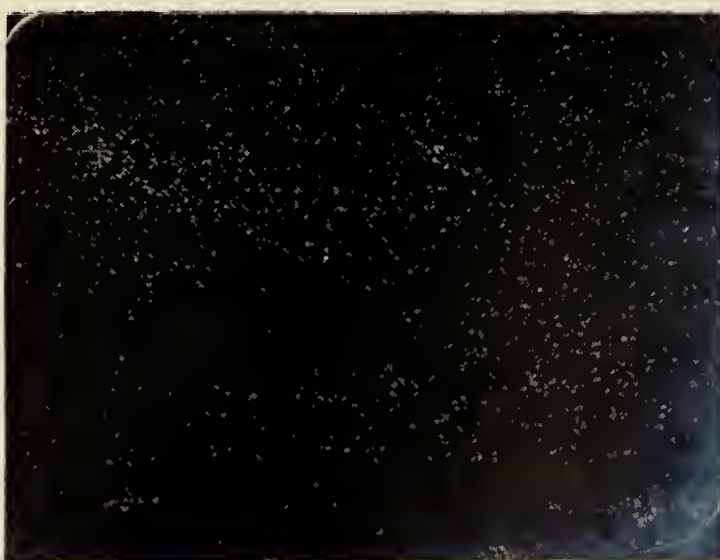
Ti



U



Fe



Ca

0 50 100
microns

Plate 4: Reflected light, backscattered electron (bs), and elemental photographs of 'brannerite' in sample DL-5.

three grains were analysed avoiding inhomogeneities as much as possible. Results are listed in table 46. The compounds may be hydrated to a small extent. The analyses show an antipathetic relationship between uranium and iron, and between vanadium and titanium. Thorium was sought in all three grains and found to be absent. The 'brannerites' of Duddridge Lake differ from those reported in the literature (e.g., Ferris and Rudd, 1971) by the absence of thorium; their low uranium to titanium ratio is comparable with the brannerite from Blind River (Ferris and Rudd, 1971).

In the Duddridge Lake samples, it is felt that 'brannerite' was probably formed epigenetically as the result of incomplete 'branneritization' of ilmenite by hexavalent uranium in solution. This process combines reduction of uranium and oxidation of iron. It was incomplete as evidenced by relics of titania. Subsequent leaching may have contributed to the low U/Ti ratio of these phases. The red staining and occasional magnetite found with 'brannerite' are the products of iron oxidation. This process is similar to the one proposed by Ferris and Rudd (1971) for the formation of the Blind River 'brannerites'.

Ilmenite sometimes occurs in the same specimen as brannerite as interstitial blades; these are probably a second generation of ilmenite.

Table 46. Composition of 'brannerite' from the Duddridge Lake region in weight percentages and atomic proportions calculated for six oxygen ions.

	DL-4	DL-5(A)	DL-5(B)
Al ₂ O ₃	0.27	0.57	0.49
SiO ₂	3.37	3.57	2.86
P ₂ O ₅	0.19	0.08	1.18
CaO	0.49	0.29	0.50
TiO ₂	50.64	48.84	38.27
V ₂ O ₅	1.14	3.96	7.06
Fe ₂ O ₃	5.14	6.60	2.95
PbO	6.21	8.72	5.77
UO ₂	31.00	24.21	39.82
Total	98.45	96.85	98.90
Ti	2.13	2.03	1.85
V	0.04	0.13	0.23
sum: 'Ti'	2.17	2.16	2.08
Si	0.02	0.03	0.03
Al	0.19	0.17	0.15
P	0.01	-	0.05
Ca	0.03	0.01	0.03
Fe	0.21	0.40	0.17
Pb	0.10	0.10	0.07
U	0.38	0.25	0.44
sum: 'U'	0.94	0.97	0.94
O	6.00	6.00	6.00

3. U-Pb-Si PHASE

In samples DL-2, 3, 4 and 6, a yellow phase occurs as fillings, in small clusters and as a coating on weathered surfaces. It is often associated with carnotite and, more rarely, with uraninite. It is obviously a secondary mineral. Some optical properties were measured and microprobe analyses are done on two grains; no X-ray pattern could be obtained because the grains were very small (20 microns), and difficult to separate from carnotite.

Optical properties : These were difficult to measure because of the small size of the grains and their association with carnotite. Characteristics measured are:

colour	: pale to medium yellow in hand specimen and in thin section (in transmitted light)
birefringence	: first order
refractive index	: close to 1.633
sign	: biaxial positive
2V	: 10-15°.

Composition : Constituents identified through microprobe scanning are: silicon, lead, uranium and, in minor amounts only, titanium. In plate 5, a backscattered electron photograph shows the shape of one grain (pale grey) and scanning photographs for the main constituents show that these are uniformly distributed. The U-Pb-Si grain thus

constitutes a single compositional phase.

Quantitative analysis of two grains including the one shown in plate 5 are reported in table 47.

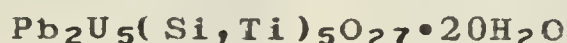
Table 47. Composition of a U-Pb-Si phase from sample DL-3 in weight percentages and atomic proportions. Water is calculated by difference and atomic proportions are given on the basis of two uranium ions.

grain	wt%			at. prop.	
	A	B		A	B
SiO ₂	12.56	11.85	Si	1.90	2.00
TiO ₂	0.60	0.35	Ti	0.04	0.08
PbO	19.14	19.23	Pb	0.82	0.82
UO ₃	60.09	60.41	U	2.00	2.00
H ₂ O	7.61	8.16	O	10.70	10.98
			H ₂ O	4.13	4.02

Results for the two grains A and B are very close. They suggest a formula of the type:

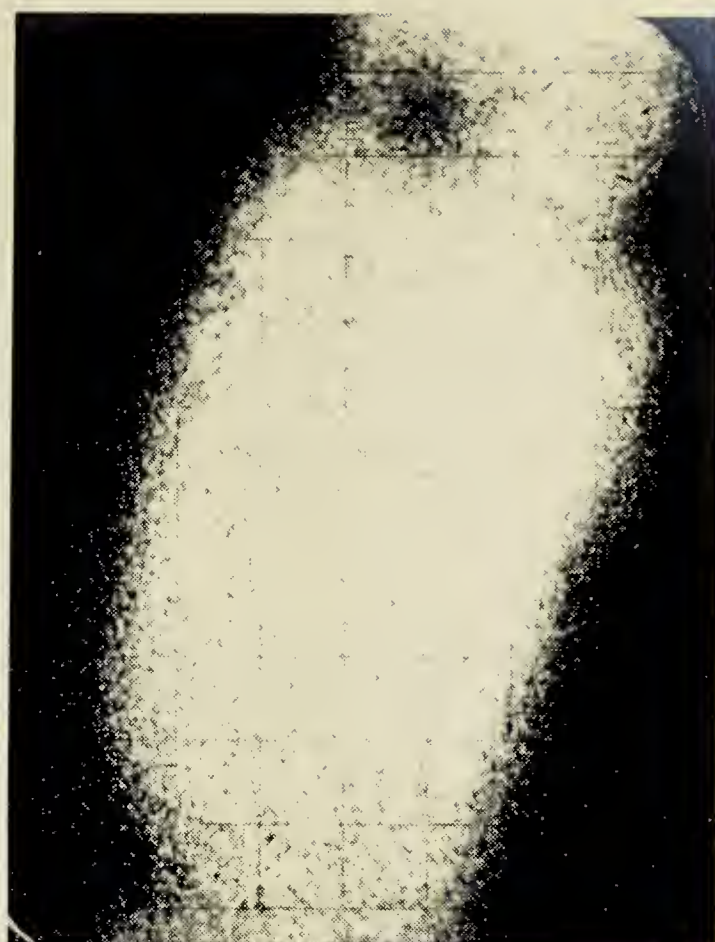
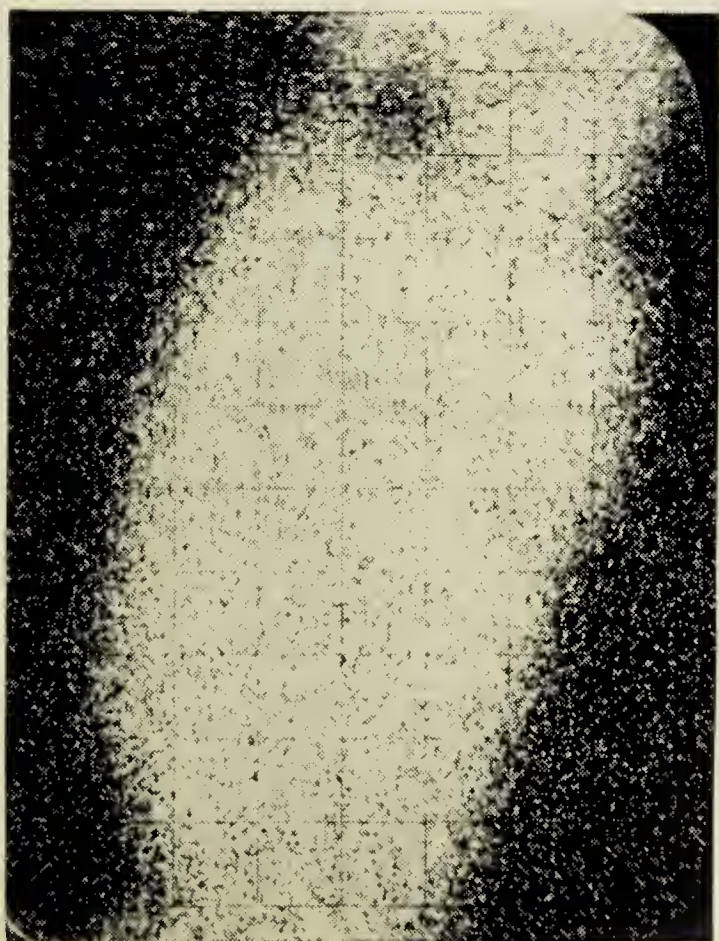
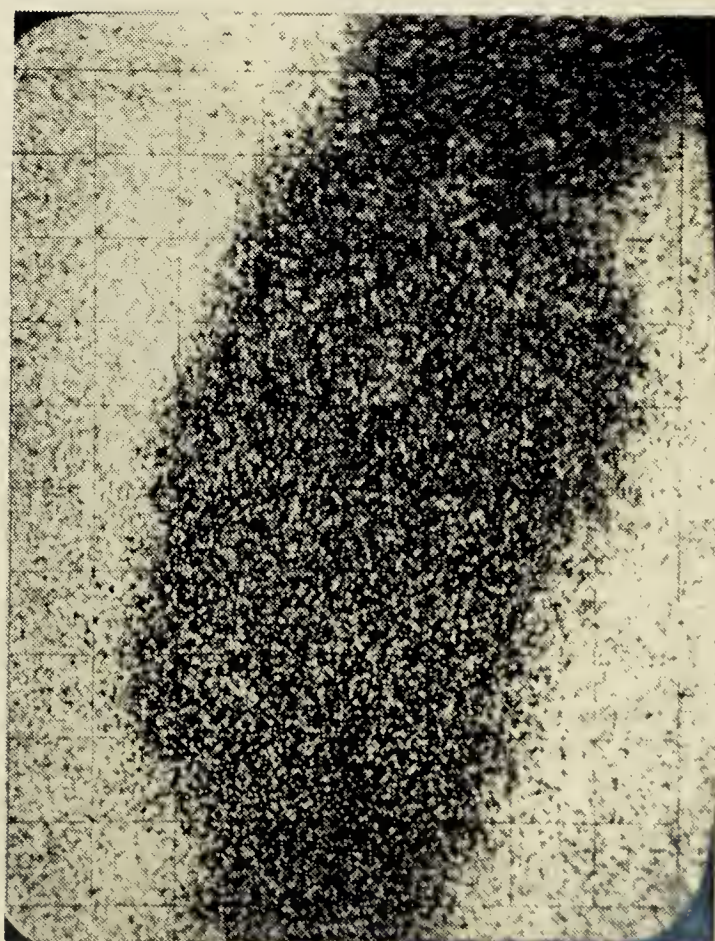


when titanium is grouped together with lead or,



when titanium is grouped together with silicon. It is not possible at this stage to give a definite formula.

The composition and optical properties of the U-Pb-Si phase are unlike those of any known uranium mineral. This phase is a new mineral which remains to be better defined preferably from a sample taken in situ rather than from a boulder.

**bs****U****Pb****Si**

0 25 50
microns

Plate 5 : Backscattered electron (bs) and elemental photographs of 'U-Pb-Si' phase in DL-3.

4. Ti-V PHASE

Small grains 10-20 microns in size, roundish to diamond shaped and with reflectance of about 18-20% in air, occur in samples DL-1 and 8. Two analyses, one for each sample, were carried out. Results are listed in table 48.

Table 48. Composition of a Ti-V phase in weight percentages and atomic proportions. The atomic proportions are calculated for a total number of cations equal to 100.

sample	wt%			at prop.	
	DL-1	DL-8		DL-1	DL-8
Al ₂ O ₃	1.78	1.78	Al	3.23	3.12
SiO ₂	2.80	2.86	Si	4.32	4.23
P ₂ O ₅	0.11	0.31	P	0.14	0.39
CaO	0.29	0.25	Ca	0.47	0.39
TiO ₂	45.12	43.57	Ti	52.48	48.54
V ₂ O ₅	30.61	36.11	V	31.25	35.34
Fe ₂ O ₃	5.63	3.86	Fe	6.55	4.32
As ₂ O ₅	n.d.	2.62	As	-	2.03
PbO	1.50	2.27	Pb	0.61	0.92
UO ₂	2.72	2.19	U	0.95	0.72
Total	90.56	95.82			

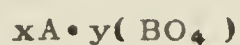
n.d.: not detected

Cations for these two analyses can be grouped together according to ionic radii, valences and coordination numbers. The simplest groups possible are:

A: Ti + Fe + Ca + U + Pb

B: As + P + V + Al + Si as RO₄ radicals

leading to a general formula of the type:



where $x = 61.06$, $y = 38.94$ for the grain DL-1

and, $x = 54.89$, $y = 45.11$ for DL-8

Proportions of A and B will be consistent for the two samples when vanadium is distributed between A and B, i.e., when it occurs not only as the radical VO_4^{3-} but also as V^{+3} in substitution for titanium and iron. For example, a shift of 6.17 vanadium ions from B to A in sample DL-8 brings its x and y values equal to those of sample DL-1. When the analyses are expressed as $x\text{A} \cdot y(\text{BO}_4)$, charges do not balance unless oxygen (or any element of negative charge) is added and the analysis written as:

$(\text{Ti,Fe})_{61.06} (\text{P,V,Al,Si})_{38.94} \text{O}_{209.73}$ for DL-1, and

$(\text{Ti,Fe,V}^{+3})_{61.06} (\text{P,V}^{+5},\text{As,Al,Si})_{38.94} \text{O}_{209.29}$ for DL-8

or, more schematically:



Both grains have very similar compositions though sample DL-1 yields a lower total. They are mainly titanium and vanadium compounds with significant amounts of aluminium, silicon, iron, lead, uranium, and, in DL-8, arsenic, calcium, and phosphorus. Thorium, tantalum and niobium were sought but not found. Low totals may result from the presence of light elements, such as carbon, beryllium and hydrogen, and also from failure to return always exactly to the same area at each step of the analysis.

The atomic proportions of this phase do not correspond to those of any mineral listed by Fleischer

(1976). Nor are there any known minerals which have both titanium and vanadium as major constituents. More thorough studies are needed to define this phase which appears to be a new mineral. As in the case of the U-Pb-Si phase, such studies should preferably be carried out on well localized samples.

5. RUTILE

This mineral occurs in most samples. The uranium content of rutile was verified by analysing one grain from sample DL-8. Results are listed in table 49. Thorium and

Table 49. Composition of rutile (sample DL-8) in weight percentages.

Al ₂ O ₃	0.07
SiO ₂	0.09
TiO ₂	95.58
V ₂ O ₃	3.57
Fe ₂ O ₃	0.20
UO ₂	0.53
Total	100.04

niobium were sought but not found. The total is almost 100% and the analysis appears excellent. The uranium and vanadium contents are high when compared to analyses reported by Deer *et al.*, 1973. Indeed for six rutiles the maximum value for vanadium is 0.26 wt% whilst uranium is not mentioned. Rutile

in the Duddridge Lake region thus reflects the local mineralization.

6. ZIRCON

Zircons are zoned and abundant in sample DL-10. Compositions for two grains are given below (table 50). Uranium is present in zircons only in very low concentrations.

Table 50. Compositions of zircons from the Duddridge Lake region in weight percentages and atomic proportions. The latter are calculated for four oxygen ions.

	DL-1	DL-10		DL-1	DL-10
CaO	0.02	0.02	Ca	-	-
Fe ₂ O ₃	0.03	0.39	Fe	-	0.01
ZrO ₂	64.96	66.17	Zr	0.99	0.99
Hf ₂ O ₃	0.57	0.79	Hf	0.01	0.01
UO ₂	0.10	0.06	U	-	-
			sum: 'Zr'	1.00	1.01
SiO ₂	32.24	32.71	Si	1.01	1.00
Al ₂ O ₃	0.01	0.01	Al	-	-
			sum: 'Si'	1.01	1.00
Total	97.9	100.15	O	4.00	4.00

7. MONAZITE

Monazites were identified in samples DL-5 and 7; they are zoned and not abundant. No complete analyses were done but thorium and uranium contents were estimated by comparing count rates (peak minus background) with those of monazites from Baie Johan Beetz. Results are listed in table 51. Clearly, monazite is enriched in thorium rather than in uranium. However, all monazites from these samples probably do not have thorium and uranium contents close to those listed in table DL-9, since they are zoned and variable in size.

Table 51. Thorium and uranium weight percentages in two monazites from sample DL-10

Sample	Th	U
DL-10(A)	5.53	0.34
DL-10(B)	5.91	0.33

8. APATITE

Apatite is a possible host for uranium. However, in the Duddridge Lake area its uranium content is nil or, at any rate, below the limit of detection of the electron microprobe using wavelength dispersive analysis. No complete analyses were done for this mineral.

C- CONCLUSIONS

The samples from the Duddridge Lake region are enriched in uranium, vanadium, copper and cobalt. This association is not accompanied by thorium. The main uranium-rich minerals are uraninite, brannerite, two new minerals, a U-Pb-Si and a Ti-V phase, and carnotite; the latter two are also vanadium-rich phases. Copper minerals observed are: chalcopyrite and bornite; cobalt minerals are cobaltite and safflorite. Rutile is not an important uranium bearer but nevertheless it is unusually rich in uranium and vanadium and thus reflects the regional mineralization. Yellow staining of the specimens and the occurrence and habit of carnotite and the U-Pb-Si phase, indicate that they were affected by significant weathering.

Any hypotheses for the genesis of the mineralization in the area studied must take account of :

- 1- the association of uranium, vanadium and copper, common in epigenetic sandstone hosted deposits and the presence of cobalt which is generally absent in sedimentary deposits but encountered in vein type deposits such as those of the Great Bear Lake district;
- 2- the absence of thorium in uraninite and 'brannerite' which probably indicates the epigenetic nature of the mineralization;
- 3- the fact that uranium is enriched in both meta-sediments (arkose and quartzite) and basement rock. This suggests remobilization of already existing uranium concentration during metamorphism;
- 4- the age of uraninite: this suggests a type, or at least a period, of deposition different from that of the vein deposits of the Athabasca basin;
- 5- the apparent absence of chloritic and argillitic alteration associated with vein type deposits such as those at Rabbit Lake;
- 6- the lateral continuity of the mineralization over 40 miles, its restriction to the basal horizon of the stratigraphic sequence and its occurrence as lenses all reveal the stratabound character of the mineralization;
- 7- the fact that the sedimentary environment of the supracrustal rocks changes upward and westward from continental to marine: this does not eliminate the

possibility of having pegmatite or vein type deposits but nevertheless offers controls for sedimentary deposition.

From the above considerations we may conclude that the Duddridge Lake mineralization originated at moderate to low temperature. The model favoured is one of epigenetic (or diagenetic) deposits redistributed during metamorphism (1700 - 1750 Ma). It should be noted that certain aspects, such as the uranium-vanadium-copper association and the type of rock hosting the ore minerals (arkose), suggest a Colorado type sedimentary deposit. On the other hand, the presence of cobalt and location of the mineralization in the vicinity of the limit between continental and marine domains, together with the presence of restricted basin-type sediments overlying the mineralized rocks, suggest a similitude with the Shinkolowbe deposit in the Copper Belt of Katanga.

CHAPTER IX

CHARLEBOIS LAKE

A- DESCRIPTION

1. LOCALIZATION

This region (fig. 11) is part of the Churchill Province. It is located in the Athabasca region of northern Saskatchewan, about 15 km north of Black Lake, 35 km northeast of Stony Rapids and 220 km east of Uranium City.

PREVIOUS WORK

Mapping of the Charlebois Lake area has been done at a scale of 1 mi:1 inch by Mawdsley (1957). The geology has been described by the same author (1952, 1957, 1958) and, on a larger scale, by Beck (1967, 1969, 1970) who studied the uranium deposits of the Athabasca region. Morra (1977) has prepared a thesis on the geology of the

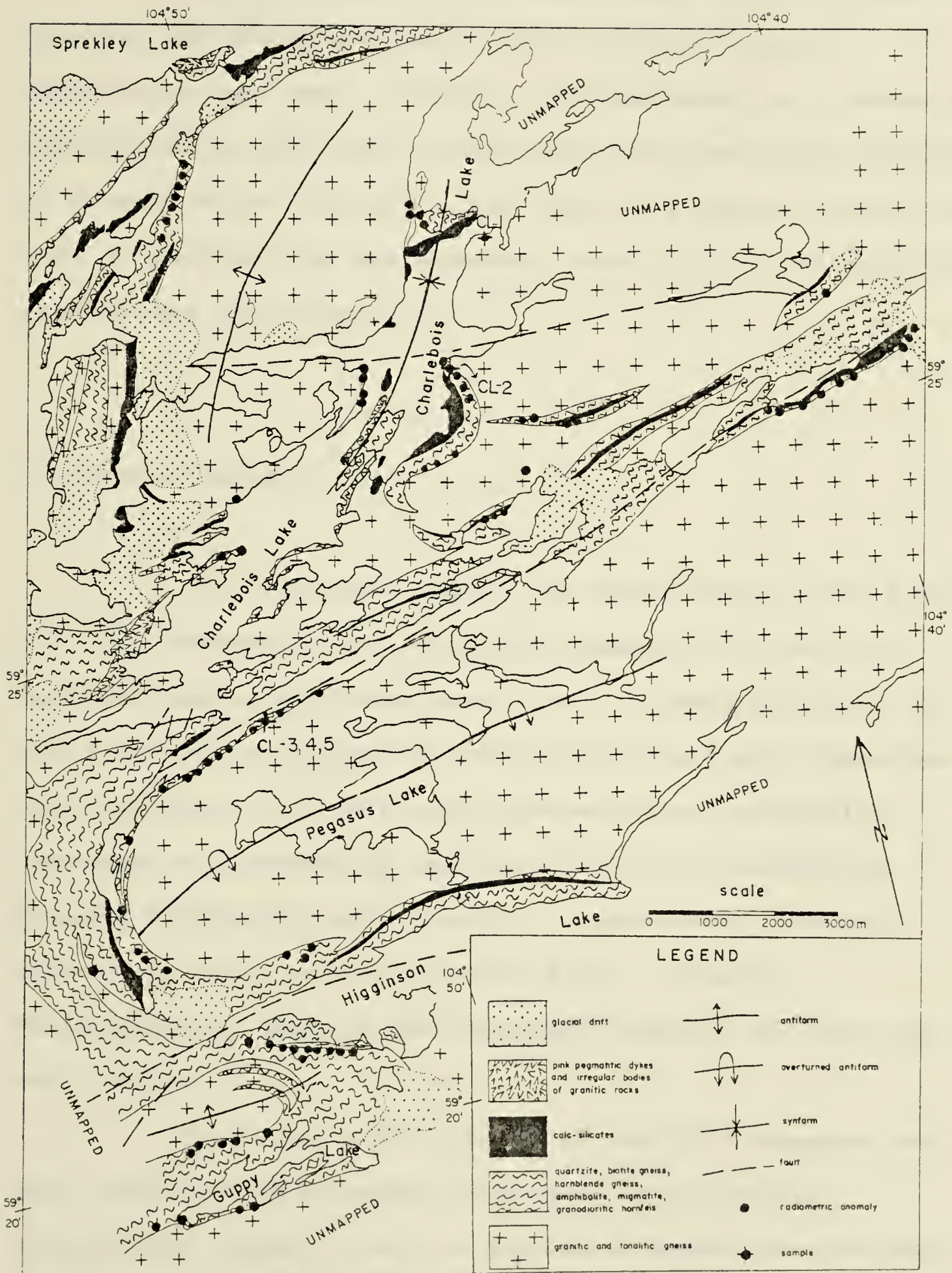


Fig. 11 Charlebois Lake area (simplified after Morra, 1977):

Charlebois Lake area.

Radioactivity in the area (fig. 11) was first reported in 1948 (Mawdsley, 1952). Prospecting and exploration was then initiated and continued in a sporadic fashion until 1974 when rights over the area were acquired by Fosago Exploration Ltd. who initiated Morra's work with a view to determining the economic potential of the numerous radioactive occurrences.

2. GENERAL GEOLOGY

The Athabasca region, as described by Beck (1969, p 8), is underlain by a basement complex of Archean or Aphebian age constituted mostly of "...paragneisses with minor sedimentary rocks to which the term Tazin Group has been applied." All have been metamorphosed and partly replaced or intruded by granites during the Hudsonian Orogeny (1750-1950 my). Locally, conglomerate, arkose, sandstone, siltstone and basalt flows, probably Paleohelikian, rest on the basement complex. All are cut by basic dykes.

This region "is one of the world's largest and most important mineralogic provinces of vein-type pitchblende deposits and, in addition, contains numerous other radioactive showings of economic interest including pegmatite and occurrences of uraninite in crystalline

basement rocks" (Beck, 1969, p. 31).

In the Charlebois Lake area, Morra (1977) has distinguished eight lithologic units; they are from upper to lower:

H - dykes and irregular bodies of pink pegmatite

G - quartzites

F - biotite gneiss

E - hornblende gneiss and amphibolite

D - calc - silicate rocks

C - migmatite

B - granodioritic granofels

A - granitic and tonalitic gneiss

The name Charlebois Lake Complex has been applied to unit A to G by Morra (1977).

The Charlebois Lake area (fig. 11) is underlain mostly by granitic and tonalitic gneisses while units B to G occur as bands bringing out the structure of the area.

3. DESCRIPTION OF LITHOLOGICAL UNITS

The following brief description is based on that of Morra (1977) except where otherwise stated.

A- Granitic and tonalitic gneisses

These occur mainly in the core of an antiformal structures. Layers of amphibolite are intercalated in the upper part of these gneisses where they grade into granodioritic granofels and/or migmatites.

B- Granodioritic granofels

This unit was named pegmatitic granite by Mawdsley (1952). It ranges in composition from diorite, to tonalite, to alkali-feldspar granite. It is distinguished from the granitic gneiss mainly by its coarser grain size; indeed the grain size ranges from 0.5 to 1 mm in the granofels and from 3 to 30 mm in the granitic gneiss. This unit "occurs almost wholly along and close to the granite and gneiss contacts with the metasediments..." Mawdsley (1952, p 369). 'Granite and gneiss' correspond to granitic and tonalitic gneiss (unit A) on the map (fig. 11). Zones of migmatites (unit C), and veins and pockets of quartz are associated with the granofels.

C- Migmatites

These are felsic bands composed chiefly of quartz, plagioclase and microcline intercalated with biotite or hornblende rich bands. This rhythmic variation is imputed to compositional variation in the original sediments and to exudation during their metamorphism. Mawdsley (1952) interprets the migmatites as being of igneous origin as he

terms them injection migmatites.

D- Calc-silicate rocks

This unit includes amphibole-diopside gneiss, talc-serpentine-carbonate marble, and sericite-phlogopite/biotite-diopside gneiss. It "forms the bulk of what appears to be a definite horizon within the folded metasediments of the area" (Mawdsley, 1952, p. 368).

E- Hornblende gneiss, amphibolite; F- biotite gneiss

These two units are intimately associated. The amphibolite is not foliated while the biotite and the hornblende gneiss are well foliated.

G- Quartzite

This unit only occurs in minor amounts usually as thin beds and lenses.

H- Pink pegmatite dykes and irregular bodies of granitic rocks

These cut across all the aforementioned units in the Charlebois Lake area. They are essentially composed of pink microcline, plagioclase and quartz. Dykes are present southeast of Charlebois Lake and north of Guppy Lake, small bodies also occur north of Guppy Lake and between Charlebois Lake and Sprekley Lake.

4. STRATIGRAPHY

The stratigraphic relations between the various units have been interpreted somewhat differently by Morra (1977) and by Mawdsley (1952). Table 52 compares both interpretations. The main divergence expressed in this table arises from the situation of units A, B and C. These are considered to be the lower members of a sedimentary suite, namely the Charlebois Lake Complex, by Morra (1977) while Mawdsley (1952) describes them as intrusive rocks in a sedimentary sequence, the Tazin Group. In the Beaverlodge area, Tremblay (1968) has defined two lithological sequences of the Tazin Group, separated by a northeast fault. By comparing the above stratigraphic sequence with that of Tremblay, it can be seen that they cannot be directly correlated and, that members such as the calc-silicate rocks and the quartzite beds can be compared to more than one single unit of the Tazin Group of the above area. Indeed, the Tazin Group in the Beaverlodge area comprises at least two units composed one in part and the other wholly of calc-silicate rocks; they are unit 3 and unit 9 in the western part of Tremblay's map (1968). Quartzites are numerous in the Beaverlodge area, and Tremblay has distinguished at least 12 map-units containing such rocks.

Thus the attempt to correlate the lithological suite A to G with the Beaverlodge area and, to define it relative to the Tazin Group, was unsuccessful.

Table 52: Stratigraphy of the Charlebois Lake area, according to Mawdsley (1952) and Morra (1977).

Mawdsley (1952)	Morra (1977)
<p>Pleistocene and Recent sediments</p> <p>----- unconformity -----</p> <p>Coarse pegmatite (H)*</p> <p>----- intrusive contact -----</p> <p>Fine pegmatite and migmatite (B,C)</p> <p>----- intrusive contact -----</p> <p>Granite gneiss and granite (A)</p> <p>----- intrusive contact -----</p> <p>Metamorphosed sediments and possibly minor amounts of metavolcanics and dyke rocks: impure quartzite, biotite schists, hornblende schists, diopside-rich gneisses and schists, and other calcareous meta-sediments. (D,E,F,G)</p> <p>----- Early Archean -----</p> <p>----- Early Proterozoic -----</p> <p>----- Paleozoic -----</p> <p>----- Mesozoic -----</p> <p>----- Tertiary -----</p> <p>----- Quaternary -----</p>	<p>Pleistocene and Recent sediments</p> <p>----- unconformity -----</p> <p>(H) Pink pegmatite dykes and irregular bodies</p> <p>----- intrusive contact -----</p> <p>(G) Quartzite</p> <p>(F) Biotite gneiss</p> <p>(E) Hornblende gneiss and amphibolite</p> <p>(D) Calc-silicate rocks</p> <p>(C) Migmatite**</p> <p>(B) Granodiorite granofels</p> <p>(A) Granitic and tonalitic gneiss</p> <p>Charlebois L. Complex</p> <p>Aphebian</p> <p>** The stratigraphic position of the migmatite remains uncertain as it is locally in contact with the granitic gneiss.</p>

* Capital letters indicate corresponding units.

5. STRUCTURE

The dominating structural features of the Charlebois Lake area are three major antiforms oriented south to southwest. They are separated in one case by a synform (between Sprekley Lake and Charlebois Lake) and in the other by a fault (between Charlebois Lake and Pegasus Lake).

The cores of the antiforms are occupied by granitic to tonalitic gneisses, while stratiform bands of units B to G appear pinched between more rigid blocks of the granitic and tonalitic gneisses. This suggests that the latter might have been a basement complex beneath units B to G.

The general concordance and parallelism between the granodioritic granofels and migmatites and the upper metasediments suggest that these are all part of a sedimentary sequence. It should also be noted in figure 11 that the calc-silicate horizon follows the antiformal structure around Pegasus Lake as a single band, while two bands of it appear northeast of the antiform; they are separated by the upper hornblende gneiss and amphibolite. This suggests the presence of a synform parallel to the northeast trending fault shown by Morra (1977).

6. METAMORPHISM

The metamorphic mineral assemblages identified in the Charlebois Lake area are listed in table 53. They place the degree of metamorphism in the intermediate to upper amphibolite facies. Quantitatively insignificant retrograde metamorphism in the whole area (unit A to G) and short distance migration of potassium in the migmatites have also been reported (Morra, 1977).

Table 53. Metamorphic mineral assemblages from the Charlebois Lake area (after Morra, 1977).

units	assemblages
A,B,C-	quartz-oligoclase-microcline-biotite-chlorite
A,B,C-	quartz-oligoclase-microcline-biotite-muscovite
E	- quartz-andesine-biotite-hornblende
C	- quartz-andesine-microcline-biotite-sillimanite
F	- quartz-oligoclase-microcline-muscovite-biotite-sillimanite-garnet
E	- quartz-andesine-hornblende-diopside
D	- sericite-diopside-actinolite-hornblende
D	- carbonate-talc-serpentine

7. MINERALIZATION

The Charlebois Lake area is part of a uranium mineralogic province. Except for the dykes and small bodies of pink pegmatite, all rock-types encountered in the area are enriched in uranium by at least a factor of 3 relative to the average concentration in similar rock-types (Morra, 1977); similarly they are enriched in thorium by at least a factor of 1.5 and as much as 6 in the case of granitic gneiss (Morra, 1977). The Th/U ratio is close to 1.5 in the granitic gneiss, the biotite gneiss, the amphibole gneiss and in the amphibolite; it is approximately 0.8 in the calc-silicate rocks and 0.3 in the migmatites and granodioritic granofels (Morra, 1977). All the important showings occur in a more or less continuous fashion in the granofels and in the migmatite between the granitic gneiss and the calc-silicate horizon. The latter is always barren of mineralization but the gneiss generally has higher radioactivity when in contact with 'showings'.

Uranium occurs mainly as uraninite partially altered to 'gummite', and in a lesser amount, in betafite (?), thucholite, secondary uranophane and metamict zircon. Molybdenite, apatite, sphene, pyrrhotite and magnetite are also common in the 'showings'.

Controversial hypotheses for the formation of the uranium deposits have been presented; according to Morra (1977, p.v), "geological and radiometric data suggest that

the mineralization present in the Charlebois-Higgenson Lake area may have originally been of syngenetic sedimentary origin, prior to its metamorphism and that the parent rocks of the granitic and tonalitic gneiss of the area constitute the most likely source-rocks of the uranium deposits". Based on Mawdsley's work (1952), Beck (1969) describes the mineralization as 'lit-par-lit' type deposits, i.e., uranium rich pegmatites intrusive in to the metasediments.

Whatever the interpretation, it is certain that the radioactive showings occur in the granofels and in the migmatites. Their more or less continuous distribution around the granitic gneiss and in the folds emphasises the structure of the area.

B- ANALYSIS

Five samples were collected in the Charlebois Lake region (fig. 11). All were chosen from zones of high radioactivity. Identification and petrographic descriptions are given in appendix IV.

The main constituents are quartz, orthoclase, plagioclase, biotite, muscovite with minor amounts of uraninite, monazite, zircon and occasionally, apatite, pyrite, hematite and galena. β -uranophane occurs as a coating on some of the samples.

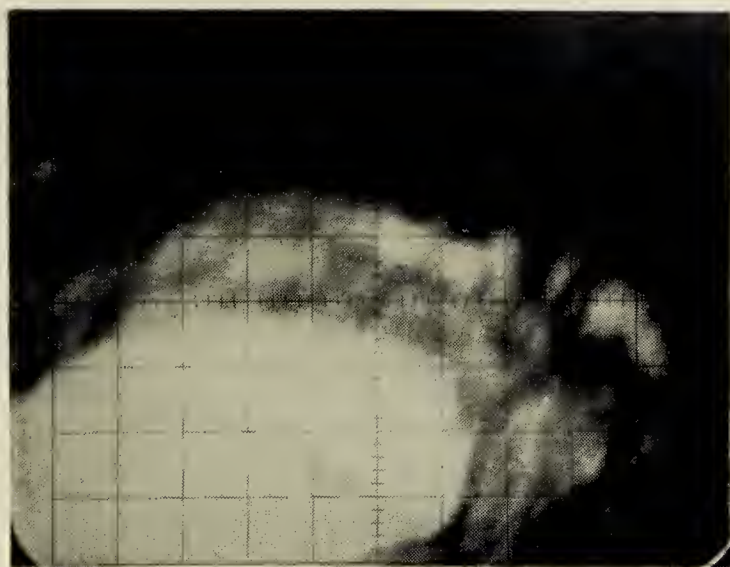
Uraninite and β -uranophane were investigated in detail; uranium and thorium in monazite were determined qualitatively; one analysis of zircon is presented. The analysis for β -uranophane is given in a previous chapter (analysis of standard materials). No uranium or thorium were detected in the apatite.

1. APPEARANCE OF URANINITE AND MONAZITE

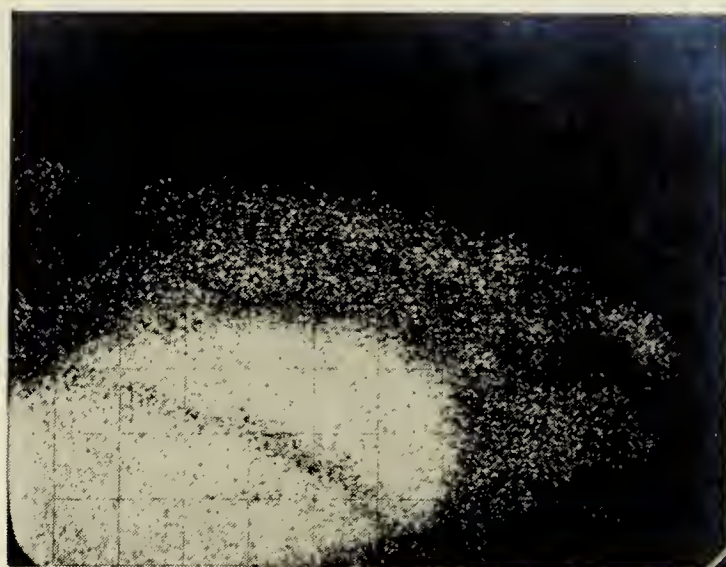
In some samples (CL-2, 4, and 5A) uraninite, monazite and also zircon occur mostly included in, or in contact with, biotite; in the other samples (CL-1, 3 and 5B), it is distributed randomly.

In transmitted light, uraninite is present as dark green to brown material rimmed by a reddish zone. Grains included in feldspar and quartz are somewhat less altered than those included in, or in contact with, biotite. But nevertheless in most cases, they are fractured and altered, with only a few fragments of uraninite remaining which are suitable for microprobe analysis. Monazite is zoned and, like uraninite, it is surrounded by a reddish rim.

Chemical relations between uraninite (or monazite), its reddish rim, and its host mineral were investigated. Backscattered electron and X-ray scanning photographs were taken for a particularly good looking uraninite and a monazite (plates 6 and 7, respectively). The



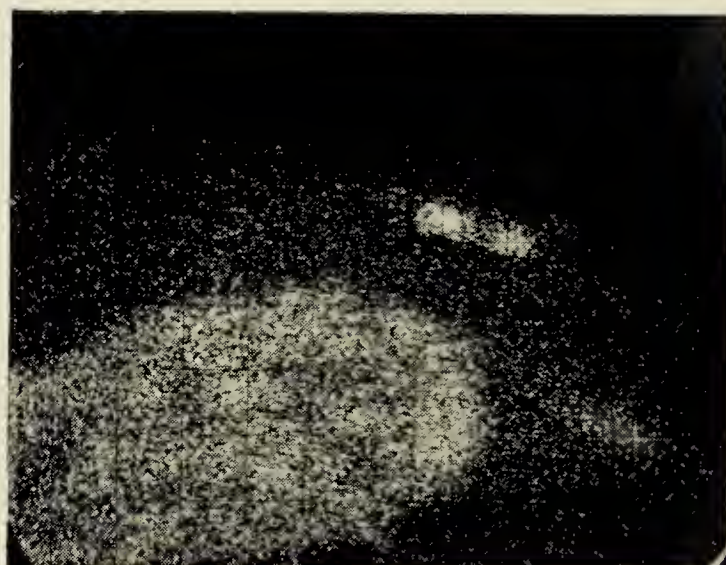
bs



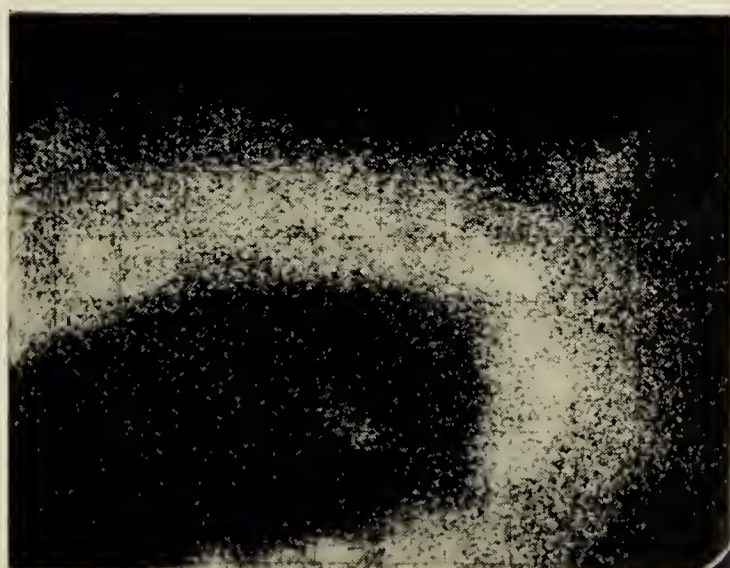
U



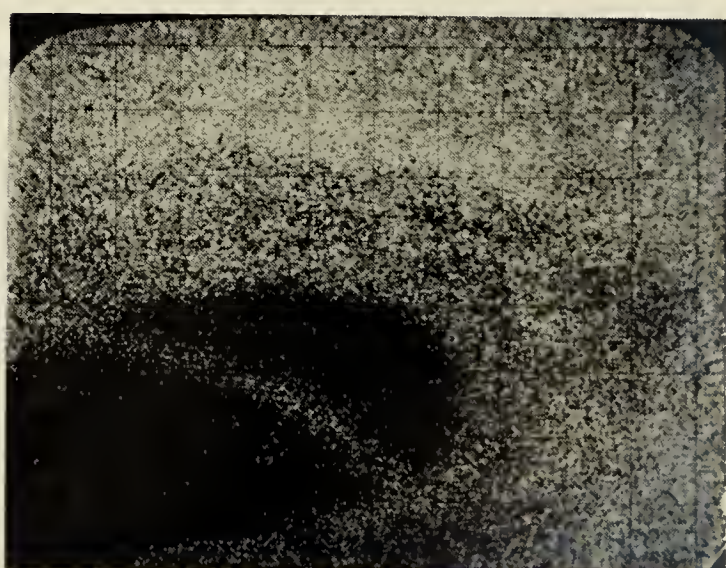
Th



Pb



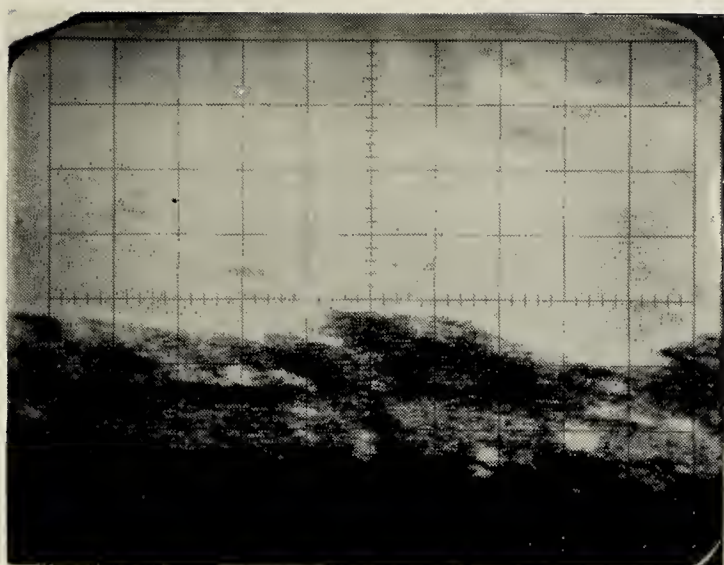
Fe



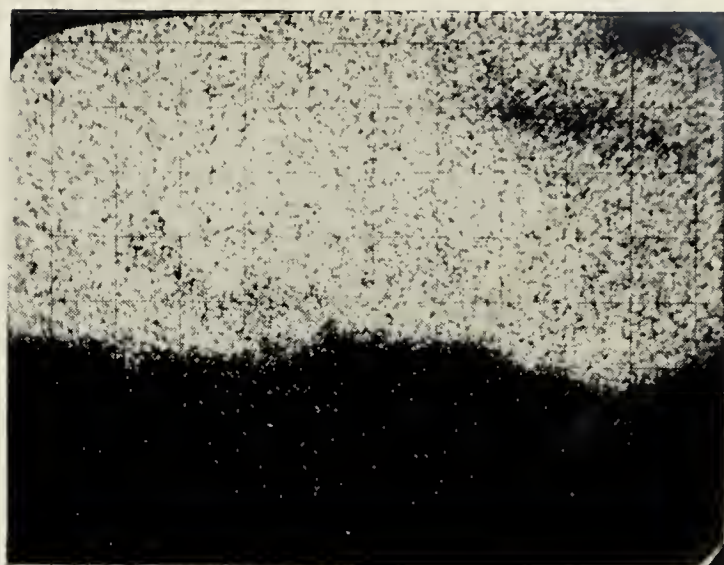
Si

0 50 100
microns

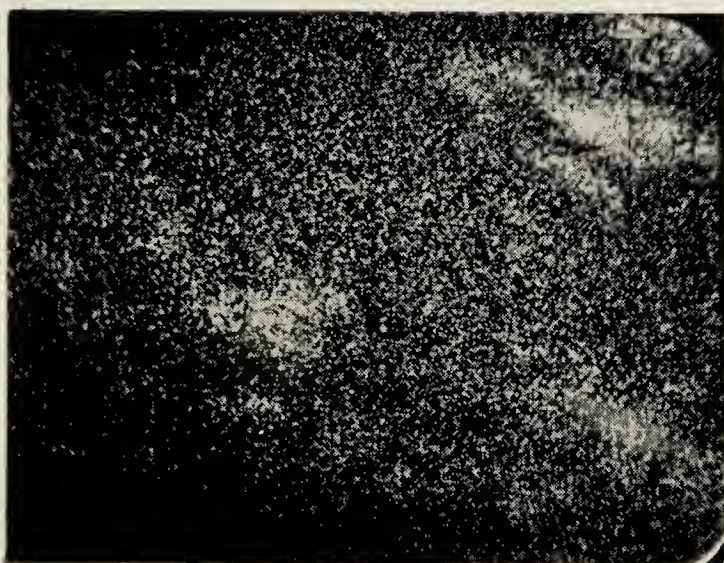
Plate 6 : Backscattered electron (bs) and elemental photographs of uraninite in CL-1.



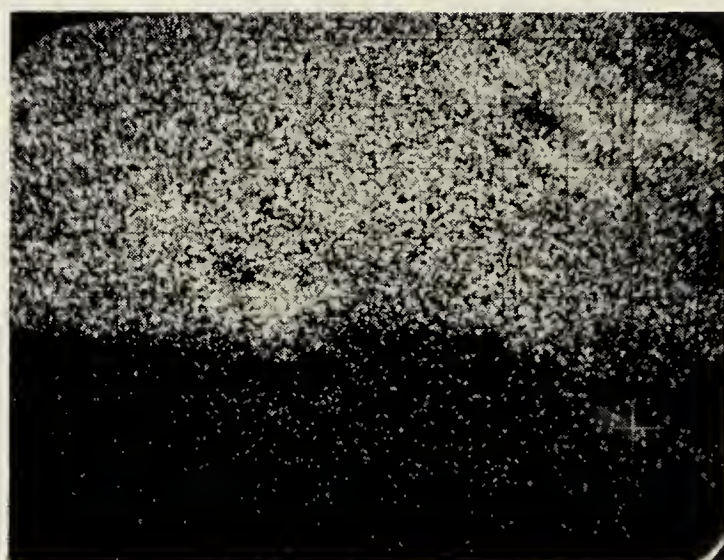
bs



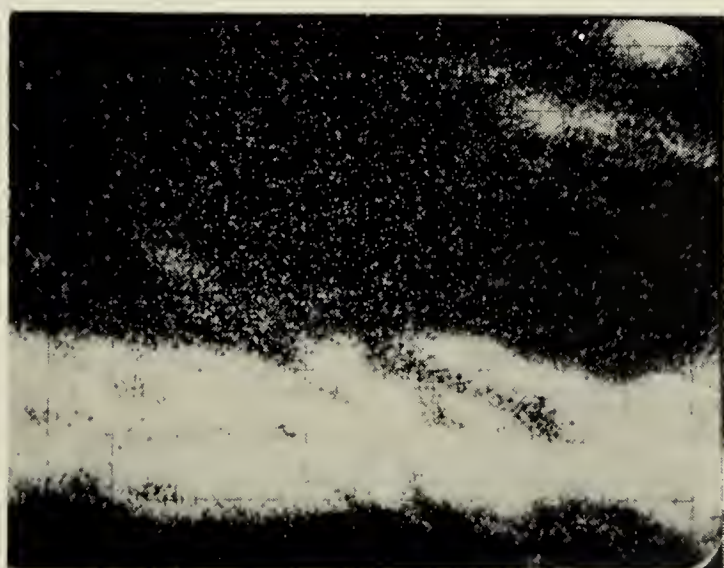
P



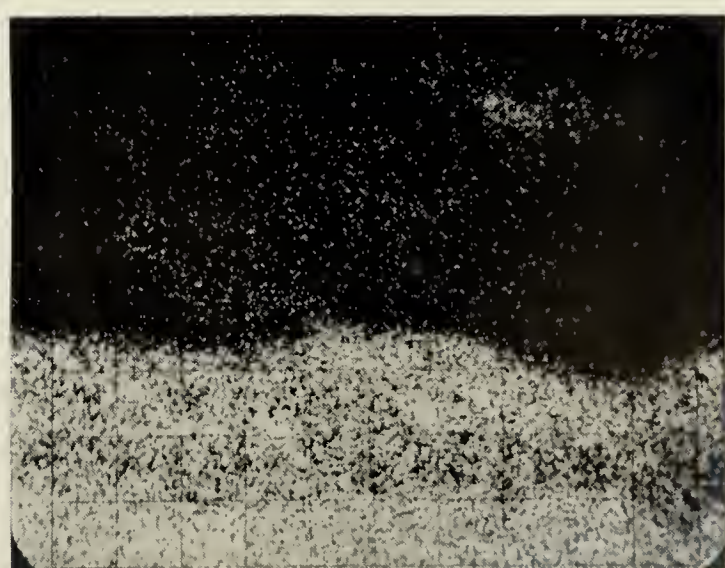
Th



U



Fe

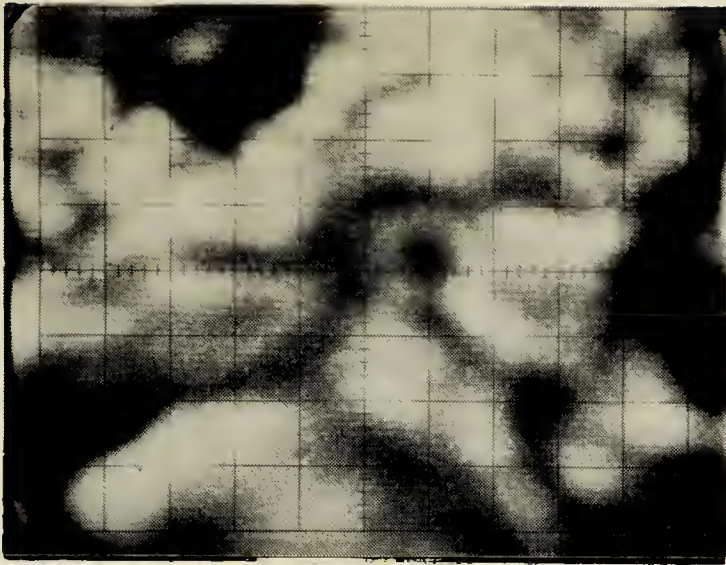


Si

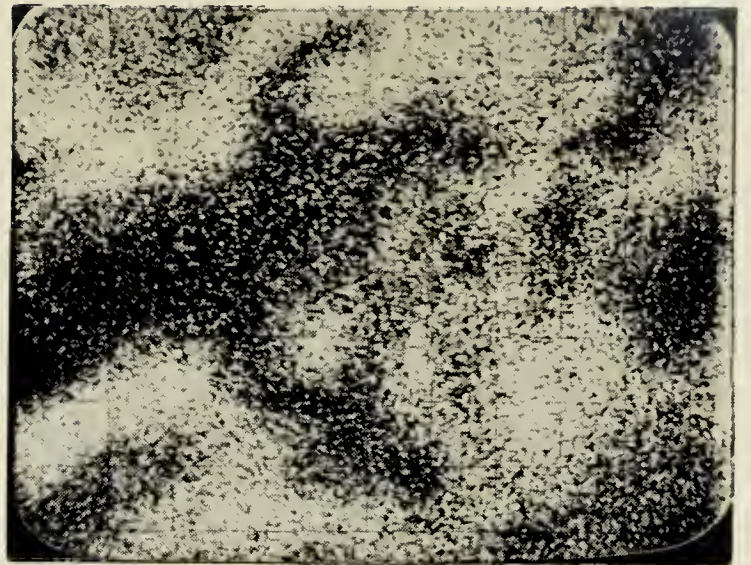
0 50 100
microns

Plate 7 : Backscattered electron (bs) and elemental photographs of monazite in CL-1.

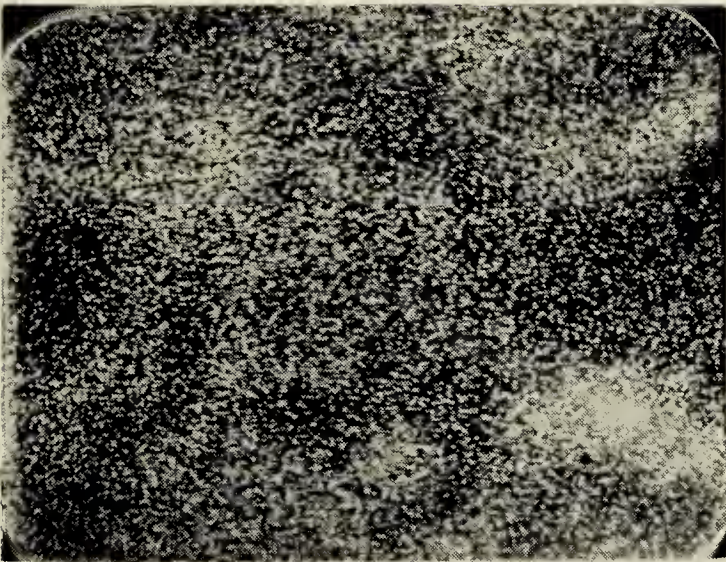
main constituents of uraninite are uranium, thorium and lead with minor amounts of silicon, calcium and iron. The main constituents of monazite are phosphorus, rare-earths and thorium with minor amounts of uranium, iron and silicon. In the backscattered electron photographs the white areas represent uraninite (plate 6) and monazite (plate 7), the dark areas are their host mineral (feldspar) and the intermediate grey represents their reddish rims. In both cases the rims show a high concentration of iron. They are enriched in lead and uranium relative to the feldspar and in silicon (and other feldspar constituents) relative to uraninite and monazite. Thorium is restricted to uraninite and monazite grains, and phosphorus to the monazite grain. Backscattered electron and X-ray scanning photographs of a typical uraninite are also presented (plate 8). The backscattered electron photograph shows a fractured grain or a cluster of grains of high average atomic number (white spots). X-ray scanning photographs show that uranium and thorium vary sympathetically, and are abundant in only part of the 'grain'; lead is concentrated with iron in other parts, and, finally, silicon is present throughout the area but in higher concentrations where uranium and thorium are low and where iron is intermediate. In the present case, the thorium distribution cannot be used because of the high background. Indeed, thorium variations are low, and therefore its photograph indicates changes in the average atomic number of the grains rather than in the thorium



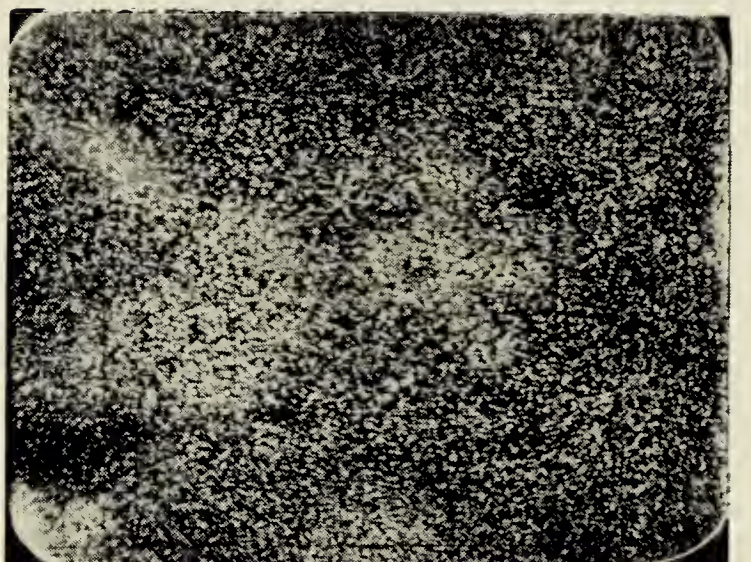
bs



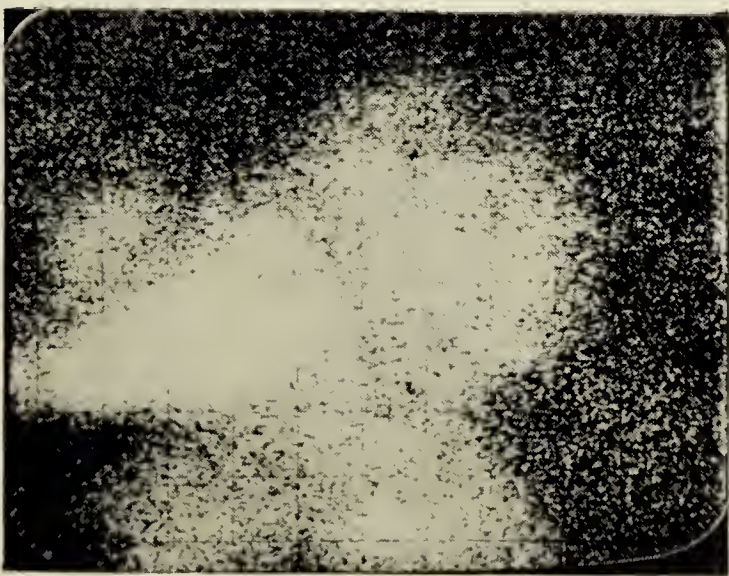
U



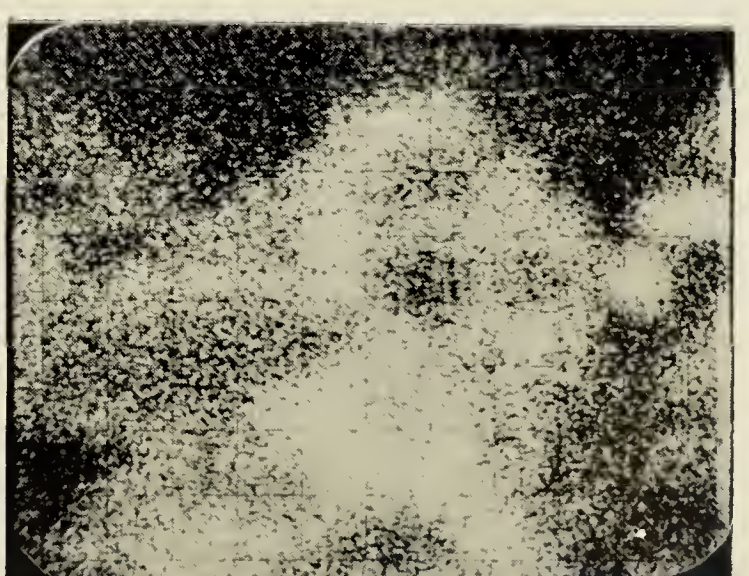
Th



Pb



Fe



Si

0 25 50
microns

Plate 8 : Backscattered electron (bs) and elemental photographs of uraninite in CL-5.

distribution.

X-ray powder photographs of some reddish coated uraninite yielded two patterns, one of uraninites, and a second of hematite.

It should be noted also that the reddish rims are prominent when uraninite and monazite are related to biotite, less when these are included in feldspar and almost absent when included in quartz.

It is proposed that the rims form by migration of uranium out of uraninite and monazite (lead behaves as uranium at least in uraninite), and by migration of iron toward uraninite or monazite. Oxygen produced during radiogenic decay of uranium and thorium oxidizes the iron of the biotite around the uraninite or monazite grain and creates a concentration gradient which, in turn, induces further diffusion of Fe^{+2} towards uraninite or monazite resulting in a hematite coating.

2. URANINITE

Five uraninite grains were analysed (table 54). Low totals are imputed to the poor quality of the grain, the possible presence of a larger portion of uranium occurring as U^{+6} , and also to the likely presence of volatiles such as helium. The analyses show that the thorium to uranium ratio is uniform in the various samples. Rare-earths were sought

Table 54. Composition in weight percentages of uraninites from the Charlebois Lake region. Lead is given a valence of two and, uranium a valence of four with an amount of hexavalent uranium equal to the amount of lead present.

Sample	CL-1	CL-5A1	CL-5A2	CL-5B1	CL-5B2
Al ₂ O ₃	0.70	0.25	0.26	0.13	0.21
SiO ₂	3.79	2.22	4.24	0.64	1.03
CaO	1.55	0.31	1.40	0.67	0.62
Fe ₂ O ₃	0.10	0.59	0.97	0.10	0.34
PbO	16.08	14.33	14.31	18.86	17.28
ThO ₂	7.84	5.17	5.31	5.80	5.37
UO ₂₋₃	66.26	69.04	68.36	68.14	67.21
Total	96.32	91.91	94.85	94.34	92.07

but not found in these uraninites.

Age

Approximate ages were calculated by the method described for the Baie Johan Beetz uraninites. As can be

Table 55. Approximate ages for uraninites from the Charlebois Lake region.

sample	age (Ma)
CL-1	1783
CL-5A1	1546
CL-5A2	1558
CL-5B1	2054
CL-5B2	1910

seen in table 55, the five uraninites yield a wide range of ages. The lower values, 1546 and 1558 Ma were obtained from a rock specimen containing galena. It is reasonable to

assume that galena formed from radiogenic lead expelled from uraninite. This would obviously decrease the apparent age of the latter. Thus 1546 Ma and 1558 Ma are not representative of the age of the mineralization, but may reflect a subsequent period of readjustment. Three values remain. Uraninite CL-1 which yielded 1783 Ma has a pronounced migration rim (plate 6). It is therefore expected that the lead to thorium plus uranium ratio has been altered and that 1783 Ma is not representative of any definite period. Uraninite CL-5B-2 is somewhat altered and yielded 1910 my; sample CL-5B1 appeared fresh and yielded 2054 my.

The only conclusions that can be drawn from the approximate apparent ages is that most uraninites have not behaved as closed systems since their formation, and that mineralization in the area has a minimum age of 2054 my.

3. MONAZITE

Monazites are common in the samples. Like uraninites, they are often surrounded by a hematitized rim. No complete quantitative analyses of monazite were done, but the thorium and uranium contents were estimated by comparing their count rates (peak less background) with those of monazites from Baie Johan Beetz.

The thorium content of monazite varies not only from one grain to another (table 56), but also within single

Table 56. Uranium and thorium weight percentages of two monazites from the Charlebois Lake region (CL-1, CL-5A).

Sample	UO ₂	ThO ₂
CL-1	0.49	14.95
CL-5A	0.42	4.00; 9.87

grains (4.00 and 9.87 wt% ThO₂ were obtained from two different areas of the same grain. Uranium, on the other hand, is low and uniform.

4. ZIRCON

Zircons in the samples are colourless to brownish in transmitted light; they do not give rise to radiogenic haloes when included in biotite. Analysis of one grain (table 57) shows a low uranium content compared, for example, to the average content of zircons from Baie Johan Beetz (0.66 wt% UO₂). Thorium was sought but not found. The absence of haloes presumably results from the low content of radiogenic elements.

Table 57. Composition of zircon from one sample of the Charlebois Lake region in weight percentages and atomic proportions. The latter are calculated for four oxygen ions.

CaO	0.01	Ca	<0.01
Fe ₂ O ₃	0.75	Fe	0.02
ZrO ₂	64.83	Zr	0.97
Hf ₂ O ₃	1.24	Hf	0.01
UO ₂	0.16	U	<0.01
		sum: 'Zr'	1.00
Al ₂ O ₃	0.02	Al	<0.01
SiO ₂	32.89	Si	1.01
		sum: 'Si'	1.01
Total	99.90	O	4.00

C- CONCLUSIONS

Samples from the Charlebois Lake region are enriched in uranium and thorium. Uranium is present mainly in uraninite, thorium in monazite and to a smaller extent, in uraninite. β -uranophane is an alteration product which coats some of the samples. Betafite and thucholite, previously reported in the area (Morra, 1977), were not found in the samples studied.

Hypotheses for the genesis of mineralization must account for:

- 1- the association of uranium and thorium, indicating a relatively high temperature of formation;
- 2- the fact that all rock-types encountered in the area, with the exception of dykes and small bodies of pink pegmatite, are enriched in uranium and thorium;

- 3- the stratigraphic and lithological control of the mineralization;
- 4- the restriction of significant anomalies to the granofels and migmatites located between the granitic gneiss and the calc-silicate horizon;
- 5- an approximate age of 2054 Ma for uraninite and the mineralization.

Considering the above facts, it appears that mineralization in the migmatites and granofels occurred in two stages. Firstly by the deposition of uranium and thorium enriched sediments. Indeed, all meta-sedimentary rocks of the area are enriched in uranium and thorium as is their source, the granitic gneiss (Morra, 1977). A secondary enrichment occurred when mineralizing fluids possibly expelled from the granitic gneiss during metamorphism, propagated through the migmatites and granofels horizon, thereby increasing and redistributing the uranium and thorium. These fluids were probably limited in their migration by the overlying impervious horizon of calc-silicates. This second stage probably occurred during the Hudsonian orogeny and may well be synchronous with the first major uranium mineralizing event (epigenetic deposits) in the Beaverlodge area: 1975-1950 my (Tremblay, 1972). In the latter region we know that a period of faulting and shearing accompanied by uranium redistribution took place around 1240 Ma ago (Tremblay, 1972). Similar events may have

occurred in the Charlebois Lake area but their effects were not strong enough to induce uranium redistribution and formation of vein type deposits. It follows that faults which cross the Charlebois Lake area may be related to the family of faults of the Beaverlodge area which have been repeatedly active after the Hudsonian orogeny.

This hypothesis differs from the one proposed by Morra (1977) by the assumption that a second stage of enrichment took place. It does not imply, nor does it exclude, as in Beck's hypothesis (1969), the intrusion of important amounts of granitic material.

CHAPTER X

CONCLUSION

This work has demonstrated the usefulness of the electron microprobe in the study of uranium and thorium minerals. It has also brought out various aspects in need of improvement, especially the establishment of analytical standards, correction procedures and to a lesser extent, with the time required for an analysis.

The most reliable standards were found to be simple synthetic compounds such as oxides. Carbides, fluorides and silicides could be used provided they can be obtained as single phase grains of more than 50 microns.

It appears that corrections applied by FEPAC give better results than those applied by COR-2. Owing to the fact that FEPAC does not print out detailed corrections, the source of the differences in the results could not be traced back. Because FEPAC recalculates many of the parameters needed for the various corrections, it is not necessary to create and store an extensive data file for this programme. Compared to COR-2, this approach is more flexible and more

amenable to use by workers not familiar with the detail of the programme. FEPAC, however, cannot be installed directly in most computing systems without carrying out language modifications.

In general, correction procedures remain somewhat inadequate. Improvement could result from the determination and refinement of empirical factors for X-ray lines shorter than the uranium and thorium M absorption edges through more analyses of a larger number of simple compounds. However, better understanding of the ZAF effects through basic studies would be more satisfactory and of wider usefulness.

Compared to other methods of analysis, the electron microprobe is rapid. This could be further improved by using a fully automated instrument. The use of EDA with an appropriate correction programme would also reduce considerably the time required for analysis and have the advantage of determining simultaneously all elements needed. Such an approach was beyond the scope of this study. It is also doubtful whether the resolution of present-day solid-state detector systems such as the one in use at the Department of Geology of the University of Alberta (Smith and Gold, 1976) is sufficient to unravel the problem of overlapping L-lines of the rare-earth group and other heavy elements which are commonly present in primary uranium- and thorium-minerals. However, secondary uranium minerals often have a simpler chemistry and may be more amenable to this approach.

In the study of uranium compounds, uranium minerals, and some of their deposits, the electron microprobe has proven useful in five main ways.

- 1- It is possible to identify uranium minerals on the basis of their composition, and moreover to analyse quantitatively such minerals and other uranium compounds with both precision and accuracy. Indeed, precision and accuracy achieved on uraninites were sufficient to allow the calculation of meaningful ages and to distinguish between uraninites of different 'ages'.
- 2- It was possible to define the mineralogy of the three regions considered, and also to identify minerals which were not identifiable by microscopic examination and would, therefore, have required tedious separations and chemical analyses. Even then, it might not have been possible to make the determination due to possible contamination, or to an insufficient amount of material; such was the case of the U-Pb-Si phase from Duddridge Lake. It was also possible to study compositional variability and internal zoning of certain phases such as allanite, and monazite.
- 3- When analysing separated minerals, a doubt always arises as to whether minor elements are due to the presence of impurities or to chemical substitution.

Investigation of the nature and extent of chemical substitution is thus facilitated and put on firmer ground by microanalysis of single grains, as exemplified by the analyses of allanite, zircon and 'brannerite'.

- 4- Two new minerals were partly defined, namely a U-Pb-Si phase, and a Ti-V phase. These were analysed quantitatively but require additional data before they can be named according to the rules set by the International Mineralogical Association.
- 5- Mineralizing events were dated. Ages can be calculated for individual grains after simultaneous analyses of the elements concerned. Though it yields less information than the mass-spectrometer, which determines isotopes, the electron microprobe has the advantage of being able to perform point analyses; it is, however, limited to uranium- or thorium-rich minerals containing sufficient amounts of radiogenic lead (say, at least 2 wt%). Mineralized rocks and in particular those that have reached ore-grade are the result of a succession of events that occurred over a period of time which is generally longer than the resolution of present day geochronological methods. In such rocks a complex mineralogy reflects the complexity of the mineralizing events. The microprobe permits the distinction between the different varieties of a mineral species, between

fresh and altered material, and between zoned and unzoned phases which can seldom be isolated by mineral separation techniques. Furthermore, it is possible to perform quantitative analyses on each of these phases. Thus, in a sample or suite of samples, rather than the average age of mineralization, one can obtain ages of mineralizing events and relate them to the corresponding phases. Having thus defined the problem, one can proceed to more precise methods such as mass-spectrometry, if need be.

Some potential applications of electron microprobe analysis of uranium-bearing minerals have not been investigated here. However, with the findings of this study it is possible to foresee fields for such applications.

The structures of many uranium and thorium minerals remain to be determined and others, to be refined. We now have a way in which single-crystal X-ray crystallography can be brought to greater value by the non-destructive, precise analysis of the grain on which a structure is determined. This, of course, applies not only to uranium and thorium minerals, but to all compounds and more specifically to the naturally occurring 'impure' minerals.

In sedimentology, the accurate definition of heavy minerals and, in particular, the age of those bearing uranium, enables one not only to characterize a formation or

marker-bed, but also helps towards a better understanding of the paleogeography of a given period by providing a more accurate definition of the source material of the sediments.

An expanding field of research is pollution control work. The recognition and identification of radioactive particles as contaminants in various environments might be advantageously done through microprobe analysis.

Another field, maybe more important, is the realm of mineral exploration and beneficiation. With an increasing demand for uranium, low-grade deposits, for example the so-called 'uranium porphyries', which were, up to now, economically marginal, become more and more attractive. For such deposits, it is important:

- 1- to know what portion of the uranium is in uranium-rich phases amenable to pre-concentration in order to decide what constitutes a potential ore; and
- 2- to define accurately those phases in ore-grade materials as a preliminary to the development of extraction methods.

This, of course, applies not only to low-grade ore but also to the secondary recovery of mine tailings where some mineral phases may not have been extracted at the time of the original treatment.

BIBLIOGRAPHY

- Abeledo, M.E.J. de, Benyacar, M.A.R. de, and Galloni, E.E.
(1960): Ranquillite, a calcium uranyl phosphate. Am.
Mineral. 45, 1078-1086.
- Adda, Y., Beyeler, M. and Kirianenko, A. (1960): Effect of
pressure on the intermetallic compound formed by
diffusion between uranium and copper. C.R.A.S. 250, 115-
117 (in French).
- Adda, Y., Kirianenko, A., Beyeler, M. and Maurice, F.
(1961): Determination of equilibrium diagrams by
diffusion in the solid state. Mém. Sci. Rev. Mét. 58,
716-723 (in French).
- Adler, H.H. and Puig, J.A. (1961): Observations on the
thermal behavior of brannerite. Am. Mineral. 46, 1086-
1096.

- Agrinier, H., Chantret, F., Geffroy, J., Héry, B., Bachet, B. and Vachey, H. (1972): Une nouvelle espèce minérale: La méta-lodevite (arséniate hydraté d'uranium et de zinc). Bull. Soc. fr. Minéral. Cristallogr. 25, 360-364.
- Albee, A.L. and Ray, L. (1970): Correction factors for the electron probe microanalysis of silicates, oxides, carbonates, phosphates and sulfates. Anal. Chem. 42, 1408-1414.
- Alberman, K.B. and Anderson, J.S. (1949): The oxides of uranium. Chem. Soc. London J. Supp. 2, S303-S311.
- Alberman, K.B., Blakey, R.C. and Anderson, J.S. (1951): The oxides of uranium - part II, Binary systems $\text{UO}_2\text{-CaO}$. Chem. Soc. London J. (1951) 1351-1356.
- Alcock, C.B. and Grievson, P. (1961): A thermodynamic study of the compounds of U with Si, Ge, Sn and Pb. J. Inst. Metals 90, 304-310.
- Alekseeva, M.A., Chernikov, A.A., Shashkin, Dp.P., Konkova E.A. and Gavrilova, I.N. (1974): Strelkinite, a new uranyl vanadate. Zapiski Vses. Mineral. Obshch. 103, 576-580 (in Russian). From: Am. Mineral. 60, 488.

- Ambartsumian, Ts. L. (1957): Thermal investigations of uranium minerals. In: Geology of uranium: Sov. J. Atomic Energy Supp. 6, 74-102. Consultants Bur. Inc, N.Y. (1958).
- Andersen, C.A. (1973): Analytical methods and applications of the ion microprobe mass analyser. In: Andersen, C.A. ed.; Microprobe analysis; John Wiley and Sons, 531-553.
- Appleman, D.E. (1956): Crystal structure of liebigite (abstract) Bull. Geol. Soc. Am. 67, 1666.
- Appleman, D.E. (1957): Crystal-chemical study of johannite (abstract): Bull. Geol. Soc. Am. 68, 1696.
- Appleman, D.E. and Evans, H.T. (1965): The crystal structure of synthetic anhydrous carnotite $K_2(UO_2)_2V_2O_8$ and its cesium analogue $Cs_2(UO_2)_2V_2O_8$. Am. Mineral. 50, 825-842.
- Baldwin, A.B. (1970): Uranium and thorium occurrences on the north shore of the Gulf of St. Lawrence. C.I.M. Bull. 63, 699-707.

Bambynek, W., Crasemann, B., Fink, R.W., Freund, H.U., Mark, H., Swift, C.D., Price, R.E. and Venugopala Rao, P. (1972): X-ray fluorescence yields, Auger and Coster-Krönig transition probabilities. Rev. Mod. Phys. 44, 716-813.

Barthel, F. and Mehnert, K.R. (1970): Die Verteilung von Uran und thorium im Malsburger Granit. N. Jb. Miner. Abh 114, 18-47.

Barton, J.M. (1971): A geochronological and stratigraphic study of the Precambrian rocks north of Montreal. Thesis (Ph.D.) McGill Univ.

Barton, J.M. and Doig, R. (1973): Time-stratigraphic relationships east of the Morin anorthosite pluton, Quebec. Am. J. Sci. 273, 376-384.

Bearden, J.A. (1967): X-ray wavelengths. Rev. Mod. Phys. 39, 78-124.

Beck, L.S. (1967): A preliminary report on uranium deposits in the Athabasca Region. Sask. Dept. Mineral. Res. Rept. 112, 16 pp.

- Beck, L.S. (1969): Uranium deposits of the Athabasca Region, Saskatchewan. Sask. Dept. Mineral. Res. Rept. 126, 140 pp.
- Beck, L.S. (1970): Genesis of uranium in the Athabasca Region and its significance in exploration. Can. Min. Met. Bull. 63, 367-377.
- Belova, L.N. (1958a): Arsenuranylite, the arsenic analogue of phosphuranylite. Zapiski Vses. Mineral. Obschch. 87, 589-602. (in Russian). From: Am. Mineral. 44, 208.
- Belova, L.N. (1958b): Barium uranophane. Proc. 2nd Intern. Conf. Peaceful Uses of Atomic Energy, Geneva (1958) 2, 295.
- Belova, L.N., Litenkova, V.I. and Novorossova, L.E. (1963): Phosphorus analogue of troegerite. Vaprosy Priklad. Radiogeol. Sbornik, 174-177. (in Russian). From: Chem. Abstracts, 61, 10457.
- Bence, A.E. and Albee, A.L. (1968): Empirical correction factors for the electron microanalysis of silicates and oxides. J. Geol. 76, 382-403.

- Benyacar, M.A.R. de, and Abeledo, M.E.J. de (1974): Phase transistion in synthetic troegerite at room temperature. Am. Mineral. 59, 763-767.
- Berger, M.J. and Selzter, S.M. (1964): Tables of energy losses and ranges of electron and positrons . Nat. Acad. Sci. Nat. Res. Council Publ. 1133, 205-268. From: Heinrich, K.F.S. (1973).
- Berman, R.M. (1957): The role of lead and excess oxygen in uraninite. Am. Mineral. 42, 705-731.
- Bethe, M.J., Rose, M.E. and Smith, L.P. (1938): Multiple scattering of electrons. Proc. Am. Phil. Soc. 78, 573-585. From: Heinrich, K.F.J. (1973).
- Blais, R. (1955): Pashashibou area, Drucourt and Costebelle townships, Saguenay County. Quebec. Dept. Mines; P.R. 316, map 1114.
- Borom, M.P. and Hanneman, R.E. (1967): Local compositional changes in alkali silicate glasses during electron microprobe analysis. J. Appl. Phys. 38, 2406.

Bourne, J.H., Stott, G., Borduas, B. and, Lalonde, A.

(1977): Lac de Morhiban and Natashquan River map-areas, Quebec. Rept. Activities, part A, Geol. Surv. Can. Paper 77-1A, 199-204.

Branche, G., Bariland, P., Chantret, F., Pouget, R. and Rimsky, A. (1963): La vanuralite, un nouveau minéral uranifère. C.R.A.S. (France) 25, 5374-5376.

Branche, G., Chervet, J. and Guillemin, C. (1951): Nouvelles espèces uranifères françaises. Bull. Soc. fr. Mineral. Cristallogr. 74, 457-488.

Brasseur, H. (1962): Essai de représentation des oxydes doubles $mX^{++}O, UO_3.nH_2O$ par une formule générale. Bull. Soc. fr. Minéral. Cristallogr. 85, 242-245.

Brasseur, H. and Potdevin, H. (1960): Considérations sur les propriétés et les constitutions de certains minéraux uranifères. Z. Kristall. 113, 132-141.

Büchner, A.R. (1973): Bestimmung der mittleren Ordnungszahl von Legierungen bei der quantitativen Mikrosondenanalyse. Arch. Eisenhüttenwes 44, 143-147.

- Bultemann, H.W. and Moh, G.H. (1959): Bergenit, ein neues Mineral der Phosphuranylit-gruppe. N. Jb. Miner. Mh. (1959) 232-233.
- Buryanova, E.Z., Stroková, G.S. and Shitov, V.A. (1965): Vanuranylite, a new mineral. Zapiski Vses. Mineral. Obshch. 94, 437-443. (in Russian). From: Am. Mineral. 51, 1548.
- Butler, J.R. (1958): Rare-earths in some niobate-tantalates. Min. Mag. 31, 763-780.
- Castaing, R. (1951): Application des sondes électroniques à une méthode d'analyse chimique et cristallographique. Thèse doctorat, Paris. From: Kirianenko et al. (1963).
- Castaing, R. (1960): Electron probe microanalysis. Adv. in Electronics and electron Physics 12, 317-386.
- Castaing, R. and Deschamps, J. (1955): Sur les bases physiques de l'analyse ponctuelle par spectrographie X. J. Phys. Radium, 16, 304-317. From: Kirianenko et al. (1963).

- Cesbron, F. (1970): Nouvelles données sur la vanuralite.
Existence de la méta-vanuralite. Bull. Soc. fr. Minéral.
Cristallogr. 93, 242-248.
- Cesbron, F. and Morin, N. (1968): Une nouvelle espèce
minérale: la curiënite. Etude de la série francevillite-
curiënite. Bull. Soc. fr. Minéral. Cristallogr. 91,
453-459.
- Cesbron, F., Bachet, B. and Oosterbosch, R. (1965): La
demesmaekerite, sélénite hydraté d'uranium, cuivre, et
plomb. Bull. Soc. fr. Minéral. Cristallogr. 88, 422-425.
- Cesbron, F., Brown, W.L., Bariand, P. and Geffroy, J.
(1972): Rameauite and agrinierite, two new hydrated
complex uranyl oxides from Margnac, France. Mineral.
Mag. 38, 781-789.
- Cesbron, F., Oostrebosch, R. and Pierrot, R. (1969): Une
nouvelle espèce minérale: la marthozite, uranylsélénite
de cuivre hydraté. Bull. Soc. fr. Minéral. Cristallogr.
92, 278-283.

Cesbron, F., Pierrot, R. and Verbeek, T. (1970): La roubaultite, $\text{Cu}_2(\text{UO}_2)_3(\text{OH})_{10} \cdot 5\text{H}_2\text{O}$, une nouvelle espèce minérale. Bull. Soc. fr. Minéral. Cristallogr. 93, 550-554.

Cesbron, F., Pierrot, R. and Verbeek, T. (1971): La derriksite, $\text{Cu}_4(\text{UO}_2)(\text{SeO}_3)_2(\text{OH})_3 \cdot \text{H}_2\text{O}$, une nouvelle espèce minérale. Bull. Soc. fr. Minéral. Cristallogr. 94, 534-537.

Chakrabarty, M.R. (1969): Formation and properties of uranium glasses. Ceram. Bull. 48, 1076-1078.

Chernikov, A.A. (1957): Conditions of formation of natroautunite. In: The geology of uranium. Atomnaya Energiya. Supp. 6. Consultants Bureau, N.Y. (1958), 66-69.

Chernikov, A.A., Krumetskaia, O.V. and Sidel'nikova, V.D. (1957): Ursilite-A new silicate of uranium. In: The geology of uranium. Atomnaya Energiya. Supp. 6. Consultants Bureau, N.Y. (1958), 61-65.

- Chernikov, A.A., Shaskin, D.P. and Gavrilova, I.N. (1975): Sodium boltwoodite. Doklady Akad. Nauk. S.S.S.R. 221, 195-197. (in Russian) From: Am. Mineral. 61, 1054-1055.
- Chervet, J (1960): Les minéraux secondaires. In: Roubault, M. ed.; Les minerais uranifères français et leur gisements; tome 1, 89-299; Presses universitaires de France.
- Christ, C.L. and Clark. J.R. (1960): Crystal chemical studies of some uranyl oxide hydrates. Am. Mineral. 45, 1026-1061.
- Church, A.H. (1875): On the composition of autunite. Chem. Soc. London J. 2, 109. From: Frondel (1958).
- Clark, J.R. (1960): X-ray study of alteration in the uranium mineral wyartite. Am. Mineral. 45, 200-208.
- Claveau, J. (1944): Geology of the Wakeham-Forget Lakes region, north shore of Gulf of St. Lawrence. Ph.D. thesis, Univ. Toronto. From: Grenier, 1957.
- Colby, J.W. (1964): Microprobe analysis of binary systems containing uranium. Adv. in X-ray analysis 8, 352-362.

Colby, J.W. (1968): MAGIC IV - A computer program for quantitative electron microprobe analysis. Bell Telephone Labs, Allentown, Penn. (1972): also, Adv. X-ray Analysis 11, 287-305. From: Springer (1976b).

Coleman, R.G., Ross, D.R. and Meyrowitz, R. (1966): Zellerite and metazellerite, new uranyl carbonates. Am. Mineral. 51, 1567-1579.

Cooper, G.E. (1957): Johan Beetz area, Electoral district of Saguenay. Dept. Mines, Quebec; G.R. 74, 54 pp.

Courtois, A. (1968): Contribution à la connaissance de la cristallographie de l'ion uranyle dans les oxides hydratés étude structurale de la curite ($3\text{PbO} \cdot 8\text{UO}_3 \cdot 5\text{H}_2\text{O}$) et de la becquerelite ($\text{CaO} \cdot 6\text{UO}_3 \cdot 11\text{H}_2\text{O}$). Thèse (3e cycle) Nancy (France).

Criss, J.W. and Birks, L.S. (1966): Intensity formulae for computer solution of multicomponent electron probe specimens. In: McKinley, T.D. Heinrich, K.F.J. Wittry, D.B. ed.: The electron microprobe, John Wiley, 217-236.

- Cumming, G.L. and Scott, B.P. (1976): Rb/Sr dating of rocks from the Wollaston Lake Belt, Saskatchewan. Can. J. Earth Sci. 13, 355-364.
- Dahlkamp, F.J. and Tan, B. (1977): Geology and mineralogy of the Key Lake U-Ni deposits, northern Saskatchewan, Canada. In: Geology, mining and extractive processing of uranium. Institution of Mining and Metallurgy, London. 145-157.
- Davidson, C.F. and Bowie, S.H.U. (1951): On thucholite and related hydrocarbon-uraninite complexes, with a note on the origin of the Witwatersrand gold ores. G.B. Geol. Serv. Bull. 3, 1-19.
- Dépatie, J. (1965): Geology of l'Ours Lake area, Duplessis County. Quebec Dept. Nat. Res.; P.R. 559, map 1644.
- Deer, W.A. Howie, R.A. and Zussman, J. (1963): Rock-forming minerals, 5 vol., Longmans.
- Deliens, M. (1975): Une association de molybdates d'uranium de Shinkolobwe (région du Shaba, République du Zaïre). Ann. Soc. Geol. Belg. 98, 155-160.

- Desautels, P.E. (1967): The morphology of mckelveyite. Am. Mineral. 52, 860-863.
- Dooley, J.R. jr. (1976): High speed radioluxograph with single scintillation sensitivity for autoradiography of geologic samples. Proc. Int. Conf. Nucl. Photogr. Solid State Track Detectors, 8th; Bucarest, Roumania; p 453.
- Douglas, R.J.W. ed. (1970): Glacial map of Canada, no. 1253A. From: Geology and economic minerals of Canada. Geol. Surv. Can. Econ. Rept. 1.
- Drake, M.J. and Weill, D.F. (1972): New rare-earth element standards for electron microprobe analysis. Chem. Geol. 10, 179-201.
- Edgar, A.D. (1973): Experimental petrology, basic principles and techniques. Clarendon Press, Oxford, 217 pp.
- Elston, J. (1960): In: Pascal, P. (1960): Nouveau traité de chimie minérale, tome XV, premier fascicule: Uranium et transuraniens.

- Emerson, D.O. and Wright, H.D. (1957): Secondary uranium minerals at the M. Wilson mine in the Boulder batholith, Montana. *Am. Mineral.* 42, 222-239.
- Epshtein, G.Yu. (1959): On the molybdates of uranium - moluranite and iriginite. *Zapiski Vses. Mineral. Obshch.* 88, 564-570. (in Russian) From: *Am. Mineral.* 45, 257-258.
- Eskova, E.M., Semenov, E.I., Khomyakov, A.P., Kazakova, M.E. and Sidorenko, O.V. (1974): Laplandite, a new mineral. *Zapiski Vses. Mineral. Obshch.* 103, 571-575. (in Russian). From: *Am. Mineral.* 60, 487.
- Eskova, E.M., Semenov, E.T., Khomyskov, A.P., Merkov, A.N., Lebedeva, S.I. and Dubakina, L.S. (1974): Umbozerite, a new mineral. *Dokl. Akad. Nauk. S.S.S.R.* 216, 169-174 (in Russian). From: *Am. Mineral.* 60, 341.
- Fairchild, J.G. (1929): Base exchange in artificial autunites. *Am. Mineral.* 14, 265-275. From: Frondel (1958).
- Feraday, M.A. (1971): The oxidation, hydriding and aqueous corrosion of U_3Si alloys. AECL-3862, 33 pp.

- Ferris, C.S. and Ruud C.O. (1971): Brannerite: its occurrences and recognition by microprobe. *Quat. Col. Sc. Mines* 66, 35 pp.
- Fink, R.W. Jobson, R.C. Mark, H. and Swift, C.F. (1976): Atomic fluorescence yields. *Rev. Mod. Phys.* 38, 513-540.
- Fisher, F.G. and Meyrowitz, R. (1962): Brockite, a new calcium thorium phosphate from the Wet Mountains, Colorado. *Am. Mineral.* 47, 1346-1355.
- Flahaut, J. (1963): Thorium. In: Pascal, P. ed. *Nouveau traité de chimie minérale*, tome IX, 997-1195.
- Fleisher, M. (1975): Glossary of mineral species. Mineralogical Record Inc, 145 pp. Maryland.
- Frarey, M.J. (1950): Ile-à-la-Crosse Map Area, Saskatchewan. *Geol. Surv. Can. Pap.* 50-25, 10 pp.
- Frenzel G., Otteman, J. and Kurtze, W. (1975): Uran-Verezungen und uranhaltige Rutile in einem permovulkanischen Tuffit von Boarezzo (Valganna, Varese): *N. Jb. Miner. Abh* 124, 75-102.

- Friskney, C.A. and Haworth, C.W. (1967): Heat flow problems in electron probe micro-analysis. J. Appl. Phys. 38, 3796-3999.
- Frondel C. (1952): Studies of uranium minerals (X): uranopilite. Am. Mineral. 37, 950-959.
- Frondel, C. (1951): Studies of uranium minerals (VIII): Sabugalite, an aluminium-autunite. Am Mineral. 36, 671-680.
- Frondel, C. (1953): Hydroxyl substitution in thorite and zircon. Am. Mineral. 38, 1007-1018.
- Frondel, C. (1956): Mineral composition of gummite. Am. Mineral. 41, 539-568.
- Frondel, C. (1958): Systematic mineralogy of uranium and thorium. U. S. Geol. Surv. Bull. 1064, 400 pp.
- Frondel, C., Riska, D. and Frondel, J.W. (1956): X-ray powder data for uranium and thorium minerals. U.S. Geol. Surv. Bull. 1036-G, 91-153.

- Fuchs, L.H. and Gebert, E. (1958): X-ray studies of synthetic coffinite, thorite and uranothorites. Am. Mineral. 43, 243-248.
- Fuchs, L.H. and Hoekstra, H.R. (1959): The preparation and properties of uranium(IV) silicate. Am. Mineral. 4, 1057-1063.
- Gaines, R.V. (1965): Moctezumite, a new lead uranyl tellurite. Am. Mineral. 50, 1158-1163.
- Gaines, R.V. (1969): Cliffordite - A new tellurite mineral from Moctezuma, Sonora, Mexico. Am. Mineral. 54, 697-701.
- Gaines, R.V. (1971): Schmitterite - a new uranyl tellurite from Moctezuma, Sonora. Am. Mineral. 56, 411-415.
- Gallagher, M.J. and Atkin, D. (1966): Meta-ankoleite, hydrated potassium uranyl phosphate. Bull. Geol. Surv. G.B. 25, 49.
- Galy, J. and Meunier, G. (1971): A propos de la cliffordite UTe_3O_8 . Le système UO_3-TeO_8 à $700^\circ C$. Structure cristalline de UTe_3O_8 . Acta Cryst. B27, 608-616.

- Geffroy, J. and Sarcia, J.A. (1960): Les mineraux noirs.
In: Roubault, M. ed.; Les mineraux uranifères français et leurs gisements. tome 1, 1-86.
- Getseva, R.V. (1956): Hydronasturan and urgite - new minerals of the group of hydrated uranium oxides.
Atomnaya Energiya 3, 135-136. From: Am. Mineral. 42, 442.
- Getseva, R.V. and Sarel'eva, K.T. (1956): Rukovotsno po opredeleniiu uranorykh mineralov. (Handbook for the determination of uranium minerals), Moscow, 260 pp.
Ferutite, 126-128. From: Am. Mineral. 43, 382-383.
Lermontovite, 199-200. From: Am. Mineral. 43, 379.
Lodochnikite, 132-133. From: Am. Mineral. 43, 380.
Moluranite, 196. From: Am. Mineral. 43, 381-382.
Orlite, 239. From: Am. Mineral. 43, 381.
Ufertite, 132. From: Am. Mineral. 43, 378.
Sogrenite, 250-251. From: Am. Mineral. 43, 382.
- Gorzhevskaya, S.A., Lugovskoi, G.P. and Sidorenko G.A. (1963): The first find of samieresite in the Soviet Union. Doklady Akad. Nauk. S.S.S.R. 162, 1148-1151. (in Russian). From: Am. Mineral. 51, 1551-1552.

- Gotman, Ya.D. and Khapaev, I.A. (1958): Thorutite - a new mineral of the group of titanates of thorium. *Zapiski Vses. Mineral. Obshch.* 87, 201-202. From: *Am. Mineral.* 43, 1007.
- Goulet, N. (1971): Etude pétrologique, structurale et géochronologique des formations cristallines du quart nord-est de la feuille Saint-Gabriel-de-Brandon (Province de Grenville; Bouclier canadien). Thèse (3e cycle) Univ. Grenoble (France), 203 pp.
- Grandstaff, D.E. (1974): Microprobe analyses of uranium and thorium in uraninite from the Witwatersrand, South-Africa, and Blind River, Ontario, Canada. *Trans. Geol. S. Afr.* 77, 291-294.
- Granger, H.G. (1963): Mineralogy. In: *Geology and technology of the Grants uranium region*. New Mexico Bur. Mines Mineral Resources Mem. 15, 21-37. From: *Am. Mineral.* 49, 439.
- Grenier, P.E. (1957): Beetz Lake area, Electoral district of Saguenay. Quebec Dept. Mines; G.R. 73, 77 pp.

Gross, E.B. and Corey A.S. (1958): Heinrichite and metaheinrichite, hydrated barium uranyl arsenate minerals. *Am. Mineral.* 43, 1134-1143.

Guillemin, C. and Protas, J. (1959): Ianthinite et wyartite. *Bull. Soc. fr. Minéral. Cristallogr.* 82, 80-86.

Hamilton, P.K. and Kerr, P.F. (1959): Umohoite from Cameron, Arizona. *Am. Mineral.* 44, 1248-1260.

Haughton, D.R. (1976): A multiple media geochemical survey of a boulder train associated with the Duddridge Lake uranium deposit, Saskatchewan. In: Dunn, C.E. ed.; *Uranium in Saskatchewan. Proc. Symp 10 Nov. 1976; Sask. Geol. Soc. Sp. Publ.* 3, 256-296.

Hauseux, M.A. (1976): Mode of uranium occurrence in a migmatic granite terrain, Baie Johan Beetz, Quebec. Paper presented at the 78th Annual General Meeting of the Canadian Institute of Mining and Metallurgy in Quebec City, April 25-29, 1976.

- Hénoc, J. (1968): Quantitative electron probe microanalysis. U.S. Nat. Bur. Stand. Sp. Publ. 29, 197pp; Heinrich, K.F.S. ed.; In: Hénoc, et al. (1973).
- Hénoc, J., Heinrich, K.F.J. and Myklebust, R.L. (1973): A rigorous correction procedure for quantitative electron probe microanalysis (COR-2) NBS TN-769, 132 pp.
- Hecht, F. (1933): Quantitative Mikro-Gesamtanalysen von Ceylan-Thorianeten. Mikrochemie 12, 193. From: Frondel (1958).
- Heinrich, K.F.J. (1958): Mineralogy and geology of radioactive raw materials. McGraw Hill.
- Heinrich, K.F.J. (1966) X-ray absorption uncertainty. In: McKinley T.D., Heinrich, K.F.J. and Wittry, D.B. eds. (1966): The electron microprobe. John Wiley and Sons, 296-377.
- Heinrich, K.F.J. (1973): Present state of the classical theory of quantitative electron probe microanalysis. In: Hénoc, et al. (1973); appendix 1; NBS Tech. Note 521, 83.

- Heinrich, K.F.J. and Yakowitz, H. (1975): Absorption of primary X-rays in electron-probe microanalysis. Anal. Chem. 47, 2408-2411.
- Henmi, K. (1951): Rare element minerals produced in Haicheng hsien, southern Manchuria. Geol. Soc. Japan J. 57, 345. From: Frondel (1958).
- Hess, F.L. and Foshag, W.F. (1927): Crystalline carnotite from Utah. U.S. Nat. Mus. Proc. 72, Art.12. From: Frondel (1958).
- Heynes, M.S.R. and Rawson, H. (1961): An investigation into some high melting point glass systems and their use as solvents for uranium dioxide. J. Phys. Chem. Glasses 2, 1-11.
- Hidden, W.E. and Mackintosh, J.B. (1889): A description of several yttria and thoria minerals from Llano county, Texas. Am. J. Sci. 38, 481. From: Frondel (1958).
- Hillebrand, W.F. (1924): Carnotite and tyuyamunite and their ores in Colorado and Utah. Am. J. Sci. 8, 201-216. From: Frondel (1958).

- Honea, R.M. (1961): New data on boltwoodite, an alkali uranyl silicate. *Am. Mineral.* 46, 12-25.
- Hounslow, A.W. (1976): Mineralogy of uranium and thorium; a tabular summary. *Col. Sc. Mines Res. Inst.*
- Hutton, O.C. (1957): Kobaite from Paringa river, South Westland, New Zealand. *Am. Mineral.* 42, 342-353.
- Kamhi, S.R. (1959): An X-ray study of umohoite. *Am. Mineral.* 44, 920-925.
- Keil, K. (1973): Applications of the electron microprobe in geology. In: Andersen, C.A. ed. *Microprobe analysis*. John Wiley and Sons, 189-240.
- Keil, K. and Snetsinger, K.G. (1973): Applications of the laser microprobe to geology. In: Andersen, C.A. ed.; *Microprobe analysis*; John Wiley and Sons, 457-476.
- Kirianenko, A., Maurice, F., Calais, D. and Adda, Y. (1963): Analysis of heavy elements ($Z > 80$) with the Castaing microprobe: application to the analysis of binary systems containing uranium. In: Pattie, H.H., Coslett, V.E. and Engstrom, A. eds.; *X-ray Optics and X-ray microanalysis*, Academic Press, N.Y. 559-576.

Kleykamp H. (1973): Mikrosonden-untersuchungen an
Bestrahltem Urancarbid. J. Nuclear Mat. 47, 271-277.

Kobayashi, M. (1912): On the composition of
thorianite. Tohoku Imp. Univ. Sci. Repts. Ustser 1, 201-
206. From: Frondel (1958).

Kopchenova, E.V. and Skoortsova, K.V. (1957): Sodium
uranospinite. Doklady. Akad. Nauk. S.S.S.R. 114, 634-
636. (in Russian). From: Am. Mineral. 43, 383-384.

Kopchenova, E.V., Skvortsova, K.V., Silantieva, N.I.,
Sidorenko, G.A. and Mikhailova, L.V. (1962) Mourite, a
new supergene uranium - molybdenum mineral. Zapeski
Vses. Mineral. Obshch. 91, 67-71 (in Russian). From: Am.
Mineral. 47, 1217.

Krauskopf, K.B. (1967): Introduction to geochemistry.
McGraw-Hill, Inc, 721 pp.

Lacroix, A (1922): Minéralogie de Madagascar. Paris. From:
Frondel (1958).

Lambertson, W.A. Mueller, M.H. and Gunzel, F.H. (1953):

Uranium oxide phase equilibrium systems: IV, $\text{UO}_2\text{-ThO}_2$.

J. Am. Ceram. Soc. 36, 397-399.

Lambertson, W.A., and Mueller, M.H. (1953): Uranium oxide
phase equilibrium systems: III, $\text{UO}_2\text{-ZrO}_2$. J. Am. Ceram.
Soc. 36, 365-367.

Lang, S.M., Knudsen, F.P., Fillmore, C.L. and Roth, R.S.

(1956): Natl. Bur. Standards, Circ. 568 , 17. From:

Levin, E.M., Robbins, C.E. and McMurdie, H.F. (1964):

Phase diagrams for ceramists. Ed: Reser, M.K. Am. Ceram.
Soc. 601 pp.

Leo, G.W. (1960): Autunite from Mt. Spokane, Washington.

Am. Mineral. 45, 99-128.

Lima de Faria, J. (1965): Identification of metamict

minerals by X-ray powder photographs. Estudos, Ensaios e
Documentos Lisbon 112, Junta de Invest. do Ultramar, 74
pp.

Lineweaver, J.L. (1963): Oxygen outgassing caused by

electron bombardment of glass. J. Appl. Phys. 34, 1786-
1791.

Livingstone, A. Atkin, D. Hutchison, D. and Al-Hermezi, H.M.
(1976): Iraqite, a new rare-earth mineral of the ekanite
group. Mineral. Mag. 40, 440-445.

Mawdsley, J.B. (1952): Uraninite-bearing deposits,
Charlebois Lake area, northeastern Saskatchewan. Can.
Min. Metall. Bull. 482, 366-367.

Mawdsley, J.B. (1957): The geology of the Charlebois Lake
area. Sask. Dept. Mineral Res. Rept. 24.

Mawdsley, J.B. (1958): The radioactive pegmatites of
Saskatchewan. 2nd Int. Conf. Peaceful Use At. En. 2,
484-490.

McBurney, T.C. and Murdoch, J. (1959): Haiweeite, a new
uranium mineral from California. Am. Mineral. 44, 839-
843.

McPhee, D.S. (1959): Preliminary report on Aguanish area,
Saguenay electoral district. Quebec Dept. Mines; P.R.
403, 6 pp.

Meunier, G. and Galy, J. (1973): Structure cristalline de la schmitt rite synth tique $UTeO_5$. Acta Cryst. B29, 1251-1255.

Milton, C., Ingram, B., Clark, J.R. and Dvornik, E.J. (1965): Mckelveyite, a new hydrous sodium, barium rare-earth uranium carbonate mineral from the Green River formation, Wyoming. Am. Mineral. 50, 593-612.

Money, P.L. (1968): The Wollaston Lake fold-belt, Saskatchewan-Manitoba. Can. J. Earth Sc. 5, 1489-1504.

Money, P.L. (1965): The geology of the area around Needle Falls, Churchill River, comprising the Eulas Lake area (west half), Sandfly Lake area (east half) and Black Bear Island area (west half), Saskatchewan. Sask. Dept. Min. Res. Rept. 88, 70 pp.

Money, P.L. (1967): The Precambrian geology of the Needle Falls area, Saskatchewan. Ph.D. thesis, Univ. of Alberta (unpublished).

Money, P.L., Baer, A.J., Scott, B.P. and Wallis, R.H.

(1970): The Wollaston Lake Belt, Saskatchewan, Manitoba, Northwest Territories. In: Baer, A.J. ed.; Basins and geosynclines of the Canadian Shield; Geol. Surv. Can. Pap. 70-40, 170-200.

Morra, F.P. (1977): Geology and U deposits of the Charlebois-Higginson Lake area, North Saskatchewan. M.Sc. thesis, Univ. of Alberta, (unpublished).

Morten, R.D. and Sassano, G.P. (1972): Reflectance and micro-indentation hardness vs. chemical composition in some Canadian uraninites. N. Jb. Miner. Mh. 8, 350-360.

Munday, R.J.C. (1973): Mudjatik (NE), Saskatchewan. In: Sask. Dept.. Min. Res. Sum. Rept. 18-23.

Munday, R.J.C. (1974a): Ile-à-la-Crosse 73-0-E east half. Sask. Dept. Min. Res. preliminary geol. map.

Munday, R.J.C. (1974b): Reconnaissance Geological Survey of 73-0-NE and 73-0-SE. In: Beck, L.S. and Macdonald, R. eds.; Sum. Rept. of field investigations by the Saskatchewan Geological Survey, 1974, 20-24.

Munday, R.J.C.: (1972) Mudjatic (SE), Saskatchewan. In:
Sask. Dept.. Min. Res. Sum. Rept. 22-25.

Muto, T., Meyrowitz, R. and Pommer, A.M. (1959):
Ningyoite, a new uranous phosphate mineral from Japan.
Am. Mineral. 44, 633-650.

Nekrasova, Z.A. (1957): The hydrous uranyl and ammonium
phosphate (uramphite): $\text{NH}_4(\text{UO}_3)(\text{PO}_4) \cdot 3\text{H}_2\text{O}$. In: The
geology of uranium. Atomnaya Energiya, Supp. 6.
Consultants Bureau, N.Y. (1958), 56-60.

Nekrasova, Z.A. (1958): The form of the occurrence of
uranium in some coals. GEN P/2083. From: Geffroy and
Sarcia, 1960.

Nováček, R. (1935): Revision of the secondary uranium
minerals from Jachymov (in Czechoslovakian). Narodni
Mus. Casopis. oddel přírod. Orčnik. 19, 100-107. From:
Fronde! (1958).

Olds, L.E. (1961): In: Levin, E.M., Robbins, C.E. and
McMurdie, H.F. (1964): Phase diagrams for ceramists.
Am. Ceram. Soc. 139, fig. 353.

- Outerbridge, W.T., Staatz, M.H., Meyrowitz, R. and Pommer, A.M. (1960): Weeksite, a new uranium silicate from the Thomas Range, Juab county, Utah. *Am. Mineral.* 45, 39-52.
- Oztunali, O. (1959): Uber die Struktur von Brannerit. *N. Jb. Miner. Mh.* (1959) 187-188.
- Pabst, A. (1954): Brannerite from California. *Am. Mineral.* 39, 109-117.
- Patchett, J.E. and Nuffield, E.W. (1960): Studies of radioactive compounds, X-ray, synthesis and crystallography of brannerite. *Can. Mineral.* 6, 483-490.
- Pearson, D.E. (1972): Mudjatic (S.W.), Saskatchewan. In: *Sask. Dept.. Min. Res. Sum. Rept.* 30-39.
- Perez y Jorba, M., Mondange, H. and Collongues, R. (1961) Sur les composés formés par la thorine avec les oxydes de métaux tétravalents. *Bull. Soc. chim. fr.* (1961), 79-81.
- Philibert, J. (1963): A method for calculating the absorption correction in electron probe microanalysis. *Proc. Third Int. Cong. X-ray Optics and X-ray analysis*, Academic Press, N.Y. 379-392.

- Pierrot, R., Toussaint, J. and Verbeek, T. (1965): La quilleminite, une nouvelle espèce minérale. Bull. Soc. fr. Minéral. Cristallogr. 88, 132-135.
- Pisani, F. (1861): Analyse de l'uranite d'Autun et de la chalkolite de Cornouailles. C.R.A.S. 52, 817. From: Frondel (1958).
- Polikarpova, V.A. (1957): New data on nenadkevite. From: The geology of uranium. Atomnaya Energiya. Supp. 6. Consultants Bureau, N.Y. (1958), 43-55.
- Poole, D.M. and Thomas, P.M. (1962) Quantitative electron-probe microanalysis. J. Inst. Metals, 90, 228.
- Poole, W.H., Sandford, B.V., William, H. and Kelly, D.G. (1970): Geology of southeastern Canada. In: Douglas, R.J.W. ed.; Geology and economic minerals of Canada. Geol. Surv. Can.; Ec. Rept. 1, 227-304.
- Povilaitis, M.M. (1963): On the new mineral lodochnikite, absite, and thorutite. Zapiski Vses. Mineral. Obshch. 92, 113-123. (in Russian). From: Am. Mineral. 48, 1419-1420.

- Protas, J. (1959): Contribution a l'étude des oxydes d'uranium hydratés. Bull. Soc. fr. Minéral. Cristallogr. 82, 239-272.
- Protas, J. (1964): Une nouvelle espèce minérale: la compregnacite, $K_2O \cdot 6UO_3 \cdot 11H_2O$. Bull. Soc. fr. Minéral. Cristallogr. 87, 365-371.
- Pudovkina, Z.V., Dubakina, L.T., Levedeva, S.I and Pyatenko, Yu.A. (1974): Study of Brazilian zirkelite. Zapiski Vses. Mineral. Obshch. 103, 368-372. (in Russian). From: Am. Mineral. 60, 341.
- Ramdohr, P. (1969): The ore minerals and their intergrowths, 3rd edition. Pergamon Press, p 1027.
- Ramdohr, P., Otteman, J. and Schidrowski, M. (1965): Mikroskop, Microsonde und Schätzung der Uran-Blei-Alter. Max-Planck Inst. Kernph. Heidelberg, 18 pp.
- Reed, S.J.B. (1965): Characteristic fluorescence corrections in electron-probe microanalysis. Brit. J. Appl. Phys. 16, 913-926.

Rogova, V.P., Belova, L.N., Kiziyarov, G.N. and Kuznetsova, N.N. (1974): Calciouranoite, a new hydroxide of uranium. Zapiski Vses. Mineral. Obshch. 103, 103-109. (in Russian). From: Am. Mineral. 60, 161.

Rogova, V.P., Belova, L.N., Kiziyarov, G.N. and Kuznetsova, N.N. (1973): Bauranoite and metacaltsuranoite, new minerals of the group of hydrous uranium oxides. Zapiski Vses. Mineral. Obshch. 102, 75-81. (in Russian). From: Am. Mineral. 58, 111.

Ross, M. (1963): The crystallography of meta-autunite. Am. Mineral. 48, 1389-1393.

Ross, M. and Evans, H.T. jr. (1965): Studies of the torbernite minerals (III): role of the interlayer oxonium, potassium, and ammonium ions, and water molecules. Am. Mineral. 50, 1-12.

Ross, M. and Evans, T.H. jr. (1964): Studies of the torbernite minerals (I): The crystal structure of abernathyite and the structurally related compounds $\text{NH}_4(\text{UO}_3\text{AsO}_4) \cdot 3\text{H}_2\text{O}$ and $\text{K}(\text{H}_3\text{O})(\text{UO}_3\text{AsO}_4) \cdot 6\text{H}_2\text{O}$. Am. Mineral. 49, 1578-1602.

- Ross, M., Evans, T.H. jr. and Appleman, D.E. (1964):
Studies of the torbernite minerals (II): The crystal structure of meta-torbernite. *Am. Mineral.* 49, 1603-1621.
- Ruh, R. and Wadsley, A.D. (1966): The crystal structure of ThTi_2O_6 (brannerite). *Acta Cryst.* 21, 974-978.
- Rupnitskaya, L.S. (1958): Calcium uranium molybdate, $\text{Ca}(\text{UO}_3)_3(\text{MoO}_4)_3(\text{OH})_2 \cdot 8\text{H}_2\text{O}$. *Proc. 2nd. Intern. Conf. Peaceful Uses of Atomic Energy, Geneva. (1958)* 2, 286.
- Schidrowski, M. (1966a): The radioactive components of the Witwatersrand conglomerates I Pitchblende in conglomerate of the Orange Free State gold fields. (in German). *N. Jb. Mineral. Abh.* 10, 183-202.
- Schidrowski, M. (1966b): The radioactive components of the Witwatersrand conglomerates II Brannerite and 'uraninite ghosts'. (in German). *N. Jb. Mineral. Abh.* 10, 310-321.
- Schidrowski, M. (1966c): The radioactive components of the Witwatersrand conglomerates III The carbonaceous substance 'Thucolite'. (in German). *N. Jb. Mineral. Abh.* 10, 55-71.

- Schoep, A. (1930): Les minéraux du gîte uranifère du Katanga. Mus. Congo belge Ann, sér. 1, tome 1, Fasc. 2, 43p. From: Frondel (1958).
- Sergeev, A.S. (1964): Pseudo-autunite, a new hydrous calcium phosphate. Mineral. Geokhim. Leningrad Univ. Skornik Statei, 1, 31-39 (in Russian). From: Am. Mineral. 50, 1505-1506.
- Sharma, K.N.M. (1973): Geology of the Victor Lake area, Duplessis County. Quebec. Dept. Nat. Res; P.R. 607, 11 pp.
- Sharma, K.N.M. and Jacoby, R. (1973): Jérémie and Gaudreault Lakes area, Duplessis County, Quebec. Quebec Dept. Nat. Res. Open File Rept. GM 28442, 16 pp.
- Sibbald, T.I.I. (1973): Mudjatik (NW), Saskatchewan. In: Sask. Dept. Min. Res. Sum. Rept, 35-42.
- Sibbald, T.I.I., Munday, R.J.C. and Lewry, J.F. (1976): The geological setting of uranium mineralization in northern Saskatchewan. In: Dunn, C.E. ed.; Uranium in Saskatchewan, Proc. Symp. 10 Nov. 1976. Sask. Geol. Soc. Sp. Publ. 3, 51-98.

- Simpson, E.S. (1930): Contributions to the mineralogy of Western Australia. Royal Soc. West. Australia J. 16, 25-33. From: Frondel (1958).
- Skvortsova, K.V. and Sidorenko, G.A. (1965): Sedovite, a new supergene mineral of uranium and molybdenum. Zapiski Vses. Mineral. Obshch. 9, 548-554. (in Russian). From: Am. Mineral. 51, 530.
- Smellie, J.A.T. (1972): Preparation of glass standards for the use in X-ray microanalysis. Min. Mag. 38, 614-617.
- Smellie, J.A.T., Cogger, N. and Herrington, J. (1978): Standards for quantitative microprobe determination of uranium and thorium with additional information on the chemical formulae of davidite and euxenite-polycrase. Chem. Geol. 22, 1-10.
- Smith, D.G.W. and Gold, C.M. (1976): A scheme for fully quantitative energy dispersive analysis. Adv. in X-ray analysis, 19, 191-201.
- Smith, D.K. (1959): An X-ray crystallographic study of schroeckingerite and its dehydration product. Am. Mineral. 44, 1020-1025.

- Smith, D.K. and Stohl, F.V. (1972): Crystal structure of Beta-uranophane. G.S.A. Mem. 135, 281-288.
- Smith, M.L. and Marienko, J. (1971): Comparison of mourite from Karnes County, Texas with mourite from the U.S.S.R. Am. Mineral. 56, 163-173.
- Smith, T.H. (1926): Mineralogical Notes; No.2: Australian Museum Rec. 15, 68. From: Frondel (1958).
- Soboleva, M.V. and Pudovkina, I.A. (1957): Mineraly Urana, Spavochnik. (Uranium Minerals Handbook), Moscow, 404 pp.
- Lermontovite, 181-182. From: Am. Mineral. 43, 379.
- Lodochnikite, 347-350. From: Am. Mineral. 43, 380.
- Moluranite, 252-253. From: Am. Mineral. 43, 380.
- Orlite, 129-130. From: Am. Mineral. 43, 381.
- Sogrenite, 257-259. From: Am. Mineral. 43, 382.
- Ufertite, 132. From: Am. Mineral. 43, 382.
- Unnamed, 201-202. From: Am. Mineral. 43, 382.
- Sobry, R. (1971): Water and interlayer oxium in hydrated uranates. Am. Mineral. 56, 1065-1076.

- Sobry, R. (1973a): Etudes des uranates hydratés-I: Propriétés radiocristallographiques des uranates hydratés de cations bivalents. *J. inorg. nucl. Chem.* 35, 1515-1524.
- Sobry, R. (1973b): Etude des uranates hydratés-II: Examen des propriétés vibrationnelles des uranates hydratés de cations bivalents. *J. inorg. nucl. Chem.* 35, 2753-2768.
- Sobry, R. and Rinne, M. (1973): A least-squares method for the identification of resonant groups from N.M.R. powder spectra. Identification of oxonium and hydroxyl ions in hydrated uranates. *J. Magn. Res.* 12, 152-167.
- Springer, G. (1976a): FEPAC: The Falconbridge procedure for computing electron-probe analysis corrections. FRL-153, 28 pp.
- Springer, G. (1976b): Correction procedures in electron-probe analysis. In: Smith, D.G.W. ed.; Short course in microbeam techniques. Min. Ass. Can. 45-62.
- Springer, G. (1976c): Iterative procedures in electron-probe analysis corrections. *X-Ray Spectrometry* 5, 88-91.

- Springer, G. and Nolan, B. (1976): Mathematical expressions for the evaluation of X-ray emission and critical absorption energies, and mass absorption coefficients. Can. J. Spect. 21, 134-138.
- Steacy, H.R., Plant, A.G. and Boyle, R.W. (1974): Brannerite associated with native gold at the Richardson mine, Ontario. Can. Miner. 12, 360-363.
- Steiger, R.H. and Jäger, E. (1977): Subcommittee on geochronology convention on the use of decay constants in geo- and cosmochemistry. E. Pl. Sc. Lett. 36, 359-362.
- Steinöcher, V. and Nováček, R. (1939): On β -uranotile. Am. Mineral. 24, 324-338.
- Stephenson, D.A. (1964): Iriginite from South Dakota. Am. Mineral. 49, 408-413.
- Threadgold, I.M. (1960): The mineral composition of some uranium ores from the South-Alligator River area, Northern Territory. Australian CSIRO, Mineralogical Invest. Tech. Paper, 2, 53 pp.

- Tremblay, L.P. (1968): Geology of the Beaverlodge mining area, Saskatchewan. Geol. Surv. Can. Mem. 367, 265 pp.
- Tröger, W.E. (1967): Optische Bestimmung der gesteinsbildenden Minerale. E. Schweizerbart'sche Verlagsbuchhandlung, p 79.
- Van Wambeke, L. (1972): Eylettersite, un nouveau phosphate de thorium appartenant à la série de la crandallite. Bull. Soc. fr. Minéral. Cristallogr. 95, 98-105.
- Vlasov, K.A. (1964): Geochemistry and mineralogy of rare elements and genetics type of their deposits: Vol. 2: Mineralogy of rare elements. Ac. Sc. USSR, 945 pp.
- Walenta, K. (1958a): Die sekundären Uranmineralien des Schwarzwaldes. Jahresheft geol. Landesamt Baden-Württemberg, 3, 17-51. From: Am. Mineral. 45, 254.
- Walenta, K. (1958b): Die sekundären Uranmineralien des Schwarzwaldes. Techn. Hochschule, Stuttgart, preliminary report. From: Bull. Soc. fr. Minéral. Cristallogr. 81, 67-68.

- Walenta, K. (1965a): Die Uranglimmergruppe. Chemie der Erde 24, 254-278.
- Walenta, K. (1965b): Hallimondite, a new uranium mineral from the Michael mine near Reichenbach (Black Forest, Germany). Am. Mineral. 50, 1143-1157.
- Walenta, K. (1972): Grimselit, ein neues Kalium-Natrium-Uranylkarbonat aus dem Grimselgebiet (Oberhasli, Kt. Bern, Schweiz) Schweiz. Mineral. Petrog. Mitt. 52, 93-108.
- Walenta, K. and Wimmenauer, W. (1961): Die Mineralbestand des Michaelganges im Weiler bei Lahr (Schwarzwald): Jahreshefte geol. Landesamtes Baden-Wurttemberg 4, 7-37. From: Walenta, K. (1965).
- Weisbach, A. (1877): Uber Uranocircit, ein neues Glied der Gruppe des sogenannten Uranglimmers. From: Frondel (1958).
- Wells, R.C., Fairchild, J.G. and Ross, C.T. (1933) Thorianite from Easton, Pa. Am. J. Sc. 226, 45-54.

- Wilder D.R., Carrell M.A. and Wirkus, C.D. (1963) Uranium glasses. U.S.A.E.C. Contract W-7405 UC-25 Conf. 506-3, 28 pp.
- Willis, B.T.M. (1963): Position of oxygen atoms in UO_2 .₁₃. Nature 197, 755-756.
- Winkler, H.G.F. (1974): Petrogenesis of metamorphic rocks, 3rd. edition. Springer-Verlag, 320 pp.
- Wirkus, C.D. and Wilder, D.R. (1960a): Uranium glasses: I-Fundamental considerations. U.S.A.E.C. Tech. Rept. IS-107, Contract W-7405, 19 pp.
- Wirkus, C.D. and Wilder, D.R. (1960b): Uranium glasses: II-Uranium silicate glasses. U.S.A.E.C. Tech. Rept. IS-158, contract W-7405, 29 pp.
- Wirkus, C.D. and Wilder, D.R. (1961): Uranium glasses: III-Uranium phosphate glasses. U.S.A.E.C. Tech. Rept. IS-168, contract W-7405, 23 pp.
- Wirkus, C.D. and Wilder, D.R. (1962): Uranium-bearing glasses in the silicate and phosphate systems. J. Nucl. Mat. 5, 140-146.

- Wynne-Edwards, H.R. (1972): The Grenville Province. In: Price, R.A. and Douglas, R.J.W. eds.; Variations in tectonic styles in Canada. Geol. Ass. Can. Sp. Paper 11, 263-334.
- Wynne-Edwards, H.R. (1976): Proterozoic ensialic orogeneses: the millipede model of ductile plate tectonics. Am. J. Sc. 276, 927-953.
- Young, E.J., Weeks, A.D. and Meyrowitz, R. (1966): Coconinoite, a new uranium mineral from Utah and Arizona. Am. Mineral. 51, 651-663.
- Ziebold, T.O. and Ogilvie, R.E. (1963): Quantitative analysis with the electron microanalyser. Anal. Chem. 35, 621-627.

APPENDIX I

PERMANENT DATA FILE FOR COR-2

The original data file of COR-2 (Hénoc et al., 1973) was modified from the original version supplied to the laboratory by the National Bureau of Standards, Washington. Complete data for Ce, Pr, Sm, Eu, Gd, Tb, Dy, Ho, Er and Tm have been added. Certain parameters, mainly Coster-Krönig coefficients and fluorescence yields, were updated or added to the original file. Values for some of the Coster-Krönig coefficients (for relatively light elements such as the first series of transition elements) were added for the sake of completeness. They are not commonly called upon in routine analysis of geological materials.

The file is listed in table 59, its format has not been modified from that of the original version. The symbols *, ** and & in table 59 ARE NOT PART OF THE COMPUTER FILE, they indicate the following:

- *- modified line of data from the original version;
- ** - first line of data for an element added to the original data file;

8- first line of data for each element.

Table 58. Format for the computer file listed in table 59.
 * indicates that the numbers are right justified in the field. To avoid confusion between line of data and emission line, the former is designated as card and the latter as line. (After Hénoc et al., 1973.)

card	use	columns	format	description
1	once at beginning of table	1-3*	I3	Number of elements in permanent data file
2	first card for each element	1-2*	I2	Atomic number
		3-4*	I2	Number of absorption edges listed in the file
		5-10	F6.3	Atomic weight
		3 fields of 6	3F6.4	Coster-Krönig coefficients
		11-28		f_{12}, f_{23}, f_{13}
		29-34	F6.2	Absorbtion constant C_{λ}
		2 fields of 4 (35-42)	2F4.2	Absorption exponents n_K, n_{KL}
3	card for each line	1-7	F7.5	Wavelength at absorption edge
		8-13	F6.4	Jump for the edge
		14-19	F6.5	Fluorescence yield
		20	I1	Number of lines listed for the edge
4	card for each line	1-7	F7.5	Wavelength of line
		8-13	F6.4	Weight of the line with respect to the sum of line intensities in this series

Table 59. Listing of the permanent data file for COR-2. The format of this file and the symbols &, * and ** are explained in table 58 and at the beginning of appendix I.

77				
1 1 1007		1 290		&
200				
3 1 6939		14 288		&
120				
4 1 9012		35 286		&
111				
5 1 1081		74 285		&
676				
6 2 12011		135 284 273		&
4368 2622	00091			
447 1				
99				
7 2 14007		221 283 273		&
3099 2576	00151			
316 1				
99				
8 2 16		334 282 273		&
2332 24	00601			
2362 1				
99				
9 2 19		49 281 273		&
17913 1933	000941			
1832 1				
99				
11 2 2299		905 279 273		&
11569 184	025 2			
11575 12				
119101 88				
99				
12 2 2431		1175 279 273		&
95122 15	028 2			
95207 12				
989 88				
99				
13 2 2698		1487 278 273		&
79481 14	038 2			
79605 12				
83393 88				
99				
14 2 2809		185 277 273		&
6738 1296	043 2			
67530 12				
712542 88				
99				
15 3 30974		225 277 273		&
5784 1232	060 2			
5796 12				
61568 88				

Table 59 cont'd.....

00									
94									
16	2	32064			27	276	273		ε
5019	1167		082	2					*
50316	12								
53722	88								
757									
17	2	35453			317	276	273		ε
43971	1112		09552						*
44034	12								
47278	88								
609									
19	3	39102			425	275	273		ε
34365	101		138	2					*
34539	12								
37414	88								
00									
421									
20	3	4008			484	274	273		ε
30703	96		163	2					*
30897	12								
33584	88								
00									
3513									
21	3	4496			551	274	273		ε
2762	929		190	2					*
27796	12								
30309	88								
00									
3014									
22	3	479	3130		6290	621	273	273	ε*
24973	887		221	2					*
25139	12								
27485	88								
00									
2729									
23	3	5094			698	273	273		ε
22694	8703		253	2					*
22844	12								
250356	88								
00									
238882									
24	2	52	3170		636	78	273	273	ε*
20702	8497		283	2					*
208487	12								
22897	88								
167									
25	2	5494			867	272	273		ε
18964	824		313	2					*

Table 59 cont'd.....

19102	126										
21018	874										
1624											
26 3 5585	3020	0700	652	9580	272	273					ε*
174346	8108	342	2								*
175661	102										
193604	895										
17202			1								
1726	857										
00											
27 3 5894				1055	271	273					ε
160815	7962	366	2								*
162079	10										
178897	88										
00											
15618											
28 3 5869	3250	0997	622	11590	271	273					ε*
148807	7769	414	2								*
150014	107										
165791	893										
00											
14242			1								
14271	857										
29 5 6354		109		12680	271	273					ε*
138059	7659	443	2								*
139222	12										
154056	88										
112709	117										
13014	139										
13288	573	00561									
13336	1										
110.6											
30 4 6538	3220		624	138	270	273					ε
12834	7505	479	2								*
129525	12										
143516	88										
1106	117										
11862	139										
12131											
31 5 6972				1498	270	273					ε
11958	7376	528	2								*
120789	12										
134008	88										
9517	117		1								
10365	1										
10828	139		1								
11023	1										
111	4246	006	1								
11292	1										
99											
32 5 7259	2660	0249	671	1622	270	273					ε*

Table 59 cont'd.....

6644	139	024	1						
70759	1								
6865	439	024	1						
73183	1								
38265									
38 5 8762	2490	1150	646	2513	268	273			ε*
76973	6976	702	2						*
78292	16								
87526	84								
5592	117	008	2						
63672	59								
64026	41								
6173	139	024	1						
66239	1								
6387	4314	024	1						
68628	1								
345									
39 5 8891	2510	1175	57	2681	267	273			ε*
72766	695	711	2						*
74072	16								
82884	84								
5217	117	008	2						
59832	59								
60186	41								
5756	139	024	1						
6212	1								
5962	424	024	1						
64488	1								
3147									
40 5 9122	2530	1200	585	2851	267	273			ε*
68883	696	730	2						*
70173	16								
78593	84								
4879	117	008	2						
5633	59								
56681	41								
5378	139	024	2						
53843	10								
5836	90								
5579	4166	024	2						
55863	7								
60705	93								
288									
41 5 9291	2550	1225	56	3039	267	273			ε*
65298	7035	748	2						*
66576	16								
7462	84								
4575	117	008	2						
53102	59								
53455	41								
5031	139	024	2						

Table 59 cont'd.....

58545	85								
34369	117	01	2						
40346	58								
40711	36								
37228	139	03	2						
37246	16								
414622	83								
39074	380	03	2						
390887	16								
436767	84								
18532									
47 510788	0152	1520	786	439	265	271			E*
48589 673	834	2							*
49707 15									
55941 85									
3254 117	00352								
383313 58									
387023 36									
3514 139	025	2							
35226 16									
393473 83									
3698 371	021	2							
370335 16									
415443 84									
1724									
48 511240	42	25	36	4648	265	271			E
46407 6855	840								*
30489 117	05	2							
364495 58									
3682 36									
33257 139	06	2							
333564 16									
373823 83									
35047 372	02	2							
351408 16									
395635 84									
1608									
49 511482	46	30	25	4914	264	271			E
44371 689	850								*
29260 117	05	2							
346984 58									
350697 36									
31473 139	06	2							
316213 16									
355531 83									
33237 361	02	2							
333838 16									
377192 84									
1505									
50 511869	0620	1490	737	5188	264	271			E*
4246 592	859								*

Table 59 cont'd.....

27769	117	03	2					
33058	58							
33433	36							
29831	139	06	2					
30012	16							
33849	83							
31557	3539	05	2					
31751	16							
35999	84	000						
14028								
51 512176		1640	1380	316	842	270		E*
40668	58	867						*
26388	117		2					
315258	58							
319014	36							
28294	139	069	2					
285159	16							
322567	83							
30003	346	049	2					
302335	16							
343941	84							
1313								
52 51276		31	13		885	27		E
3897	58	875						*
25101	117	04	2					
30089	58							
30466	36							
26882	139	07	2					
27124	16							
30768	83							
28558	3403	06	2					
28822	16							
32892	84							
1234								
53 51269		63	23		94	270		E
37381	57	882						*
2388	117	05	2					
291207	58							
287429	36							
25542	139	09	2					
258244	16							
293744	83							
27196	339	07	2					
375053	16							
31486	84							
11544								
55 5132905		628	175		1034	269		E
34451	55	889						*
21673	117		2					
26285	58							
26666	36							

Table 59 cont'd.....

20791	3085	120	2						
21194	16								
24630	84								
13									
60 914424	1860	1410	319	0132		267			E*
28453	53	920							*
1739	117	075	2						
21268	59								
21669	39								
1844	139	133	2						
18779	16								
21669	84								
19967	3044	135	2						
2036	16								
23704	84								
78668	116								
88242	1207								
9559	1158								
123856	1895								
126769	1895								
62 515035	206	137	317	14400	000267				E**
3000	55	927							
16002	117	085	2						
19624	59								
20009	39								
16953	139	150	2						
17272	16								
19981	84								
18457	3000	145	2						
18822	16								
21988	84								
99									
63 515196	41	43	66	151		266			E**
3000	52	930							
15381	117	100	2						
18867	59								
19255	39								
16271	139	185	2						
16574	15								
19203	85								
17761	2944	174	2						
18118	16								
21209	84								
10									
64 515725	205	135	351	158		267			E**
3000	55	932							
14784	117	096	2						
18150	59								
18540	39								
15632	139	159	2						
16574	16								

Table 59 cont'd.....

18468	84						
17117	290	155	2				
17455	16						
20468	84						
99							
65 515892	204	134	313	165	267		E**
30000	55	934					
14223	117	101	2				
17472	59						
17864	39						
15023	139	166	2				
15303	16						
17768	84						
16497	289	160	2				
16830	16						
19765	84						
99							
66 516250	203	133	311	172	266		E**
3000	55	936					
13692	117	100	2				
16822	59						
17210	39						
14445	139	184	2				
14727	16						
17106	84						
15916	288	180	2				
16237	16						
19088	84						
99							
67 516496	202	138	309	178	265		E**
3000	55	938					
13190	117	112	2				
16203	59						
16595	39						
13905	139	203	2				
14174	16						
16475	84						
15368	286	203	2				
15671	16						
18450	84						
99							
68 516726	204	144	325	185	264		E**
3000	55	946					
12706	117	112	2				
15616	59						
16007	39						
13386	139	213	2				
13641	16						
15873	84						
14835	284	210	2				
15140	16						

Table 59 cont'd.....

731018095	55	2	19	222	262	£
18394 47	956					*
10613 117	28	2				
130678 61						
134581 39						
11137 139	25	2				
113794 15						
132698 85						
12553 2615	25	2				
128454 16						
152197 84						
4585 116	005					
502 1207	0084					
565 1158	00451					
6312 1						
687 1892	017	1				
7023 1						
7128 1892	019	1				
7252 1						
2105						
741018392	01770	1200	328	231	261	£*
17837 47	0957					*
102467 117	0305	2				
126269 61						
130162 39						
10745 139	0311	2				
109855 15						
128181 85						
12155 260	22	2				
124460 1593						
147639 8407						
4407 116	005					
4815 1207	0084					
5435 1158	00451					
6092 1						
659 1895	017	1				
6757 1						
683 1895	019	1				
6983 1						
2105						
75101862	325		458	239	261	£
17302 47	959					
9894 117	11	2				
122031 61						
125917 39						
10371 139	33	2				
106099 15						
123858 85						
11773 2574	20	2				
12066 16						
14329 84						

Table 59 cont'd.....

4236	116	005					
462	1207	0084					
5234	1158	00451					
5885	1						
633	1895	017	1				
6504	1						
656	1895	019	1				
6729	1						
199							
76101902	3			46	247	260	£
16787	46	961					*
9558	117	1	2				
117955	61						
121844	39						
10014	139	35	2				
102503	15						
119727	85						
11408	2544	21	2				
116979	16						
13912	84						
4071	116	005					
4433	1207	0084					
5043	1158	00451					
5682	1						
6073	1904	017	1				
6267	1						
630	1904	019	1				
6490	1						
1890							
77101922	19			46	256	26	£
16292	46	962					*
9236	117	10	2				
114085	61						
117958	39						
9671	139	37	2				
99085	18						
115781	82						
11058	252	23	2				
113532	17						
135128	82						
3915	116	005					
4260	1207	0084					
4861	1158	00451					
55	1						
583	1895	017	1				
6038	1						
605	1895	019	1				
6262	1						
179							
781019523	17			50	263	259	£
15818	46	963					*

Table 59 cont'd.....

8931	117	35	2						
110394	61								
114223	39								
93414	140	31	2						
95797	18								
111990	82								
10723	248	275	2						
110200	17								
131304	82								
3774	116	005							
4414	1207	0084							
471	1158	00451							
5319	1								
5665	1895	017	1						
5828	1								
581	1895	019	1						
6047	1								
172									
791019697	0830	1320	644	272		259		E*	
015359	46	964						*	
086376	117	08	2						
106785	61								
110651	39								
090259	139	343	2						
92650	18								
108353	82								
10400	247	31	2						
107022	18								
127640	82								
3616	116	005							
3936	1207	0084							
4518	1158	00451							
5145	1								
5374	1895	017	1						
5624	1								
5584	1895	019	1						
584	1								
1627									
801020059	1010	1080	618	281		258		E*	
14918	46	966						*	
8353	117		2						
103358	61								
107222	39								
8722	139	39	2						
89646	18								
104868	82								
10091	2438	40	2						
103975	18								
12412	82								
3478	116	005							
3783	1207	0084							

Table 59 cont'd.....

4355	1158	00451					
4978	1						
5157	1895	017	1				
5431	1						
536	1895	019	1				
5645	1						
154012							
811020437	17	25	56	289	258		ε
14495	45						
80786	117	09	2				
100062	61						
103918	39						
8435	139	43	2				
86752	18						
101513	82						
9795	2404	27	2				
101031	18						
120739	82						
33471	116	005					
36297	1207	0084					
41933	1158	00451					
4823	1						
49889	1888	017	1				
5249	1						
5189	1888	019	1				
546	1						
14664							
821020719	16		6	298	257		ε
14088	56	968					*
78168	117	37	2				
96911	61						
10075	39						
81566	139	24	2				
83973	18						
98291	82						
95112	2394	35	2				
98221	18						
117501	82						
321967	116	005					
348827	1207	0084					
404318	1158	00451					
4674	1						
479502	1895	017	1				
5076	1						
499114	1895	019	1				
5286	1						
13874							
8310209	0690	1010	656	307	256		ε*
13694	45	963					*
7571	117	12	2				
93855	61						

Table 59 cont'd.....

97690	39								
7887	139	32	2						
81311	18								
95198	82								
9234	236	35	2						
95518	183								
114386	817								
3094	116	005							
3359	1207	0084							
3904	1158	00451							
4532	1								
4572	1895	017	1						
4909	1								
4764	1895	019	1						
5118	1								
132									
901223204	002100000000	575	377		253			ε*	
11037	42	975						*	
6059	117	197	2						
75479	61								
79257	39								
6299	139	56	2						
65313	21								
76521	79								
7607	194	39	2						
79354	19								
956	81								
2393	116	005							
2572	1207	0084							
3068	1200	00451						*	
3679	1								
3557	1200	017	1					*	
3941	1								
3729	1550	019	1					*	
41381	1								
9371	2200	000001						*	
10688	120	000001						*	
12928									
921223803	1			55	397	253		ε	
10723	42	976						*	
5695	117	25	2						
71029	61								
74799	39								
5919	139	59	2						
61477	21								
71998	79								
7223	2069	44	2						
75468	19								
91064	81								
2235	116	005							
2394	1207	0084							

Table 59 cont'd.....

2884	1158	00451	
3479	1		
3333	1550	017 1	*
3716	1		
3497	1550	019 1	*
391	1		
8614	022500	0001	*
9747	2300	000001	*

99

APPENDIX II

SUGGESTIONS FOR THE ANALYSIS OF U AND Th-MINERALS

A- PREPARATION FOR MICROPROBE ANALYSIS OF U AND Th-MINERALS

The following is concerned with the analysis of minerals in a rock sample. For mineral separates, only steps 2 and 5 need be carried out.

- 1- The saw cut surfaces of a rock sample are put on a film to locate the radioactive phases either by autoradiography or radioluxography.
- 2- The selected portions of the sample are impregnated with epoxy resin, and made into polished thin sections.
- 3- Autoradiographs or radioluxographs of the thin sections are made.
- 4- The thin sections are studied under the microscope, with reference to the radiographs. Lines are drawn, in India ink, from the edge of the section to the vicinity of grains to be analysed, and

photomicrographs (X50) of these grains, including the end of the ink line, are taken. A map of the section, showing the ink lines, is sketched. In this way, the grains can be rapidly located during analysis, and the exact point or area of analysis marked on the photomicrograph.

- 5- The sections are coated to ensure good conductivity.¹ A qualitative study is made to identify the elements present and check for homogeneity (see section B below), using EDA² and/or WDA³. Points or areas to be analysed are thus selected.

B- TESTS FOR HOMOGENEITY

Homogeneity can be tested qualitatively at different levels. Broad differences of composition are detected most readily by EDA, while more subtle differences will be detected by WDA.

¹ This, of course, may vary from one laboratory to another.

² energy dispersive analysis

³ wavelength dispersive analysis

1. ENERGY DISPERSIVE ANALYSIS

This is done by comparing spectra for different areas, either by making Polaroid photographs of the spectra from the oscilloscope display or transferring the spectra from the multichannel analyser to a chart or X-Y recorder, and then comparing them visually. In all cases, the spectra should be recorded over similar periods of time; 400 to 1000 second counting time with an operating potential of 15 kV, and a probe current of $0.3 \cdot 10^{-6}$ A gave satisfactory results with the instrument used in the present study. These conditions vary with instrumentation, and with the scale of the variations sought.

2. WAVELENGTH DISPERSIVE ANALYSIS

This is done by traversing a grain and recording simultaneously the intensities of two or more elements on a chart or X-Y recorder; or by taking X-ray, backscattered electron and sample current scanning photographs of small areas. The first is used mainly for millimetre scale variations, while the second is suitable for micron scale variations.

C- OPERATING CONDITIONS

Basic data and suggestions for the analysis of uranium, thorium, and associated elements, including emission lines and standards, are listed in table 60.

Suitable analytical conditions for an ARL-EMX microprobe, or instrument with similar characteristics, are:

- operating potential : 15 kV;
- probe current : 1×10^{-7} A;
- beam diameter : 0.5 to 20 microns;
- counting period : 50 sec.;
- number of counting periods on 'peaks' : 10;
- number of counting periods on 'backgrounds': 5.

By taking numerous short 'counts' (here, 50 s) rather than a single longer 'count' equivalent in time (here, 500 s for 'peak' positions), it is possible to avoid spurious values which could arise from electronic failure and contamination. A total period of 500 s gives adequate statistics for most concentrations for the instrument used in this study.

Suitable standards are listed in table 60. A compromise must be reached, taking into account the following considerations:

- 1- the average atomic number of the standard should, ideally, be similar to that of the specimen;
- 2- the element concerned should be present in both

standard and sample in similar amounts, with the proviso that it should have a concentration of at least 3 wt% in the standard;

- 3- it is convenient to use the same standard for different elements.

The analysing crystal is selected according to the wavelength range required, and the efficiency of the suitable crystals, while retaining the possibility of maximum use of the available spectrometers. Suitable crystals for the analysis of uranium, thorium, and commonly associated elements are listed below (table 61).

Table 60: Basic data and suggestions for the analysis of uranium, thorium, and commonly associated elements for an operating potential of 15 kV. Elements (El.) are listed with analytical lines (Line) and their wavelength (Wlength); standards; possible interferences (Int.); and remarks (R). 'M' stands for metal.

El.	Line	Wlength	Standards	Int.	R
H					1
N					1
C					1
O					1
Na	K α	11.9090	feldspar		2
Mg	K α	9.8889	forsterite, diopside		
Al	K α	8.3390	feldspar, corundum		
Si	K α	7.7261	quartz, most silicates		
P	K α	6.1549	Ca ₂ P ₂ O ₇ , xenotime		
S	K α	5.3728	galena, pyrite		
K	K α	3.7424	feldspar	U-M α	3
K	K β	3.4539	"		3
Ca	K α	3.3596	feldspar, Ca ₂ P ₂ O ₇		
Ti	K α	2.7496	M, rutile, ilmenite		
V	K α	2.5047	M, vanadinite		
Mn	K α	2.1030	M, rhodonite, alabandite		
Fe	K α	1.9373	hematite, pyrite, Fe-silicates		
Co	K α	1.7902	M, cobaltite		
Cu	K α	1.5418	M, cuprite, chalcopyrite		
Zn	K α	1.4363	M, zincite, willemite		
As	L α	9.6714	M, arsenopyrite, niccolite		
Se	L α	8.4901	NbSe ₂ , eucarite, naumannite		
Y	L α	6.4484	M, xenotime, glasses		
Zr	L α	6.0702	M, zircon		
Nb	L α	5.7240	M, NbS ₂ , glasses		
Mo	L α	5.4062	M, molybdenite, wulfenite		
Te	L α	3.2891	M, Ag ₂ Te, Bi ₂ Te ₃		
Ba	L α	2.7751	barite		
La	L α	2.6650	glasses	REE-L	4
Ce	L α	2.5611	glasses	REE-L	4
Nd	L α	2.3700	glasses	REE-L	4
Sm	L α	2.1994	glasses	REE-L	4
Gd	L α	2.0460	glasses	REE-L	4
Dy	L α	1.9087	glasses	REE-L	4
Ho	L α	1.8447	glasses	REE-L	4
Er	L α	1.7842	glasses	REE-L	4
Yb	L α	1.6718	glasses	REE-L	4
Ta	L α	1.5218	M, Ta ₂ O ₅ , KTaO ₃		
Pb	M α	5.2916	M, galena		
Bi	M α	5.1238	M, Bi ₂ Te ₃ , BiS ₃		
Th	M α	4.1448	ThO ₂ , glasses		
U	M α	3.9168	UO ₂ -UO ₃ , glasses	Th-M γ	5
U	M β	3.7160	" "	K-K α	3

table 60, cont'd.....

- 1- This element is not analysed, its concentration is calculated as indicated in section E of this appendix.
 - 2- Sodium K-lines occur in the same range of energy as some uranium N-absorption edges. Data relevant to the analysis of sodium in the presence of uranium are lacking. The effect of the N-absorption edges remains to be quantified and corrected for, if required.
 - 3- Interferences exist between K-K α and U-M β , and between U-M α and Th-M γ . When thorium is absent, U-M α and K-K β are used; when all three elements occur together, Th-M α , K-K β , and U-L α can be used; U-L α (17.162 kV) requires an operating potential of at least 22 kV to excite it and obtain sufficient intensity. Problems relative to the usage of U-L lines are considered in detail in chapter IV.
 - 4- In practice, overlaps between the various rare-earths affect mainly the background reading positions. It is a good practice to determine the background positions for each set of standard and specimen, and to use standards containing no more than four rare-earths; the latter should be of spaced atomic number (say, 5).
 - 5- Th-M β and U-M α overlap each other. U-M β is slightly affected by Th-M γ ; this is only a minor line, hence an overlap coefficient is easily determined. In the presence of thorium, U-M β is used, and an overlap coefficient is applied to the measured intensities (prior to data reduction).
-

Table 61: Elements and lines recorded with some common crystals used in WDA.

Crystal	Elements	Lines
K acid phthalate (KAP)	Al-O	K
Rb acid phthalate (RAP)	Al-O	K
Mica	S-Na	K
Thallium acid phthalate (TAP)	Al-O	K
Ammonium dihydrogen phosphate (ADP)	Ti-Mg	K
	Ba-As	L
	Pb-U	M
Ethylene diamine dextrotartrate (EDDT)	V-Si	K
	Nd-Y	L
	Pb-U	M
Pentaerythritol (PET)	V-Si	K
	Nd-Y	L
	Pb-U	M
Quartz (SiO ₂)	Co-P	L
	Er-Zr	L
Lithium fluoride (LiF(200))	Se-K	K
	Ta-As	L

D- DATA PROCESSING

At present, two programmes are known to effect reduction of microprobe data, including full 'ZAF' corrections for M-lines, i.e., COR-2 (Hénoc *et al.*, 1973) and FEPAC (Springer, 1976). These must be adapted to the local computer. COR-2 refers to a permanent data file for constant parameters used at various steps in the reduction.

This file must be extended for uranium, thorium, and rare-earth analysis.¹ FEPAC uses a set of equations to calculate most parameters as required.

Whether data are recorded on tapes, cassettes, punched cards, or paper depends on the installation. Depending on the mode of recording, ratios of intensities (sample divided by standard) will be calculated by desk calculator, or by computer programmes. When recorded, corrections for variations in the probe current to aperture current ratio should be applied to the raw data by independent programmes. Corrections for overlaps are not included in the above mentioned programmes, and need to be applied prior to final reduction.

E- ELEMENTS NOT ANALYSED

Light elements are not analysed quantitatively by microprobe; they are determined either by stoichiometry or by difference. When oxygen is the only light element present, it can be calculated stoichiometrically. When additional elements, such as hydrogen, carbon, and fluorine are expected, they are treated together with oxygen, and the sum of light elements is calculated by difference. The

¹ Such a completed file is listed in appendix I

computed average atomic number of a phase will not differ much whether all light elements are attributed an atomic number of 8, or if their weighted average atomic number is calculated, since in most minerals, oxygen is, by far, the most abundant light element (i.e., the weighted average atomic number for the light elements would be close to 8 in most cases).

APPENDIX III

SAMPLE TEMPERATURE BENEATH THE ELECTRON BEAM

According to Friskney and Haworth (1967), the rise in temperature at a point bombarded by electrons, located at a distance 'r' from the centre of the electron beam, can be calculated as follows:

$$T(r) = \frac{3W_0(3-r^2/r_0^2)(1+2\ln(R/r_0-r^2/r_0^2))}{4 \times 3.1416 [lK_1(13-3r^2/r_0^2) + 3Kr_0(1+2\ln(R/r_0-r^2/r_0^2))]}$$

where: $T(r)$ = temperature increment at a distance 'r' from the centre of the beam

r_0 = radius of the beam

R = radius of the specimen

K_1 = thermal conductivity of the coating

K = thermal conductivity of the specimen

W_0 = total power absorbed

l = thickness of the coating.

For the following values:

$r_0 = 1 \cdot 10^{-4} \text{ cm}$

$R = 1 \text{ cm}$

$$W_0 = 15 \text{ kV} \times 1.0 \cdot 10^{-6} \text{ amp} \cdot 10^{-1}$$

(Only about 1/10 of the current passes through the last 300 micron aperture in the ARL-EMX instrument used and with the operating conditions suggested.)

$$= 1.5 \cdot 10^{-6} \text{ watts}$$

$$K = 0.004 \text{ cal/sec} \cdot \text{cm} \cdot ^\circ\text{C} \text{ (as obsidian)}$$

$$= 0.016 \text{ watt/cm} \cdot ^\circ\text{C}$$

$$K_1 = 0.5 \text{ watt/cm} \cdot ^\circ\text{C} \text{ (i.e. about 1/4 of the conductivity of aluminium)}$$

$$l = 200 \text{ \AA}.$$

At the centre of the beam, $r=0$ and:

$$r/r_0 = 0$$

the equation thus becomes:

$$T(0) = \frac{3W_0 \times 3(1+2\ln(R/r_0))}{4 \times 3.1416[(13lK_1) + 3Kr_0(1+2\ln(R/r_0))]}$$

$$T(0) = \frac{9 \times 1.5 \cdot 10^{-3} \text{ w} (1+2\ln 10^4) \text{ cm} \cdot ^\circ\text{C} \text{ cm} \cdot ^\circ\text{C}}{4 \times 3.1416[2 \times 10^{-6} \text{ cm} \times 0.5 \text{ w} \times 13 \times 3 \times 0.016 \text{ w} \cdot 10^{-4} \text{ cm} (1+2\ln 10^4)]}$$

$$T(0) = 197^\circ\text{C} \text{ then,}$$

if the room temperature is 21°C , then,

the temperature at the centre of the beam is 218°C

APPENDIX IV

IDENTIFICATION AND PETROGRAPHIC DESCRIPTIONS OF SAMPLES

Table 62 Identification of the samples from the Baie
Johan Beetz region

Table 63 Petrographic descriptions of the samples from
the Baie Johan Beetz region

Table 64 Identification of the boulder samples from the
Duddridge Lake region

Table 65 Petrographic descriptions of the samples from
the Duddridge Lake region

Table 66 Identification of the samples from the
Charlebois Lake region

Table 67 Petrographic descriptions of the samples from
the Charlebois Lake region

All the percentages (%) given in the petrographic
descriptions were estimated visually.

Table 62 Identification of the samples from the Baie Johan
Beetz area

number	rock type
JB-1	white pegmatite
JB-2	white granite with uranophane and allanite
JB-3	pink granite
JB-4	pink biotite granite
JB-5	white biotite granite (at contact with pink biotite pegmatite)
JB-6	pink biotite-garnet gneiss
JB-7	pink biotite-garnet gneiss
JB-8	biotite and apatite rich granite
JB-9	fracture filling in granite
JB-10	muscovite-biotite pink to green granite
JB-11	medium pink to green granite
JB-12	coarse greenish granite
JB-13	coarse greenish granite
JB-14	garnet bearing medium green granite
JB-15	shear zone in white pegmatite
JB-16	pink pegmatite
JB-17	shear zone in medium green granite (sample JB-18)
JB-18	medium green granite

Table 63 Petrographic descriptions for samples from the
Baie Johan Beetz region

Sample JB-1

mineral	%	description
quartz	15	undulose extinction
microcline	10	altered; cloudy brownish appearance
plagioclase	75	An ₁₅ ; cloudy brown appearance, more altered than microcline
muscovite	<1	small patches and veinlets in plagioclase
chlorite	<1	
titanobetafite	1	yellow to red, almost opaque, metamict, biaxial
uraninite	<1	roundish
monazite	<1	automorphous
xenotime	<1	automorphous
apatite	<0.1	

Uraninite, monazite, and xenotime tend to cluster together.

Texture : granoblastic

Average grain size : 1 cm; accessories: 0.1 mm

table 63 cont'd.....Sample JB-2

mineral	%	description
<hr/>		
quartz	15	undulose extinction
microcline	50	altered; cloudy brown appearance
plagioclase	30	An ₃₀ , more altered than microcline
muscovite	<1	small patches and veinlets in plagioclase
uraninite	<1	roundish
monazite	<1	automorphous

Monazite and uraninite tend to cluster together; no apatite or xenotime were observed.

Texture : granoblastic

Average grain size : 1 cm; accessories: 0.1 mm

table 63 cont'd.....Sample JB-3

mineral	%	description
<hr/>		
quartz	40	undulose extinction, round grains included in feldspar
microcline	40	perthitic, light brownish surface with large plagioclase exsolution
Fe-muscovite	1	in veinlets associated with ilmenite and included in microcline
uraninite	<1	roundish
ilmenite	<1	
rutile	4	
calcite	<1	interstitial between rutile and ilmenite

Ilmenite, rutile and calcite are found together with minor amounts of Fe-muscovite; they are remnants of a large broken grain (2x4mm). The rutile is automorphous and displays rhombohedral shapes.

Texture : granoblastic

Average grain size : 1 cm; accessories 0.5 mm

table 63 cont'd.....Sample JB-4

mineral	%	description
<hr/>		
quartz	10	undulose extinction
microcline	5	altered brownish surface
plagioclase	65	An ₂₀ altered brownish surface
biotite	20	brown
muscovite	<1	associated with biotite
uraninite	1	often fractured
monazite	1	automorphous
xenotime	<1	automorphous
zircon	<0.1	automorphous

The uraninite is often fractured. Seen in transmitted light, the black grains appear to be composed of two phases under reflected light. One phase, uraninite, is grey, more reflectant and fractured or 'exploded', the second is grey to slightly greenish and fills in the fractures or constitutes a major part of the 'opaque grain' (30 to 95%), it is believed to be carbonaceous matter.

The radioactive grains do not tend to cluster together.

Texture : granoblastic

Average grain size : 0.5 cm; accessories: 0.3 mm

table 63 cont'd.....Sample JB-5

mineral	%	description
<hr/>		
quartz	80	undulose extinction
microcline	<1	altered; cloudy surface
plagioclase	5	An ₂₅ , altered; cloudy surface
biotite	15	brown, dark red to nearly black in section parallel to (001)
uraninite	<0.1	roundish
apatite	<1	
monazite	1	automorphous
zircon	<0.1	automorphous
muscovite	<1	associated with uraninite in biotite

The biotite is chloritized or turning green. It contains very finely disseminated uraninite grains easily detected by their wide radiogenic haloes.

Texture : granoblastic

Average grain size : 0.5 cm; accessories: 0.3 mm

table 63 cont'd.....Sample JB-6

mineral	%	description
<hr/>		
quartz	8	undulose extinction
microcline	60	perthitic with large plagioclase exsolutions; slightly altered
plagioclase	10	as exsolution in microcline
biotite	20	two generations (brown-green and brown)
garnet	1	fractured
muscovite	<1	associated with biotite
chlorite	<1	
uraninite	1	two phases as in section JB-5
apatite	<1	
monazite	<1	automorphous

Two generations of biotite were recognized, the first one, more important (15%), is brown and green, and contains uraninite; the second is brown, cuts grains of the first generation and is uraninite free.

Texture : granoblastic

Average grain size : 0.5 cm; accessories: 0.3 mm

table 63 cont'd.....Sample JB-7

mineral	%	description
<hr/>		
quartz	30	undulose extinction
microcline	60	altered; cloudy brownish appearance
plagioclase	2	
biotite	1	brown to almost black
garnet	8	often hosting uraninite
monazite	<1	automorphous
xenotime	<1	automorphous
zircon	<1	automorphous
uraninite	<1	two phases, as in section JB-5
apatite	<1	

Xenotime, monazite, zircon, uraninite and apatite tend to cluster together.

Texture : granoblastic

Average grain size : 1 cm; accessories: 0.3 mm

table 63 cont'd..... Sample JB-8

mineral	%	description
<hr/>		
quartz	5	interstitial, undulose extinction
microcline	70	altered, brownish, perthitic with large exsolutions
plagioclase	3	zoned, An ₃₀ at the centre with a rim of about An ₂₀ the centre is very altered; the rim is fresh.
biotite	20	green to dark red (almost black)
muscovite	<0.1	associated with biotite
titanobetafite	<0.1	
monazite	2	automorphous
zircon	1	automorphous
apatite	<1	

Monazite and zircon cluster together. They are strongly radioactive and usually occur in contact with, or close to, biotite.

Texture : granoblastic

Average grain size : 0.5 cm; accessories 0.3 mm

table 63 cont'd.....Sample JB-9

mineral	%	description
<hr/>		
quartz	25	undulose extinction
microcline	18	altered; turbid surface
plagioclase	10	altered, brownish turbid surface
allanite	8	pale brown at the centre, with a darker rim
xenotime	20	automorphous, altered
samarskite	2	automorphous
uraninite	5	automorphous
thorogummite	2	fractured, often as a rim around xenotime
zircon	1	clear, zoned

This sample had a very altered aspect. This is reflected in the thin section by intense fracturing especially around xenotime and samarskite.

Xenotime is zoned and has a brownish centre with a pale yellow rim. Some grains show exsolution of a Th phase.

Uraninite is rimmed by a thin red coating.

Texture : granoblastic

Average grain size : 1mm

table 63 cont'd.....Sample JB-10

mineral	%	description
<hr/>		
quartz	15	undulose extinction
microcline	5	altered, cloudy appearance
plagioclase	75	An ₃₀ ; very altered, cloudy brown surface with fine flakes of mica; antiperthitic
biotite	3	brown to dark red to almost black
chlorite		chloritized partly or wholly
muscovite	<1	associated with biotite
xenotime	<1	automorphous
monazite	<1	automorphous
uraninite	<1	roundish
titanobetafite	<0.1	

Monazite and xenotime tend to cluster together.

Texture : granoblastic

Average grain size : 1 cm; accessories: 0.3 mm

table 63 cont'd.....Sample JB-11

mineral	%	description
<hr/>		
quartz	55	undulose extinction
microcline	25	altered brownish surface, finely perthitic
plagioclase	20	zoned, An ₁₇ at the centre with a rim of about An ₂₅ . The centre is very altered with distinct flakes of mica; the rim is fresh.
biotite	4	brown to dark red to almost black, chloritized
chlorite	<1	associated with biotite
muscovite	1	associated with biotite and plagioclase
titanobetafite	<1	
uraninite	<0.1	roundish
apatite	<0.1	automorphous
zircon	<0.1	automorphous
monazite	<0.1	automorphous

Titanobetafite, uraninite, apatite, zircon and monazite cluster together, and occur in contact with, or close to, biotite.

Texture : granoblastic

Average grain size : 0.5 cm; accessories: 0.5 mm

table 63 cont'd.....Sample JB-12

mineral	%	description
<hr/>		
quartz	30	undulose extinction
K-feldspar	20	slightly altered;l Carlsbad twinning only.
plagioclase	40	An ₁₀₋₁₅ ; slightly altered
biotite	1	brownish green
stilpnomelane	<0.1	
sphene	1	automorphous with seams of magnetite
monazite	<0.1	automorphous
allanite	1	automorphous, yellow to green
zircon	<1	automorphous, zoned
apatite	<0.1	automorphous
titanobetafite	<0.1	
uraninite	<0.1	roundish
magnetite	<0.1	included in sphene

Monazite, zircon, allanite, apatite, titanobetafite and uraninite cluster together and occur in contact with or included in biotite.

Texture : granoblastic

Average grain size : 2 mm; accessories: 0.2 mm

table 63 cont'd.....Sample JB-13

mineral	%	description
<hr/>		
quartz	50	undulose extinction
microcline	40	slightly altered
plagioclase	8	zoned, An ₁₀ at the centre with a rim of about An ₁₇ . The centre is very altered with distinct flakes of mica; the rim is fresh
biotite	2	chloritized
chlorite		alteration of biotite
muscovite	<1	associated with biotite
titanobetafite	<0.1	
uraninite	<0.1	automorphous
monazite	<0.1	automorphous
zircon	<0.1	automorphous

Texture : granoblastic

Average grain size : 0.2-1 cm; accessories: 0.2 mm

table 63 cont'd.....Sample JB-14

mineral	%	description
<hr/>		
quartz	45	undulose extinction
microcline	20	slightly perthitic with recrystallized seams of muscovite and quartz; very slightly altered
plagioclase	20	An ₂₀ ; slightly altered
biotite	3	chloritized
chlorite		mostly from alteration of biotite and in minute cracks in microcline
muscovite	<1	associated with feldspar
stilpnomelane	3	fractured, altered
samarskite	<1	
xenotime	<0.1	automorphous
ilmenite	<1	automorphous
brookite	<0.1	automorphous
magnetite	<0.1	as exsolution in brookite

The whole thin section shows damage due to expansion or fracture of stilpnomelane.

Texture : granoblastic

Average grain size : 0.5-1 cm; accessories: 1-0.1 mm

table 63 cont'd.....Sample JB-15

mineral	%	description
<hr/>		
quartz	1	interstitial
K-feldspar	5	
plagioclase	15	An ₁₇₋₂₀ ; slightly altered
muscovite	7	
allanite	63	automorphous; zoned; pale green centre with a darker rim
samarskite	4	
xenotime	4	
uraninite	1	sub-automorphous
ilmenite	2	
brookite	<0.1	inclusion in ilmenite

Allanite is the main constituent of this thin section
samarskite, xenotime, uraninite, ilmenite and brookite occur
 in the plagioclase.

Texture : granoblastic

Average grain size : 1 cm; accessories: 1 mm

table 63 cont'd.....Sample JB-16

mineral	%	description
<hr/>		
microcline	45	slightly altered
plagioclase	50	slightly altered; a rim of about An ₂₀ is barely distinguishable from the centre An ₁₅
muscovite	1	associated with microcline and in patches and veinlets
samarskite	<1	
xenotime	<1	
allanite	5	automorphous; zoned (pale green centre with a darker rim)
uraninite	<1	automorphous

This section resembles section JB-15 but the allanite is less abundant, other minor minerals such as: samarskite, xenotime and uraninite occur in feldspar mostly in contact with or close to the allanite.

Texture : granoblastic

Average grain size : 1 cm; accessories: 1 mm

table 63 cont'd.....Sample JB-17

mineral	%	description
<hr/>		
quartz	85	mosaic extinction
biotite	4	pale brown, with eyes of quartz between cleavage planes
sphene	4	automorphous; dark pink, often with inclusions of zircon
allanite	4	sub-automorphous; zoned (pale green centre with a dark green or brown rim)
zircon	<1	automorphous
uraninite	<1	automorphous
brookite	<1	
samarskite	<0.1	

Sphene, allanite, zircon, uraninite, brookite and samarskite
cluster together and occur in contact with or close to
biotite.

Texture : granoblastic

Average grain size : 1 cm; accessories: 1 mm

table 63 cont'd.....Sample JB-18

mineral	%	description
<hr/>		
quartz	50	undulose extinction
microcline	20	slightly altered; finely perthitic
plagioclase	28	An ₂₅ ; very altered with distinct flakes of mica, cloudy appearance
biotite	2	brown to green
muscovite	<1	associated with biotite and plagioclase
chlorite	<1	alteration product; pseudomorph of an hexagonal section but the presence of the primary mineral was not detected
zircon	<1	automorphous

Texture : granoblastic

Average grain size : 1 cm; accessories: 1 mm

Table 64 Identification of the boulder samples from the
 Duddridge Lake region

number	rock type
<hr/>	
DL-1	meta-arkose
DL-2	meta-arkose
DL-3	meta-arkose
DL-4	meta-arkose
DL-5	migmatite
DL-6	grey dyke
DL-7	meta-quartzite
DL-8	quartzitic meta-arkose
DL-9	meta-arkose
DL-10	meta-conglomerate

Table 65 Petrographic descriptions for samples from the
Duddridge Lake region

Sample DL-1

mineral	%	description
<hr/>		
quartz	55	undulose extinction
microcline	35	altered; turbid surface
plagioclase	5	fresh about An ₁₀ , diffuse twinning
biotite	5	pale brown
calcite	<0.1	
zircon	<0.1	
chalcopyrite	1	automorphous
ilmenite	1	fine interstitial blades
'brannerite'	<0.1	roundish, with reddish haloes
Ti-V phase	<0.1	roundish, with reddish haloes

'brannerite' grains tend to cluster together. They are surrounded by red staining.

Texture : porphyroblastic

Average grain size : 1mm; accessories: 0.1 mm (ilmenite) to 0.01

table 65 cont'd.....Sample DL-2

mineral	%	description
<hr/>		
quartz	45	most grains are discrete and show no undulose extinction
microcline	5	altered; turbid surface
plagioclase		altered; turbid surface, An ₄₋₁₀
biotite	3	brown
muscovite	2	pale brown to colourless
'brannerite'	<1	associated with red staining
U-Pb-Si phases	<1	as crack filling and in small pockets
rutile	<0.1	

Biotite and muscovite either cluster together to form small pockets or occur separately as dispersed grains throughout the sample.

Texture : equigranular to mortar

Average grain size : 0.5 mm; accessories: 0.01 mm

table 65 cont'd.....Sample DL-3

mineral	%	description
<hr/>		
quartz	50	undulose extinction
microcline	18	altered; turbid surface
plagioclase	20	altered; turbid surface, An ₅₋₁₀
biotite	2	brown
muscovite		alteration of plagioclase
calcite		alteration of plagioclase
uraninite	3	soft, occurs in bands of discrete grains
'brannerite'	1	
U-Pb-Si phase	1	as cluster and fracture filling
carnotite	<0.1	associated to U-Pb-Si phase

The composition of the plagioclase is difficult to estimate because it is damouritized and its twinning is diffuse.

'brannerite' occurs as grains dispersed between the major constituents of the rock and as inclusions in feldspar.

Texture : equigranular

Average grain size : 0.5 mm; accessories: 0.01 mm

table 65 cont'd.....Sample DL-4

mineral	%	description
<hr/>		
quartz	55	undulose extinction in the larger grains, normal extinction in smaller grains
microcline	30	fresh
plagioclase	7	fresh, An ₅ ; diffuse twinning
biotite	2	pale brown to pale green, chloritized
zircon	<0.1	zoned
uraninite	1	roundish
U-Pb-Si phase	1	mostly associated with uraninite
pyrite	<0.1	automorphous
'brannerite'	<1	roundish
magnetite	<0.1	associated with uraninite

Uraninite and 'brannerite' occur as interstitial grains and included in quartz and feldspars where they display large reddish black haloes. Interstitial grains do not display haloes in adjacent feldspars or quartz. Both are soft and altered and, occasionally show replacement by, or overgrowths of, magnetite.

Red to yellow staining is abundant between grains and in cleavage planes.

Texture : equigranular

Average grain size : 0.5 mm; accessories: 0.01 mm

table 65 cont'd.....Sample DL-5

mineral	%	description
<hr/>		
quartz	60	undulose extinction
microcline	25	fresh
plagioclase	10	generally fresh with some large flakes of hydromuscovite; An ₁₀₋₁₂
biotite	2	chloritized
muscovite	1	
uraninite	<1	roundish
'brannerite'	1	roundish
monazite	<0.1	
pyrite	<0.1	
rutile	<0.1	

Uraninite and 'brannerite' occur as in sample DL-4. They are less abundant than in the latter specimen; iron staining is also less abundant.

Texture : mortar to equigranular

Average grain size : 1mm; accessories: 0.01 mm

table 65 cont'd.....Sample DL-6

mineral	%	description
quartz	45	undulose and plain extinction
microcline	16	little alteration
plagioclase	30	little alteration; An ₃₋₁₅ ; diffuse twinning
biotite	1	brown
uraninite	1	very altered, roundish
U-Pb-Si phase	2	mostly associated with uraninite
chalcopyrite	<0.1	
arsenopyrite	<1	
cobaltite	<1	
ilmenite	1	fine interstitial blades
rutile	<0.1	
'brannerite'	<0.1	

Uraninite is mostly interstitial. It is altered and occurs as remnants in yellow reddish patches.

Rutile and Ti-V oxide are intergrown.

Arsenopyrite and cobaltite often form mixed grains.

Texture : porphyroblastic, gneissic

Average grain size : 1 mm, accessories: 0.01 mm

table 65 cont'd.....Sample DL-7

mineral	%	description
quartz	55	undulose extinction
microcline	10	altered; turbid surface
plagioclase	30	altered, damouritized, very diffused twinning; about An ₁₅
calcite	<1	associated with plagioclase
biotite	1	pale brown
muscovite	5	
zoisite	<1	
chalcopyrite	4	often associated with muscovite
sphene	1	with segregation of rutile and ilmenite
rutile	<0.1	associated with sphene
ilmenite	<0.1	associated with sphene
apatite	<0.1	automorphous
monazite	<0.1	automorphous
'brannerite'	<0.1	very altered
U-Pb-Si phase	<0.1	

Texture : equigranular

Average grain size : 1mm, accessories: 0.01 mm

table 65 cont'd.....Sample DL-8

mineral	%	description
<hr/>		
quartz	50	in large grains with mosaic extinction
microcline	10	fresh
plagioclase	30	fresh, An ₁₅
biotite	3	brown
ilmenite	1	fine interstitial blades
rutile	1	automorphous, often with a reddish halo
cobaltite	5	automorphous
safflorite	<0.1	
chalcopyrite	<0.1	
zircon	<0.1	
'brannerite'	<0.1	roundish, with reddish halo
Ti-V oxide	<0.1	

Cobaltite often occurs as clusters of grains growing on the edges of rutile.

Texture : porphyroblastic, schistose

Average grain size : 1 mm; accessories: 0.01 mm

table 65 cont'd.....Sample DL-9

mineral	%	description
<hr/>		
quartz	40	undulose extinction
microcline	10	altered; turbid surface
plagioclase	48	almost fresh, some damouritization, An ₁₃
biotite	1	pale brown to pale green
muscovite	<1	
calcite	<0.1	
ilmenite	1	fine interstitial blades
chalcopyrite	<0.1	
'brannerite'	<0.1	roundish, surrounded by yellow staining
apatite	<0.1	automorphous

Texture : equigranular, slightly foliated

Average grain size : 1 mm; accessories: 0.01 mm

table 65 cont'd.....Sample DL-10

mineral	%	description
<hr/>		
quartz	60	as pebbles in large sutured grains and as smaller grains in the matrix
biotite	13	brown
muscovite	2	
garnet	1	altered to quartz and mica, and epidote, fractured
epidote	1	replacement of garnet
ilmenite	15	
monazite	5	automorphous
zircon	3	automorphous
apatite	1	automorphous

Texture : granoblastic

Average grain size : coarse fraction: 5 mm

:matrix: 0.5 mm to 0.03 (accessories)

The coarse grained fraction of this meta-conglomerate consists of quartz pebbles while the matrix is a intimate mixture of biotite, ilmenite and mica with epidotized garnet, zircon, apatite, monazite and finer grained quartz.

Table 66 Identification of the samples from the
Charlebois Lake region

number	rock type

CL-1	migmatite
CL-2	migmatite
CL-3	migmatite
CL-4	pegmatite
CL-5	migmatite

Table 67 Petrographic descriptions of the samples from
the Charlebois Lake region

Sample CL-1 (average of two polished thin-sections)

mineral	%	description
quartz	7	undulose extinction
orthoclase	20	altered; turbid appearance; not twinned
plagioclase	62	zoned; altered damouritized centre of undetermined composition with a fresher rim of about An ₂₅
biotite	10	reddish brown, to almost black, with chloritized zones
muscovite	1	in feldspar and as small flakes around biotite
uraninite	<0.1	mostly remnants
monazite	<0.1	automorphous, pinkish to yellowish, metamict
zircon	<0.1	automorphous, clear, zoned, metamict
pyrite	<0.1	lamellar mostly included in biotite in cleavage planes

Monazite, zircon and uraninite do not appear to be associated with biotite. Both zircon and monazite have low birefringence (first order white), this is imputed to metamictization. When in contact with biotite, monazite has a radiogenic halo, while zircon does not. Included in biotite, cubic shapes of yellowish dark green to brown material appear to be remnants of uraninite; they are rimmed by a reaction zone. One grain of uraninite appeared fresh, it is included in plagioclase.

Texture :equigranular

Average grain size : 5 mm; accessories: 0.5 mm

table 67 cont'd.....Sample CL-2

mineral	%	description
<hr/>		
quartz	20	undulose extinction
orthoclase	29	not twinned, cloudy surface
microcline	1	twinned, cloudy surface
plagioclase	40	altered, damouritized, about An ₃₀
biotite	10	brown
monazite	< 1	automorphous, yellowish to pinkish, metamict
zircon	<1	automorphous, clear, zoned, metamict
uraninite	<0.1	remnants, hematitized
pyrite	<0.1	lamellar, mostly included in biotite between cleavage planes

Cubic shapes of yellowish dark green to brown material appear to be remnants of uraninite. They are rimmed by a reaction zone or the host mineral (biotite or feldspar). Monazite zircon and uraninite are mostly included in or in contact with, biotite. The biotite occasionally shows kink structure around the included grains. Zircon, though metamict, imprints no radiogenic halo in the biotite while monazite does.

Texture : mortar

Average grain size : 3-6 mm; accessories: 0.5 mm

table 67 cont'd.....Sample CL-3 (average of two thin-
sections)

mineral	%	description
<hr/>		
quartz	40	undulose to mosaic extinction
orthoclase	15	slightly altered; brownish surface, not twinned
plagioclase	30	altered, damouritized; about An ₂₅
biotite	15	brown
zircon	<0.1	in biotite, with radiogenic haloes
uraninite	<0.1	hematitized remnants with reddish haloes

Texture : equigranular to gneissic

Average grain size : 5 mm (equigranular), 1mm (gneissic)

accessories: 0.1 mm (uraninite), 0.05 mm (zircon)

table 67 cont'd.....Sample CL-4 (average of two thin-sections)

mineral	%	description
quartz	40	undulose to mosaic extinction
orthoclase	5	altered; turbid surface, not twinned
plagioclase	40	zoned; fresh rim, generally not twinned, of about An ₁₅ with twinned lamouritized centre of lower refractive indices (An ₁₀ ?)
biotite	15	brown
muscovite	1	occurs around biotite
monazite	<0.1	automorphous, yellowish to pinkish, metamict
zircon	<0.1	automorphous, clear, zoned, metamict
uraninite	<0.1	remnants
galena	<0.1	lamellar, mostly included in biotite in cleavage planes

Monazite biotite and uraninite are mostly associated with biotite. They occur as in sample CL-2.

Texture : equigranular to mortar

Average grain size : 2-5 mm; accessories: 0.1 mm

table 67 cont'd.....Sample CL-5A

mineral	%	description
<hr/>		
quartz	5	undulose extinction
orthoclase	5	altered; turbid brownish surface
plagioclase	35	altered, damouritized, about An ₂₅
biotite	55	brown
muscovite	<1	occurs around biotite
zircon	<0.1	automorphous, zoned, clear, metamict
monazite	<0.1	automorphous, yellowish to pinkish, metamict
pyrite	<1	
galena	<0.1	
uraninite	<0.1	remnants

Monazite and zircon are mostly associated with biotite.

Monazite gives rise to radiogenic haloes in biotite while zircon does not.

Texture : schistose

Average grain size : 1-2 mm; accessories: 0.5 mm

table 67 cont'd.....Sample CL-5B

mineral	%	description
<hr/>		
quartz	5	undulose extinction
microcline	45	perthitic, moderately altered; turbid surface
plagioclase	45	zoned very altered damouritized centre of about An ₂₅ with a fresher rim of about An ₂₀
muscovite	1	
biotite	3	brown
apatite	<1	automorphous
hematite	<0.1	
uraninite	<0.1	remnants

Texture : equigranular to mortar

Average grain size : 5 mm; accessories: 0.2 mm

B30223